

**Ultrastructural Organisation and
Molecular Interactions in the
Hypertrophic Cartilage Extracellular
Matrix**

Sian Hancock

2005

UMI Number: U585538

All rights reserved

INFORMATION TO ALL USERS

The quality of this reproduction is dependent upon the quality of the copy submitted.

In the unlikely event that the author did not send a complete manuscript and there are missing pages, these will be noted. Also, if material had to be removed, a note will indicate the deletion.



UMI U585538

Published by ProQuest LLC 2013. Copyright in the Dissertation held by the Author.
Microform Edition © ProQuest LLC.

All rights reserved. This work is protected against
unauthorized copying under Title 17, United States Code.



ProQuest LLC
789 East Eisenhower Parkway
P.O. Box 1346
Ann Arbor, MI 48106-1346

This thesis is dedicated to

James Plimmer

Robert & Pamela Hancock

Max & Jean James and Ronnie Hancock

*Thank you for your love, encouragement and support (emotional and financial!)
throughout my studies, I could not have done it without you.*

Diolch yn fawr.

Acknowledgements

I am indebted to my supervisor Professor Vic Duance for his guidance, support and encouragement, he always had 'two minutes' to spare me and his door was always open - *Cheers Vic.*

I would like to thank my co-supervisor Dr Alvin Kwan for offering advice, practical assistance and reagents when required.

Members of Laboratory C5.11; past and present*, have made the past few years a good memorable experience. I was fortunate to be surrounded by a group of bright knowledgeable people and I am grateful to them all.

- | | |
|-------------------------|-----------------------|
| * Dr Sophie Gilbert | |
| * Dr Emma Blain | Dr Rob Young |
| * Dr Philippa Callender | Dr Steve Luckman |
| * Dr Debbie Mason | Dr Anne Vaughn-Thomas |
| * Lindsay Davies | Dr Jim Huggett |
| * Sophie Flood | Dr Elaine Rees |
| * Waiel Al-Amoudi | |

Your good advice, practical assistance, time and friendship have been very much appreciated.

The practical assistance of Dr David Williams with the Biacore 3000 instrument, Dr Ant Hann, Dr Rob Young and Mr Mike Turner with electron microscopy was invaluable.

Thank you to Dr Clare Hughes and Dr Larry Fisher for the kind donation of antibodies.

I acknowledge the financial assistance of the Anatomical Society and Cardiff University.

Abstract

Type X collagen is a member of the family of network-forming collagens, it contains a triple helical domain flanked by two non-collagenous (NC) domains, NC2 at the N-terminal and NC1 at the C-terminal. It is expressed and synthesised by hypertrophic chondrocytes of the epiphyseal growth plates during the process of endochondral ossification (EO). This process involves replacement of a cartilaginous anlagen by bone, the coordination of chondrocyte proliferation, maturation and hypertrophy are followed by calcification of hypertrophic cartilage, vascular invasion and deposition of a bone matrix. A precise functional role for type X collagen has not been defined, although its temporal and spatial expression has linked it to endochondral ossification. A family of Small Leucine Rich Proteoglycans (SLRPs) have been demonstrated to be important for collagen biology. In particular, the well characterised decorin and biglycan, interact with numerous collagen types, non-collagenous proteins and growth factors. Decorin and biglycan have also been linked to the mineralisation process. This led to the hypothesis that type X collagen interacts with decorin and biglycan in the hypertrophic cartilage extracellular matrix.

Interactions of type X collagen with decorin and biglycan were investigated using a solid phase assay and surface plasmon resonance (SPR). The interaction of type X collagen with decorin and biglycan was found to be of high affinity, with dissociation constants in the nanomolar range. Through using different domains of the type X collagen molecule; the NC1 domain, the triple helical region or whole type X collagen, it was demonstrated that the interactions are likely to be mediated by the NC1 domain. The interaction of type X collagen with decorin and biglycan was found to be independent of the presence of the glycosaminoglycan chain(s) on decorin and biglycan, indicating the protein cores of decorin and biglycan are involved. Negative staining and transmission electron microscopy were used to visualise the interactions of type X collagen with decorin and biglycan labelled gold particles. The localisation of gold particles to the ends of type X collagen molecules supports the finding that the interactions are mediated by NC1. Recombinant fragments of the NC1 domain were synthesised in an attempt to further determine regions of NC1 important for the interactions with decorin and biglycan, these fragments have to date provided no additional information. Using RT-PCR decorin was demonstrated to be co-expressed with type X collagen by hypertrophic chondrocytes. Immunohistochemistry was utilised to study the localisation of type X collagen, decorin and biglycan in the hypertrophic cartilage extracellular matrix. All of the interacting components were shown to co-localise. The co-expression and co-localisation studies indicate that these interactions could occur *in vivo*.

The characterised interactions of type X collagen with decorin and biglycan are likely to have functional roles in EO. Potentially; they may be involved in regulation and assembly of a type X collagen pericellular matrix, they may adopt a structural role providing mechanical stability to an extracellular matrix undergoing dynamic remodelling, they could be involved in sequestering growth factors in the hypertrophic cartilage and hence be involved in modulating interactions of growth factors with their signalling receptors. These postulated functions are all possible in the normal development and growth of a long bone. Type X collagen, decorin and biglycan have all been implicated in pathology; the interactions could alternatively be involved in pathological calcification. Molecular interactions that contribute to the molecular assembly of the growth plate are fundamental to its functions. Characterisation of such interactions will aid in defining precise roles for molecules such as type X collagen, decorin and biglycan during the process of EO.

Ultrastructural Organisation and Molecular Interactions in the Hypertrophic Cartilage Extracellular Matrix

| | |
|--------------------------|-----|
| Acknowledgements | i |
| Abstract | ii |
| Table of Contents | iii |
| List of Figures | x |
| Abbreviations | xiv |

Chapter 1: Introduction

| | |
|---|----|
| 1.1 The Skeleton | 1 |
| 1.1.1 Endochondral Bone Formation | 1 |
| 1.1.2 The Epiphyseal Growth Plate | 3 |
| 1.2 Molecular Composition of Hypertrophic and Articular Cartilage | 6 |
| 1.2.1 The Collagen Superfamily | 6 |
| 1.2.1.1 Collagen Biosynthesis | 6 |
| 1.2.1.2 Fibril Forming Collagens | 10 |
| 1.2.1.3 Fibril-associated Collagens with Interrupted Triple Helices (FACIT Collagens) | 10 |
| 1.2.1.4 Network Forming Collagens | 11 |
| 1.2.1.5 Filamentous Collagens | 11 |
| 1.2.1.6 Membrane Bound Collagens | 12 |
| 1.2.1.7 Multiplexin (multiple triple-helix domains and interruptions) Collagens | 12 |
| 1.2.1.8 Others | 12 |
| 1.2.1.9 The Cartilage Collagens | 13 |
| 1.2.2 Proteoglycans | 16 |
| 1.2.2.1 Hyaluronan (HA) | 16 |
| 1.2.2.2 Aggrecan | 16 |
| 1.2.2.3 Perlecan | 19 |
| 1.2.3 Other ECM Components | 21 |
| 1.2.3.1 Matrilins | 21 |
| 1.2.3.2 Cartilage Oligomeric Matrix Protein | 21 |
| 1.3 Type X Collagen | 22 |
| 1.3.1 Three Distinct Domains of Type X Collagen: the triple helix, NC1 and NC2 | 24 |
| 1.3.1.1 The Triple Helix | 24 |
| 1.3.1.2 The NC1 Domain | 24 |
| 1.3.1.3 The NC2 Domain | 27 |
| 1.3.2 Ultrastructural Assembly and Function of Type X Collagen | 27 |
| 1.3.3 The Type X Collagen Gene | 30 |

| | | |
|-----------|---|----|
| 1.3.4 | Type X Collagen Localisation other than Growth Plate | 31 |
| 1.3.5 | Schmid Metaphyseal Chondrodysplasia (SMCD) | 32 |
| 1.3.6 | Type X Collagen Transgenic and Knockout Mice | 33 |
| 1.3.6.1 | Transgenic Type X Collagen Mice | 33 |
| 1.3.6.2 | Collagen X Null Mice | 35 |
| 1.4 | Small Leucine Rich Proteoglycans (SLRPs) | 36 |
| 1.4.1 | Class I SLRPs | 39 |
| 1.4.1.1 | Decorin and Biglycan | 39 |
| 1.4.1.2 | Genomic Organisation of Decorin and Biglycan | 43 |
| 1.4.1.3 | Localisation of Decorin and Biglycan | 43 |
| 1.4.1.4 | Interactions of Decorin and Biglycan with Collagens | 45 |
| 1.4.1.5 | Interactions of Decorin and Biglycan with Non-Collagenous Proteins | 47 |
| 1.4.1.6 | Interaction of Decorin and Biglycan with Growth Factors | 47 |
| 1.4.1.7 | Decorin and Biglycan Transgenic Mice | 48 |
| 1.4.1.7.1 | Biglycan-deficient mouse | 49 |
| 1.4.1.7.2 | Decorin-deficient mouse | 49 |
| 1.4.1.7.3 | Biglycan/Decorin-deficient mouse | 49 |
| 1.4.2 | Class II SLRPs | 50 |
| 1.4.3 | Class III SLRPs | 52 |
| 1.5 | Cellular Control, Remodelling, Mineralisation and Angiogenesis during Endochondral Ossification | 53 |
| 1.5.1 | Cellular Control of Growth Plate Chondrocytes | 53 |
| 1.5.1.1 | Indian hedgehog and Parathyroid Hormone-related Protein | 53 |
| 1.5.1.2 | Transforming Growth Factor- β (TGF- β) | 54 |
| 1.5.1.3 | Fibroblast Growth Factors (FGFs) and their Receptors (FGFRs) | 54 |
| 1.5.1.4 | Bone Morphogenetic Proteins (BMPs) | 55 |
| 1.5.1.5 | Other Growth Factors and Hormones | 55 |
| 1.5.2 | Matrix Remodelling During the Process of EO | 57 |
| 1.5.3 | Mineralisation in the Growth Plate | 60 |
| 1.5.4 | Angiogenesis during the Process of EO | 61 |
| 1.5.4.1 | Vascular Endothelial Growth Factor | 61 |
| 1.5.4.2 | Connective Tissue Growth Factor | 62 |
| 1.6 | Aims and Objectives of the Project | 63 |
| 1.6.1 | Background and Hypothesis | 63 |
| 1.6.2 | Aims and Objectives | 63 |
| 1.6.2.1 | Specific objectives | 64 |

Chapter 2: Generation of Reagents for Interaction Analysis

| | | |
|-------|------------------------|----|
| 2.1 | BACKGROUND | 65 |
| 2.1.1 | Native Type X Collagen | 65 |
| 2.1.2 | Recombinant NC1 Domain | 65 |

| | | |
|-----------|--|----|
| 2.1.3 | Decorin and Biglycan Sources | 65 |
| 2.2 | MATERIALS AND METHODS | 67 |
| 2.2.1 | Purification of Type X Collagen | 67 |
| 2.2.1.1 | <i>Hypertrophic Chondrocyte Culture - Tissue Preparation</i> | 67 |
| 2.2.1.2 | <i>Hypertrophic Chondrocyte Culture - Cell Preparation</i> | 67 |
| 2.2.1.3 | <i>Storage of Collected Medium</i> | 67 |
| 2.2.1.4 | <i>Ammonium Sulphate Precipitation</i> | 68 |
| 2.2.1.5 | <i>Differential Salt Fractionation</i> | 68 |
| 2.2.1.6 | <i>Hydroxyproline Assay</i> | 68 |
| 2.2.2 | Isolating Different Domains of Type X Collagen | 71 |
| 2.2.2.1 | <i>Preparation of the Triple Helical Domain</i> | 71 |
| 2.2.2.2 | <i>Preparation of Human Recombinant NC1 Domain</i> | 71 |
| 2.2.2.2.1 | <i>Purification of 6XHis-tagged NC1 under Native Conditions</i> | 71 |
| 2.2.3 | Enzymatic Digestion of Decorin and Biglycan | 71 |
| 2.2.3.1 | <i>Chondroitinase ABC Treatment</i> | 71 |
| 2.2.4 | Analysis of Proteins and Proteoglycans | 72 |
| 2.2.4.1 | <i>Sample preparation</i> | 72 |
| 2.2.4.2 | <i>Sodium Dodecyl Sulphate PolyAcrylamide Gel Electrophoresis (SDS-PAGE)</i> | 72 |
| 2.2.4.3 | <i>Coomassie Blue Staining</i> | 72 |
| 2.2.4.4 | <i>Western Blotting</i> | 73 |
| 2.2.4.4.1 | <i>Preparation of Membrane</i> | 73 |
| 2.2.4.4.2 | <i>Transfer of Proteins from Polyacrylamide Gels to Membranes</i> | 74 |
| 2.2.4.4.3 | <i>Immuno-probing of Membranes</i> | 74 |
| 2.2.4.4.5 | <i>Detection of Immunoreactive Bands</i> | 75 |
| 2.2.4.4.6 | <i>Enhanced Chemiluminescence (ECL) Detection</i> | 75 |
| 2.2.4.4.7 | <i>NBT/BCIP Detection</i> | 76 |
| 2.3 | RESULTS | 77 |
| 2.3.1 | Purification of Type X Collagen | 77 |
| 2.3.2 | Analysis of Salt Fractions by SDS-PAGE | 77 |
| 2.3.3 | Confirmation of Collagen Types by Western Blotting | 77 |
| 2.3.4 | Preparation of the Triple Helical Domain of Type X Collagen | 81 |
| 2.3.5 | Preparation of Human Recombinant NC1 Domain | 81 |
| 2.3.5.1 | <i>Analysis of Recombinant NC1 by SDS-PAGE and Western Blotting</i> | 81 |
| 2.3.6 | Deglycosylation of Decorin and Biglycan | 85 |
| 2.4 | DISCUSSION | 88 |

Chapter 3: Interaction Studies of Type X Collagen with Decorin and Biglycan

| | | |
|-------|--|----|
| 3.1 | BACKGROUND | 91 |
| 3.1.1 | Molecular Interactions in a Solid Phase Assay | 91 |
| 3.1.2 | Biomolecular Interaction Analysis (BIA) Technology | 94 |

| | | |
|---------|--|-----|
| 3.1.2.1 | Surface Plasmon Resonance (SPR) – Basic Principle | 94 |
| 3.1.2.2 | Sensor Chip Technology | 95 |
| 3.1.3 | Visualising Interacting Molecules Using Negative Staining | 98 |
| 3.2 | MATERIALS AND METHODS | 99 |
| 3.2.1 | Basic Solid Phase Assay | 99 |
| 3.2.1.1 | <i>Competitive Solid Phase Assay</i> | 99 |
| 3.2.2 | Biomolecular Interaction Analysis | 100 |
| 3.2.2.1 | <i>Immobilisation of Ligands on CM5 Sensor Chips</i> | 100 |
| 3.2.2.2 | <i>Kinetic Assays on the BIAcore</i> | 100 |
| 3.2.2.3 | <i>Data Preparation and Analysis using BIAevaluation 3.0</i> | 101 |
| 3.2.3 | Negative Staining Electron Microscopy | 101 |
| 3.2.3.1 | <i>Preparation of Gold Colloids</i> | 101 |
| 3.2.3.2 | <i>Preparation of Decorin and Biglycan Gold Probes</i> | 101 |
| 3.2.3.3 | <i>Concentration of Gold Particle Populations by Centrifugation</i> | 101 |
| 3.2.3.4 | <i>Estimation of Gold Particle Sizes</i> | 102 |
| 3.2.3.5 | <i>Grid Preparation and TEM</i> | 102 |
| 3.3 | RESULTS | 103 |
| 3.3.1 | Solid Phase Assays | 103 |
| 3.3.1.1 | <i>Decorin interacts with type X collagen in a solid phase assay</i> | 103 |
| 3.3.1.2 | <i>Interaction of decorin with type X collagen can be competitively inhibited by decorin</i> | 103 |
| 3.3.1.3 | <i>Interaction of decorin with type X collagen can be competitively inhibited by biglycan</i> | 104 |
| 3.3.1.4 | <i>Biglycan interacts with type X collagen in a solid phase assay</i> | 108 |
| 3.3.1.5 | <i>Interaction of biglycan with type X collagen can be competitively inhibited by biglycan</i> | 108 |
| 3.3.1.6 | <i>Interaction of biglycan with type X collagen can be competitively inhibited by decorin</i> | 109 |
| 3.3.1.7 | <i>Pepsinised Type X Collagen Does Not Interact With Decorin or Biglycan</i> | 113 |
| 3.3.2 | Biomolecular Interaction Analysis Results | 115 |
| 3.3.2.1 | <i>Immobilisation of Ligands to the Sensor Chip Surface</i> | 115 |
| 3.3.2.2 | <i>BIAcore Analysis of Type X Collagen and NC1 Domain Interactions with Decorin</i> | 115 |
| 3.3.2.3 | <i>BIAcore Analysis of Type X Collagen and NC1 Domain Interactions with Biglycan</i> | 124 |
| 3.3.2.4 | <i>Interactions of Type X Collagen with Decorin and Biglycan are Mediated Via The NC1 Domain and are Independent of the Presence of GAG Chains</i> | 129 |
| 3.3.3 | Interactions Visualised by Negative Staining | 130 |
| 3.3.3.1 | <i>Production of Decorin and Biglycan Labelled Gold Particles (4 – 5nm diameter)</i> | 130 |
| 3.3.3.2 | <i>Type X Collagen in Multimeric and Aggregated Forms</i> | 134 |
| 3.3.3.3 | <i>Type X Collagen Interacts with Decorin and Biglycan</i> | 134 |
| 3.4 | DISCUSSION | 139 |

Chapter 4: Construction of Expression Clones, Expression and Purification of Recombinant Proteins and Interaction Analysis of NC1 Fragments with Decorin and Biglycan

| | | |
|---------|---|-----|
| 4.1 | BACKGROUND | 144 |
| 4.1.1 | Bacterial Expression of NC1 Recombinant Fragments | 144 |
| 4.1.2 | Regulation of Expression: pREP4 plasmid | 144 |
| 4.1.3 | Purification of 6xHis-tagged proteins by Ni-NTA affinity chromatography | 145 |
| 4.2 | MATERIALS AND METHODS | 149 |
| 4.2.1 | Amplification of NC1 Fragments by Polymerase Chain Reaction (PCR) | 149 |
| 4.2.1.1 | <i>PCR Using Primers Adapted with Restriction Sequences</i> | 149 |
| 4.2.1.2 | <i>Agarose Gel Electrophoresis</i> | 151 |
| 4.2.1.3 | <i>Purification of DNA from Agarose Gels using QIAEX II (Qiagen)</i> | 151 |
| 4.2.2 | Cloning NC1 Fragments into the Cloning Vector pGEM®-T | 151 |
| 4.2.2.1 | <i>Ligating PCR Products into the pGEM®-T Vector</i> | 152 |
| 4.2.2.2 | <i>Transformation of Competent E. coli (JM109) with pGEM®-T.</i> | 152 |
| 4.2.2.3 | <i>DNA purification using the Wizard® Plus SV Miniprep System (Promega)</i> | 152 |
| 4.2.2.4 | <i>Sequencing Reaction</i> | 153 |
| 4.2.3 | Restriction Digestion of NC1 PCR Products | 157 |
| 4.2.3.1 | <i>Linearisation of pQE-30 Expression Vector</i> | 157 |
| 4.2.3.2 | <i>Ligation of NC1 Fragments into pQE-30 Expression Vector</i> | 157 |
| 4.2.4 | Preparation of Competent E. Coli Cells | 158 |
| 4.2.4.1 | <i>M15[Prep4] Cells</i> | 158 |
| 4.2.4.2 | <i>XL-1 Blue Cells</i> | 158 |
| 4.2.4.3 | <i>Transformation of Competent M15 and XL-1 Cells</i> | 159 |
| 4.2.5 | E. coli Culture Growth for Preparative Purification | 159 |
| 4.2.5.1 | <i>Preparation of Cleared E. coli Lysates Under Native Conditions</i> | 160 |
| 4.2.5.2 | <i>Preparation of E. coli Cellular Debris Under Denaturing Conditions</i> | 160 |
| 4.2.5.3 | <i>Purification of 6xHis-tagged Proteins from E. coli Lysate Under Native Conditions</i> | 160 |
| 4.2.5.4 | <i>Purification of 6xHis-tagged Proteins from E. coli Cellular Debris Under Denaturing Conditions</i> | 161 |
| 4.2.6 | SDS-PAGE and Western Blot Analysis | 161 |
| 4.2.6.1 | <i>Western Blotting using Specialised Membrane</i> | 161 |
| 4.2.6.2 | <i>Immuno-detection Using Qiagen's Penta-His Antibody</i> | 162 |
| 4.2.7 | Determination of Protein Concentration | 162 |
| 4.2.8 | Optimisation of Antibody Dilutions Required for Interaction Analysis | 162 |
| 4.2.8.1 | <i>Interaction Analysis using Basic Solid Phase Assay</i> | 163 |
| 4.3 | RESULTS | 164 |
| 4.3.1 | Amplification, TA Cloning and DNA Sequencing of NC1 Fragments | 164 |
| 4.3.2 | Sub-cloning into the pQE-30 expression vector | 169 |
| 4.3.3 | Confirming the presence of NC1 Fragments in the pQE-30 expression vector in transformed | |

| | |
|--|-----|
| <i>E. coli</i> | 175 |
| 4.3.4 Recombinant Protein Production and Purification | 183 |
| 4.3.4.1 Analysis of the Positive Control Protein, DHFR | 184 |
| 4.3.4.2 Analysis of the NC1 Fragment, F1/R1 | 187 |
| 4.3.4.3 Analysis of the NC1 Fragment, F1/R2 | 190 |
| 4.3.4.4 Analysis of the NC1 Fragment, F2/R2 | 193 |
| 4.3.4.5 Analysis of the NC1 Fragment, F2/R3 | 196 |
| 4.3.5 Interaction Analysis | 199 |
| 4.3.5.1 Optimisation of Antibody Dilutions | 199 |
| 4.3.5.2 Interaction Analysis using NC1 Recombinant fragments F1/R1, F1/R2, F2/R2 and F2/R3 | 199 |
| 4.4 DISCUSSION | 202 |

Chapter 5: Expression and Localisation of Interacting Components Type X Collagen, Decorin and Biglycan in Hypertrophic Cartilage.

| | |
|--|-----|
| 5.1 BACKGROUND | 207 |
| 5.1.1 Confirming Hypertrophic Chondrocyte Expression | 207 |
| 5.1.2 Confirming Localisation of Interacting Components Type X Collagen, Decorin and Biglycan in Epiphyseal Growth Plate Cartilage | 207 |
| 5.2 MATERIALS AND METHODS | 208 |
| 5.2.1 RNA Preparation | 208 |
| 5.2.1.1 Homogenisation of Cartilage in Trizol® | 208 |
| 5.2.1.2 Phase Separation | 208 |
| 5.2.1.3 RNA Precipitation, Washing and Re-dissolving | 208 |
| 5.2.1.4 DNase Treatment of Isolated RNA | 209 |
| 5.2.1.5 Re-Extraction of RNA Post-DNase Treatment | 209 |
| 5.2.2 cDNA Synthesis by Reverse Transcription of RNA (RT-PCR) | 209 |
| 5.2.3 Primer Design | 210 |
| 5.2.4 Polymerase Chain Reaction (PCR) | 210 |
| 5.2.4.1 PCR product Cloning & Sequencing | 211 |
| 5.2.5 Preparation of Tissue for Histology and Immunohistochemistry | 211 |
| 5.2.5.1 Dissection and Preparation of Cryosections | 211 |
| 5.2.5.2 Dissection, Fixation and Decalcification Prior to Paraffin Wax Sectioning | 211 |
| 5.2.5.3 Paraffin Wax Sectioning | 211 |
| 5.2.5.4 Pre-staining treatment | 212 |
| 5.2.5.5 Masson's Trichrome Staining | 212 |
| 5.2.5.6 Haematoxylin and Eosin Staining | 212 |
| 5.2.6 Immunohistochemistry | 213 |
| 5.2.6.1 Type X Collagen Staining | 213 |
| 5.2.6.2 Decorin and Biglycan Staining | 213 |

| | | |
|-------|--|-----|
| 5.3 | RESULTS | 215 |
| 5.3.1 | Generation of cDNA for PCR Analysis | 215 |
| 5.3.2 | Type X Collagen and Decorin are Expressed by Hypertrophic Chondrocytes | 215 |
| 5.3.3 | Expression of Biglycan by Hypertrophic Chondrocytes Not Confirmed | 221 |
| 5.3.4 | Cellular Morphology of the Growth Plate | 221 |
| 5.3.5 | Localisation of Type X Collagen in the Hypertrophic Zone of the Growth Plate | 224 |
| 5.3.6 | Localisation of Type X Collagen in Other Joint Structures | 224 |
| 5.3.7 | Localisation of Decorin and Biglycan in the Growth Plate | 224 |
| 5.4 | DISCUSSION | 229 |

Chapter 6: General Discussion

| | | |
|-------|---|-----|
| 6.1 | Background | 232 |
| 6.2 | Summary of Findings | 232 |
| 6.3 | Proposed Biological Significance of the Identified Interactions | 235 |
| 6.3.1 | Involvement in Endochondral Ossification | 235 |
| 6.3.2 | Involvement in Pathology | 239 |
| 6.4 | Future work | 240 |
| 6.5 | Closing comments | 241 |

| | |
|------------------------------|------------|
| Chapter 7: References | 242 |
|------------------------------|------------|

List of Figures

| | |
|--|-----|
| Figure 1.1: Schematic diagram of the process of endochondral bone formation. | 2 |
| Figure 1.2: A schematic representation of a longitudinal section through the epiphyseal growth plate. | 5 |
| Figure 1.3: Schematic representation of fibrillar collagen biosynthesis. | 8 |
| Figure 1.4: A table summarising collagen groups with associated members. | 9 |
| Figure 1.5: Schematic diagram showing the arrangement of collagen molecules in cartilage heterotypic fibrils. | 15 |
| Figure 1.6: Schematic illustration of the high molecular weight proteoglycan aggregate found in cartilage. | 18 |
| Figure 1.7: Schematic illustration of the modular protein core of the heparan sulphate proteoglycan perlecan. | 20 |
| Figure 1.8: Schematic representation of the collagen X gene (COL10A1), messenger RNA and protein. | 23 |
| Figure 1.9: Structure of the collagen X NC1 trimer and the Ca ²⁺ cluster. | 26 |
| Figure 1.10: Rotary shadowing electron micrographs of the extended network of type X collagen aggregates. | 29 |
| Figure 1.11: Members of the different SLRP classes are shown, with genomic, protein and GAG details. | 38 |
| Figure 1.12: Schematic representation of a Class I SLRP. | 41 |
| Figure 1.13: Molecular model of the decorin core protein, displaying the 'horse-shoe-like' conformation. | 42 |
| Figure 1.14: Schematic illustration detailing some of the signalling molecules involved in the cellular control of events occurring at the growth plate. | 56 |
| Figure 1.15: Schematic illustration of the MMPs involved in endochondral ossification, different functional domains are highlighted. | 59 |
| Figure 2.1: Schematic illustration of the steps involved in the differential salt fractionation process of preparing collagen. | 70 |
| Figure 2.2: SDS-PAGE and Western blot analysis of samples generated by differential salt fractionation. | 79 |
| Figure 2.3: Anti-type II and anti-type X collagen western blot analysis of samples obtained by differential salt fractionation. | 80 |
| Figure 2.4: SDS-PAGE and Western blot analysis of the 2M precipitate sample generated by differential salt fractionation. | 83 |
| Figure 2.5: SDS-PAGE and Western blot analysis of the fractions generated by Ni-NTA agarose column purification. | 84 |
| Figure 2.6: SDS-PAGE and Western analysis of decorin before and after deglycosylation. | 86 |
| Figure 2.7: SDS-PAGE and Western analysis of biglycan before and after deglycosylation. | 87 |
| Figure 3.1: Interaction analysis using basic and competitive solid phase assays. | 93 |
| Figure 3.2: Schematic diagram of refraction and total internal reflection. | 96 |
| Figure 3.3: Applying SPR to biomolecular analysis. | 97 |
| Figure 3.4: Type X collagen interacts with decorin in a solid phase assay. | 105 |
| Figure 3.5: The interaction of type X collagen with decorin can be competitively inhibited by decorin. | 106 |
| Figure 3.6: The interaction of type X collagen with decorin can be competitively inhibited by biglycan. | 107 |
| Figure 3.7: Type X collagen interacts with biglycan in a solid phase assay. | 110 |

| | |
|--|-----|
| Figure 3.8: The interaction of type X collagen with biglycan can be competitively inhibited by biglycan. | 111 |
| Figure 3.9: The interaction of type X collagen with biglycan can be competitively inhibited by decorin. | 112 |
| Figure 3.10: Solid phase assay demonstrating interactions of decorin and biglycan with whole type X collagen but not with pepsinised type X collagen. | 114 |
| Figure 3.11: An example of sensogram responses during the process of ligand immobilisation and control flow cell preparation. | 116 |
| Figure 3.12: Sensograms showing a concentration range of decorin being injected over a type X collagen chip surface. | 117 |
| Figure 3.13: Baseline stability of control and ligand coated flow cells analysed between cycles of analyte injection. | 118 |
| Figure 3.14: Sensogram showing dissociation phase curve fitting for a concentration range of the analyte decorin, being injected over a type X collagen chip surface. | 120 |
| Figure 3.15: Sensogram showing an association phase curve fitting for a concentration range of the analyte decorin, being injected over a type X collagen chip surface. | 121 |
| Figure 3.16: Sensogram showing a dissociation phase curve fitting for a concentration range of the analyte decorin, being injected over a NC1 domain chip surface. | 122 |
| Figure 3.17: Sensogram showing an association phase curve fitting for a concentration range of the analyte decorin, being injected over an NC1 domain chip surface. | 123 |
| Figure 3.18: Sensogram showing a dissociation phase curve fitting for a concentration range of the analyte biglycan, being injected over a type X collagen chip surface. | 125 |
| Figure 3.19: Sensogram showing an association phase curve fitting for a concentration range of the analyte biglycan, being injected over a type X collagen chip surface. | 126 |
| Figure 3.20: Sensogram showing a dissociation phase curve fitting for a concentration range of the analyte biglycan, being injected over a NC1 domain chip surface. | 127 |
| Figure 3.21: Sensogram showing an association phase curve fitting for a concentration range of the analyte biglycan, being injected over an NC1 domain chip surface. | 128 |
| Figure 3.22: Electron micrographs of the line grating grid used for measuring and size estimation purposes. | 131 |
| Figure 3.23: Estimation of decorin labelled gold particle diameter. | 132 |
| Figure 3.24: Estimation of biglycan labelled gold particle diameter. | 133 |
| Figure 3.25: Electron micrographs of type X collagen stained with 1% uranyl formate. | 135 |
| Figure 3.26: Electron micrograph after negative staining with 1% uranyl formate of type X collagen interacting with decorin labelled gold particles. | 136 |
| Figure 3.27: Electron micrograph after negative staining with 1% uranyl formate of type X collagen interacting with decorin labelled gold particles. | 137 |
| Figure 3.28: Electron micrograph of type X collagen interacting with biglycan labelled gold particles; negatively stained with 1% uranyl formate. | 138 |
| Figure 4.1: pQE vector map with characteristics required for protein expression highlighted. | 146 |
| Figure 4.2: Vector map showing positions of features important for protein expression and diagram detailing restriction sites present in the multiple cloning sites of vectors pQE -30, -31 and -32. | 147 |
| Figure 4.3: Interaction between neighbouring residues in the 6xHis tag and Ni-NTA matrix. | 148 |

| | |
|--|-----|
| Figure 4.4: Sequence of the NC1 domain of human type X collagen COL10A1 mRNA (gi:18105031). | 150 |
| Figure 4.5: pGEM-T vector map and multiple cloning site. | 155 |
| Figure 4.6: Protocol for the Wizard Plus SV Minipreps DNA purification system. | 156 |
| Figure 4.7: PCR products generated using different combinations of the NC1 primers. | 165 |
| Figure 4.8: Sequence analysis of the NC1 clone F1/R1. | 167 |
| Figure 4.9: Sequence analysis of the NC1 clone F1/R2. | 168 |
| Figure 4.10: Sequence analysis of the NC1 clone F2/R2. | 168 |
| Figure 4.11: Sequence analysis of the NC1 clone F2/R3. | 169 |
| Figure 4.12: Sequences of the restriction sit adapted NC1-F and NC1-R primers, restriction sites are highlighted in blue. | 170 |
| Figure 4.13: 1% agarose gel electrophoresis of PCR amplified products with NC1 primers containing 5' restriction sites from plasmid DNA. | 172 |
| Figure 4.14: 1% agarose gel electrophoresis of linearised pQE-30 expression vector after <i>Bam</i> H I and <i>Pst</i> I restriction digest. | 173 |
| Figure 4.15: Sub-cloning steps used to generate NC1 fragment expression vectors. | 174 |
| Figure 4.16: Gel electrophoresis of PCR amplified products from plasmid DNA samples from different colonies of M15[pREP4] cells transformed with different NC1 fragments. | 177 |
| Figure 4.17: Gel electrophoresis of PCR amplified products from plasmid DNA samples from different colonies of XL-1 Blue cells transformed with different NC1 fragments. | 178 |
| Figure 4.18: Nucleotide and protein sequence of the recombinant fragment F1/R1. | 179 |
| Figure 4.19: Nucleotide and protein sequence of the recombinant fragment F2/R3. | 180 |
| Figure 4.20: Nucleotide and protein sequence of the recombinant fragment F1/R2. | 181 |
| Figure 4.21: Nucleotide and protein sequence of the recombinant fragment F2/R2. | 182 |
| Figure 4.22: SDS-PAGE and western blot analysis of samples generated under native conditions using the Ni-NTA agarose to purify 6xHis-tagged DHFR. | 185 |
| Figure 4.23: SDS-PAGE and western blot analysis of samples generated under denaturing conditions using the Ni-NTA agarose to purify 6xHis-tagged DHFR. | 186 |
| Figure 4.24: SDS-PAGE and western blot analysis of samples generated under native conditions using the Ni-NTA agarose to purify 6xHis-tagged F1/R1 recombinant fragment. | 188 |
| Figure 4.25: SDS-PAGE and western blot analysis of samples generated under denaturing conditions using the Ni-NTA agarose to purify 6xHis-tagged F1/R1 recombinant fragment. | 189 |
| Figure 4.26: SDS-PAGE and western blot analysis of samples generated under native conditions using the Ni-NTA agarose to purify 6xHis-tagged F1/R2 recombinant fragment. | 191 |
| Figure 4.27: SDS-PAGE and western blot analysis of samples generated under denaturing conditions using the Ni-NTA agarose to purify 6xHis-tagged F1/R2 recombinant fragment. | 192 |
| Figure 4.28: SDS-PAGE and western blot analysis of samples generated under native conditions using the Ni-NTA agarose to purify 6xHis-tagged F2/R2 recombinant fragment. | 194 |
| Figure 4.29: SDS-PAGE and western blot analysis of samples generated under denaturing conditions using the Ni-NTA agarose to purify 6xHis-tagged F2/R2 recombinant fragment. | 195 |

| | |
|--|-----|
| Figure 4.30: SDS-PAGE and western blot analysis of samples generated under native conditions using the Ni-NTA agarose to purify 6xHis-tagged F2/R3 recombinant fragment. | 197 |
| Figure 4.31: SDS-PAGE and western blot analysis of samples generated under denaturing conditions using the Ni-NTA agarose to purify 6xHis-tagged F2/R3 recombinant fragment. | 198 |
| Figure 4.32: Graph of antibody dilutions optimisation . | 201 |
| Figure 4.33: The nucleotide sequence of the NC1 products generated by PCR. | 203 |
| Figure 5.1: RNA samples isolated from the caudal and cephalic regions of embryonic chick sternum. | 217 |
| Figure 5.2: Type X collagen, decorin and GAPDH PCR products run on an agarose gel. | 218 |
| Figure 5.3: 100% sequence identity of the type X collagen PCR product, the query, with the chicken type X collagen gene, the subject, sequence analysis was performed using the NCBI Blast search engine. Positions of forward and reverse primers are highlighted in red. | 219 |
| Figure 5.4: 100% sequence identity of the decorin PCR product, the query, with the chicken decorin mRNA sequence, the subject, analysis was performed using the NCBI Blast search engine. Positions of forward and reverse primers are highlighted in red. | 220 |
| Figure 5.5: Six week old mouse tibia unfixed and decalcified 15µm cryosections stained with H & E. | 222 |
| Figure 5.6: Histological staining with Masson's Trichrome of 10µm wax sections of 6 week old mouse fixed and decalcified tibia. | 223 |
| Figure 5.7: Immunolocalisation of type X collagen in the tibial growth plate of 6 week old C57 black mice. | 225 |
| Figure 5.8: Immunolocalisation of type X collagen in the articular cartilage of 6 week old C57 black mice. | 226 |
| Figure 5.9: Immunolocalisation of decorin in the growth plate of 6 week old C57 black mice. | 227 |
| Figure 5.10: Immunolocalisation of biglycan in the growth plate of 6 week old C57 black mice. | 228 |
| Figure 6.1: Potential roles of an interaction between type X collagen and the SLRPs decorin and biglycan. | 238 |

Abbreviations

| | |
|----------------|---|
| Acc No | accession number |
| ADAMTS | a disintegrin and metalloproteinase domain with thrombospondin motifs |
| ALP | alkaline phosphatase |
| APS | ammonium persulphate |
| ATP | adenosine triphosphate |
| BCA | bicinchoninic acid |
| BIA | biomolecular interaction analysis |
| BMP | bone morphogenetic protein |
| bp | base pairs |
| BSA | bovine serum albumin |
| cDNA | complementary deoxyribonucleic acid |
| CHO | Chinese hamster ovary |
| CMD | carboxymethyl dextran |
| CMP | cartilage matrix protein |
| COMP | cartilage oligomeric matrix protein |
| CS | chondroitin sulphate |
| CTGF | connective tissue growth factor |
| Da | Daltons |
| DHFR | dihydrofolate reductase |
| DMEM | Dulbecco's modified eagle's medium |
| DNA | deoxyribonucleic acid |
| DNase | deoxyribonuclease |
| dNTP | deoxynucleotide 5'-triphosphate |
| DS | dermatan sulphate |
| DTT | dithiothreitol |
| ECL | enhanced chemiluminescence |
| ECM | extracellular matrix |
| <i>E. coli</i> | <i>Escherichia coli</i> |
| EDS | Ehlers Danlos syndrome |
| EDTA | ethylene diaminetetra-acetic acid |
| EGF | epidermal growth factor |
| EO | endochondral ossification |
| FACIT | fibril-associated collagens with interrupted triple helices |
| FGF | fibroblast growth factor |
| FGFR | fibroblast growth factor receptor |
| FITC | fluorescein isothiocyanate |
| G | globular |
| g | gravitational force |
| GAG | glycosaminoglycan |
| GAPDH | glyceraldehydes-3-phosphate dehydrogenase |
| HA | hyaluronan |
| HAP | hydroxyapatite |
| HEPES | N-2'-hydroxyethyl-piperazine-N-2'ethane sulphonic acid |
| His | histidine |
| HRP | horse radish peroxidase |
| IGF | insulin-like growth factor |
| Ihh | Indian hedgehog |
| IPTG | isopropyl β -D-thiogalactoside |

| | |
|----------------|--|
| ka | association rate constant |
| kd | dissociation rate constant |
| K _D | equilibrium dissociation constant |
| kDa | kilo dalton |
| KO | knock-out |
| KS | keratin sulphate |
| LA | laminin A |
| LB | luria broth |
| LDL-R | low density lipoprotein receptor |
| LE | laminin epidermal growth factor-like |
| LG | globular subdomain of laminin chain |
| LRR | leucine-rich repeat |
| MAPK | mitogen-activated protein kinase |
| MED | multiple epiphyseal dysplasia |
| MCS | multiple cloning site |
| MMP | matrix metalloproteinase |
| mRNA | messenger ribonucleic acid |
| MT-MMP | membrane type – matrix metalloproteinase |
| NBT/BCIP | nitro blue tetrazolium/bromo-4-chloroindol-3-yl phosphate |
| NC | non-collagenous |
| NEM | N-ethylmaleimide |
| NMD | nonsense-mediated decay |
| NTA | nitrilotriacetic acid |
| OD | optical density |
| OPD | o-phenylenediamine |
| PBS | phosphate buffered saline |
| PCR | polymerase chain reaction |
| PG | proteoglycan |
| PKB | protein kinase B |
| PMSF | phenylmethanesulphonyl fluoride |
| ppt | precipitate |
| PRELP | proline arginine-rich end leucine-rich repeat protein |
| PSACH | pseudochondroplasia |
| Ptc | Patched |
| PTHrP | parathyroid hormone related protein |
| R ² | correlation coefficient |
| RNA | ribonucleic acid |
| RNase | ribonuclease |
| rpm | revolutions per minute |
| RT | reverse transcription |
| RU | resonance unit |
| SBTI | soybean trypsin inhibitor |
| SC | short chain |
| SDS-PAGE | sodium dodecyl sulphate polyacrylamide gel electrophoresis |
| SLRP | small leucine rich proteoglycan |
| SMCD | Schmid metaphyseal chondrodysplasia |
| spnt | supernatant |
| SPR | surface plasmon resonance |
| T _m | denaturation temperature |
| TBE | tris borate EDTA |

| | |
|-------|--|
| TEM | transmission electron microscopy |
| TEMED | tetramethylethylenediamine |
| TGF | transforming growth factor |
| TIR | total internal reflection |
| TNF | tumour necrosis factor |
| UTR | untranslated region |
| x-gal | 5-bromo-4-chloro-3-indolyl- β -D-galactopyranoside |
| VEGF | vascular endothelial growth factor |

Chapter 1: Introduction

1.1 The Skeleton

The skeleton derives from mesoderm, which gives rise to a loosely organised tissue known as mesenchyme. Skeletal elements can form via two different mechanisms. The process of intramembranous ossification involves mesenchymal cells directly differentiating into bone, the craniofacial skeleton forms via this mechanism. The process responsible for the formation of most of the vertebrate appendicular and axial skeleton is endochondral ossification (EO). Mesenchymal cells differentiate into cartilage which then provides a template for bone morphogenesis (Ortega et al., 2004).

1.1.1 Endochondral Bone Formation

In brief, mesenchymal cells differentiate into chondrocytes, which produce a cartilage matrix (figure 1.1). A cartilaginous model of the future bone forms. Chondrocytes at the diaphysis of these future bones begin to hypertrophy, this changes the matrix that they produce, and subsequently the matrix begins to calcify. As this calcified cartilage enlarges, the perichondrium differentiates into an outer connective tissue sheath containing fibroblasts and an inner osteoblastic layer of cells, a thin layer of periosteal bone forms around the diaphysis. The end of the embryonic period is marked by invasion of blood vessels via the periosteal bone shaft into the calcified hypertrophic cartilage. Invading blood vessels bring haemopoietic stem cells, osteoblasts and osteoclasts. A primary or a diaphyseal ossification centre forms, where the cartilage cells and matrix have begun to disintegrate. Cartilaginous remnants are then used as a scaffold for the formation of trabecular bone. Resorption of a central core forms the marrow cavity. A secondary or an epiphyseal ossification centre forms, at the growing cartilaginous ends in long bones. The primary and secondary centres of ossification are separated by a transverse plate of cartilage that extends across the bone. This is the epiphyseal growth plate which remains until an individual stops growing (Mundlos, 1994) (Price et al., 1994).

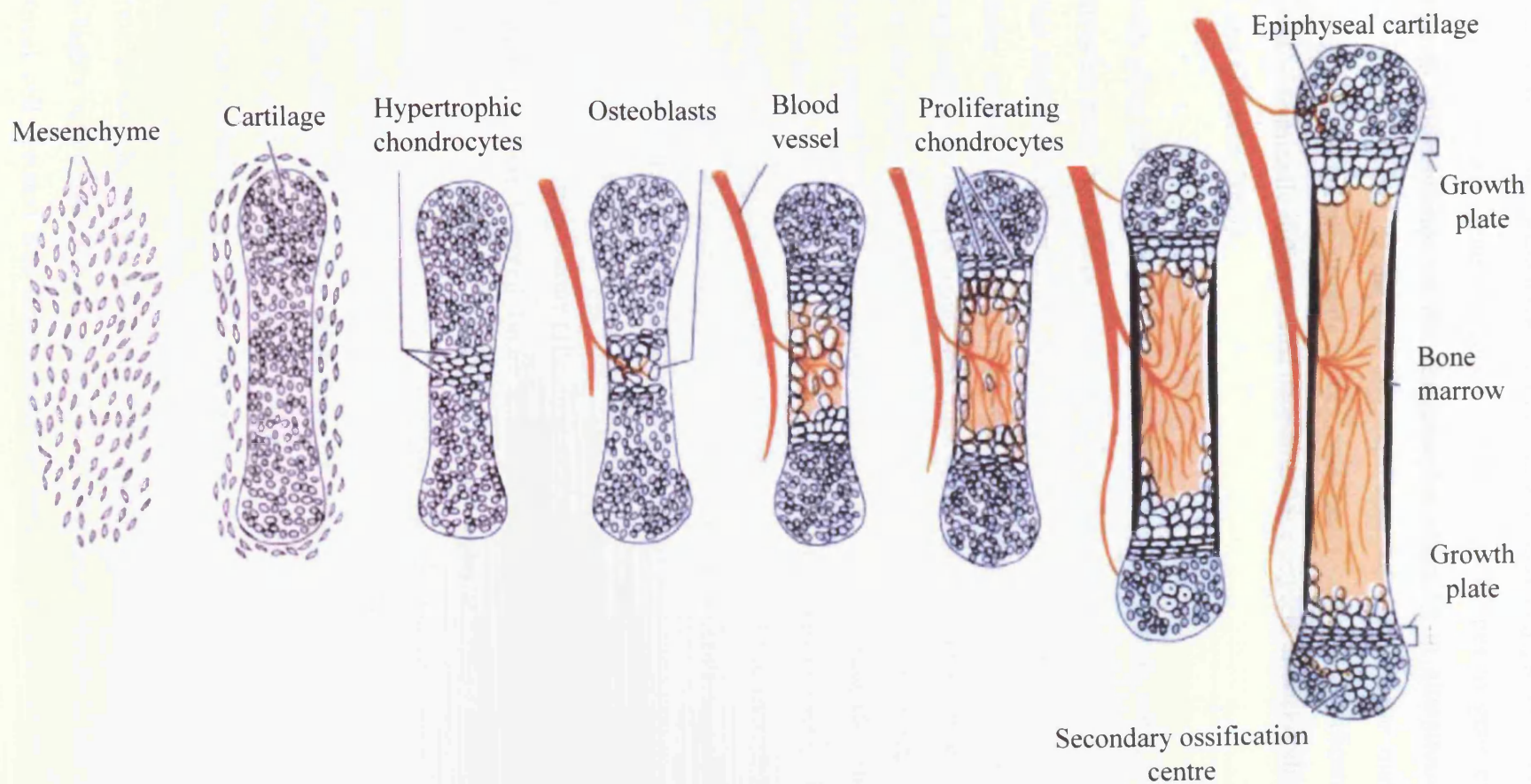


Figure 1.1: Schematic diagram of the process of endochondral bone formation.
 Taken from www.classes.aces.uiuc.edu/ansci312/bone/boneelect.htm.

1.1.2 The Epiphyseal Growth Plate

Longitudinal growth of the skeleton is a tightly regulated process which occurs at the growth plate (figure 1.2), via the mechanism of EO. Locally produced growth factors and systemic hormones act on growth plate chondrocytes triggering changes in gene expression. These events lead to differentiation of the chondrocytes resulting in alterations in chondrocyte phenotype, including size of the cell and expression of extracellular matrix components, secreted enzymes, numerous growth factors, and their receptors. Calcification of the matrix and removal of terminally differentiated chondrocytes complete endochondral bone formation (Ballock and O'Keefe, 2003).

The growth plate can be divided into discrete zones: the resting zone, proliferating zone, prehypertrophic zone, hypertrophic zone and the calcified zone, which contain chondrocytes at different stages of differentiation. The chondrocytes synthesise and are surrounded by an extracellular matrix (ECM), composed of an organised network of macromolecules, comprising collagens and proteoglycans (discussed later). The reserve or resting zone is adjacent to the epiphysis, it contains spherical chondrocytes which are separated by abundant extracellular matrix, these cells exhibit low rates of proliferation (Kember, 1978). In the proliferative zone, cells undergo rapid division forming columns of flattened cells, and matrix synthesis results in longitudinal growth. The chondrocytes of the hypertrophic zone have a cellular volume up to tenfold bigger than those of the proliferative zone. This is the main factor which contributes to longitudinal growth. Hypertrophic chondrocytes are metabolically active cells, with overall matrix synthesis per cell increased approximately three-fold, compared to the proliferative zone (Hunziker et al., 1987). The zone of calcified cartilage is the transitional region between bone and cartilage. Matrix calcification occurs in the longitudinal septae between the columns of chondrocytes and this calcified matrix becomes the scaffolding for bone deposition in the metaphysis. The fate of hypertrophic chondrocytes in this region is subject to contradictory reports. Originally it was believed that the chondrocytes die by apoptosis which may be triggered by the metaphyseal vasculature. Apoptosis of hypertrophic chondrocytes has been proposed to exert effects on the process of endochondral ossification, including intracellular calcium accumulation and release, matrix calcification, matrix resorption, attraction of blood vessels and osteoblast precursors, and stimulation of bone formation (Gibson, 1998). Alternatively it has been suggested that these cells are highly active and may differentiate into osteoblasts (Hunziker and Schenk, 1984). An asymmetrical cell division was demonstrated to take place in an embryonic chick culture

system, one daughter cell dies by apoptosis and the other differentiates into an osteogenic cell (Roach et al., 1995), however, this has not been demonstrated in other species.

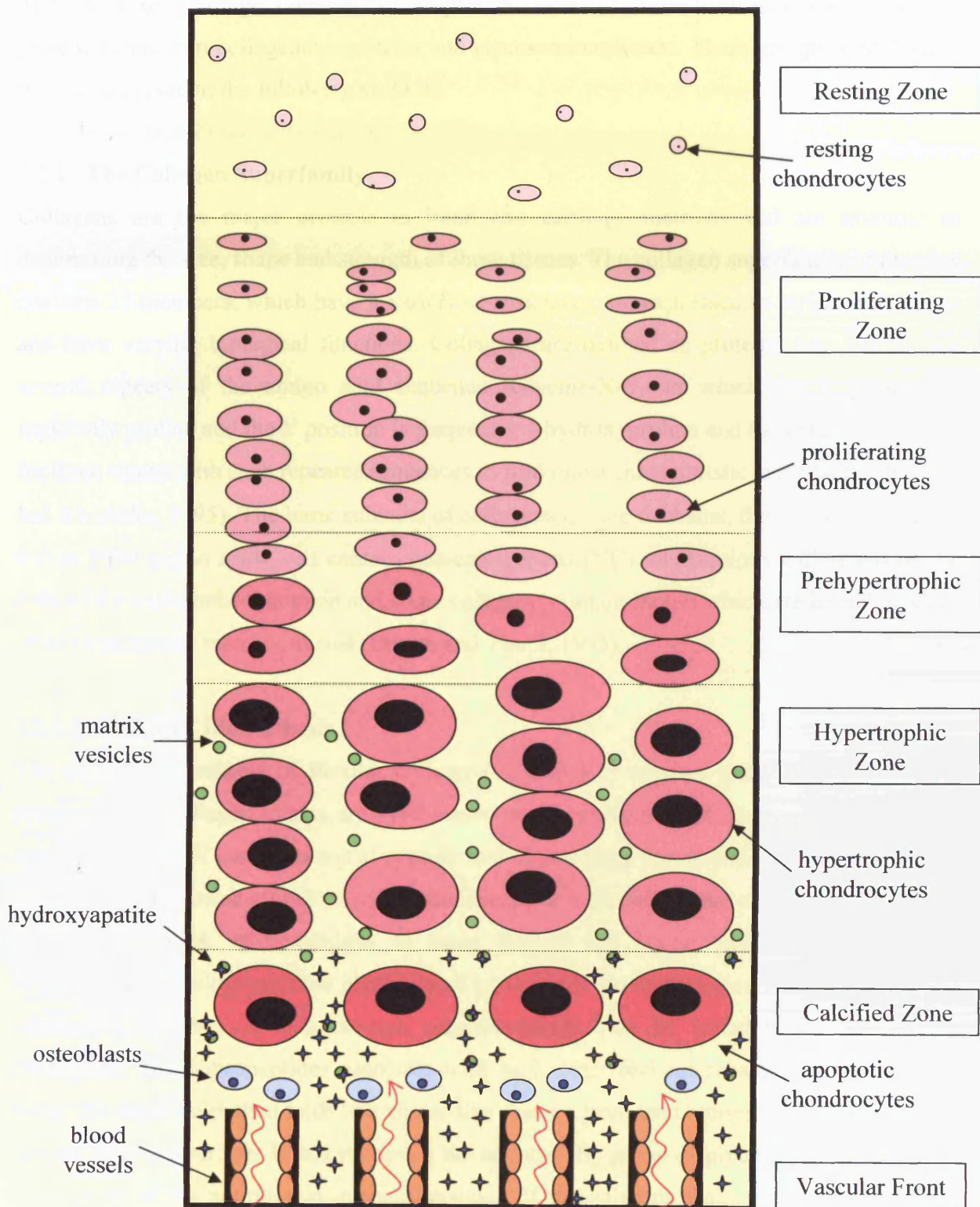


Figure 1.2: A schematic representation of a longitudinal section through the epiphyseal growth plate. Distinct morphological regions and cell types are highlighted.

1.2 Molecular Composition of Hypertrophic and Articular Cartilage

The ECM of cartilage contains a complex network of molecules including collagens, proteoglycans, non-collagenous proteins and glycosaminoglycans. These groups of molecules will be discussed in the following sections.

1.2.1 The Collagen Superfamily

Collagens are the major proteins in bone and cartilage matrices and are essential in determining the size, shape and strength of these tissues. The collagen superfamily of proteins contains 27 members, which have a variety of structures, are expressed in different locations and have varying biological functions. Collagens are defined as proteins that: (a) contain several repeats of the amino acid sequence -Glycine-X-Y- in which the X position is frequently proline and the Y position is frequently 4-hydroxyproline and (b) have the potential for three chains with such repeated sequences to fold into a characteristic triple helix (Prockop and Kivirikko, 1995). The basic subunits of collagens are the α -chains, they vary in size from 600 to 3000 amino acids, can contain non-collagenous (NC) interruptions within and on the ends of the triple helical domain and some collagens contain motifs which are homologous to other extracellular matrix proteins (Brown and Timpl, 1995).

1.2.1.1 Collagen Biosynthesis

The correct biosynthesis of fibrillar collagens (figure 1.3) requires many post-translational events. Pre-procollagen chains are synthesised on the ribosomes of the rough endoplasmic reticulum. They all contain a signal peptide that targets them for secretion into the lumen of the rough endoplasmic reticulum where modifications begin within the cell. After removal of the signal peptide, hydroxylation of some proline and lysine residues occurs. Some hydroxylysine residues are then glycosylated by the addition of galactose with or without the addition of glucose. A mannose-rich oligosaccharide may be added to the C-terminus propeptide. The C-propeptides associate with each other and interchain disulphide bonds form. The triple helix then folds in a zipper-like manner from the C-terminus. The triple helix is stabilised by hydrogen bonds involving the amino (NH) group of glycine and the carboxyl (CO) group of the amino acid in the X position of the adjacent chain. Further stabilisation involves the hydroxyl groups of hydroxyproline residues forming hydrogen bonds through water bridges (Myllyharju and Kivirikko, 2001).

After secretion of the procollagen from the cell, the N and C-terminus propeptides are cleaved by N-proteinases and C-proteinases, respectively. The collagens then self assemble into fibrils. Some lysine and hydroxylysine residues are oxidised into reactive aldehydes by the extracellular enzyme lysyl oxidase. The reactive aldehydes form covalent crosslinks which stabilise the fibrils (Prockop and Kivirikko, 1995).

This process is typical of the fibrillar collagens but many of the non-fibrillar collagens undergo different post-translational processes. Some collagens do not contain propeptides but have large non-collagenous domains at either end of their triple helix, these domains are not removed by proteinases. Other collagen types require the addition of N-linked oligosaccharides or the addition of glycosaminoglycan (GAG) chains. Some collagens such as types XIII and XVII assemble their triple helical domains from the N-terminus to the C-terminus (Myllyharju and Kivirikko, 2001).

The collagen superfamily contains twenty seven members at present, and can be divided into groups based on their molecular structures and the supramolecular assemblies which they adopt (figure 1.4).

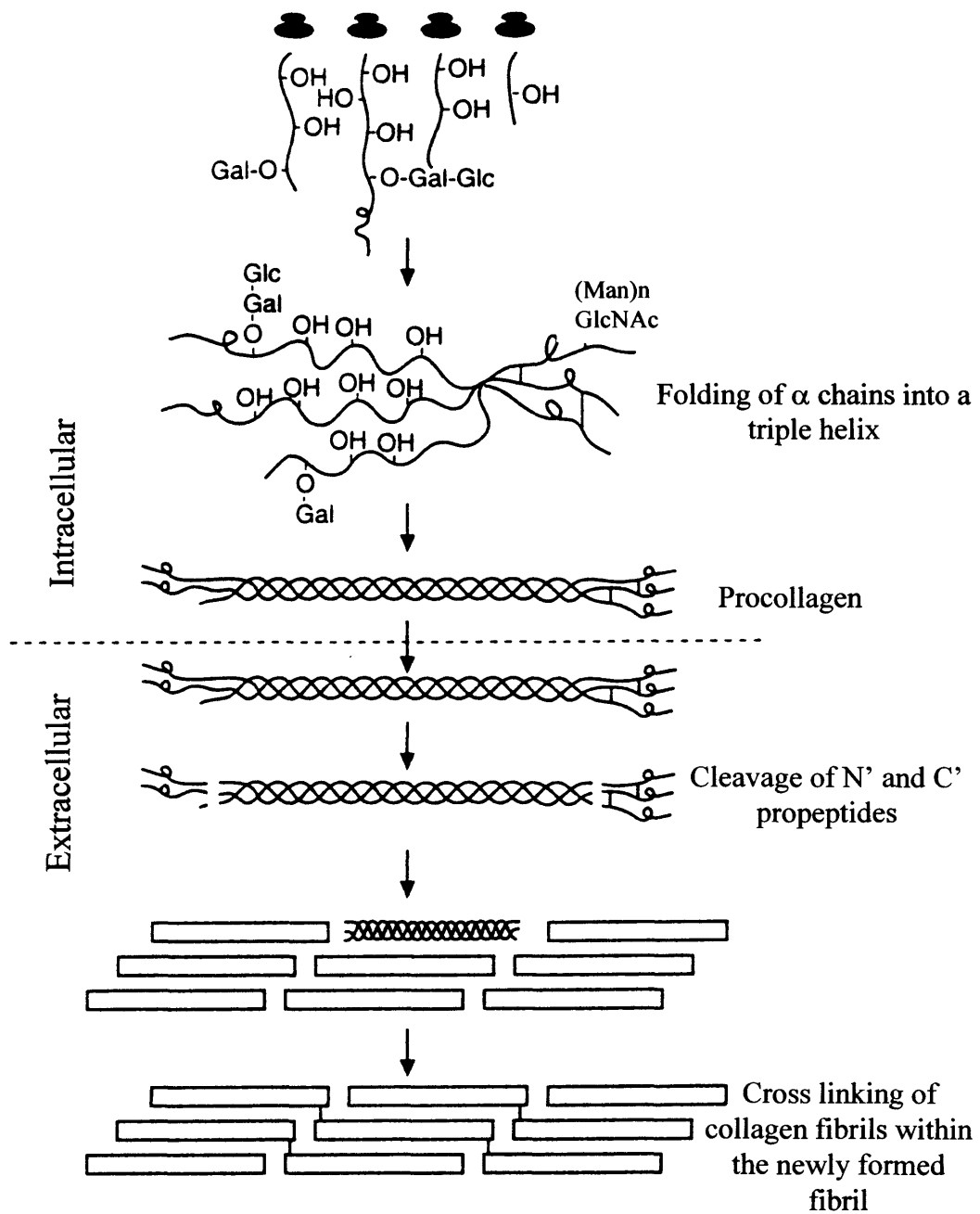


Figure 1.3: Schematic representation of fibrillar collagen biosynthesis.
Adapted from Myllyharju & Kivirikko, 2001.

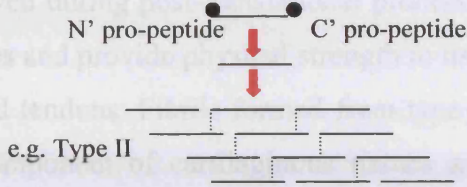

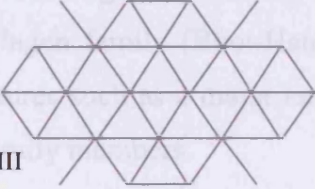

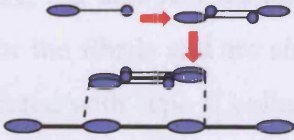
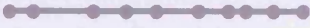
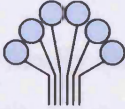
| Collagen Family | Members | Example |
|--------------------------|---|--|
| Fibrillar Collagens | Types I, II, III, V, XI, XXIV, XXVII |  <p>N' pro-peptide C' pro-peptide</p> <p>e.g. Type II</p> |
| FACIT Collagens | Types IX, XII, XIV, XVI, XIX, XX, XXI, XXII |  <p>e.g. Type IX</p> |
| Network Collagens | Types IV, VIII, X |  <p>e.g. Type VIII</p> |
| Membrane Bound Collagens | Types XIII, XVII, XXIII, XXV |  <p>e.g. Type XIII</p> |
| Filamentous Collagens | Types VI, VII |  <p>e.g. Type VI</p> |
| Multiplexins | Types XV, XVIII, XXVI |  <p>e.g. Type XV</p> |
| Others | C1q |  <p>e.g. C1q</p> |

Figure 1.4: A table summarising collagen groups with associated members. An example of a member of each group is illustrated in a schematic diagram.

1.2.1.2 Fibril Forming Collagens

Fibril forming collagens include types I, II, III, V, XI, XXIV and XXVII, they contain around 1000 amino acids in each α -chain in their triple helical domain and assemble into cross-striated fibrils (Kielty and Grant, 2002). Types I, II and III are initially synthesised with N- and C-terminus pro-peptides which are removed during post-translational processing. Type I collagen fibrils are packed into parallel bundles and provide physical strength to tissues which experience extensive forces, such as bone and tendons. Fibrils formed from type II collagen are narrower and are the major collagen component of cartilaginous tissues and vitreous humour. Type III collagen fibrils are prevalent in elastic tissues such as the skin, intestine and aorta. Type V and XI collagens also undergo post-translational processing, but retain an N-terminus globular domain. They are usually found within fibrils formed from collagen types I-III, type V collagen is found in most non-cartilaginous tissues which contain types I and III collagen fibrils, whereas, type XI collagen is found in cartilaginous tissues. Type XXVII collagen has recently been assigned to the fibrillar collagen family (Boot-Handford et al., 2003). However it contains some unusual molecular features such as a major helical domain that is short and interrupted when compared with other family members.

1.2.1.3 Fibril-associated Collagens with Interrupted Triple Helices (FACIT Collagens)

Collagen types IX, XII, XIV, XVI, XIX, XX, XXI and XXII are members of the FACIT family, these collagens are characterised by short triple-helical domains interrupted by non-collagenous sequences (Kielty and Grant, 2002). Types IX, XII and XIV collagens decorate the surface of fibrillar collagens. They organise and anchor the fibrils and are able to interact with other matrix components. Type IX collagen is associated with type II collagen, whereas types XII and XIV collagens are usually associated with type I collagen. Type XVI collagen is broadly distributed and has 11 NC domains, more than all other family members. Type XIX has been localised to many developing embryonic tissues and to specific adult tissues, such as brain.

Type XX collagen has recently been assigned to the FACIT family (Koch et al., 2001), its expression was found in many chick embryo tissues, being most prevalent in corneal epithelium. Collagen type XXI has also been assigned to the FACIT collagens (Chou and Li, 2002), its genomic organisation is similar to that of other FACIT members. Expression of collagen XXI is highest at fetal stages, it is an extracellular component of blood vessel walls and is secreted by smooth-muscle cells.

1.2.1.4 Network Forming Collagens

The family of network forming collagens consists of types IV, VIII and X collagens. Type VIII and X collagens demonstrate structural similarities at nucleotide and amino acid levels, and are approximately half the size of fibrillar collagens (Kielty and Grant, 2002). Type VIII collagen is expressed by endothelial cells and is found in the specialised 'basement membrane' laid down by corneal endothelial cells, Descemet's membrane and in most blood vessels. The hexagonal lattice-like network that it forms is mediated via interactions of its NC1 domain. Recent microscopic analysis of recombinant molecules led to the proposal of a model for collagen VIII assembly, in which four homotrimers form a tetrahedron stabilized by central interacting C-terminus NC1 trimers. Tetrahedrons could then act as building blocks of three-dimensional hexagonal lattices generated by secondary interactions involving terminal and helical sequences (Stephan et al., 2004). Type X collagen is discussed in more detail later.

Type IV collagen contains a large C-terminus non-collagenous domain (NC1) and a short non-collagenous domain at its N-terminus, the N-terminus domain along with a short stretch of the triple helical region is known as the 7S domain (Kielty and Grant, 2002). The triple helical region contains around 20 imperfections in its Gly-X-Y sequence, giving a more flexible molecule. Type IV collagen is found in basement membranes, sheet like structures that are associated with epithelial and endothelial cells. Type IV collagen forms these sheet like assemblies via interactions involving its NC1 and 7S domains.

1.2.1.5 Filamentous Collagens

Type VI and VII collagens are the only members of the filamentous collagens family. Type VI collagen contains a short triple helical domain flanked by large N- and C-terminus globular domains (Kielty and Grant, 2002). Its characteristic extensive filamentous assembly is found in many connective tissues, including skin and cornea. The type VI molecules assemble into dimers in an anti-parallel fashion which aggregate laterally to form disulphide bonded tetramers. Type VI collagen tetramers are the basic unit of beaded filaments or type VI microfibrils. Type VII collagen is found in anchoring fibrils, specialised extracellular structures which anchor basement membranes to the stroma (Kielty and Grant, 2002). Type VII collagen dimers associate laterally in a non-staggered array to form tightly packed fibrous structures. The three armed NC1 domains contain motifs homologous to adhesive proteins, thus are spatially and chemically suitable to interact with basement membrane proteins.

1.2.1.6 Membrane Bound Collagens

Types XIII, XVII, XXIII and XXV collagens are members of the membrane bound collagen family, all containing a hydrophobic trans-membrane segment (Kielty and Grant, 2002). Their short N-terminus region is intracellular while their collagenous regions are situated extracellularly. Membrane-associated collagens are expressed in mesenchymal tissues. Type XIII contains four NC domains, whereas type XVII contains sixteen. Type XVII is a component of anchoring filaments tethering the epithelia via hemidesmosomes to basement membranes. Furin mediated proteolytic processing of type XVII yields a 120 kDa soluble triple-helical extracellular domain of unknown function. It has been suggested that it may influence signal transduction and or cell attachment to the basement membrane during proliferation and differentiation (Hirako et al., 1998). Type XXIII collagen has recently been assigned to this family, after being identified in rat prostate carcinoma cells (Banyard et al., 2003). It shows structural homology with the other members of the family. Type XXV collagen has been linked with Alzheimer's disease amyloid plaques (Hashimoto et al., 2002), as a membrane-tethered component and a secreted extracellular domain.

1.2.1.7 Multiplexin (multiple triple-helix domains and interruptions) Collagens

Types XV and XVIII collagens contain multiple collagenous and non-collagenous domains (Kielty and Grant, 2002). Their tissue distribution is distinct, with type XV collagen being highly expressed in muscle tissues and high levels of XVIII being found in the liver. It has been suggested that both collagens may contribute to the structural and functional integrity of basement membranes. Endostatins derived from the C-terminus of collagens XV and XVIII have been shown to inhibit angiogenesis (Sasaki et al., 2000). Whether these collagens/endostatins have roles in the angiogenesis which occurs in the epiphyseal growth plate is not known. Type XXVI collagen has been characterised and is expressed in the testis and ovary (Sasaki et al., 2000), it was demonstrated to have homologies with types XIII and XXV collagens.

1.2.1.8 Others

Another group within the superfamily has many members containing triple-helical collagenous domains but are not defined as collagens. An example of such a molecule is C1q of complement (Myllyharju and Kivirikko, 2001). The collagenous sequences in these proteins contribute structure. Triple helix formation leads to the alignment of the non-

collagenous subunits, thereby leading to correct functioning. Many of these proteins have roles in immunity.

1.2.1.9 The Cartilage Collagens

Type II collagen is the most abundant collagen in cartilage (Kielty and Grant, 2002). Type II is composed of three identical $\alpha 1(\text{II})$ chains that wind into the characteristic triple helix, type II collagen forms heterotypic fibrils with less abundant type IX and XI collagens (figure 1.5). Type XI collagen integrates into the interior of type II fibrils and type IX associates with the exterior of the fibril. These fibrils form highly ordered arrangements that constitute a regular three-dimensional network throughout the cartilage matrix, providing the ECM with strength and resilience. The fibrils have sites which are available for interaction with other ECM components.

Type IX collagen is a heterotrimer [$\alpha 1(\text{IX})$ $\alpha 2(\text{IX})$ $\alpha 3(\text{IX})$], the three chains are products of three distinct genes (Eyre and Wu, 1995). There are long and short forms of type IX collagen, which differs depending on the presence or absence of a large globular domain (NC4) at the amino terminus of the $\alpha 1$ chain. In the hypertrophic cartilage of the growth plate the short form of type IX collagen is the dominant form whereas in articular cartilage type IX is present mainly in the long form, thus the expression of these different forms is tissue specific and developmentally regulated (Olsen, 1992). The $\alpha 2$ chain of type IX collagen can also bear a chondroitin sulphate chain which allows this collagen to be classified as a proteoglycan. Type XI collagen is a heterotrimer [$\alpha 1(\text{XI})$ $\alpha 2(\text{XI})$ $\alpha 3(\text{XI})$]. The $\alpha 1(\text{XI})$ and $\alpha 2(\text{XI})$ chains are products of separate genes, while the $\alpha 3(\text{XI})$ chain is coded for by the same gene as the $\alpha 1(\text{II})$ chain, but undergoes different post-translational hydroxylation and glycosylation (Burgeson et al., 1982). The α -chains of type XI collagen can participate in the formation of heterotypic molecules with type V collagen (Fichard et al., 1994). Genetic mutations in the genes which code for the different components of the heterotypic fibril, lead to a variety of diseases with different severities (Mundlos and Olsen, 1997). Mutations in the COL2A1, COL9A2 and the COL11A2 gene loci can lead to achondrogenesis type II, multiple epiphyseal dysplasia and a Stickler-like dysplasia, respectively (Horton, 1996).

Type VI collagen microfibrils in cartilage are primarily localised around the chondrocytes in the pericellular capsule known as a chondron (Poole et al., 1988). It is rich in the integrin binding motif, the RGD sequence, and has been demonstrated to bind to the surface of

chondrocytes. Pericellular type VI collagen staining has been shown around the resting and early proliferating chondrocytes of the growth plate, however the staining became progressively diffuse and was virtually absent by the end of the proliferating zone, there was no staining for type VI collagen observed pericellularly around hypertrophic chondrocytes of the growth plate (Sherwin et al., 1999).

1.2.2 Protoglycans

Protoglycans (PGs) are complex molecules which fulfil a variety of biological functions. Their protein cores are substituted with sulphated glycosaminoglycans (GAGs), which can vary in their composition, size and number. Hyalactan and small leucine-rich proteoglycan (decorin) are examples of families of protoglycans. Hyalactan aggregates (figure 1.5a) are formed by multiple protoglycans binding to an extended hyaluronan chain (HA). They bind via a globular binding region on the protein core, the rigidity of the PG-HA bond is increased by the participation of a 40 kDa link protein (figure 1.5b) (Humphreys et al., 1994).

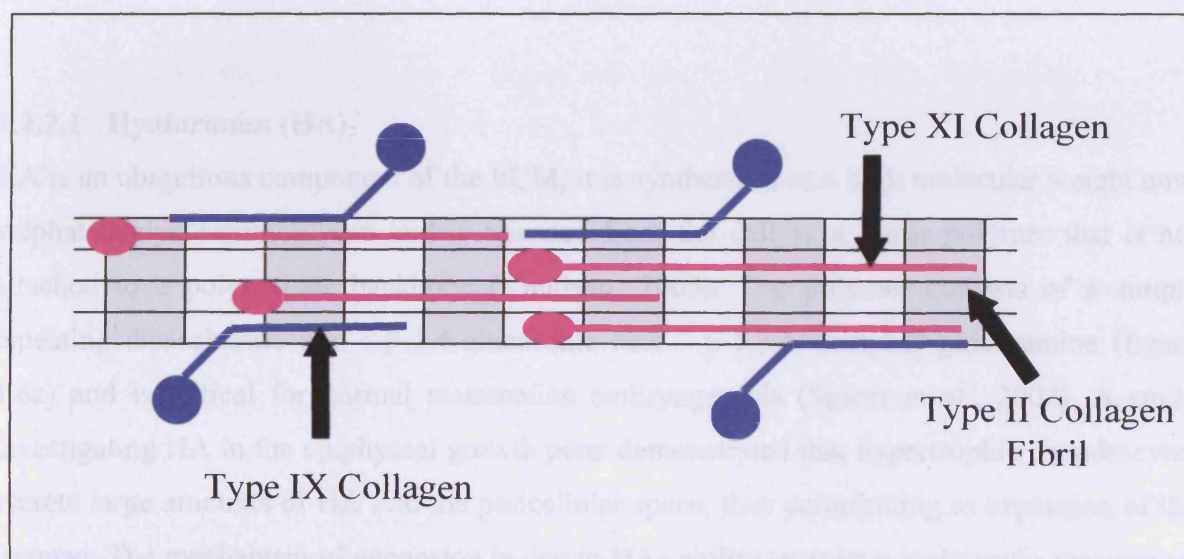


Figure 1.5: Schematic diagram showing the arrangement of collagen molecules in the heterotypic fibrils found in cartilage.

1.2.2.2 Aggrecan

Aggrecan is the predominant protoglycan (PG) found in cartilage ECM and because it forms large multimolecular complexes with hyaluronan it is a member of the hyalactan family. Other family members include versican, perlecan and osteonectin. Aggrecan has a multi-domain protein core of approximately 220 kDa (figure 1.5c) its domains have distinct functional roles. The globular G1 domain is located at the N-terminus and binds non-covalently to hyaluronan (and a stabilising link protein), thereby facilitating the formation of multimolecular aggregates

1.2.2 Proteoglycans

Proteoglycans (PGs) are complex molecules which fulfil a variety of biological functions. Their protein cores are substituted with sulphated glycosaminoglycans (GAGs), which can vary in their composition, size and number. Hyalactans and small leucine rich proteoglycans (discussed later) are examples of families of proteoglycans. Hyalactan aggregates (figure 1.6a) are formed by multiple proteoglycans binding to an extended hyaluronan chain (HA). They bind via a globular binding region on the protein core, the stability of the PG-HA bond is increased by the participation of a 40 kDa link protein (figure 1.6b) (Hardingham et al., 1984).

1.2.2.1 Hyaluronan (HA)

HA is an ubiquitous component of the ECM, it is synthesised as a high molecular weight non-sulphated glycosaminoglycan and is released from the cell as a linear polymer that is not attached to a polypeptide backbone (Knudson, 2003). The polymer consists of a simple repeating disaccharide unit : β -1,4-glucuronic acid - β -1,3-N-acetyl-D-glucosamine (figure 1.6c) and is critical for normal mammalian embryogenesis (Spicer et al., 2002). A study investigating HA in the epiphyseal growth plate demonstrated that hypertrophic chondrocytes secrete large amounts of HA into the pericellular space, thus contributing to expansion of the lacunae. The mechanism of expansion is due to HAs ability to exert a hydrostatic pressure on the surrounding territorial matrix, therefore HA is partially responsible for the interstitial growth of the epiphyseal plate which, in turn, determines the rate of bone elongation (Pavasant et al., 1996). HA is removed from the zone of erosion during the process of EO by osteoprogenitor cells that express CD44 on their surfaces (Pavasant et al., 1994). CD44 is a cell surface transmembrane glycoprotein receptor for HA which mediates both cell-cell and cell-matrix interactions (Knudson, 2003).

1.2.2.2 Aggrecan

Aggrecan is the predominant proteoglycan (PG) found in cartilage ECM and because it forms large multimolecular complexes with hyaluronan it is a member of the hyalactan family. Other family members include versican, brevican and neurocan. Aggrecan has a multi-domain protein core of approximately 220 kDa (figure 1.6d) its domains have distinct functional roles. The globular G1 domain is located at the N-terminus and binds non-covalently to hyaluronan (and a stabilising link protein), thereby facilitating the formation of multimolecular aggregates

comprised of up to 100 monomers (Caterson et al., 2000). A second globular domain G2 is separated from the G1 domain by a short interglobular domain. Adjacent to the G2 domain is a short keratan sulphate attachment domain (KS) and two chondroitin sulphate attachment domains (CS1 and CS2). Over 100 CS and KS chains may be present in the GAG attachment regions. At the C-terminus there is another globular domain termed G3, the function of which remains unclear. Its lectin-like properties suggest the possibility of interaction with other matrix components, though it has also been suggested that it is involved in intracellular trafficking during aggrecan synthesis (Roughley, 2001).

The functional role of aggrecan is dependant on its characteristics, its ability to form multimolecular complexes with hyaluronan and the high content of sulphated GAGs. In cartilage, each aggrecan monomer occupies a large hydrodynamic volume, and when subjected to compressive forces, water is displaced from individual monomers. The swelling of the tissue is dissipated readily when the compressive forces are removed and the water molecules are drawn back into the tissue (Iozzo, 1998). Aggrecan shows a similar distribution in the growth plate to type II collagen. The highest rate of expression being seen in chondrocytes of the proliferating and upper hypertrophic zones (Mundlos, 1994). As the chondrocytes undergo hypertrophy aggrecan expression is down regulated (Wai et al., 1998). Other hyalactan family members have not been linked to the growth plate.

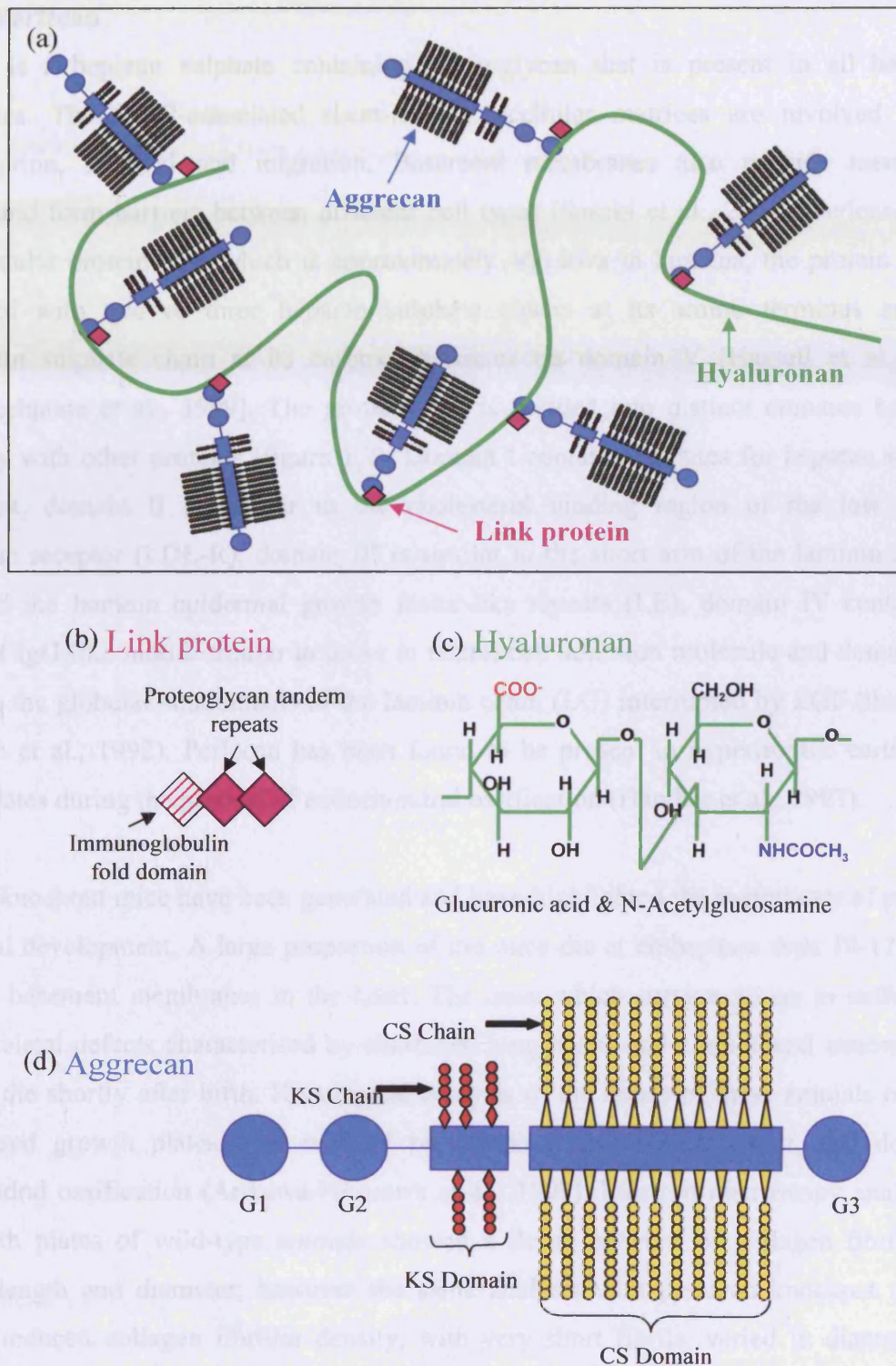


Figure 1.6: (a) Schematic illustration of the high molecular weight proteoglycan aggregate found in cartilage and its component parts. (b) Link protein with domains highlighted. (c) Hyaluronan repeating disaccharide. (d) Aggrecan monomer, showing different domains and sites of GAG attachment.

1.2.2.3 Perlecan

Perlecan is a heparan sulphate containing proteoglycan that is present in all basement membranes. These cell-associated sheet-like extracellular matrices are involved in cell differentiation, survival and migration. Basement membranes also provide mechanical stability and form barriers between different cell types (Sasaki et al., 2004). Perlecan has a large modular protein core which is approximately 466 kDa in humans, the protein core is substituted with two or three heparan sulphate chains at its amino terminus and one chondroitin sulphate chain at its carboxy terminus on domain V (Hassell et al., 2003; Tapanadechpone et al., 1999). The protein core is divided into distinct domains based on homology with other proteins (figure 1.7). Domain I contains the sites for heparan sulphate attachment, domain II is similar to the cholesterol binding region of the low density lipoprotein receptor (LDL-R), domain III is similar to the short arm of the laminin A (LA) chain and the laminin epidermal growth factor-like repeats (LE), domain IV contains 21 repeats of IgG-like motifs similar to those in neural cell adhesion molecule and domain V is similar to the globular subdomains of the laminin chain (LG) interrupted by EGF-like motifs (Murdoch et al., 1992). Perlecan has been found to be present in hypertrophic cartilage of growth plates during the process of endochondral ossification (Handler et al., 1997).

Perlecan knockout mice have been generated and have highlighted the importance of perlecan in skeletal development. A large proportion of the mice die at embryonic days 10-12 due to defective basement membranes in the heart. The mice which survive go on to suffer from severe skeletal defects characterised by shortened long bones and craniofacial abnormalities and then die shortly after birth. Histological analysis of the bones of these animals revealed disorganised growth plates with reduced proliferation and differentiation, and defective endochondral ossification (Arikawa-Hirasawa et al., 1999). Electron microscopy analysis of the growth plates of wild-type animals showed a dense network of collagen fibrils with uniform length and diameter, however the same analysis with perlecan knockout animals revealed reduced collagen fibrillar density, with very short fibrils, varied in diameter and lacking a dense network. This has led to the suggestion that perlecan may have a special function in maintaining the cartilage ECM, possibly by being involved in the storage, stability, or inactivation of MMPs within the growth plate matrix (Gustafsson et al., 2003).

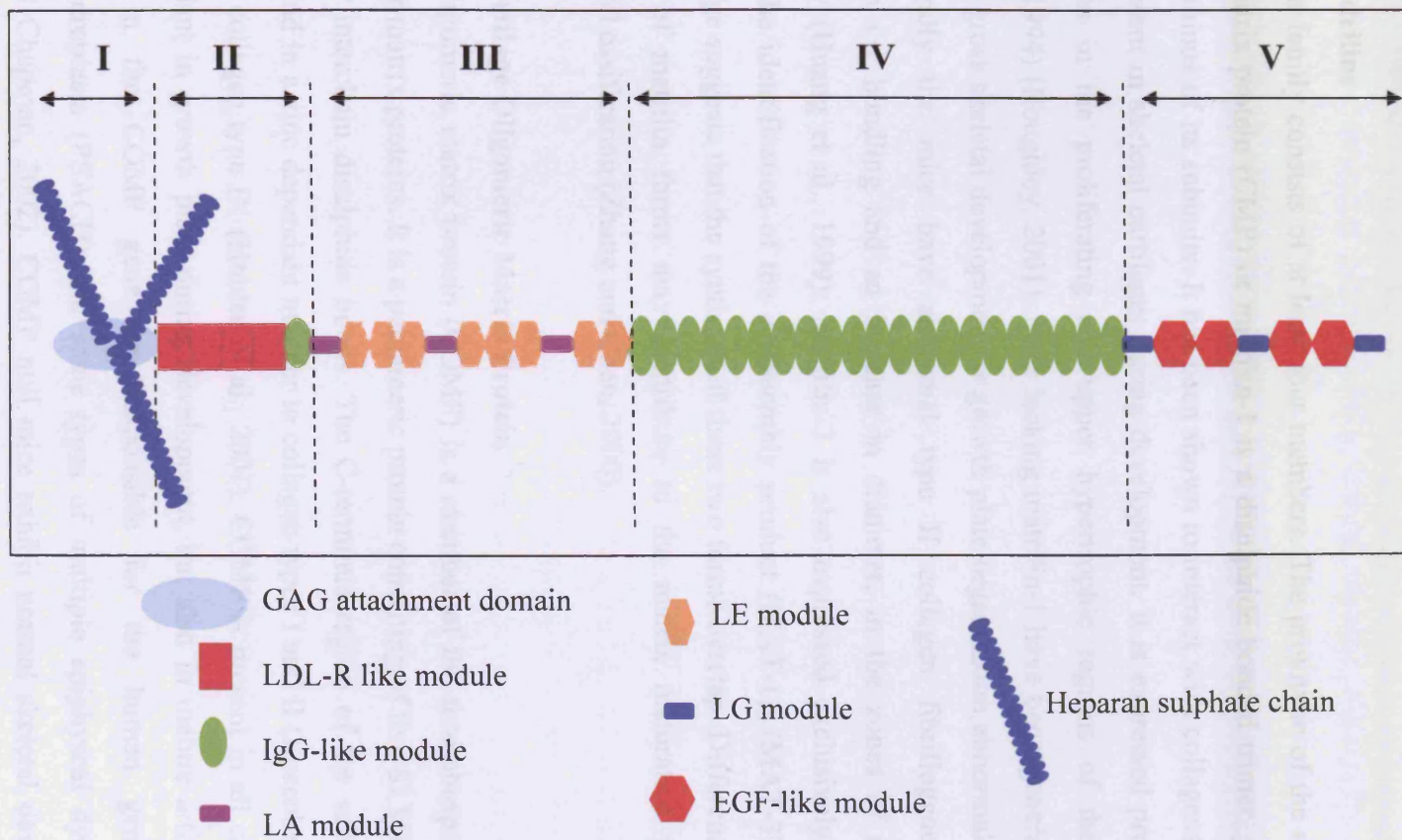


Figure 1.7: Schematic illustration of the modular protein core of the heparan sulphate proteoglycan perlecan (adapted from Jiang and Couchman, 2003).

1.2.3 Other ECM Components

The extracellular matrix of cartilage contains protein components, which are neither collagens nor proteoglycans. Some examples which are relevant to development and growth plate are described below.

1.2.3.1 Matrilins

The matrilin family consists of at least four members. The prototype of the matrilin family, cartilage matrix protein (CMP) or matrilin-1 is a disulphide bonded trimer, joined near the carboxy terminus of its subunits. It has been shown to interact with collagens and aggrecan. CMP is present in skeletal cartilages during development. It is expressed predominantly by chondrocytes in the proliferating and upper hypertrophic regions of the growth plate (Mundlos, 1994) (Roughley, 2001). Mice lacking matrilin-1 have been generated and do not display any gross skeletal development or growth plate organisation abnormalities. However, ultrastructurally the mice have abnormal type II collagen fibrillogenesis and fibril organisation i.e. bundling and an increase in diameter, in the zones of maturation and hypertrophy (Huang et al., 1999). Matrilin-3 is also expressed exclusively in developing cartilage. The identification of the co-assembly product (MAT-1)₂ (MAT-3)₂ from growth plate cartilage suggests that the synthesis of these two forms overlap. Difference in the spatial expression of matrilin forms may contribute to the matrix maturation process during endochondral ossification (Zhang and Chen, 2000).

1.2.3.2 Cartilage Oligomeric Matrix Protein

Cartilage oligomeric matrix protein (COMP) is a member of the thrombospondin family of extracellular matrix proteins. It is a pentameric protein consisting of five 87 kDa subunits held together by interchain disulphide bonds. The C-terminus region of the subunits has been shown to bind in a zinc dependant manner to collagen types I and II (Rosenberg et al., 1998) and also to collagen type IX (Holden et al., 2001). COMP is present in all cartilages, being most abundant in growth plate during development, but also in mature articular cartilage. Mutations in the COMP gene are responsible for the human genetic disorders pseudochondroplasia (PSACH) and some types of multiple epiphyseal dysplasia (MED) (Briggs and Chapman, 2002). COMP null mice exhibit normal skeletal development, and show no anatomical, histological or ultrastructural abnormalities and show no signs of PSACH or MED. These results suggest that mechanisms such as, folding defects or

extracellular assembly abnormalities due to dysfunctional mutated COMP, cause the phenotype in PSACH and MED, not the reduced amount of COMP (Svensson et al., 2002).

1.3 Type X Collagen

Type X collagen is a member of the network forming collagen family. It is a homotrimer comprising three $\alpha 1(X)$ chains (figure 1.8). It has a short triple helical region, compared to the major fibrillar collagens found in cartilage (type II collagen) and bone (type I collagen). This triple helical region is flanked by two non-collagenous (NC) domains, NC2 at the amino terminus and a much larger NC1 at the carboxyl terminus.

Discovery of type X collagen occurred simultaneously by two groups in the early 1980's (Gibson et al., 1982; Gibson et al., 1981; Schmid and Linsenmayer, 1983). Collagen type X was isolated from culture medium of chick chondrocytes undergoing hypertrophy and was described as a short chain (SC) collagen (Schmid and Linsenmayer, 1983). The molecular weight of the native molecule was described as 59 kDa, which reduced to 45 kDa after limited pepsin digestion. The 45 kDa form was identified as being collagenous, while the 59 kDa form also had non-collagenous regions. A low molecular weight collagen of the same size and characteristics was also described by another group of scientists studying collagen synthesis by chick sternal chondrocytes maintained in long term culture in collagen gels, they named their molecule G collagen (Gibson et al., 1982; Gibson et al., 1981). The name type X collagen was introduced shortly after in a paper which described the synthesis of type X collagen to occur almost exclusively in the cartilaginous zone of hypertrophying chondrocytes within the developing long bones (Kielty et al., 1985).

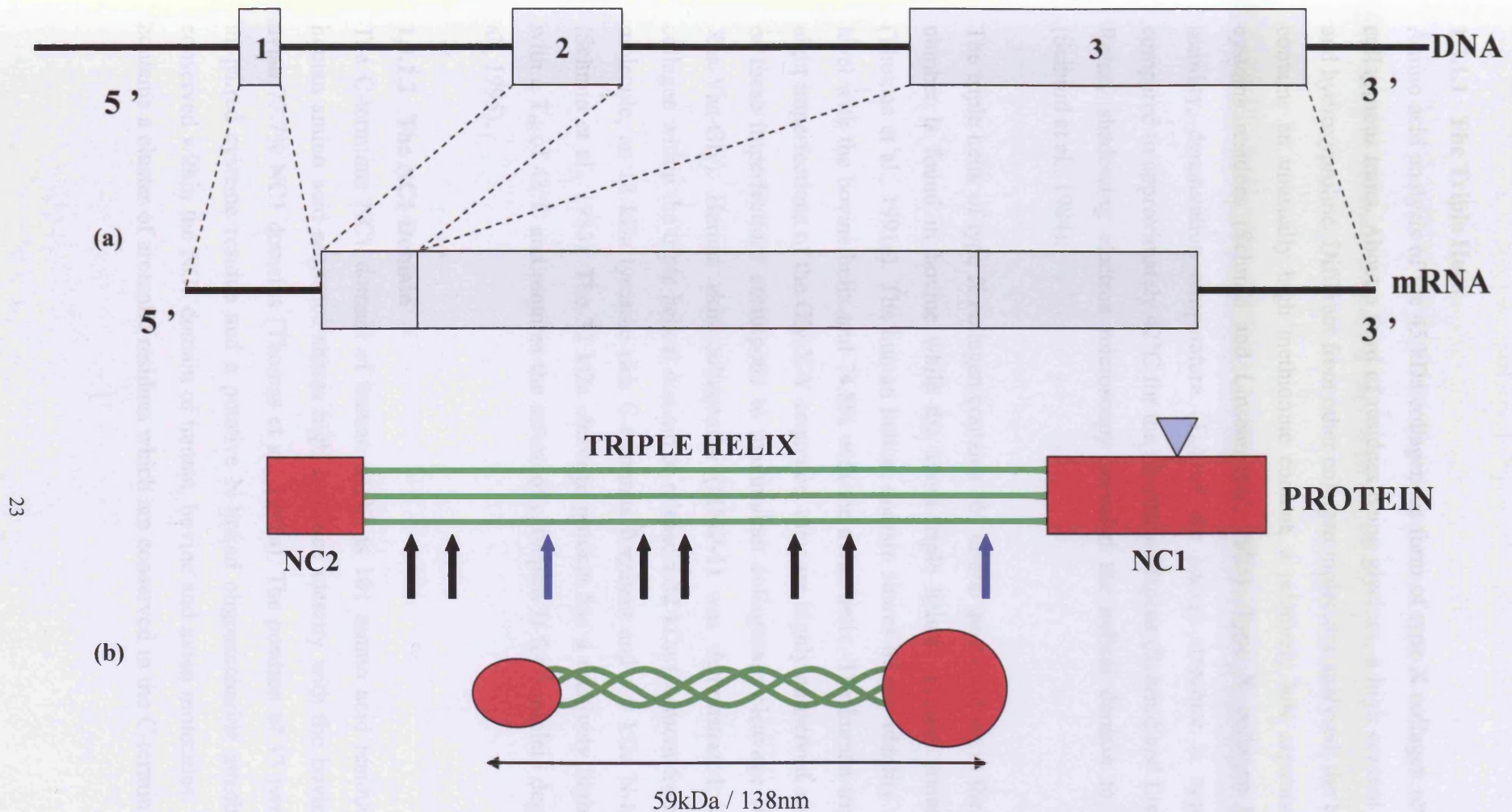


Figure 1.8: Schematic representation of the collagen X gene (COL10A1), exons are labelled 1, 2 and 3, messenger RNA and protein. Protein domains are labelled, NC2, triple helix and NC1. Arrows underneath the helical region represent disruptions in the Glycine-X-Y repeat sequence, and blue arrows are the sites for collagenase cleavage. A light blue triangle on the NC1 domain represents a possible oligosaccharide attachment region.

1.3.1 Three Distinct Domains of Type X Collagen: the triple helix, NC1 and NC2

1.3.1.1 The Triple Helix

Amino acid analysis of the 45 kDa collagenous form of type X collagen revealed the typical collagenous traits. About a third of residues being glycines, a high content of hydroxylysine and hydroxyproline. Different from other collagen molecules analysed, the type X triple helix contains an unusually high methionine content, a relatively low arginine content and no cysteine residues (Schmid and Linsenmayer, 1983). Type X collagen has high thermal stability, denaturation temperature (T_m) of the helical structure is approximately 47°C compared to approximately 42°C for the fibrillar collagens (Schmid and Linsenmayer, 1984). Rotary shadowing electron microscopy revealed the helical domain to be a 138nm rod (Schmid et al., 1984).

The triple helix of type X collagen contains 463 amino acid residues in the human, the same number is found in bovine while the avian triple helical domain contains 460 residues (Thomas et al., 1991a). The human helical domain shares 86.6% identity at the amino acid level with the bovine helix and 74.8% with the avian helix. The human triple helix contains eight imperfections of the Gly-X-Y sequence, they are highly conserved across species. Two of these imperfections correspond to mammalian collagenase cleavage sites (Gly-Ile-Yaa-Xaa-Yaa-Gly). Human skin collagenase (MMP-1) was demonstrated to cleave type X collagen within the triple helical domain to release a 32 kDa fragment from the centre of the molecule, an 18 kDa tyrosine rich C-terminus fragment and a 9 kDa N-terminus fragment (Schmid et al., 1986). The 32 kDa cleavage product has a relatively high thermal stability with a T_m of 43°C and requires the action of cathepsin B for complete degradation (Sires et al., 1995).

1.3.1.2 The NC1 Domain

The C-terminus NC1 domain of human $\alpha 1(X)$ is 161 amino acid residues in length. The human amino acid sequence shares high sequence identity with the bovine 89.4% and the avian 77.7% NC1 domains (Thomas et al., 1991a). The position of 13 tyrosine residues, an un-paired cysteine residue and a putative N-linked oligosaccharide attachment site are all conserved within the NC1 domain of human, bovine and avian molecules. The NC1 domain contains a cluster of aromatic residues which are conserved in the C-termini of collagen VIII

and in the collagen like complement factor C1q. This cluster is part of a larger region of 130 amino acids which displays a hydrophilicity profile very similar to that of the C-terminus of type II collagen (Brass et al., 1992). This conserved region probably causes the trimerisation of the NC1 domain, which in turn leads to the association and alignment of the $\alpha 1(X)$ chains. The NC1 domain forms an exceptionally stable trimer without any disulphide bonds, which is only dissociated after heat denaturation at 100°C (Zhang and Chen, 1999).

The crystal structure of the human collagen X NC1 trimer has been resolved revealing some interesting features (figure 1.9). The NC1 domain is a trimer of ten-stranded β sandwich subunits. A cluster of four calcium ions buried inside the apex of the NC1 trimer interact with aspartic acid residues, the interaction of the protein loops with the calcium ions is likely to contribute significantly to the stability of the NC1 trimer. The molecular surface of the NC1 trimer contains three strips, consisting of eight partially exposed aromatic residues which creates a hydrophobic surface patch involved in the higher order association of type X collagen trimers (Bogin et al., 2002).

The NC1 domain has been demonstrated to be involved in mediating cell-adhesion properties of type X collagen, particularly to $\alpha 2\beta 1$ integrin expressing cells. The intracellular-extracellular connection that the NC1 domain could mediate between the hypertrophic chondrocytes and the ECM may potentially have regulatory roles during the process of EO (Luckman et al., 2003). Thus, the NC1 domain is crucial for the assembly of type X collagen molecules and hence crucial for the functions of type X collagen.

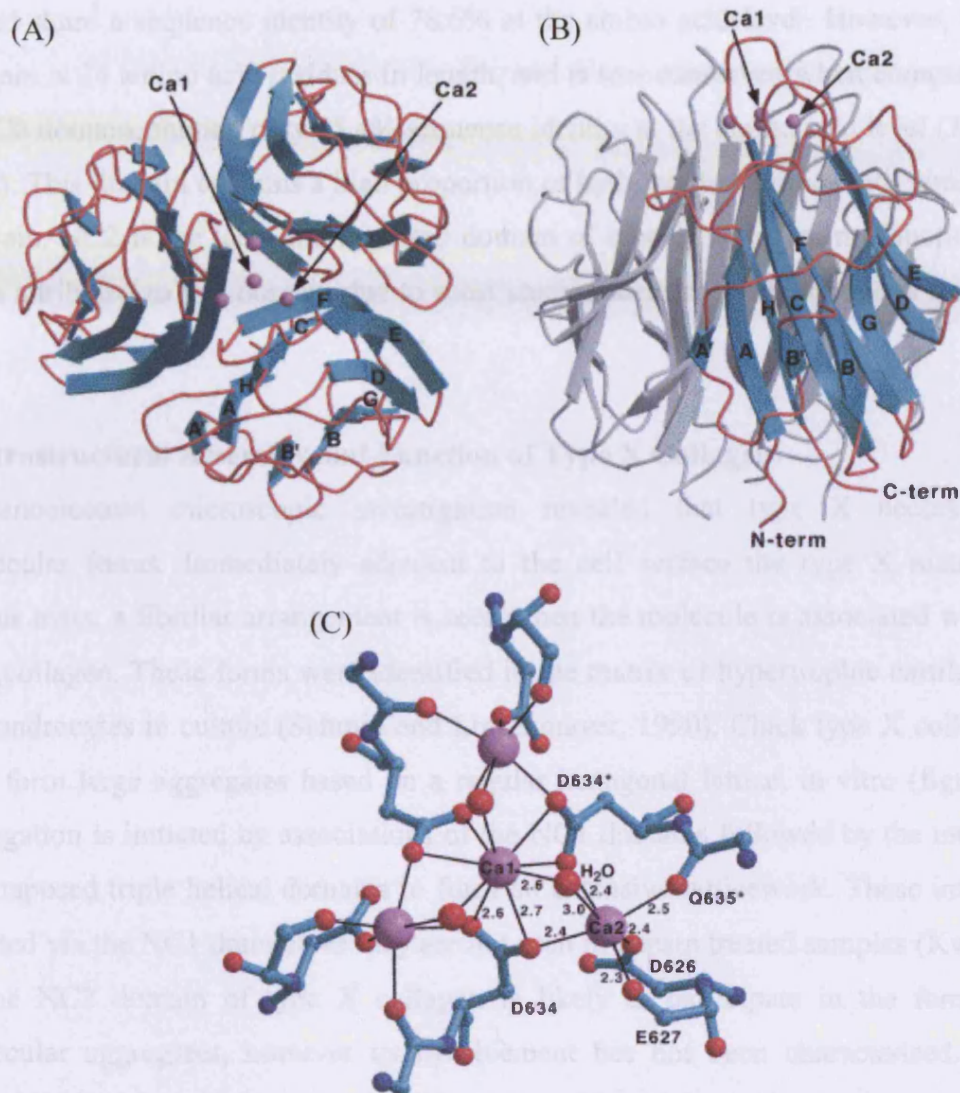


Figure 1.9: Structure of the collagen X NC1 trimer and the Ca^{2+} cluster (taken from Bogin et al., 2002).

(A) Cartoon representation of the NC1 trimer viewed down the crystallographic 3-fold axis. Beta strands are labelled A, A', B, B', C-H and calcium ions are represented as purple spheres.

(B) As in (A) but rotated 90° about the horizontal axis.

(C) Ca^{2+} ions and water molecules are represented as large purple and small red spheres, respectively. Ca1 is situated on the 3-fold symmetry axis of the collagen X NC1 trimer. Residues coordinating the Ca^{2+} ions are shown as ball and stick models and are labelled.

1.3.1.3 The NC2 Domain

The N-terminus NC2 domain of human and bovine $\alpha 1(X)$ are both 38 amino acid residues in length, and share a sequence identity of 78.6% at the amino acid level. However, the avian NC2 domain is 34 amino acid residues in length, and is less conserved when compared to the human NC2 domain, sharing only 55.4% sequence identity at the amino acid level (Thomas et al., 1991a). This domain contains a high proportion of hydrophobic amino acids similar to the NC1 domain. NC2 is the least characterised domain of type X collagen, no functional roles have been attributed to this domain due to most studies focusing their attentions on the NC1 domain.

1.3.2 Ultrastructural Assembly and Function of Type X Collagen

An immunoelectron microscopic investigation revealed that type X occurs in two supramolecular forms. Immediately adjacent to the cell surface the type X matrix forms filamentous mats, a fibrillar arrangement is seen when the molecule is associated with fibrils of type II collagen. These forms were identified in the matrix of hypertrophic cartilage tissue and of chondrocytes in culture (Schmid and Linsenmayer, 1990). Chick type X collagen was shown to form large aggregates based on a regular hexagonal lattice, in vitro (figure 1.10). The aggregation is initiated by associations of the NC1 domains followed by the interactions of the juxtaposed triple helical domains to form an extensive latticework. These interactions are mediated via the NC1 domain, as they are not seen in pepsin treated samples (Kwan et al., 1991). The NC2 domain of type X collagen is likely to participate in the formation of supramolecular aggregates, however its involvement has not been characterised. Type X collagen is similar to collagen type VIII in sequence and in protein structure. They have almost identical triple helical domains containing eight imperfections in the Glycine-X-Y repeat structure (Yamaguchi et al., 1989). Type VIII collagen provides an open porous structure in Descemet's membrane. It has been suggested that type X collagen may have a comparable function, providing an open temporary matrix permissive to vascular invasion and mineralisation (Sutmuller et al., 1997). Type X collagen may function as a scaffold preventing collapse of the matrix, as the proteoglycans and collagen II are degraded in the hypertrophic region of growth plate cartilage.

Despite being initially described 20 years ago, attributing a precise functional role for type X collagen has proven elusive. Due to its restricted distribution to the hypertrophic zone of the growth plate, the role of type X collagen in the process of endochondral ossification is of

particular interest. It has been proposed that type X collagen may be degraded more readily than type II collagen, since type X has two sites for vertebrate collagenase compared to the one site in type II collagen, thus assisting vascular invasion. Another possibility is that type X collagen may be involved in matrix calcification since it appears before the onset of mineralisation.

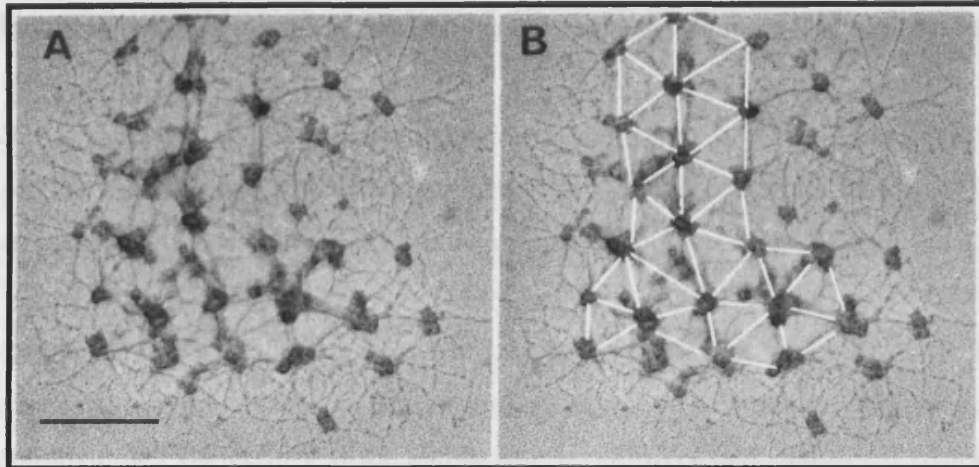


Figure 1.10: Rotary shadowing electron micrographs of the extended network of type X collagen aggregates. (A) Regularly spaced nodules of aggregated NC1 domains are interconnected with structures formed via interactions between adjacent triple helices. (B) The hexagonal nature of the type X collagen lattice is highlighted in this micrograph. Bar = 200nm. Figure taken from Kwan et al., 1991.

1.3.3 The Type X Collagen Gene

The type X collagen gene has been well characterised in a number of species, analysis of the nucleotide sequence has revealed homology across species, with all species studied sharing the same genomic organisation containing three exons (figure 1.8a). The chicken type X collagen gene was the first to be analysed, exon 1 97 basepairs (bp), codes for most of the 5'-untranslated region (UTR) of the mRNA, exon 2 (159bp) codes for the signal peptide and a short non-triple-helical domain (NC2), while exon 3 (2136bp) contains the coding region of the entire triple helix, the large non-triple-helical carboxyl domain (NC1) and the 3'-UTR (LuValle et al., 1988). This exon structure is unusual when compared to other known vertebrate collagen genes. The fibrillar collagen genes (types I, II, III, V and XI) are large containing around 50 exons and have a highly conserved exon structure in which the size of the exons coding for the triple helical domain are related to 54bp, (Gly-X-Y)₆.

The complete primary structure of the bovine $\alpha 1(X)$ collagen chain was later determined. The primary translation products of both bovine and chick type X collagen are 674 amino acids in length and there is 73% identity at the amino acid level. Sequence analyses revealed that the greatest degree of identity between the two species occurs within the triple helical domain and the NC1 domain, whereas the identity within the NC2 domain is markedly lower (Thomas et al., 1991b).

The mouse type X collagen gene has been mapped to chromosome 10 (Apte et al., 1992), and the genomic organisation is the same as chick and bovine (Elima et al., 1993); (Apte and Olsen, 1993). The human collagen X gene (COL10A1) has been assigned to the distal end of the long arm of chromosome 6 at the locus 6q21-6q22.3 (Thomas et al., 1991a); (Apte et al., 1991). The full length cDNA sequence of human collagen X was determined, it revealed that the genomic organisation was highly homologous to the chicken and mouse (Reichenberger et al., 1992). Recent sequence analysis of the porcine COL10A1 gene revealed strong evolutionary conservation of both the gene structure and amino acid sequence (Madsen et al., 2003).

1.3.4 Type X Collagen Localisation other than Growth Plate

Despite the restricted expression of type X collagen to hypertrophic chondrocytes of the growth plate, it has previously been immunolocalised to the surface of human, pig and rat articular cartilage, where it is said to be a component of normal articular cartilage (Rucklidge et al., 1996). There are also reports suggesting that there is small amounts of type X collagen in the proliferating zone of the growth plate (Jacenko et al., 2001).

Type X collagen was demonstrated to be expressed in fracture repair and in human osteoarthritic articular cartilage. Experimental fractures were created in the chicken humerus and type X collagen synthesis occurred in the fracture callus primarily within regions of the callus composed of hypertrophic cells, where matrix was undergoing vascularisation and mineralisation (Grant et al., 1987). This indicates collagen X is involved in new bone formation, as well as being involved in bone formation in development and during growth. Synthesis and extracellular deposition of type X collagen by hypertrophic cells and chondrocyte clusters in the middle zone of osteoarthritic articular cartilage was demonstrated immuno-histologically. Type X collagen synthesis was also demonstrated in suspension cultures of freshly isolated chondrocytes from osteoarthritic cartilage by SDS-PAGE and by immunoprecipitation with a specific antibody for human type X collagen (von der Mark et al., 1992). Type X collagen may be involved in the pathology of osteoarthritis, when regions of articular cartilage are calcified.

Type X collagen has more recently been localised to other regions. It has been found in the mineralised fibrocartilage at the ligament-bone interface of the bovine medial collateral ligament (Niyibizi et al., 1996) and in the mineralised fibrocartilage of the bovine Achilles tendon-calcaneus interface (Fukuta et al., 1998). The intervertebral discs of mature Beagle dogs have also been used to study type X collagen. The vertebral endplate was the predominant site of type X collagen expression, but some animals also had expression in the nucleus pulposus and in the annulus fibrosus (Lammi et al., 1998). In a study involving human intervertebral discs the presence of type X collagen was linked with disc degeneration (Roberts et al., 1998). Knee menisci of healthy and osteoarthritic rabbits and humans have also been shown to contain type X collagen (Bluteau et al., 1999). In general, expression of type X collagen outside of the hypertrophic zone of the growth plate may be part of a pathological process.

1.3.5 Schmid Metaphyseal Chondrodysplasia (SMCD)

SMCD is a relatively mild autosomal dominant disorder of the osseous skeleton resulting from growth plate cartilage abnormalities (Chan and Jacenko, 1998). The SMCD phenotype is variable and symptoms include short stature, affected spine, pelvis and long bones, coxa vara which is a reduction in the angle between the femoral neck and bone shaft and a waddling gait. Intelligence and life expectancy are unaffected by the disorder.

The link was made between SMCD and the COL10A1 gene when a 13 base pair deletion was discovered in a large Mormon kindred affected by SMCD. The mutation resulted in a frameshift which altered the C-terminus 60 amino acids of the $\alpha 1(X)$ chain, a region of the protein which is highly conserved across species. The effect of the 13 base pair deletion in this family is likely to prevent association of the mutant polypeptide during trimer formation, causing a reduction in the amount of normal type X collagen which can be synthesised. The identification of this mutation supports a role for type X collagen in endochondral ossification (Warman et al., 1993). Growth plate cartilage from SMCD patients was used to analyse type X collagen. The patient studied was heterozygous and had a premature termination mutation in the NC1 domain (Y632X). In direct analysis of growth plate cartilage tissue it was demonstrated that only the normal allele was expressed. The inability to detect mutant mRNA or mutant type X collagen protein indicated that in the patient in question, a functionally null $\alpha 1(X)$ allele leading to haploinsufficiency was the molecular basis causing SMCD (Chan et al., 1998). The proof reading machinery of the cell is likely to rapidly degrade mRNA encoding premature termination codons. Degradation of mutated mRNAs introducing premature termination codons is termed nonsense-mediated decay (NMD), a recent study found that cartilage specific NMD is an important molecular cause of SMCD (Bateman et al., 2003).

At present, around 30 mutations have been discovered in unrelated SMCD patients. Interestingly, the mutations defined include amino acid substitutions, nonsense mutations and deletions all map to the C-terminus NC1 domain. The only exception to this has been the discovery of two missense mutations found at the junction of the signal sequence and the N-terminus globular domain, of two unrelated Japanese SMCD patients (Ikegawa et al., 1997). These mutations support the haploinsufficiency theory, ineffective cleavage of the signal

peptide could impair translocation of type X collagen to the endoplasmic reticulum and subsequently secretion from the cell into the matrix.

Haploinsufficiency may not be the only mechanism underlying SMCD, clustering of both point and frameshift mutations in the NC1 domain of type X collagen contradicts this. In haploinsufficiency one would expect to find SMCD causing frameshift mutations to be randomly distributed throughout the gene. The non-random clustering of SMCD mutations in the NC1 domain is more consistent with a mechanism involving dominant interference in which the mutant chains retain the ability to trimerise (Marks et al., 1999). Confirmation of the dominant interference hypothesis came when it was found that mutant type X chains are able to form homotrimers capable of nucleating triple helix formation to form a thermally stable triple helix. The mutant chains are also able to co-assemble with wild type chains to form heterotrimers. Altered conformation and stability of these proteins could affect their secretion, expression, assembly and their interactions with other extracellular matrix proteins outside the cell (McLaughlin et al., 1999).

1.3.6 Type X Collagen Transgenic and Knockout Mice

A great deal has been learned from mice carrying spontaneous or experimentally induced mutations in extracellular matrix genes. These mouse models are of great interest not only for understanding the causes of ECM-related diseases in humans but may also allow the development of diagnostic tools. These mice have also increased our knowledge about pathogenetic mechanisms leading to ECM-dependant diseases and allowed researchers to uncover new and unexpected functions of ECM proteins. On the other hand, some mutations in mice result in much milder phenotypes than in humans, demonstrating the limitations of transgenic mouse models (Aszodi et al., 1998). Studies involving type X collagen transgenic and knock-out mice have proved inconclusive with different groups reporting variable findings.

1.3.6.1 Transgenic Type X Collagen Mice

Transgenic mice with a dominant negative mutation in collagen X were generated to test the role of collagen X in skeletal morphogenesis. Transgene constructs contained chicken $\alpha 1(X)$ cDNA with in-frame deletions within the triple helical domain of collagen X, removing either 21 or 293 amino acid residues, transgene expression was driven by appropriate chicken $\alpha 1(X)$

promoter and upstream regulatory elements. Given the high degree of homology between chicken and mouse $\alpha 1(X)$ carboxyl domains the truncated chicken polypeptides competed with endogenous mouse chains for assembly, and thus interfered with triple helical folding of trimers. Expression of the collagen X transgene constructs in mouse hypertrophic cartilage resulted in 14 transgenic lines with similar skeletal and growth abnormalities. Initially transgenic pups were indistinguishable from one another. At around post natal day 16-17, 15-20% of transgenic mice developed hunching of the back, gradual hind limb paresis, respiratory problems and died within 4 days. Dwarfism with varying severity was seen in 80% of transgenic mice. Histological analysis of the mice revealed abnormalities in growth plates, bony trabeculae and bone marrow of all tissues undergoing endochondral ossification. Growth plate compression was seen, hypertrophic cartilage was reduced and hypertrophic chondrocytes were flattened and reduced in number, organisation of chondrocyte columns was also effected. The number and size of metaphyseal trabeculae, composed of hypertrophic cartilage cores with newly deposited bone on the surface, were also reduced. It was concluded that the compressed growth plate phenotype resulted from a deficient type X pericellular matrix in the hypertrophic cartilage of these animals due to a reduced level of intact collagen X molecules (Jacenko et al., 1993).

Haematopoietic defects in transgenic type X collagen mice were later noted. These included reduced thymuses and diminished cortical lymphocytes, small spleens and absent lymph nodes. (Jacenko et al., 1996). A more exhaustive investigation demonstrated that collagen X transgenic mice exhibited impaired haematopoiesis and marrow hypoplasia. The mice displayed reduced B cells in bone marrow and spleen, and elevated splenic T cells. Marrow abnormalities are thought to occur as a result of the skeletal alterations in the chondo-osseous junction, implying that endochondral ossification contributes to the prerequisite environment in the marrow stroma for subsequent blood cell differentiation. These defects underscore an unforeseen link between hypertrophic cartilage, endochondral ossification, and establishment of the bone marrow microenvironment required for blood cell differentiation (Jacenko et al., 2002).

Ultrastructural, histological, and immunohistochemical analyses were used to demonstrate that collagen X transgenic mice have a disrupted pericellular lattice network around

hypertrophic chondrocytes of the growth plate. This was attributed to increased proteolysis of the mutant chains, or to the inability of the mutant collagen X molecules to properly aggregate with the wild type collagen. The loss of structural integrity in the pericellular matrix, alters the partitioning of hyaluronan and heparan sulphate proteoglycan in the growth plate of these animals. Aggregates, probably containing aggrecan are seen throughout the matrix of the growth plate. This data implies a potential association between collagen X and heparan sulphate and PG's with disruption of these interactions leading to a decompartmentalised chondro-osseous junction. Hyaluronan and heparan sulphate proteoglycans are implicated in haematopoiesis, therefore disruption to these molecules provides an explanation for haematopoietic failure in the collagen X transgenic or null mice (Jacenko et al., 2001).

The compartmentalisation function of type X collagen was tested by genetically altering the relative in vivo proportions of the proteoglycans perlecan and aggrecan to collagen X. The molecules were altered by either over-expressing type X collagen in transgenic mice, or by reducing the amount of proteoglycans by using perlecan and aggrecan null mice. When type X collagen was over-expressed, mRNA was restricted to the hypertrophic chondrocytes, whereas the protein could diffuse away from the hypertrophic zone into other areas of the growth plate. Type X collagen was distributed throughout the growth plate in transgenic mice over-expressing type X collagen and in perlecan null mutants. This effect was also observed, but to a lesser extent in transgenic mice that contain perlecan with reduced heparan sulphate chains (Cheah et al., 2004).

1.3.6.2 Collagen X Null Mice

Shortly after the original report on transgenic mice by Jacenko et al., 1993, type X collagen-null mice were generated, they were viable and fertile and had no gross abnormalities in long bone growth or development. Histological examination revealed growth plates with normal appearance, and mineralisation of bones appeared normal. The distribution of other matrix components, such as type II collagen, osteopontin and osteocalcin, were also assessed and appeared normal. The complete lack of type X collagen did not alter the distribution of other markers in the growth plate. These findings resulted in the suggestion that type X collagen is not essential for long bone development, alternatively it may be that other matrix components can fulfil the function of type X collagen in its absence (Rosati et al., 1994).

When type X collagen null mice were generated by a different laboratory, deficient mice developed a SMCD-like phenotype, developing coxa vara and had abnormal trabecular bone architecture (Kwan et al., 1997). Other consequences of the deficiency were reduction in the thickness of the growth plate resting zone and articular cartilage, altered bone content, and atypical distribution of matrix vesicles and proteoglycans within the growth plate. The altered distribution of matrix components was thought to have arisen by diffusion from the hypertrophic zone or by displacement as the result of forces generated by rapid endochondral bone growth. It was concluded that collagen X is important for the compartmentalisation of matrix components to the hypertrophic zone of growth cartilage, providing the proper environment for mineralisation and bone remodeling.

Contradictory to the previous reports, a variable skeleto-haematopoietic phenotype was observed in the collagen X null mice generated by Rosati et al., 1994, when they were later studied. As the colony of mice was expanded, an acute perinatal lethal phenotype was detected in 10% of the mice at week three after birth. Subtle growth plate compressions primarily within the proliferative zone of the growth plate were observed in the null mice, as well as haematopoietic changes (Gress and Jacenko, 2000).

1.4 Small Leucine Rich Proteoglycans (SLRPs)

The SLRPs belong to a larger family of proteins which contain leucine-rich repeats (LRRs). The LRRs contain twenty to thirty amino acids, with asparagine (N) and leucine (L) residues in conserved positions in the LxxLxLxxNxL motif. The LRRs have been discovered in a variety of proteins from prokaryotes and eukaryotes, they have a wide spectrum of cellular locations and functions, examples include hormone receptors, tyrosine kinase receptors, cell adhesion molecules, bacterial virulence factors, enzymes and ECM-binding proteins. A common feature among family members is involvement in protein-protein interactions (Matsushima et al., 2000).

Members of the SLRP family are structurally related and are each encoded by a different gene. They are characterised by a protein core (approximately 40 kDa) with a central region containing LRRs. They differ according to whether they contain N-linked oligosaccharides, contain GAG chains such as CS, DS or KS, are tyrosine sulphated or undergo proteolytic processing. The members of the family have been divided into three distinct classes based on their evolutionary protein conservation, the sequence of a distinct cysteine-rich region at the

N-terminus, the number of leucine repeats they have and their genomic organisation (Iozzo, 1999). Some members of the family do not fall into any of the classes and so form an 'others' category. Discovery of additional members may lead to an expansion of classes in the future. Members of each class and their characteristics are summarised in figure 1.11

| Class | Member | Type and Number of GAG Chain(s) | Cysteine-Cluster Sequence | Number of LRRs | Genomic Organisation |
|--------------|--|--|----------------------------------|-----------------------|-----------------------------|
| I | Decorin Biglycan Asporin | CS/DS (1) CS/DS (2) No GAG | CX_3CXCX_6C | 10 | 8 EXONS |
| II | Fibromodulin Lumican Keratocan PRELP Osteoadherin/osteomodulin | KS (2-3) KS (3-4) KS (3-5) KS (2-3)/No GAG? KS (2-3) | CX_3CXCX_9C | 10 | 3 EXONS |
| III | Epiphycan/PG-Lb/DSPG3 Mimican/osteoglycin Opticin/oculoglycan | CS/DS (2-3) KS (2-3) | CX_2CXCX_6C | 6 | 7 EXONS |

Figure 1.11: Members of the different SLRP classes are shown, with genomic, protein and GAG details displayed.

1.4.1 Class I SLRPs

Class I SLRPs contain ten LRRs and the N-terminus consensus sequence, CX_3CXCX_6C (where C is a cysteine and X is any amino acid), each member is encoded by eight exons (figure 1.12) Members of Class I include the well studied and characterised decorin and biglycan, along with the newest member asporin.

The protein core of asporin is similar to decorin and biglycan with regards to the number of LRRs and the conserved cysteine motif. However, asporin does not contain the N-terminus serine/glycine dipeptide sequence(s) required for xylosyl transfer and glycosaminoglycan assembly, thus asporin is probably not a proteoglycan. Instead, asporin contains a stretch of aspartic acid residues in this region. The number of aspartate residues in this acidic motif can vary from eleven to eighteen depending on species (Henry et al., 2001). Expression of asporin mRNA has been found in various human tissues, with highest levels in osteoarthritic articular cartilage, aorta, uterus, heart and liver (Lorenzo et al., 2001).

1.4.1.1 Decorin and Biglycan

Decorin and biglycan are the original members of the SLRP family and are well characterised. Their protein cores are homologous (Fisher et al., 1989) and from the N-terminus they contain a leader/signal sequence which targets the protein for secretion. A propeptide which consists of highly negatively charged residues, proposed to act as a recognition signal for the first enzyme, xylosyltransferase, involved in the biosynthesis of the GAG chain (Sawhney et al., 1991). The tetrapeptide Ser-Gly-Xaa-Gly where Xaa is any amino acid, has been demonstrated to be a recognition consensus sequence for the attachment of GAG chains to the core proteins of proteoglycans (Bourdon et al., 1987). The GAG attachment region is followed by a short cysteine-rich cluster, ten central LRRs and a hydrophobic C-terminus cysteine-rich cluster.

Decorin is substituted with one GAG chain and biglycan is substituted with two GAG chains (Iozzo, 1999), GAG attachment sites have been identified at different positions in different species (Krusius and Ruoslahti, 1986; Neame et al., 1989; Scholzen et al., 1994). Different glycosylated forms of decorin and biglycan are spatially and temporally regulated, indicating flexible post-translational modification. The composition of the GAG chain in terms of iduronate content and pattern of sulphation varies between tissues (Cheng et al., 1994), with dermatan sulphate predominating in skin and chondroitin sulphate the major form in bone

(Hocking et al., 1998). There are a number of contrasting reports regarding the processing of the propeptide, it appears that the proteins can be secreted with or without processing (Marcum and Thompson, 1991; Roughley et al., 1996). Complexity is further increased by the possibility of N-linked oligosaccharides, decorin has three potential sites within its protein core and biglycan has one.

The three dimensional structure of decorin (figure 1.13) has been modelled on the crystal structure of the porcine ribonuclease inhibitor (Weber et al., 1996). The model predicts a 'horse-shoe-like' shaped molecule with the GAG chain located on Ser 7 at one edge of the molecule, thus the GAG chain would be relatively free to protrude away from the core protein in different directions. The three N-linked oligosaccharides at Asn¹⁸⁴, Asn²²⁸ and Asn²⁷⁵, are positioned on the outer surface of the arch projecting away from the protein core. This model allows easy access of interactive protein to the inner surface. The inner surface of the arch contains charged residues that could form ionic and polar interactions with residues found in a polar sequence in the d band of collagen $\alpha 1(I)$ in the collagen triple helix. More recently this model has been challenged by the resolving of the crystal structure of bovine dimeric decorin (Scott et al., 2004). This model predicts a more open structure, with the concave surface previously implicated in decorin ligand interactions involved in a high affinity dimer interaction.

Both decorin and biglycan have been reported to be Zn²⁺ metalloproteins, with a zinc binding site located in their N-terminus region (Yang et al., 1999). The significance remains unclear, but it may be necessary for the correct conformation of the proteins, or alternatively may function as a storage pool of zinc in tissues. Decorin forms dimers in solution (Scott et al., 2003), while biglycan can form dimers and hexamers depending on conditions (Liu et al., 1994), however whether any multimeric forms occur in vivo is unknown.

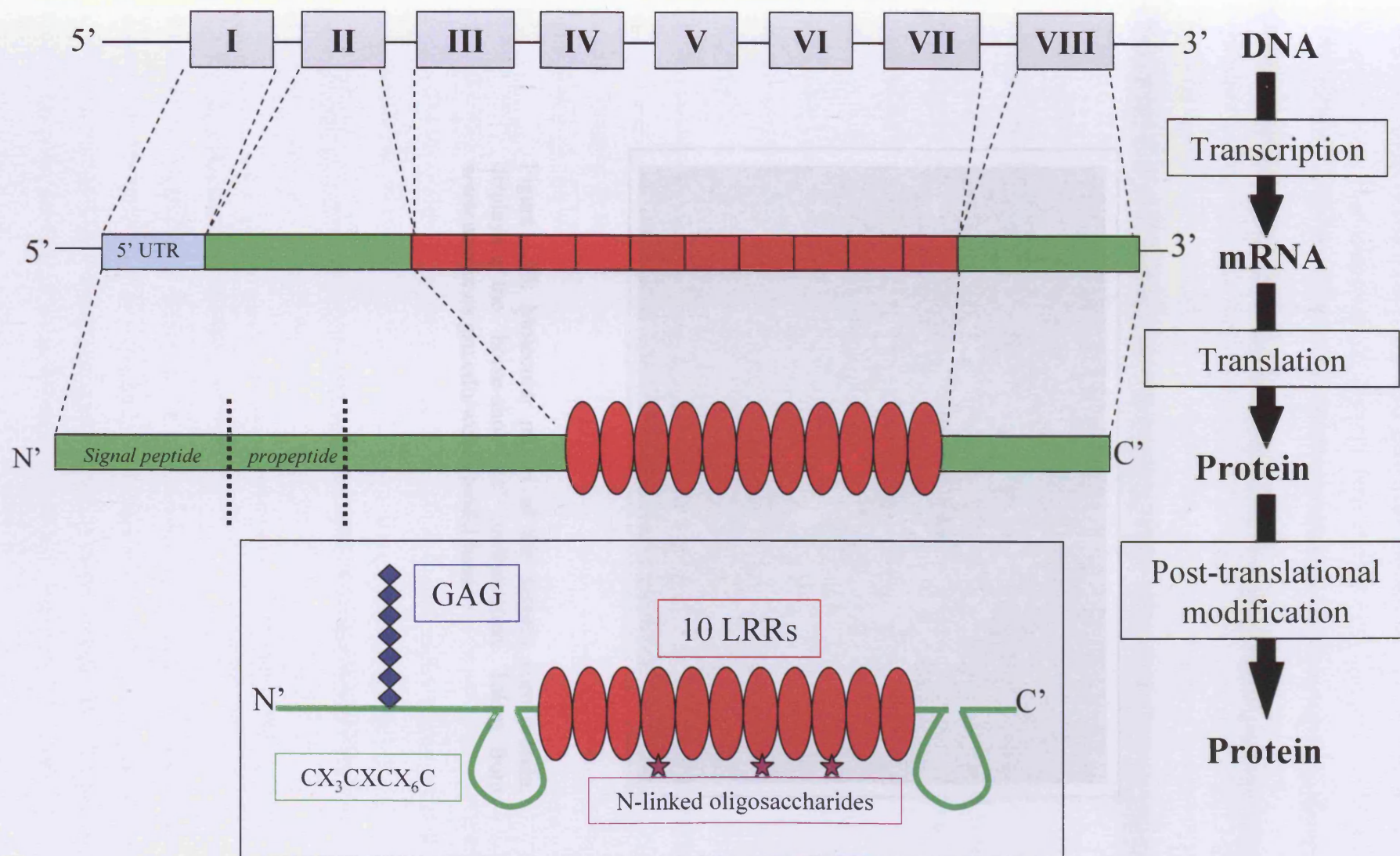


Figure 1.12: Schematic representation of a Class I SLRP. The decorin gene, mRNA and protein, before and after post-translational modification.

1.4.1.2 Genomic Organization of Decorin and Biglycan

The right kilobase pair human biglycan gene was characterized and localized to the end of the long arm of the X chromosome (Xq21-22) (Foley et al., 1991). The gene contains eight exons with the first one coding for the 5'-untranslated region of 115 codons (345 bp). The second exon codes for the signal sequence, the pro-peptide, the triple helix region, and the first cysteine-rich region. Exons three to seven code for the triple helix region. The C-terminal region is coded for by the third exon. The entire gene is 10.5 kb in size. The biglycan gene is located on the X chromosome (Foley et al., 1991). The human biglycan gene is located on the X chromosome (Foley et al., 1991). The human biglycan gene is located on the X chromosome (Foley et al., 1991).

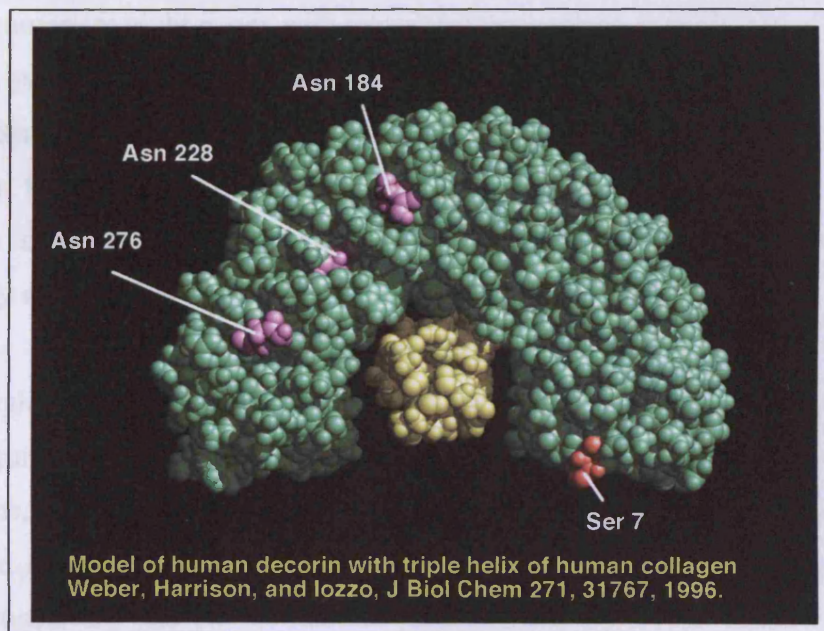


Figure 1.13: Molecular model of the decorin core protein, displaying the 'horse-shoe-like' conformation. Taken from www.astreix.cs.gsu.edu/weber/model.html

1.4.1.2 Genomic Organisation of Decorin and Biglycan

The eight kilobase pair human biglycan gene was characterised and localised to the end of the long arm of the X chromosome (Xq27-ter) (Fisher et al., 1991). The gene contains eight exons with the first one coding for the 5'-untranslated region (UTR) of the mRNA. The second exon codes for the signal sequence, the pro-peptide, the GAG attachment sites and the first cysteine-rich region. Exons three to seven code for the LRRs. The C-terminus cysteine-rich region is coded for by the final exon. The murine biglycan gene also maps to chromosome X (Chatterjee et al., 1993). The murine gene has a similar structure to the human gene although is larger. It comprises eight exons with conserved intron/exon organization (Wegrowski et al., 1995). The human (Ungefroren and Krull, 1996) and murine (Wegrowski et al., 1995) biglycan promoters contain a high GC content and multiple potential binding sites for the transcription factor SP-1. They lack TATA and CAAT boxes and contain multiple transcription start sites. These features of the promoter region are common in genes constitutively expressed at low levels or in genes related to growth.

The thirty eight kilobase human decorin gene has been mapped to chromosome 12q23. The intron-exon junctions within the coding portion of the gene are identical to those found in the biglycan gene, although the introns in decorin are larger. Two alternatively spliced leader exons termed Ia and Ib, were found in the 5' UTR, these were found to be homologous to sequences from avian and bovine decorin (Danielson et al., 1993; Vetter et al., 1993). The murine decorin gene has been mapped to chromosome 10 and differs from its human counterpart in its promoter region and lacks the leader exon Ib which is alternatively spliced (Scholzen et al., 1994). Analysis of the upstream sequence of exons Ia and Ib revealed that only the region upstream of exon Ib exhibits strong transcriptional activity (Santra et al., 1994). The Ib promoter region contains a CAAT and two TATA boxes, as well as several putative binding sites for factors such as AP-1, AP-5, NF- κ B and TGF- β . Thus, it is highly unlikely that two different transcripts are produced from the gene yielding two different proteins.

1.4.1.3 Localisation of Decorin and Biglycan

Decorin and biglycan are ubiquitously expressed and are found in many tissue types at different developmental stages. Generally, in human embryos decorin is found in tissues rich in fibrillar collagens, while biglycan is expressed by more specialised cell types such as renal tubular epithelia, keratinocytes and skeletal myofibers (Bianco et al., 1990). A screening of

human adult tissues found ubiquitous expression of both decorin and biglycan transcripts, with increased biglycan expression in a few specialised tissues such as aorta, spleen and brain (Hocking et al., 1998). During fetal development of the mouse, decorin is expressed in most mesenchymal derivatives which give rise to connective tissues, but not in cartilage and bone. In contrast, biglycan is expressed in cartilage and bone, and other sites of connective tissue such as dermis and mesothelial linings of large organs (Wilda et al., 2000).

Decorin and biglycan localisation with regard to the growth plate has also been studied. Decorin and biglycan are present in the bovine growth plate but their distribution and expression profiles vary within different zones (Alini and Roughley, 2001). Decorin was found in the reserve and proliferating zones, and its abundance decreased in the hypertrophic zone. In contrast, biglycan was found throughout the growth plate though its abundance was decreased in the proliferative and hypertrophic zones.

Biglycan was found to be associated with cartilage matrix mineralisation in a study involving the developing epiphyseal cartilage of 10-day old Wistar rats (Takagi et al., 2000). The core protein and mRNA of biglycan were localised to the hypertrophic region, and to terminally differentiated chondrocytes associated with the ossifying region of the epiphyseal plate. The presence of biglycan in the clusters of hydroxyapatite (HAP) crystals or in the crystal ghosts suggests a role in inducing or regulating the formation of apatite crystals. There is also a possibility that decorin may have some involvement in mineralisation. In vitro evidence suggests that decorin inhibits collagen matrix mineralisation when it is over-expressed in osteoblasts, thus it could potentially modulate the timing of mineralisation in vivo (Mochida et al., 2003).

Decorin and biglycan substituted with CS and deglycosylated decorin and biglycan have been demonstrated to bind to HAP. Both molecules displayed a strong association for HAP, which was predominately facilitated through the glycosaminoglycan chains. Both decorin and biglycan inhibited HAP crystal growth. Biglycan was the most efficient and the core proteins were slightly more inhibitory than the whole molecules, and when the proteoglycans were complexed with type I collagen the degree of inhibition was reduced. This could be attributed to the reduced number of binding sites on the protein available to interact with the HAP crystal surface (Sugars et al., 2003).

1.4.1.4 Interactions of Decorin and Biglycan with Collagens

Decorin and biglycan interact with many collagen types found in extracellular matrices of different tissues. Their widespread distribution and involvement in protein-protein interactions, confirms their importance in extracellular matrix biology.

Decorin has been shown to modulate the process of collagen fibril formation. It was demonstrated that an interaction between a dermatan sulphate proteoglycan and collagen causes increased stability of collagen fibrils and a change in their solubility (Toole, 1969). A later study showed an association between rat tail tendon collagen and a dermatan sulphate proteoglycan at the d band in the gap region of the collagen fibril. The orthogonal array of proteoglycan about the collagen fibril was postulated to inhibit fibril radial growth and to inhibit calcification (Scott and Orford, 1981). The discovery of an association between the two molecules started a series of studies to identify the precise regions of the proteins involved in the interaction. Chondroitinase digestion did not eliminate the small dermatan sulphate proteoglycans ability to inhibit fibrillogenesis of types I and II collagen. Alkali treatment on the other hand, which destroys the core protein, did affect the ability to inhibit fibrillogenesis, indicating that the core protein of the proteoglycan interacts with collagen. Fibrillogenesis of pepsin treated collagens was also inhibited by decorin, indicating that the interaction was with the triple helical region of collagens and did not involve the telopeptides (Vogel et al., 1984). Removal of an N-terminus stretch of 17 amino acids, including the GAG attachment site on the decorin core protein by enzymatic digestion, did not affect the inhibition of fibrillogenesis (Vogel et al., 1987).

The binding regions between decorin and collagen type I are now reasonably well characterised. By forming chimeric protein molecules of decorin and biglycan, it was found that decorin binds to collagen primarily via leucine rich repeats 4 and 5, an area of about 40 amino acids. However, it was noted that this chimera had somewhat lower affinity for collagen than wild type decorin, suggesting that additional low affinity binding sites maybe located in other parts of decorin (Svensson et al., 1995). Using rotary shadowing electron microscopy and photo affinity labelling, the binding site of decorin protein core was mapped to a narrow region near the C- terminus of type I collagen (Keene et al., 2000). A study involving endothelial cells revealed that decorin mRNA expression could be induced by interleukins-6 and -10, however decorin protein synthesis only occurred in the presence of a

type I collagen matrix (Strazynski et al., 2004), indicating the importance of the surrounding extracellular matrix during protein synthesis of ECM proteins.

The binding between fibrillar collagens and biglycan however remains unclear, and contrasting results have been found. Biglycan has been found to interact with type I collagen, probably at identical or at adjacent binding sites as that of decorin, however binding affinity was significantly less than that attributed to decorin interactions (Schonherr et al., 1995). In another study biglycan interacted strongly with type II collagen but not with type I collagen (Vynios et al., 2001).

An interaction between type V collagen with decorin and biglycan has been identified. The binding sites on the collagen may be different for each proteoglycan, preliminary studies indicate that the protein core of decorin was responsible for the interaction, while intact proteoglycan was necessary for the interaction involving biglycan (Whinna et al., 1993).

Both decorin and biglycan have been shown to bind to type VI collagen, the interaction occurs at the N-terminus region of the triple helix and is not dependant on the presence of the GAG chain on decorin or biglycan (Wiberg et al., 2001). Later, the ability of decorin and biglycan to influence the supramolecular organization of type VI collagen was investigated. Both proteins organise collagen VI into extensive hexagonal-like networks, however, biglycan with its two GAG chains is far more efficient than decorin with its one GAG chain. The GAG chains are vital for collagen VI network formation, deglycosylated decorin and biglycan lose their ability to organise collagen VI (Wiberg et al., 2002). Decorin and biglycan were demonstrated to be present in a complex with matrilin-1, acting as adapter proteins connecting the collagen VI microfibrillar networks to aggrecan and type II collagen in Swarm rat chondrosarcoma tissue (Wiberg et al., 2003). In vitro studies, have revealed that decorin can also act as a bridging molecule between types I and VI collagen, decorin interacts with these two collagens via different binding sites (Nareyeck et al., 2004).

Decorin interacts with collagen XIV. This collagen is a member of the FACIT family, and the interaction is mediated via an N-terminus fibronectin type III repeat present in the NC3 domain of type XIV (Ehnis et al., 1997). Their distribution in tissues such as tendon and skin and their localisation at the d band of collagen I fibrils, support the possibility of this interaction occurring in vivo.

1.4.1.5 Interactions of Decorin and Biglycan with Non-Collagenous Proteins

As well as interactions with members of the collagen superfamily, decorin and biglycan interact with other proteins. Decorin binds to a variety of proteins including, the cartilage-specific fibronectin isoform (Gendelman et al., 2003), fibrinogen, in a zinc dependant interaction (Dugan et al., 2003), thrombospondin, resulting in inhibition of cell adhesion (Winnemoller et al., 1992), the microfibrillar proteins MAGP-1 and fibrillin-1 (Trask et al., 2000) and the extracellular matrix 22 kDa protein (Okamoto et al., 1996).

Biglycan and decorin bind to and can modulate the haemolytic activity of the complement component C1q (Hocking et al., 1996; Krumdieck et al., 1992). The interaction is mediated via the core protein and is not affected by denaturation. An interaction between heparin cofactor II, a blood serine protease inhibitor and decorin and biglycan has been identified (Whinna et al., 1993). The activity of thrombin is inhibited by heparin cofactor II, this inhibition is enhanced in the presence of decorin or biglycan.

1.4.1.6 Interaction of Decorin and Biglycan with Growth Factors

The multifunctional cytokine, transforming growth factor- β (TGF- β), regulates a diverse range of processes important for cell growth. It has been determined that TGF- β participates in the control of cell proliferation, differentiation, adhesion, and deposition of the extracellular matrix (Hocking et al., 1998). In Chinese hamster ovary (CHO) cells, recombinant expression of decorin was accompanied by an inhibition of cell proliferation (Yamaguchi and Ruoslahti, 1988). It was proposed that this effect was due to the ability of decorin to bind to and inhibit the activity of TGF- β (Yamaguchi et al., 1990). It was later shown that decorin and biglycan bind to all isoforms of TGF- β , - β 1, - β 2 and - β 3, with dissociation constants in the nanomolar range (Hildebrand et al., 1994). Collagen bound decorin is also able to interact with TGF- β (Schonherr et al., 1998), allowing decorin to act as a reservoir for these growth factors in the extracellular milieu. The modulation of TGF- β activity by decorin and biglycan is likely to be due to the proteoglycans preventing binding of the cytokine to its receptor(s). However, in other cellular systems the ability of decorin to bind to TGF- β augments the bioactivity of the cytokine, for example the addition of decorin to osteoblastic cells enhances the binding of radiolabeled TGF- β to its receptors (Takeuchi et al., 1994).

Attempts have been made to utilise the proteoglycan-cytokine binding in a therapeutic manner. In kidney glomerulonephritis overproduction of TGF- β leads to tissue fibrosis and extracellular matrix deposition. Injection of decorin into rats with experimental glomerulonephritis inhibited the production of extracellular matrix (Border et al., 1992). Gene therapy has also been used in the same disease model with similar results (Isaka et al., 1996).

The relationship between the expression and function of the small proteoglycans and TGF- β has been speculated to involve an autocrine negative feedback mechanism (Ruoslahti and Yamaguchi, 1991). TGF- β stimulates the production of the proteoglycans and in turn they regulate the activities of this bone-enriched growth factor (Young et al., 1992). More recently it was demonstrated that decorin and biglycan interact with tumor necrosis factor- α (TNF- α) in vitro (Tufvesson and Westergren-Thorsson, 2002), whether this interaction occurs in vivo and could be physiologically relevant remains unclear.

Through studies on angiogenesis and tumourigenesis decorin has been demonstrated to be able to inhibit cellular proliferation and to be involved directly in signalling pathways. Decorin suppresses the malignant phenotype of A431 squamous carcinoma cells by activating the epidermal growth factor (EGF) receptor. Dimerisation and phosphorylation of the receptor causes the activation of the mitogen-activated protein kinase (MAPK) pathway, a mobilisation of calcium stores and an up-regulation of p21, an inhibitor of cyclin dependent kinases involved in tumour suppression, and ultimately leads to cell cycle arrest (Kresse and Schonherr, 2001). In an angiogenesis model (Schonherr et al., 1999), decorin synthesis by endothelial cells leads to capillary formation and survival of the cells. Decorin enhances the phosphorylation of protein kinase B (PKB) /Akt and subsequently induces p21 (Schonherr et al., 2001). This activation occurs independently of the EGF receptor, decorin causes phosphorylation of PKB by binding to and activating the IGF-I receptor. Whether decorin is involved in signalling via these mechanisms in chondrocytes remains to be elucidated.

1.4.1.7 Decorin and Biglycan Transgenic Mice

A number of transgenic mice have been generated which lack decorin, biglycan or both. Variable phenotypes have been observed and multiple tissues are affected. The effect on collagens in these transgenic animals confirms the importance of SLRPs for collagen assembly and ultrastructure.

1.4.1.7.1 Biglycan-deficient mouse

Targeted disruption of the biglycan gene leads to a reduced growth rate and an osteoporosis like phenotype. The biglycan-null animals grew normally until three months after birth, at which point their growth rate decreased, tibia and femur length was reduced when compared with littermates, indicating that biglycan is involved in the regulation of postnatal skeletal growth. The null-animals show reduced bone mass that becomes more pronounced with ageing, probably due to a lower osteoblast number and lower osteoblast activity (Xu et al., 1998). Thus, biglycan acts as a positive regulator of bone formation and bone mass by affecting the cellular processes of bone formation that occur during both development and adult life. Changes in dentin mineralisation and enamel thickness in biglycan-null animals, confirms the importance of biglycan in mineralised tissues (Goldberg et al., 2002).

1.4.1.7.2 Decorin-deficient mouse

Mice with a disrupted decorin gene are viable, do not show any gross anatomical abnormalities and grow to normal size. The animals have fragile skin with markedly reduced tensile strength and a thinner than normal dermis. Ultrastructural analysis of the collagens of the skin and tendons revealed abnormal packing of collagen fibrils, large variation in fibril diameter as well as fibrils with irregular and scalloped edges. Collagen fibrils in the corneas of decorin-deficient animals however appeared normal when compared to wild-type animals (Danielson et al., 1997). The phenotype of the mice resembles the cutaneous defects observed in the human Ehlers Danlos syndrome (EDS) VIIC. No observations were reported on any cartilaginous tissues in the decorin-deficient animals

1.4.1.7.3 Biglycan/Decorin-deficient mouse

Double-deficient animals revealed that the effects of decorin and biglycan deficiency are additive in the dermis and synergistic in bone (Corsi et al., 2002). The animals had a thinned dermis with loosely packed collagen bundles, which had varying fibril diameters. These changes contributed to a dermatosparaxis-like phenotype. A skeletal phenotype was observed at two months of age, the long bones of double-deficient animals were shorter and wider compared with wild type animals and were markedly osteopenic. The shorter limbs of these animals suggests abnormal functioning of the growth plate, indicating a potential involvement for decorin and biglycan within the growth plate. Collagen fibrils from bone tissue resemble 'hieroglyphics' with an overall serrated appearance. Reduced bone mass and reduced mineral content were also seen in bones of double-deficient animals. This phenotype is reminiscent of

a specific subtype of human EDS, the progeroid variant, which is characterised by a defective galactosyltransferase I enzyme necessary for the synthesis of GAG chains. The outcome of this human disease is the production of small proteoglycans devoid of GAG chains. This underlies the functional importance of the GAG chains on biglycan and decorin in bone and skin tissue (Ameys and Young, 2002).

1.4.2 Class II SLRPs

Class II SLRPs contain ten LRRs and the N-terminus consensus sequence, CX₃CXCX₉C, each member is encoded by three exons. Members of Class II include fibromodulin, lumican, keratocan, PRELP (proline arginine-rich end leucine-rich repeat protein) and osteoadherin.

Fibromodulin was originally isolated from articular cartilage but was found in other connective tissues including tendon, sclera and nucleus pulposus of the intervertebral disc (Heinegard et al., 1986). Its core protein is substituted with KS chains attached via N-glycosidic linkages to asparagines, it also contains negatively charged tyrosine sulphate residues at the N-terminus, (Antonsson et al., 1991). Fibromodulin was proposed to be a modulator of collagen fibrillogenesis and was shown to inhibit collagen fibrillogenesis in vitro (Hedbom and Heinegard, 1989).

There have been a number of investigations into the localisation of fibromodulin in growth plates of different species. These studies have proven inconclusive with many contradictory reports regarding its localisation. Fibromodulin is reported to be distributed in all regions of the bovine growth plate, however its abundance at the protein level decreases in the lower zones (Alini and Roughley, 2001). A study in mice found deposition of fibromodulin was strong around the late-hypertrophic chondrocytes of the growth plate, in young epiphyses fibromodulin was found interterritorially mainly in the uncalcified and deep-calcified cartilage, however calcified cartilage of older mice became enriched with fibromodulin (Saamanen et al., 2001). In contrast to this murine study, a different investigation also found fibromodulin to be developmentally expressed in the growth plate, however it was localised to the perichondrium and proliferating chondrocytes during endochondral ossification (Gori et al., 2001).

Mice lacking a functional fibromodulin gene exhibit thinner collagen fibrils with irregular outlines in tendon. This phenotype is associated with an approximately 4-fold increase in the

deposition of lumican, suggesting that lumican and fibromodulin share the same binding site on tendon collagen fibrils (Svensson et al., 1999). Fibromodulin-null mice display increased incidences of the degenerative changes associated with osteoarthritis in their knee joints, this is probably due to alterations in the ligaments, leading to abnormal mechanical loading of the cartilage (Gill et al., 2002).

Lumican contains three or four KS side chains which are N-linked, the linkage for the KS chain is a complex type N-linked oligosaccharide, there are additional sites which can be substituted with N-linked oligosaccharides of the high mannose type. Lumican was so named for the important role that it plays in the acquisition and maintenance of corneal transparency. Its protein core has been found in muscle and intestine as well as the cornea (Blochberger et al., 1992). Lumican expression has been localised mainly in the cartilaginous matrices during early embryonic development of the mouse, however in older embryos the expression is more prominent in the developing bone matrices. This finding led to the suggestion that lumican could potentially be involved in endochondral and intramembranous ossification (Raouf et al., 2002). Disruption of the lumican gene in mice causes the development of fragile skin and bilateral corneal opacity. These phenotypes are results of structural alterations to the organisation of irregular collagen fibrils (Chakravarti et al., 1998).

Fibromodulin and lumican double-deficient mice display severe tendon weakness, gait abnormality, joint laxity, age-dependant osteoarthritis and are smaller than wild type animals. This phenotype resembles the clinical features of EDS. Manipulations of the lumican gene in fibromodulin null mice established fibromodulin as a key regulator and lumican as a modulator of tendon strength (Jepsen et al., 2002). Mice deficient in fibromodulin alone (*lumican*^{+/+} *fibromodulin*^{-/-}) have reduced tendon stiffness, with further loss in stiffness in a *lumican* gene dose-dependent way. The tendon phenotype is partially rescued in the *fibromodulin*^{-/-} mice by an increase in lumican protein.

Keratocan is a KS proteoglycan, its restricted expression in corneal tissue suggests a role in developing and maintaining corneal transparency (Liu et al., 1998; Tasheva et al., 1998). Gene targeting was used to generate 'knockout' keratocan mice, these mice displayed subtle structural alterations in the organized packing of collagen fibrils in the corneal stroma (Liu et al., 2003). PRELP derives its name from its basic N-terminus region which is rich in arginine and proline. It was originally identified from a human articular chondrocyte cDNA library.

The protein core contains four potential N-linked glycosylation sites, however, the presence or absence of KS substitution is unclear and may vary depending on species (Bengtsson et al., 1995; Grover et al., 1996). Osteoadherin is a bone proteoglycan containing KS chains and an acidic motif at its C-terminus. The last 38 amino acids of the protein contain 16 negatively charged aspartic or glutamic acid residues, these are thought to mediate binding to the mineral hydroxyapatite (Sommarin et al., 1998).

1.4.3 Class III SLRPs

Class III SLRPs contain six LRRs and the N-terminus consensus sequence, CX₃CXCX₆C, each member is encoded by seven exons. Members of class III include Epiphykan/Pg-Lb/DS-PG3, mimecan/osteoglycin and opticon/oculoglycan.

Epiphykan was named based on its isolation from bovine epiphyseal cartilage (Johnson et al., 1997), it is a homologue of avian PG-Lb (Shinomura and Kimata, 1992) and human DSPG3 (Deere et al., 1996). The protein core is substituted with two GAG chains and one O-linked oligosaccharide at its N-terminus. Epiphykan localises to the zone of flattened chondrocytes of developing chick limb cartilage (Shinomura et al., 1983). This zone is not associated with calcification, which suggests its functions may include delaying the onset of calcification or arranging the matrix in preparation for the extensive remodeling that is associated with calcification (Johnson et al., 1997). The expression of epiphykan has been studied during mouse embryonic development and its expression was compared to type II and X collagen. The expression of epiphykan occurs later than the expression of type II collagen but before type X collagen in cartilage development. However, at the protein level epiphykan can be found in the matrix of all the zones of the growth plate (Johnson et al., 1999).

Osteoglycin/mimecan was initially isolated in a truncated form from bovine bone and was called osteoinductive factor (Bentz et al., 1989). It was subsequently characterised as one of the major keratan sulphate containing proteoglycans in the cornea, and was found to be present in other connective tissues in less abundance (Funderburgh et al., 1997). The protein core contains consensus sites for tyrosine sulphation at its N-terminus and contains an N-linked glycosylation site in its LRR region. Osteoglycin/mimecan deficient mice do not have a corneal phenotype but do have fragile skin. Ultrastructural analysis revealed that the collagen fibrils in cornea and skin are thicker than wild type and are more loosely packed (Tasheva et al., 2002).

Opticin was initially extracted from the vitreous and was later found to be expressed in ligament, skin and retina. The protein core contains six LRRs in its central domain, which are flanked by cysteine clusters including a C-terminus two-cysteine cluster containing an additional LRR. Potential O-glycosylation sites at the N-terminus were found to be substituted with sialylated O-linked oligosaccharides in bovine vitreous (Reardon et al., 2000). Differences in the post-translational modifications of opticin between species have been found, possibly suggesting that addition of carbohydrate moieties may not be necessary for all functions (Hobby et al., 2000).

The SLRP family of proteins is a diverse family with a wide variety of tissue distributions and functions. The ability of some members to bind growth factors indicates potential roles in tissue homeostasis. Their involvement in protein-protein interactions is well characterised, particularly their interactions with collagens. The abnormal collagen ultrastructure seen in transgenic mice lacking SLRPs, including decorin and biglycan, illustrates the crucial role these proteoglycans play in collagen assembly and maintenance.

1.5 Cellular Control, Remodelling, Mineralisation and Angiogenesis during Endochondral Ossification

1.5.1 Cellular Control of Growth Plate Chondrocytes

The differentiation, proliferation and hypertrophy of chondrocytes are fundamental processes during longitudinal growth, and are controlled by a variety of molecules which interplay with each other (figure 1.14). Coupled with the mineralisation, remodelling and angiogenesis that also occur during the process of EO, strict control is required to ensure correct functioning of the growth plate.

1.5.1.1 Indian hedgehog and Parathyroid Hormone-related Protein

The secreted signalling molecules Indian hedgehog (Ihh) and parathyroid hormone related protein (PTHrP) mediate a negative feedback loop of intercellular communication, which regulates the proliferation and maturation of growth plate chondrocytes. PTHrP is a paracrine factor which binds to the PTH/PTHrP receptor. Ihh is a member of the conserved family of secreted proteins which are essential for embryonic patterning, the actions of Ihh are mediated by the receptor components Patched (Ptc) and Gli (Vortkamp et al., 1996).

Ihh is expressed in the cartilage of the developing long bones, specifically in the prehypertrophic chondrocytes committed to the hypertrophic phenotype, Ihh itself inhibits transcription of the Ihh gene. Thus, the differentiation of proliferating chondrocytes is blocked by Ihh before they differentiate to Ihh-expressing cells. Ihh targets the perichondrium via Ptc and Gli and induces the secretion of PTHrP from the peri-articular region of the growth plate. The action of the secreted PTHrP on its receptor expressed by proliferating chondrocytes delays chondrocyte differentiation, thereby allowing more chondrocyte proliferation. This leads to reduced Ihh secretion and completes the negative feedback loop in which chondrocyte proliferation is maintained and hypertrophic differentiation is delayed by the action of Ihh and PTHrP (Stevens and Williams, 1999). In addition Ihh signalling is directly required for osteoblast differentiation in developing long bones (Long et al., 2004).

1.5.1.2 Transforming Growth Factor–Beta (TGF- β)

TGF's- β ($-\beta 1, -\beta 2, -\beta 3$) have been implicated in a variety of cellular events involved in the regulation of bone growth and turnover. They are produced by chondrocytes and osteoblasts and are highly concentrated in skeletal tissues. All three TGF- β isoforms and their receptors have been detected at sites of endochondral ossification. In the growth plate TGF- $\beta 1$ expression is restricted to the proliferative and upper hypertrophic zones, TGF- $\beta 2$ is found in all zones of the cartilage with highest expression seen in the hypertrophic and mineralising zones, TGF- $\beta 3$ is found in the proliferative and hypertrophic zones (Horner et al., 1998). An interplay between TGF- β and PTHrP has been identified which regulates hypertrophic differentiation in embryonic mouse metatarsal organ cultures. TGF- β acts upstream of PTHrP to regulate the rate of hypertrophic differentiation suggesting that TGF- β has both PTHrP dependent and independent effects on endochondral bone formation (Serra et al., 1999). TGF- $\beta 2$ was demonstrated to act as a signal relay between Ihh and PTHrP in the regulation of cartilage hypertrophic differentiation (Alvarez et al., 2002).

1.5.1.3 Fibroblast Growth Factors (FGFs) and their Receptors (FGFRs)

FGFs comprise a family of 22 related proteins. Family members activate four distinct FGFR tyrosine kinase molecules. FGF activity is regulated by the binding of FGF-FGFR to a heparan sulphate proteoglycan to form a trimolecular complex (Ornitz and Marie, 2002). FGFRs -1 and -3 are both expressed in the epiphyseal growth plate. They are found in different chondrocyte populations, FGFR-1 in hypertrophic chondrocytes and FGFR-3 in

proliferating chondrocytes (Peters et al., 1992). During the development of endochondral bones the expression of FGF-2, -7, -8, -9, -10 and -18 have been demonstrated (Ornitz and Marie, 2002). The importance of FGF signalling in the regulation of skeletal development has been confirmed by the identification of FGFR mutations in humans with skeletal dysplasias (Burke et al., 1998).

Through analysis of FGFR-3 mutations, it has been demonstrated that FGFR-3 is a negative regulator of chondrocyte maturation. Coordinated signalling by FGFR-3 and PTHrP has been shown to regulate chondrocyte proliferation, differentiation and apoptosis during bone development (Amizuka et al., 2004). FGF-2 treatment of rats stimulates the proliferation of chondrocytes and permits their differentiation, but inhibits vascular invasion and resorption of the cartilage matrix (Nagai and Aoki, 2002).

1.5.1.4 Bone Morphogenetic Proteins (BMPs)

BMPs are members of the TGF- β superfamily involved in regulating bone formation, their actions are transduced by a family of kinase receptors. The roles of BMPs in the growth plate have been studied and overlap with the Ihh/PTHrP signalling control mechanism. Cells of the perichondrium surrounding pre-hypertrophic and hypertrophic chondrocytes express BMP2, BMP4, BMP5 and BMP7. Pre-hypertrophic and hypertrophic chondrocytes express BMP6 and the receptor BMPRII (Vortkamp, 2001). A role for the BMPs as intermediary molecules involved in the Ihh/PTHrP has been proposed. BMPs are secreted from perichondrial cells in response to Ihh, they act via BMPRII on pre-hypertrophic chondrocytes to delay differentiation (Zou et al., 1997).

1.5.1.5 Other Growth Factors and Hormones

Growth hormone, insulin like growth factors (IGF-I & IGF-II), glucocorticoids and thyroid hormones are examples of other molecules which have roles in the regulation of normal skeletal development (Siebler et al., 2001). However, their actions and functions will not be discussed in this thesis.

1.5.1 Matrix Remodelling During the Process of EG

Matrix metalloproteinases (MMPs) are a large family of zinc-dependent proteases with a conserved domain structure (Fig. 1.13). MMPs are involved in the proteolytic degradation of the ECM (Nomaru et al., 2003). MMPs are secreted as zymogens and are processed to an active form by the removal of an inhibitory propeptide. This involves the formation of a covalent bond between the catalytic domain of the enzyme and the propeptide.

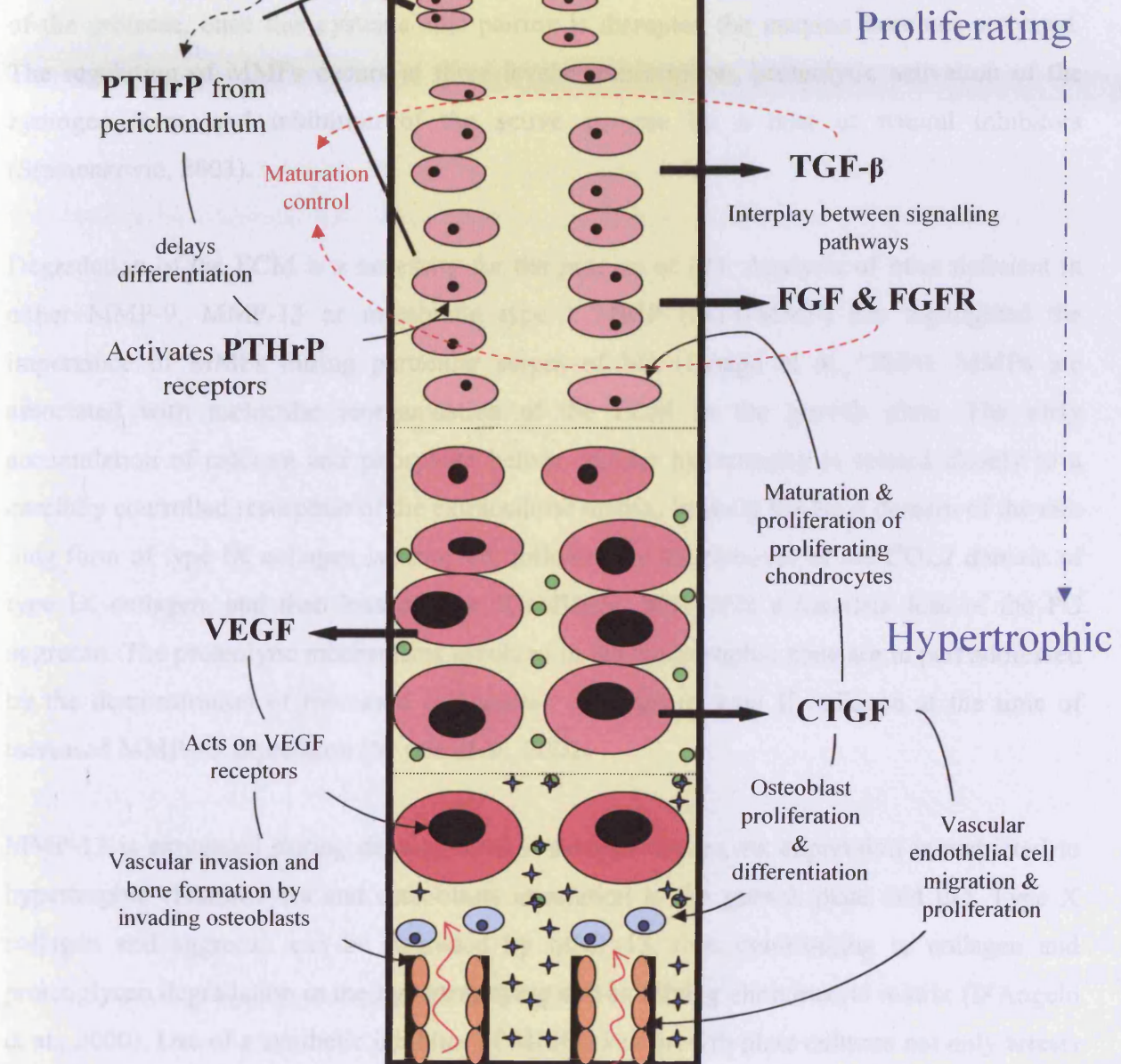


Figure 1.14. Schematic illustration detailing some of the signalling molecules involved in the cellular control of events occurring at the growth plate.

1.5.2 Matrix Remodelling During the Process of EO

Matrix metalloproteinases (MMPs) are a large family of zinc-dependent proteases with a conserved domain structure (figure 1.15) which are involved in proteolytic degradation of the ECM (Somerville et al., 2003). MMPs are synthesised as proenzymes and are processed to an active form by the proteolytic removal of an N-terminus propeptide. This involves the 'cysteine-switch' mechanism, which involves a covalent interaction between a cysteine residue in the N-terminus propeptide and the essential zinc ion bound to the catalytic domain of the protease, once this cysteine-zinc pairing is disrupted the enzyme becomes activated. The regulation of MMPs occurs at three levels: transcription, proteolytic activation of the zymogen form, and inhibition of the active enzyme by a host of natural inhibitors (Stamenkovic, 2003).

Degradation of the ECM is a necessity for the process of EO. Analysis of mice deficient in either MMP-9, MMP-13 or membrane type 1 MMP (MT1-MMP) has highlighted the importance of MMPs during particular stages of EO (Ortega et al., 2004). MMPs are associated with molecular reorganisation of the ECM in the growth plate. The early accumulation of calcium and phosphate before cellular hypertrophy is related closely to a carefully controlled resorption of the extracellular matrix. Initially the NC4 domain of the rare long form of type IX collagen is removed, followed by the removal of the COL2 domain of type IX collagen, and then loss of type II collagen, with only a transient loss of the PG aggrecan. The proteolytic mechanisms involved in the hypertrophic zone are in part addressed by the demonstration of increased collagenase cleavage of type II collagen at the time of increased MMP-13 expression (Mwale et al., 2002).

MMP-13 is expressed during development in skeletal tissues, its expression is restricted to hypertrophic chondrocytes and osteoblasts in relation to the growth plate and EO. Type X collagen and aggrecan can be degraded by MMP-13, thus contributing to collagen and proteoglycan degradation in the hypertrophying and calcifying chondrocyte matrix (D'Angelo et al., 2000). Use of a synthetic inhibitor of MMP-13 in growth plate cultures not only arrests MMP-13 activity but also inhibits mineralisation, indicating matrix resorption is essential for mineralisation to occur. Lack of degradation products leads to suppression of MMP-13 and type X collagen gene expression, indicating an important linkage between hypertrophy and matrix resorption (Wu et al., 2001).

It has been demonstrated that MMP-9 is a key regulator of growth plate angiogenesis and apoptosis of hypertrophic chondrocytes (Vu et al., 1998). Active MMP-9 is located at sites of matrix resorption where vascular invasion occurs, and is expressed in osteoclasts, endothelial cells and bone marrow stromal cells. Homozygous mice with a null mutation in the MMP-9 gene, exhibit a delay in hypertrophic chondrocyte apoptosis, vascularisation and ossification, thereby leading to an abnormal accumulation of hypertrophic cartilage. A proposed functional role for MMP-9 during EO is that it helps release angiogenic factors from the hypertrophic cartilage ECM.

MT1-MMP is a membrane bound MMP capable of mediating pericellular proteolysis of ECM components (Sato et al., 1996) as well as activating other MMP's. MT1-MMP deficient mice display skeletal dysplasia, arthritis and osteopenia. Delayed epiphyseal ossification in mutants leads to growth plate disorganization and reduced chondrocyte proliferation which may contribute to dwarfism (Holmbeck et al., 1999). MMP's -2, -3 and -7 which are not associated with the growth plate, have been demonstrated in vitro to degrade decorin into a number of fragments, cleavage sites were identified at the N-terminus and in the LRR's. TGF- β 1 can be released from a complex with decorin by the action of these MMP's (Imai et al., 1997).

In addition to the MMPs, other matrix-degrading enzymes termed 'aggrecanases' are involved in the resorption of the ECM. Aggrecanase-1 and -2 belong to the larger ADAMTS (a disintegrin and a metalloproteinase domain with thrombospondin type 1 domains) family of enzymes, and have been demonstrated to cleave aggrecan (Abbaszade et al., 1999; Tortorella et al., 1999). Evidence for aggrecanase cleavage of aggrecan has been found in areas undergoing cartilage resorption during the development of the secondary ossification centre in rat tibiae (Lee et al., 2001). It was concluded that aggrecanase and MMP activity contribute to the lysis of aggrecan, and are seen at different sites at different stages of development. Another study showed that growth plate chondrocytes are involved in proteoglycan breakdown, and that high proteoglycan-degrading activity is a marker of hypertrophic chondrocytes. Aggrecanase-2 (ADAMTS-5) was found to be involved in aggrecan breakdown during EO, the mRNA expression of aggrecanase-2 was up-regulated in hypertrophic chondrocytes in response to thyroid hormone (Makihira et al., 2003).

1.5.3 Mineralization in the Growth Plate

Deposition of mineral in the growth plate involves numerous components, including enzymes, calcium binding proteins and integrins, as well as growth factors; however, the process is not fully characterized. Matrix vesicles of cartilage contain primarily in the matrix located between adjacent hypertrophic chondrocytes, and not in the interzone between hypertrophic chondrocytes in the resting zone (Karsan et al., 2000).

Matrix vesicles are small membrane-bound vesicles that are released from hypertrophic chondrocytes and contain various enzymes, including alkaline phosphatase (ALP), and other proteins, including annexin A11, osteocalcin, osteonectin, osteopontin, osteopontin-like protein (OPLP), and osteocalcin-like protein (OLP). They are located in the longitudinal septa of the cartilage growth plate. Matrix vesicles may be a source of increased cytosolic calcium concentration, contributed to by annexin forming calcium channels in the vesicle membrane (Wang and March, 2002). Matrix vesicles exhibit calcium channel activities resulting in matrix vesicles being loaded with calcium during the initial phase of mineralization. Type V collagen is able to bind to annexin V, and it has been suggested that this may be the mechanism by which vesicles in the extracellular matrix are loaded with calcium.

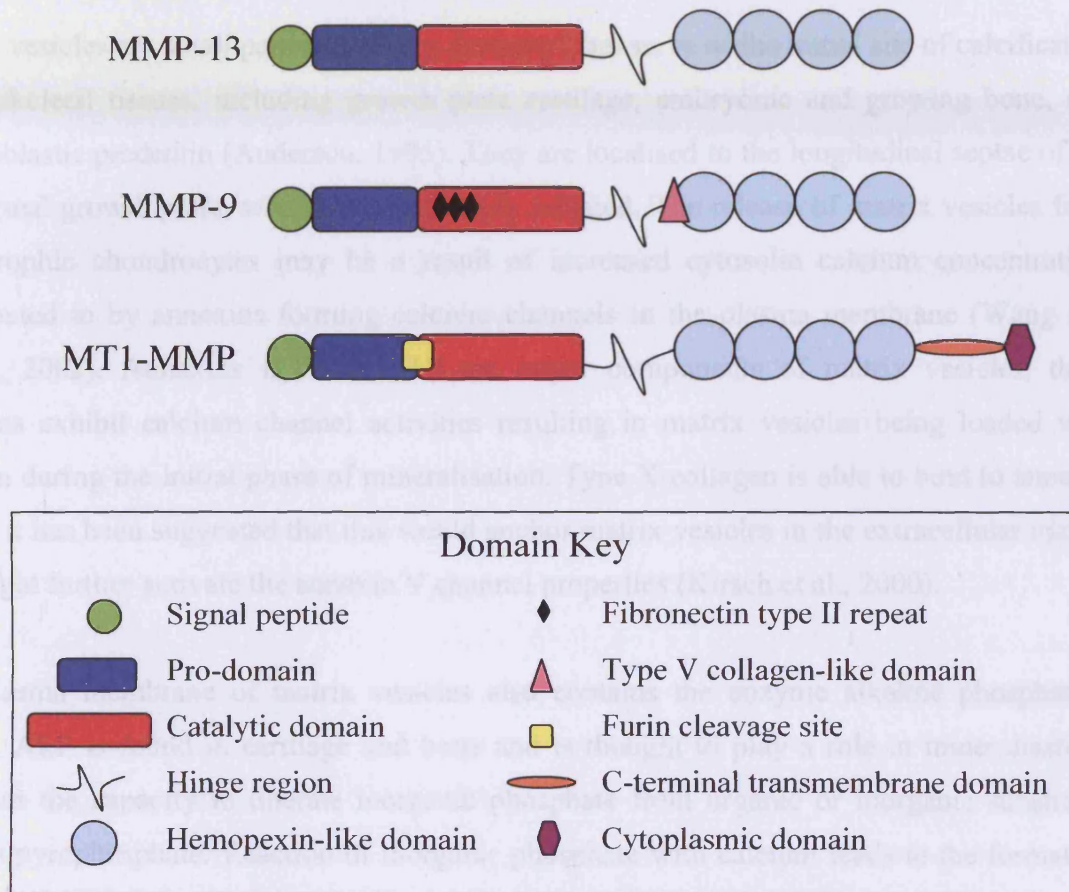


Figure 1.15: Schematic illustration of the MMPs involved in endochondral ossification, different functional domains are highlighted, (adapted from Somerville et al. 2003).

1.5.3 Mineralisation in the Growth Plate

Deposition of mineral in the growth plate involves numerous components, including enzymes, calcium binding proteins and membrane ion transport mechanisms, however the process is not fully characterised. Mineralisation of cartilage occurs primarily in the matrix located between adjacent hypertrophic chondrocyte columns, and not in the interzone between hypertrophic chondrocytes in the same column (Johnstone et al., 2000).

Matrix vesicles are small particles (50nm diameter) that serve as the initial site of calcification in all skeletal tissues, including growth plate cartilage, embryonic and growing bone, and odontoblastic predentin (Anderson, 1995). They are localised to the longitudinal septae of the epiphyseal growth plate, where calcification is initiated. The release of matrix vesicles from hypertrophic chondrocytes may be a result of increased cytosolic calcium concentration, contributed to by annexins forming calcium channels in the plasma membrane (Wang and Kirsch, 2002). Annexins II, V and VI are major components of matrix vesicles, these annexins exhibit calcium channel activities resulting in matrix vesicles being loaded with calcium during the initial phase of mineralisation. Type X collagen is able to bind to annexin V, and it has been suggested that this would anchor matrix vesicles in the extracellular matrix and might further activate the annexin V channel properties (Kirsch et al., 2000).

The plasma membrane of matrix vesicles also contains the enzyme alkaline phosphatase (ALP). ALP is found in cartilage and bone and is thought to play a role in mineralisation. ALP has the capacity to liberate inorganic phosphate from organic or inorganic substrates such as pyrophosphate. Reaction of inorganic phosphate with calcium leads to the formation of hydroxyapatite. ALP is expressed by hypertrophic chondrocytes of the growth plate, the intensity of which increases towards the chondro-osseous junction. ALP expression precedes calcification. It has been suggested that ALP is released from hypertrophic chondrocytes in the matrix vesicles, however calcification of the matrix in the upper hypertrophic zone is inhibited by matrix components such as aggrecan (Mundlos, 1994).

The role of PG's in the calcification process is not definitive. In vivo, PGs such as aggrecan may bind calcium via their chondroitin sulphate chains. This could promote hydroxyapatite formation, ALP mediates a local phosphate concentration increase, phosphate causes displacement of calcium, thus raising the calcium phosphate product above the threshold required for hydroxyapatite precipitation (Poole et al., 1989). The role of PG's as promoters

of calcification is supported by the observation that calcification is not always initiated within matrix vesicles. Calcification has been observed, in discrete focal sites containing aggrecan and chondrocalcin, which is derived from the C-terminus propeptide of type II collagen. Chondrocalcin is able to bind to annexin V and accumulates in calcifying cartilage (Kirsch and Pfaffle, 1992). However, contradictory in vitro studies on hydroxyapatite formation suggests that PGs are inhibitors of calcification (Hunter, 1991).

Initially, mineral crystals form within the matrix vesicles, they grow and increase in number and eventually penetrate the matrix vesicle membrane. The rate of crystal growth and proliferation is then dependant on the conditions of the extra-vesicular matrix. If the extracellular levels of calcium and phosphate are sufficient then continued nucleation of HA crystals on HA templates takes place (Anderson, 2003). Potentially, the type II and X collagens associated with the outer surface of the matrix vesicles may serve as a bridge for crystal propagation out into the extra-vesicular matrix (Wu et al., 1991).

A study involving isolated matrix vesicles from chicken growth plate cartilage found that the vesicles contained active MMP-2, -9 and -13, they also contained latent and active TGF- β , thought to be activated by MMP-13 (D'Angelo et al., 2001). In another study MMP-3 from matrix vesicles was implicated in the release of the large latent complex from TGF- β 1, hence activating it (Maeda et al., 2002).

1.5.4 Angiogenesis during the Process of EO

Angiogenesis of growth plate cartilage plays a fundamental role in EO. Blood vessels invade the cartilage from the metaphysis. The endothelial cell invasion induces vascular channel formation in the terminal layer of apoptotic chondrocytes, the newly formed blood vessels bring specialised cell types necessary for bone formation to the region (Gerber and Ferrara, 2000).

1.5.4.1 Vascular Endothelial Growth Factor

Vascular endothelial growth factor (VEGF) is an angiogenic growth factor which plays a role in the control of blood vessel development. VEGF and its receptors are expressed by chondrocytes in the hypertrophic cartilage (Carlevaro et al., 2000). It has been suggested that VEGF controls at least three aspects of bone development. First, it induces angiogenesis in the perichondrial regions of cartilage templates in the endochondral skeleton. Second, it

stimulates angiogenesis and chemotactic migration of osteoclastic cells into hypertrophic cartilage. Finally, it stimulates bone formation by increasing the activity of osteoblasts in endochondral bones (Zelzer et al., 2002). An essential role for VEGF in growth plate angiogenesis was demonstrated by systemic administration of a soluble receptor to VEGF to 24 day old mice. The treatment led to suppression of blood vessel invasion, impaired trabecular bone formation, expansion of hypertrophic chondrocyte zone and a decrease in cell recruitment (Gerber et al., 1999).

1.5.4.2 Connective Tissue Growth Factor

CTGF is highly expressed by hypertrophic chondrocytes, it may promote EO by acting on many cell types, including chondrocytes, osteoblasts and endothelial cells. CTGF has stimulatory effects on the proliferation, maturation and hypertrophy of cultured chondrocytes. The replacement of cartilage with bone may be promoted by the stimulatory effect that CTGF has on the proliferation and differentiation of osteoblasts. The migration and proliferation of vascular endothelial cells is stimulated by CTGF, thus, it may induce angiogenesis at the vascular front of the growth plate (Takigawa, 2003). An interaction between CTGF and the tyrosine kinase-type receptor ErbB4 in chondrocytes has been identified, raising the possibility that CTGF may transduce signals into the cells through a phosphorylation cascade (Nawachi et al., 2002). As well as this paracrine action of CTGF, a processed sub-fragment may act intracellularly and reduce proliferation and apoptosis of hypertrophic chondrocytes (Takigawa, 2003). CTGF was demonstrated to bind to an isoform of VEGF through a protein-protein interaction, and could negatively regulate the angiogenic activity of VEGF in the extracellular environment (Inoki et al., 2002).

1.6 Aims and Objectives of the Project

1.6.1 Background and Hypothesis

The ultrastructural organisation of hypertrophic cartilage found in the epiphyseal growth plate is not well understood. The prominent collagen type in this region is type X collagen, which is only expressed by prehypertrophic and hypertrophic chondrocytes. Despite being the subject of many studies during the last 20 years, characterising the molecular interactions of type X collagen and defining a precise function has remained elusive. Due to the temporal and spatial expression of type X collagen in the epiphyseal growth plate, it has been associated with the process of EO. Interactions of type X collagen with other components of the ECM are likely to be of importance in assembling and maintaining the correct matrix in hypertrophic cartilage. This in turn is essential for the correct remodelling, angiogenesis and calcification seen during EO.

The significance of the SLRP family of proteoglycans in collagen biology has been highlighted in SLRP-deficient animals. The most characterised members of this family decorin and biglycan, have been traditionally thought of as being associated with the fibrillar collagens. However, recent studies have demonstrated that these proteoglycans also interact with non-fibrillar collagens as well as with a wide variety of other proteins and molecules including growth factors and hydroxyapatite. The potential involvement of biglycan and decorin in mineralisation processes has been noted and discussed.

The work in this thesis therefore addresses the hypothesis that type X collagen interacts with decorin and/or biglycan within hypertrophic cartilage and plays a role in regulating the process of EO.

1.6.2 Aims and Objectives

The overall aim of the project was to characterise interactions of type X collagen which occur in hypertrophic cartilage using multidisciplinary approaches including biochemical, molecular and morphological analyses. Knowledge of the molecular interactions involving type X collagen, may assist our understanding of the ultrastructural organisation of this dynamic tissue during the process of EO.

1.6.2.1 Specific objectives:

- Develop a solid phase assay to study interactions.
- Characterise interactions by surface plasmon resonance.
- Visualise interactions using labelled gold probes and transmission electron microscopy.
- Produce recombinant proteins to determine which molecular domains are involved in the interactions.
- Investigate in vivo expression and localisation of interacting partners in the epiphyseal growth plate.

Chapter 2: Generation of Reagents for Interaction Analysis

2.1 BACKGROUND

2.1.1 Native Type X Collagen

To study the molecular interactions of type X collagen, relatively large quantities (in the mg range) of purified type X collagen were required. Chick collagen X can be readily isolated from spent culture medium of hypertrophic chondrocytes (Barber and Kwan, 1996). Collagen X purified from this source was used throughout the course of this study. Chick type X collagen is highly homologous to human type X collagen; they share high sequence identity at the amino acid level, for the NC2 domain 55.4%, for the triple helical domain 74.8% and for the NC1 domain 77.7% (Thomas et al., 1991). Native type X collagen prepared from this source was enzymatically digested to isolate different regions of the type X collagen molecule. These isolated domains were then used in the same interaction analyses as the whole type X collagen molecule, and gave some indication of the regions most important for the interactions.

2.1.2 Recombinant NC1 Domain

Recombinant human NC1 domain expressed in *Escherichia coli* (*E. coli*) was purified from bacterial cultures and was used in the interaction studies. The QIAexpress system (Qiagen) was the method of choice for expression, purification and detection of recombinant proteins. The vectors are designed to place an affinity tag of 6 consecutive histidine residues (6xHis-tag) at the N-terminus of the protein of interest. The 6xHis-tag rarely interferes with the secretion or the structure and functions of fusion proteins, and can be used for purification purposes (QIAGEN, 2003).

2.1.3 Decorin and Biglycan Sources

Commercially available recombinant human decorin (EMP Genetech) was used in interaction analyses. This protein is synthesised without tags from a eukaryotic vector in a human cell line, it is obtained in a secreted form from the culture supernatant. Human cell lines are the best host for the expression of recombinant human proteins, especially proteoglycans, because they produce the same post-translational modifications and recognise the same signals for synthesis, processing and secretion. Biglycan purified from bovine articular cartilage (Sigma)

was also used in interaction analyses. These sources will be used for the proteoglycans due to the large amount of material required to perform interaction analyses.

2.2 MATERIALS AND METHODS

All tissue culture reagents were obtained from Gibco Invitrogen Corporation, all other reagents were obtained from Sigma unless otherwise stated.

2.2.1 Purification of Type X Collagen

2.2.1.1 *Hypertrophic Chondrocyte Culture - Tissue Preparation*

Tibial epiphyses were removed from 17-day-old embryonic White Leghorn chicks under sterile conditions. The hypertrophic cartilage zone was removed from the epiphyseal plate using a scalpel. Tissue was placed into washing medium, Dulbecco's Modified Eagles Medium (DMEM) containing 5 mM HEPES buffer, 0.5 mM sodium pyruvate and 50 µg/ml gentamicin. Medium was changed three times to remove blood and serum. To release the cells from the ECM; tissue was incubated at 37°C for 1.5 hours with washing medium containing a final concentration of 3 mg/ml bacterial collagenase type 1A and 0.03% (w/v) trypsin solution.

2.2.1.2 *Hypertrophic Chondrocyte Culture - Cell Preparation*

The cell suspension was separated from tissue debris by brief centrifugation at 392 x g for 30 seconds. The cells were pelleted from the suspension by centrifugation at 392 x g for 4 minutes. The pellet was re-suspended in 10 ml of culture medium, DMEM containing 10% (v/v) foetal calf serum, 5 mM HEPES buffer, 0.5 mM sodium pyruvate, 50 µg/ml gentamicin, 0.25 µg/ml fungizone, 0.5 mM glutamine and 0.1 mg/ml ascorbate (Fisher Scientific, UK). The pelleting and re-suspending was repeated a further three times, to remove all tissue debris and collagenase. The chondrocytes were plated in a 420 cm² multifloor flask (TPP, Switzerland) and maintained in culture, in an atmosphere of 95% air and 5% carbon dioxide at 37°C. Culture medium was changed after the first 24 hours and every 2-3 days thereafter. Culture medium was collected after 7 days, once a confluent cell layer was established and the cultures were maintained for approximately 4 weeks.

2.2.1.3 *Storage of Collected Medium*

Culture medium was stored at -20°C with protease inhibitors, 25 mM diaminoethanetetraacetic acid disodium salt (Na₂EDTA) (Fisher Scientific, UK), 25 mM ε-amino n-caproic acid

(EACA), 2 mM phenylmethylsulfonylfluoride (PMSF) and 10 mM N-ethylmaleimide (NEM), prior to the purification protocol detailed below.

2.2.1.4 Ammonium Sulphate Precipitation

Stored culture medium was thawed and kept stirring at 4°C. Ammonium sulphate (Fisher Scientific, UK) was added to give 30% (w/v) saturation, over a period of 4-6 hours. The culture medium was allowed to stand overnight at 4°C allowing proteins to precipitate out. The insoluble protein precipitate was spun down at 12,000 x g for 2 hours at 4°C, using a Beckman JLA 10.50 rotor. The pellet was re-suspended in 50 mM Tris-HCl, containing 0.4 M NaCl, pH 7.4, and the supernatant was discarded. The re-suspended proteins were subjected to another 30% (w/v) ammonium sulphate precipitation, left to stand for 4 hours at 4°C and centrifuged as above. The pellet was then stored at -80°C until required.

2.2.1.5 Differential Salt Fractionation

Ammonium sulphate precipitated proteins were re-dissolved in 0.5 M acetic acid (Fisher Scientific, UK). They were dialysed against 0.8 M NaCl in 0.5 M acetic acid overnight at 4°C. The dialysate was centrifuged at 48,000 x g for 1 hour at 4°C, using a Beckman JA 25.50 rotor (Beckman, Germany). The pellet was re-suspended in 0.5 M acetic acid, and dialysed against 0.5 M acetic acid to de-salt, acetic acid was changed three times. This was called the 0.8 M pellet and subsequently freeze dried. The supernatant was dialysed further against 1.2 M NaCl in 0.5 M acetic acid and 2.0 M NaCl in 0.5 M acetic acid and the above procedure was repeated to get a 1.2 M and a 2.0 M pellet, see figure 2.1.

2.2.1.6 Hydroxyproline Assay

A hydroxyproline assay was performed according to the method of (Woessner, 1976) on the samples generated by differential salt fractionation to determine the hydroxyproline content and hence the collagen concentration. Samples were hydrolysed in 6 M HCl for 24 hrs at 110°C. 30 µl of samples or standards were applied in duplicate into the wells of a 96 well microtitre plate. To the wells; 70 µl of diluent (67% (v/v) propan-2-ol) and 50 µl of oxidant (50 mM chloramine T, 83.3% (v/v) stock buffer) (stock buffer 0.42 M sodium acetate trihydrate, 0.13 M tri-sodium citrate dihydrate, 26 mM citric acid, 40% (v/v) propan-2-ol) were added. The plate was placed on a plate shaker at room temperature for 5 minutes. 125 µl of colour reagent (0.7 mM Ehrlich's reagent, 13% (v/v) of 70% perchloric acid, 84.8% (v/v) propan-2-

ol) was added to the wells; mixed briefly on a shaker, then incubate at 70°C for 10-20 minutes. Absorbances of the samples and hydroxyproline standards (from 1-10 µg/ml) were measured at 550nm. The absorbance versus the concentration of standards were plotted on a graph, a function was obtained for the straight line, and subsequently used to calculate hydroxyproline content of the samples. If the samples were outside the range of the standards then the samples were diluted. Collagen content was calculated from the hydroxyproline standard curve using a determined 14% hydroxyproline content for type X collagen.

Differential Salt Fractionation

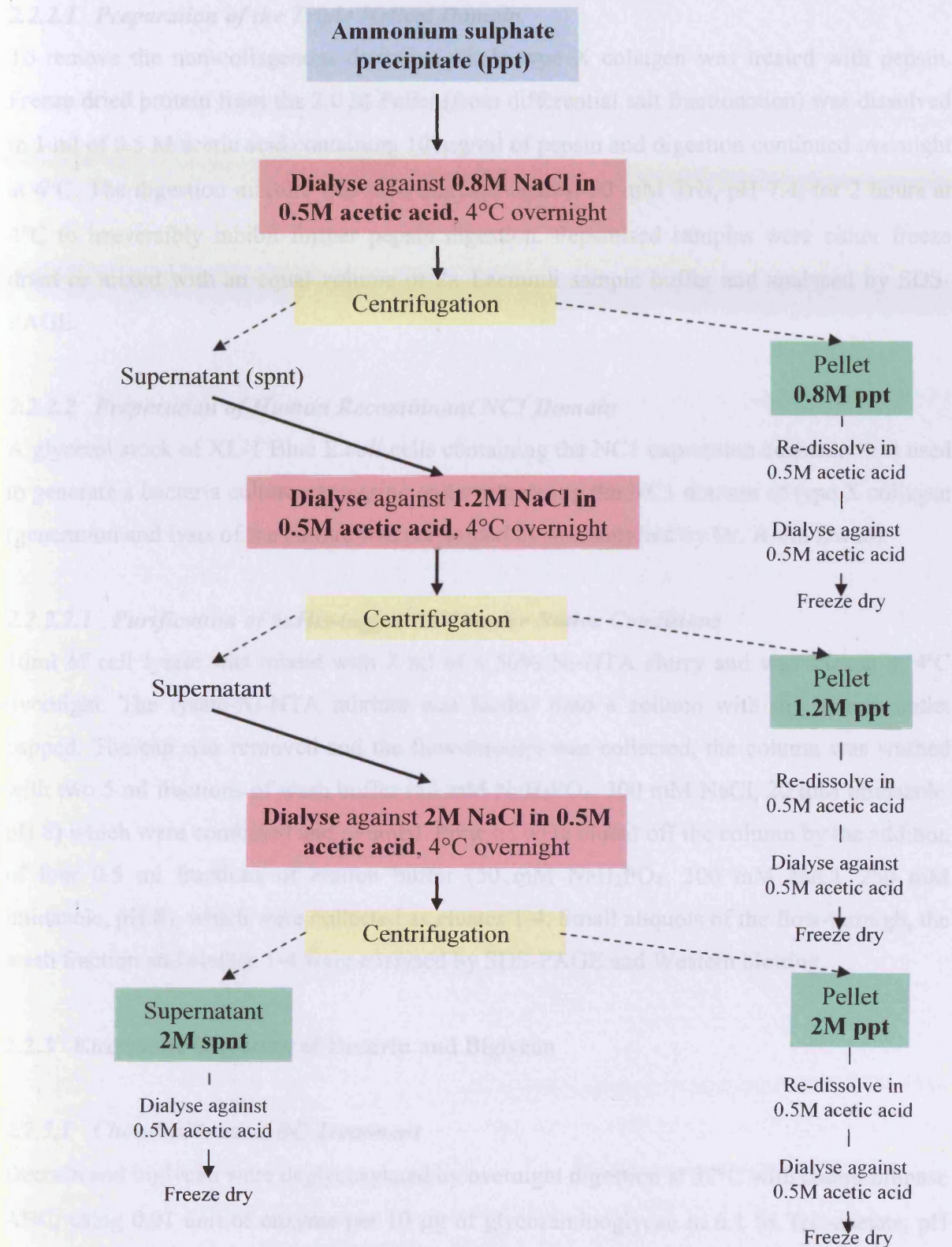


Figure 2.1: Schematic illustration of the steps involved in the differential salt fractionation process of preparing collagen. The 4 samples generated following the process are highlighted in green.

2.2.2 Isolating Different Domains of Type X Collagen

2.2.2.1 Preparation of the Triple Helical Domain

To remove the non-collagenous domains, whole type X collagen was treated with pepsin. Freeze dried protein from the 2.0 M Pellet (from differential salt fractionation) was dissolved in 1 ml of 0.5 M acetic acid containing 100 µg/ml of pepsin and digestion continued overnight at 4°C. The digestion mixture was then dialysed against 50 mM Tris, pH 7.4, for 2 hours at 4°C to irreversibly inhibit further pepsin digestion. Pepsinised samples were either freeze dried or mixed with an equal volume of 2x Laemmli sample buffer and analysed by SDS-PAGE.

2.2.2.2 Preparation of Human Recombinant NC1 Domain

A glycerol stock of XL-1 Blue *E.coli* cells containing the NC1 expression construct was used to generate a bacteria culture expressing and synthesising the NC1 domain of type X collagen (generation and lysis of the culture was performed by and supplied by Dr. Alvin Kwan).

2.2.2.2.1 Purification of 6xHis-tagged NC1 under Native Conditions

10ml of cell lysate was mixed with 2 ml of a 50% Ni-NTA slurry and was shaken at 4°C overnight. The lysate-Ni-NTA mixture was loaded onto a column with the bottom outlet capped. The cap was removed and the flow-through was collected, the column was washed with two 5 ml fractions of wash buffer (50 mM NaH₂PO₄, 300 mM NaCl, 20 mM imidazole, pH 8) which were combined and retained. Proteins were eluted off the column by the addition of four 0.5 ml fractions of elution buffer (50 mM NaH₂PO₄, 300 mM NaCl, 250 mM imidazole, pH 8), which were collected as eluates 1-4. Small aliquots of the flow-through, the wash fraction and eluates 1-4 were analysed by SDS-PAGE and Western blotting.

2.2.3 Enzymatic Digestion of Decorin and Biglycan

2.2.3.1 Chondroitinase ABC Treatment

Decorin and biglycan were deglycosylated by overnight digestion at 37°C with chondroitinase ABC, using 0.01 unit of enzyme per 10 µg of glycosaminoglycan in 0.1 M Tris-acetate, pH 6.5. Deglycosylated decorin and biglycan were then dialysed against PBS for 6 hours with 3 changes of solution. The glycosylation status of decorin and biglycan were then analysed by

SDS-PAGE and Western blotting, and the samples were subsequently used in interaction analysis.

2.2.4 Analysis of Proteins and Proteoglycans

2.2.4.1 Sample preparation

Freeze dried samples obtained from differential salt fractionation during collagen preparation; were dissolved into Laemmli sample buffer containing 10% (v/v) glycerol (Fisher Scientific, UK), 100 mM Tris, 2% (w/v) SDS (Fisher Scientific, UK) and 0.01% (w/v) Bromophenol Blue. Laemmli sample buffer (2x) was added to an equal volume of protein samples already in solution to give a final concentration of 1x sample buffer for analysis. If reduction of samples was required then 5% (v/v) 2-mercaptoethanol was added to the sample. Samples were denatured by heating to 90°C for 15 min before loading onto polyacrylamide gels.

2.2.4.2 Sodium Dodecyl Sulphate PolyAcrylamide Gel Electrophoresis (SDS-PAGE)

SDS-PAGE was used to separate proteins according to their molecular weight (Laemmli, 1970). Resolving gels 1 mm in thickness were prepared by combining the reagents in table 2.1; adding the ammonium persulphate and TEMED last, using the Miniprotean gel apparatus system (Bio-Rad). After polymerisation of the resolving gel, a 4% stacking gel was prepared by combining the reagents in table 2.1, the stacking gel was poured on top of the polymerised resolving gel and a well-creating comb inserted into the stacking gel solution. Once the stacking gel was polymerised between 5-25 µl of protein samples were loaded onto the 4% stacking gel, 5 µl of a molecular weight marker (Bio-Rad) was also loaded. Gels were electrophoresed at 200 volts for 40 minutes in Laemmli running buffer (0.025 M Tris, 0.192 M glycine and 0.1% SDS, pH 8.3) until the dye front reached the bottom of the gel.

2.2.4.3 Coomassie Blue Staining

Gels were removed from electrophoresis apparatus and placed in to Coomassie Blue stain containing: 0.25% (w/v) Coomassie Brilliant Blue R250, 10% (v/v) glacial acetic acid and 45% (v/v) methanol for a minimum of 30 minutes. The gel was incubated on a platform with gentle shaking in approximately 150 ml of stain. Gels were removed from Coomassie Blue stain and destained in 7.5% (v/v) glacial acetic acid and 10% (v/v) methanol, gels were destained overnight or in a shorter period if the destain solution was changed.

| Reagents | Resolving | | | | Stacking |
|---|-------------|-------------|-------------|-------------|--------------|
| | 7.5% | 10% | 12.5% | 15% | 4% |
| 40% (w/v) Acylamide / bisacrylamide (40:1) | 2.7ml | 3.8ml | 4.8ml | 5.5ml | 575 μ l |
| 1 M Tris pH 8.8 | 3.6ml | 3.6ml | 3.6ml | 3.6ml | --- |
| 1 M Tris pH 6.8 | --- | --- | --- | --- | 1.3ml |
| 10% (w/v) SDS | 100 μ l | 100 μ l | 100 μ l | 100 μ l | 50 μ l |
| H ₂ O | 8.2ml | 7.0ml | 6.4ml | 4.4ml | 4.1ml |
| 10% (w/v) Ammonium Persulphate | 73 μ l | 73 μ l | 73 μ l | 73 μ l | 37.5 μ l |
| TEMED | 15 μ l | 15 μ l | 15 μ l | 15 μ l | 7.5 μ l |

Table 2.1: Reagents used to make up resolving and stacking gels required for SDS-PAGE.

2.2.4.4 Western Blotting (Towbin *et al.*, 1979)

2.2.4.4.1 Preparation of Membrane

A nylon filter (Immobilon PVDF Millipore), referred to from herein as a membrane, was cut to the size of a Miniprotean mini-gel. The membrane was soaked in 100% methanol for 30 seconds, incubated in dH₂O to remove excess methanol for 2 minutes, and then equilibrated in Transfer buffer (laemmli running buffer containing 20% (v/v) methanol) for 5 minutes.

2.2.4.4.2 *Transfer of Proteins from Polyacrylamide Gels to Membranes*

Once proteins had been separated on a SDS-PAGE gel, they were transferred onto membranes at 100 volts for 1 hour in Transfer buffer. Miniprotein blotting apparatus (Bio-Rad) was assembled according to the manufacturer's instructions. Briefly, sponges and filter papers were soaked in Transfer buffer before a sandwich of sponge, filter paper, polyacrylamide gel, membrane, filter paper, sponge was assembled in a cassette. The cassette was placed into the blotting apparatus tank with the gel on the side of the negative electrode with respect to the filter. An ice pack was placed in the tank before it was filled with Transfer buffer. On application of a current through the Transfer buffer; negatively charged proteins from the gel were transferred onto the membrane.

2.2.4.4.3 *Immuno-probing of Membranes*

Membranes were removed from the blotting apparatus and were blocked for 1 hour with blocking buffer {Tris Buffered Saline (TBS), 0.15 M NaCl, 0.05 M Tris, pH 8), containing 3% (w/v) skimmed milk powder and 0.05% (v/v) Tween-20 (T-20)}. Membranes were then incubated in the presence of a primary (1°) antibody, the dilution, the diluent and length of incubation varied for primary antibodies and is detailed in table 2.2. The membrane was then washed three times for 10 minutes each time with a large volume (approximately 200 ml) of TBS containing 0.05% Tween-20. The membrane was then incubated in the presence of the appropriate secondary (2°) antibody conjugated with the enzymes either horse radish peroxidase (HRP) or alkaline phosphatase (AP). Details of the dilutions, the diluents and length of incubations are detailed in table 2.2. The membrane was washed as above, prior to detection of immunoreactive bands as described in section 2.2.4.4.5

Antibodies used during this study include:-

MA3, a monoclonal antibody raised against chick type X collagen, which recognises an epitope in the triple helical region of the molecule (supplied by Dr. Alvin Kwan, Cardiff University, UK).

AVT-6E3, a monoclonal antibody raised against a human type II collagen cyanogen bromide peptide (Young et al., 2002) (supplied by Prof. Vic Duance, Cardiff University, UK).

28.4, a monoclonal antibody raised against decorin (supplied by Dr. Clare Hughes, Cardiff University, UK)

PR-1, a monoclonal antibody recognizing a biglycan C-terminal epitope (Rees et al., 2000) (supplied by Dr. Clare Hughes, Cardiff University, UK)

Penta His antibody (Qiagen)

Sheep anti-mouse (S α M) HRP secondary antibody (Sigma), diluted in TBS containing 0.05% Tween-20.

Anti-mouse AP (Sigma), diluted in TBS containing 0.05% Tween-20 and 1% milk.

| 1° Antibody (dilution) | Diluent (of 1° Antibody) | 2° Antibody (dilution) |
|----------------------------------|-----------------------------|--------------------------------|
| MA3 (anti-type X) (1:10,000) | TBS, 0.05% T-20, 1% milk | S α M HRP (1:20,000) |
| AVT-6E3 (anti-type II) (1:10) | TBS, 0.05% T-20 | S α M HRP (1:20,000) |
| 28.4 (anti-decorin) (1:100) | TBS, 0.05% T-20, 1% milk | S α M HRP (1:20,000) |
| PR-1 (anti-biglycan) (1:50) | TBS, 0.05% T-20, 1% milk | S α M HRP (1:20,000) |
| Anti –His (1:5000) | TBS, 3% milk | S α M HRP (1:20,000) |
| | | S α M AP (1:30,000) |

Table 2.2: Combinations of primary and secondary antibodies used during this study along with their dilutions.

2.2.4.4.5 *Detection of Immunoreactive Bands*

2.2.4.4.6 *Enhanced Chemiluminescence (ECL) Detection*

ECL TM Western blotting is a light emitting non-radioactive method for detection of immobilised specific antigens, conjugated directly or indirectly with HRP labelled antibodies. Membranes were rinsed with distilled water, equal volumes of ECL reagents 1 and 2 (Amersham Biosciences) were then applied to the membrane for 2 minutes. Excess ECL reagents were removed from the membrane by blotting the membrane onto tissue paper. The membrane was sealed into a polythene bag and exposed to ECL Hyperfilm (Amersham) for

variable exposure times, from 15 minutes to overnight. Films were developed using a standard film developing protocol.

2.2.4.4.7 *NBT/BCIP Detection*

Nitro Blue Tetrazolium/-bromo-4-chloroindol-3-yl phosphate (0.48 mM NBT, 0.56 mM BCIP, 10 mM Tris and 59.3 mM MgCl₂, pH 9.2) alkaline phosphatase substrate (Sigma) was used to reveal immunoreactive bands. This ready-to-use buffered substrate for use in immunoblotting produces an insoluble dark blue-purple end product when it comes into contact with AP conjugated antibodies used in the detection of specific antigens. Membranes were rinsed with distilled water; the substrate was applied to the membrane for up to 30 minutes to allow colour development of immunoreactive bands. The membrane was then rinsed with distilled water to remove substrate and to stop further colour development.

2.3 RESULTS

2.3.1 Purification of Type X Collagen

Spent culture medium from chick hypertrophic chondrocyte cultures was subjected to a 30% ammonium sulphate precipitation. This method is a cheap and effective way of precipitating proteins out of solution, the salt attracts water molecules away from the proteins causing them to aggregate and fall out of solution. The ammonium sulphate precipitate was then re-suspended and subjected to a differential salt fractionation at acid pH. This method relies on the fact that different collagen types have different solubilities. The salt fractions prepared by differential salt fractionation (0.8 M ppt, 1.2 M ppt, 2 M ppt and 2 M spnt), were analysed by SDS-PAGE and Western blotting.

2.3.2 Analysis of Salt Fractions by SDS-PAGE

Samples were separated by SDS-PAGE on a 10% polyacrylamide gel and visualised by Coomassie brilliant blue staining (figure 2.2), approximately 5 µg of each sample was loaded. Non-reduced samples figure 2.2 (a) and reduced samples figure 2.2 (b) were run on separate gels. Type II collagen α chains can be seen in lanes 2 to 4 just below the 150 kDa molecular weight marker, as expected type II collagen has been precipitated at 0.8 M NaCl. There is a prominent band in lanes 5 and 9 around the 75 kDa molecular weight marker, this is likely to be type X collagen as the band is not affected by reduction. Type X collagen appears to have precipitated at 1.2 M NaCl and 2 M NaCl.

2.3.3 Confirmation of Collagen Types by Western Blotting

The samples that are shown in figure 2.2 were analysed by Western blotting. A monoclonal antibody raised against chick type X collagen, MA3, which recognises a region in the triple helical domain was used for detection of type X collagen. The monoclonal antibody AVT-6E3 which is raised against human type II collagen, was used for detection of type II collagen, see figure 2.3.

The high molecular weight bands just above the 250 kDa weight marker and between the 100 and 150 kDa markers seen in lanes 2-4 of figure 2.2 were confirmed to be type II collagen by Western blotting. Figure 2.3 (a) shows the α (II) chain just below the 150 kDa marker, and also shows less prominent bands above the 250 kDa marker, these could be type II procollagen as they are shown to be reducible, figure 2.2 (b). This blot confirms that there is

no type II collagen contamination in the 1.2 and 2 M ppt's, or in the 2 M spnt. The primary antibody negative control blot which was performed alongside the test blot contained no bands (not shown), confirming the specificity of the type II bands.

The Western blot for type X collagen shows the presence of type X collagen in all the fractions prepared by differential salt fractionation, figure 2.3 (b). The 0.8 M ppt fractions (lanes 2-4) contain a prominent band at around 75 kDa but also contain higher molecular weight bands, one between the 150 and 250 kDa weight markers and the other above the 250 kDa weight marker. These bands are probably high molecular weight aggregates of type X collagen and can also be seen in the other fractions. The type X collagen bands seen in the 1.2 M ppt in lane 5 and the 2 M ppt in lane 9 are more prominent, and the appearance of smearing between the bands is evidence that the film has been over exposed for the levels of type X collagen in the samples. There is also a feint band at around 75 kDa in the 2 M spnt sample in lane 12, the levels of type X collagen in this sample are probably lower as there are no high molecular weight aggregates present, and this band is not visible in the Coomassie stained gels (figure 2.2). The primary antibody negative control blot which was performed alongside the test blot contained no bands (not shown), confirming the specificity of the type X bands.

A preparation of type X collagen was sufficiently purified, when Western blot analysis demonstrated a lack of type II collagen in the sample. A hydroxyproline assay was subsequently performed on the sample to determine the type X collagen concentration.

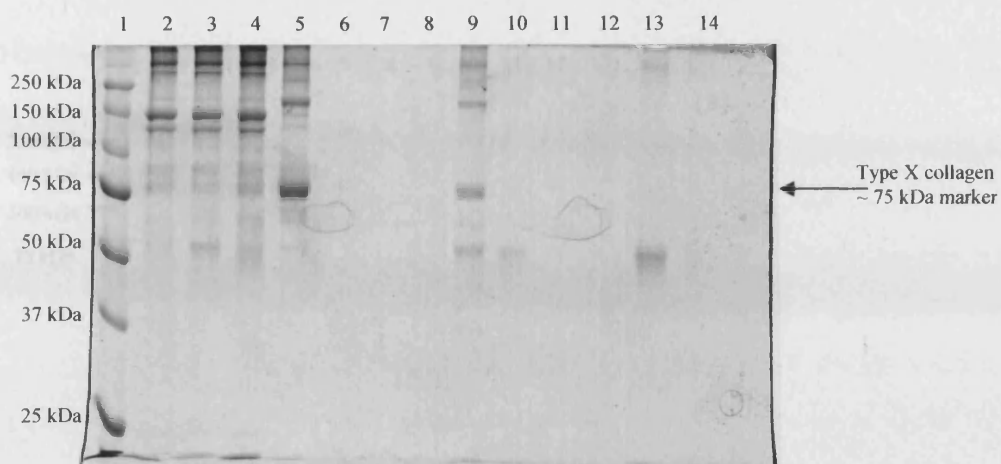


Figure 2.2 (a): SDS-PAGE analysis of samples generated by differential salt fractionation. All samples are non-reduced, 10 μ l loaded. Lane 1: Molecular weight ladder, lanes 2-4: 0.8 M ppt, lane 5: 1.2 M ppt, lane 9: 2 M ppt, lanes 10, 13 & 14: 2 M spnt.

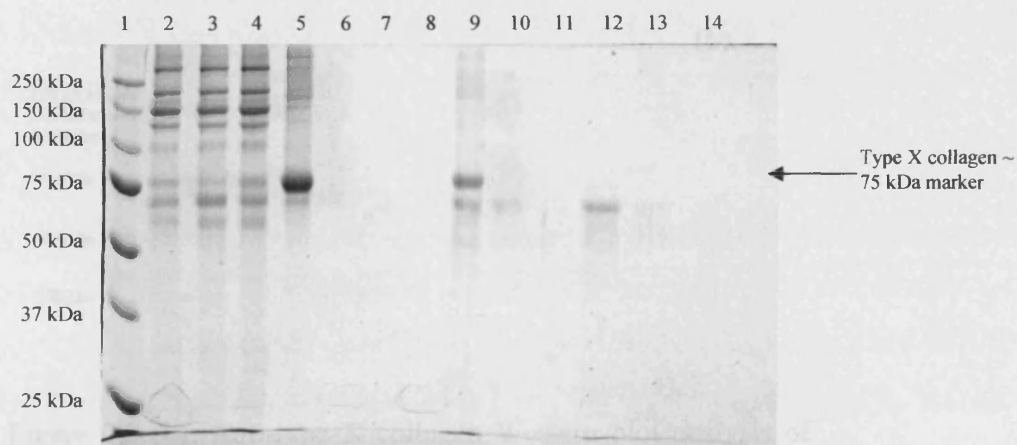


Figure 2.2 (b): SDS-PAGE analysis of samples generated by differential salt fractionation. All samples are reduced with 1% 2-mercaptoethanol, 10 μ l loaded. Lane 1: Molecular weight ladder, lanes 2-4: 0.8 M ppt, lane 5: 1.2 M ppt, lane 9: 2 M ppt, lanes 10, 12 & 13: 2 M spnt.

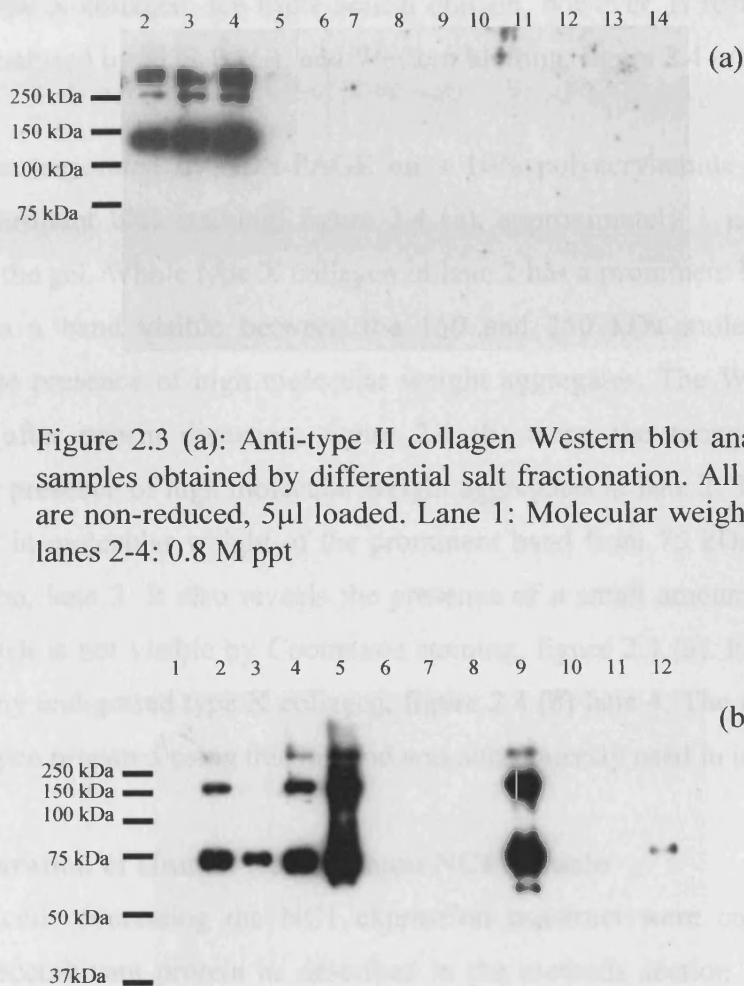


Figure 2.3 (a): Anti-type II collagen Western blot analysis of samples obtained by differential salt fractionation. All samples are non-reduced, 5 μ l loaded. Lane 1: Molecular weight ladder, lanes 2-4: 0.8 M ppt

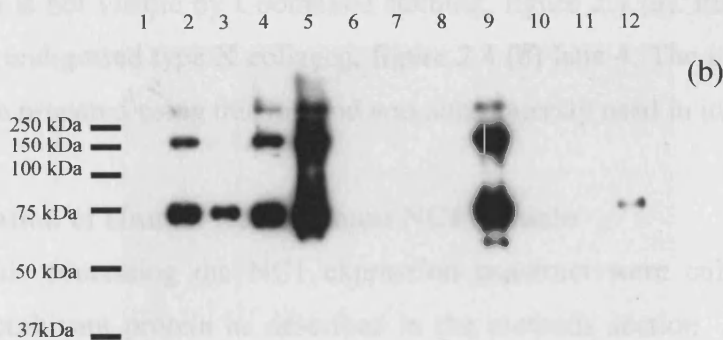


Figure 2.3 (b): Anti-type X collagen Western blot analysis of samples obtained by differential salt fractionation. All samples are non-reduced, 5 μ l loaded. Lane 1: Molecular weight ladder, lanes 2-4: 0.8 M ppt, lane 5: 1.2 M ppt, lane 9: 2 M ppt, lane 12: 2 M spnt.

2.3.4 Preparation of the Triple Helical Domain of Type X Collagen

Type X collagen isolated from culture medium by ammonium sulphate precipitation and differential salt fractionation, was digested with the enzyme pepsin, as detailed in the methods, see section 2.2.2. Pepsin is an acidic protease which will digest the non-collagenous regions of type X collagen, the triple helical domain, however, is resistant to digestion. The digest was analysed by SDS-PAGE and Western blotting, figure 2.4 (a) & (b).

Samples were separated by SDS-PAGE on a 10% polyacrylamide gel and visualised by Coomassie brilliant blue staining, figure 2.4 (a), approximately 1 μ g of each sample was loaded onto the gel. Whole type X collagen in lane 2 has a prominent band at around 75 kDa, there is also a band visible between the 150 and 250 kDa molecular weight markers, indicating the presence of high molecular weight aggregates. The Western blot of samples before and after pepsin digestion, figure 2.4 (b) using the monoclonal antibody MA3, confirms the presence of high molecular weight aggregates in lane 2. The Western blot shows the decrease in molecular weight of the prominent band from 75 kDa to just above 50 kDa after digestion, lane 3. It also reveals the presence of a small amount of undigested type X collagen which is not visible by Coomassie staining, figure 2.4 (a). Further pepsin digestion eliminates any undigested type X collagen, figure 2.4 (b) lane 4. The triple helical domain of type X collagen prepared using this method was subsequently used in interaction analysis.

2.3.5 Preparation of Human Recombinant NC1 Domain

XL-1 Blue cells containing the NC1 expression construct were cultured and induced to synthesise recombinant protein as described in the methods section. An *E. coli* lysate was prepared under native conditions, the lysate was combined with Ni-NTA agarose and 6xHis-tagged proteins were purified using a column procedure. Small aliquots of the flow-through, the wash fraction and eluates 1-4 were combined with 3x Laemmli sample buffer, to yield a final concentration of 1x sample buffer and were analysed by SDS-PAGE and Western blotting.

2.3.5.1 Analysis of Recombinant NC1 by SDS-PAGE and Western Blotting

Samples were reduced with 5% 2-mercaptoethanol prior to analysis. 15 μ l of each sample (eluates 1-4) were loaded on 10% gels with and without heat denaturation. 15 μ l of each sample was loaded on to the gel. The Coomassie stained gel figure 2.5 (a), reveals the presence of distinct bands in eluates 3 and 4 (lanes 7, 8, 11 & 12), a distinct band between the

37 and 50 kDa molecular weight markers can be seen in both samples. The expected molecular weights of the NC1 trimer, dimer and monomer are approximately 50 kDa, 38 kDa and 20 kDa, respectively. Distinct bands can be seen in eluates 3 and 4 (lanes 7 & 8) just below the 25 kDa molecular weight marker; which are not present in the samples which have not been heat denatured (lanes 11 & 12).

These bands were confirmed to be His-tagged proteins by Western blot analysis using a penta-His antibody. Two different detection methods were used; the substrate BCIP/NBT was used in combination with an AP conjugated secondary, figure 2.5 (b) and ECL detection was used in combination with a HRP conjugated secondary, figure 2.5 (c). Both blots confirm the presence of recombinant NC1 in eluates 3 and 4 (lanes 7, 8 11 & 12), with the samples that had been heat denatured samples (lanes 7 & 8) also having lower molecular weight bands.

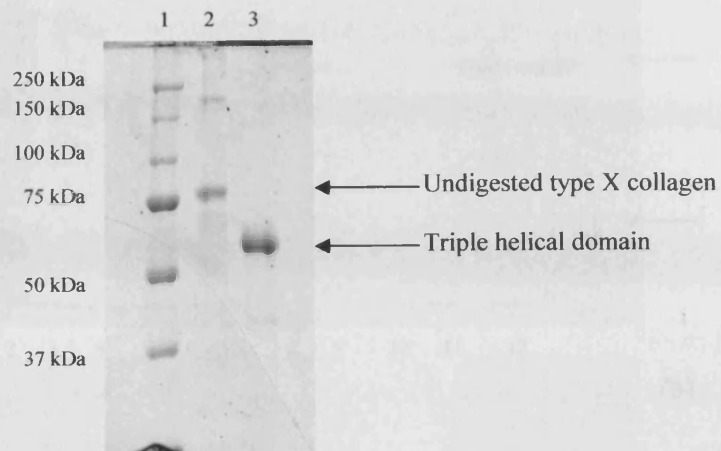


Figure 2.4 (a): SDS-PAGE analysis of the 2 M ppt sample generated by differential salt fractionation. Lane 1: molecular weight ladder, lane 2: undigested type X collagen (1 µg), lane 3: pepsinised type X collagen (1 µg).

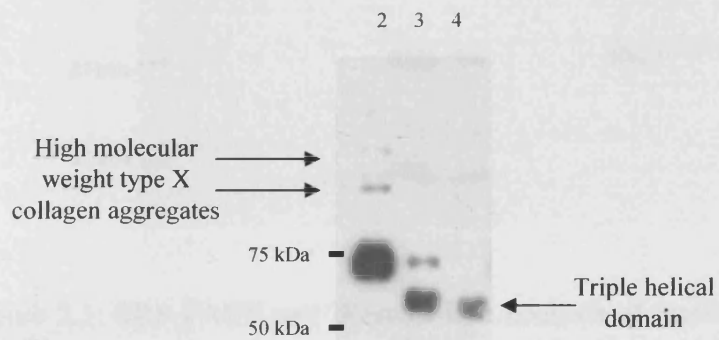


Figure 2.4 (b) Western blot analysis of the 2M ppt sample generated by differential salt fractionation. Lane 2: undigested type X collagen (1 µg), lane 3: pepsinised type X collagen (1 µg), lane 4: double digested type X collagen (1 µg).

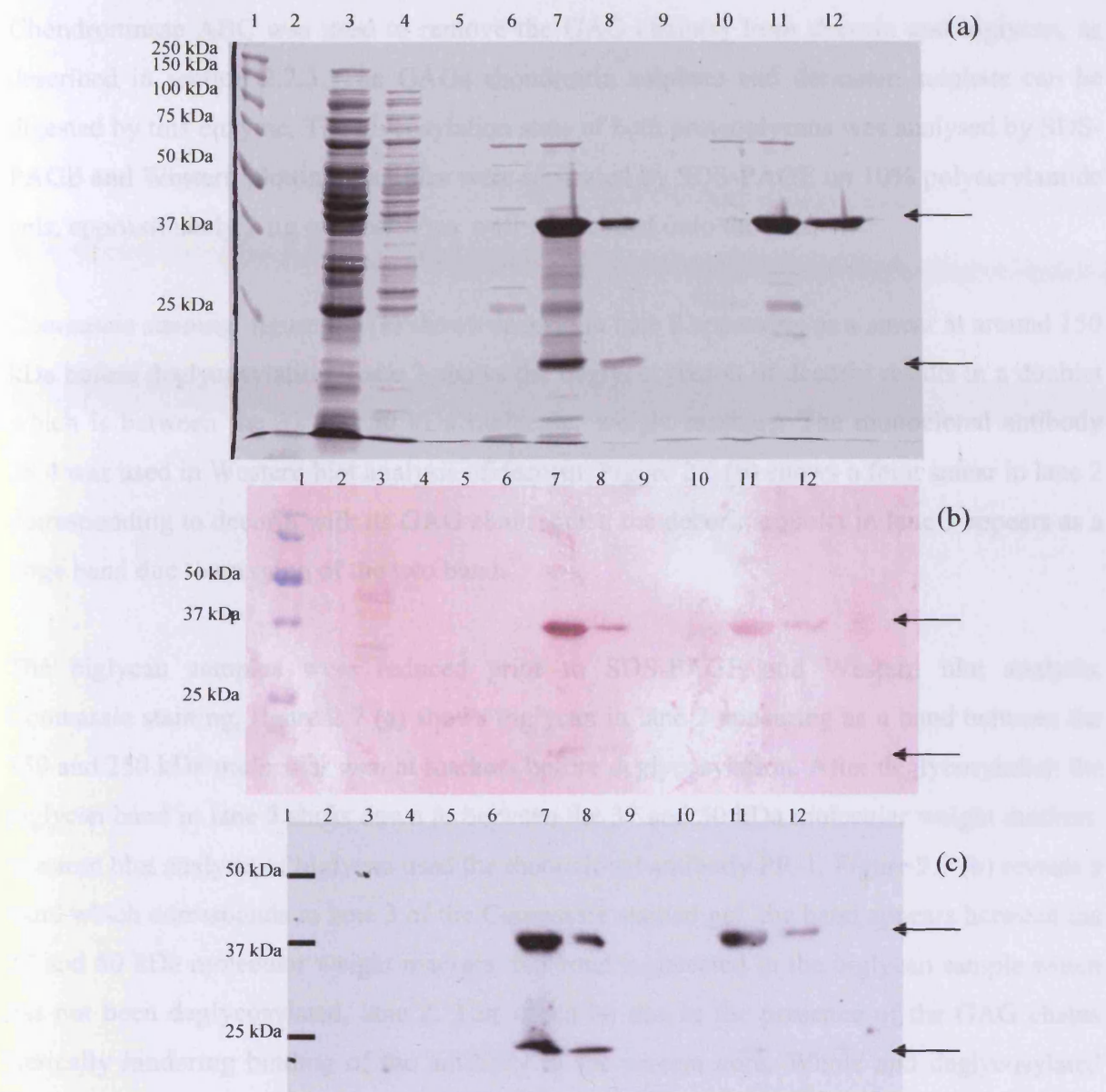


Figure 2.5: SDS-PAGE and Western blot analysis of fractions generated by Ni-NTA agarose column purification. (a) Coomassie stained 10% polyacrylamide gel, lane 1: molecular weight ladder, lane 3: column flow-through, lane 4: column wash, lane 5: eluate 1 (heat-denatured), lane 6: eluate 2 (heat-denatured), lane 7: eluate 3 (heat-denatured), lane 8: eluate 4 (heat-denatured), lane 9: eluate 1, lane 10: eluate 2, lane 11: eluate 3, lane 12: eluate 4. (b) Anti His-tag Western blot analysis of samples as in Coomassie stained gel using BCIP/NBT substrate (c) Anti His-tag Western blot analysis of samples as in Coomassie stained gel using ECL substrate.

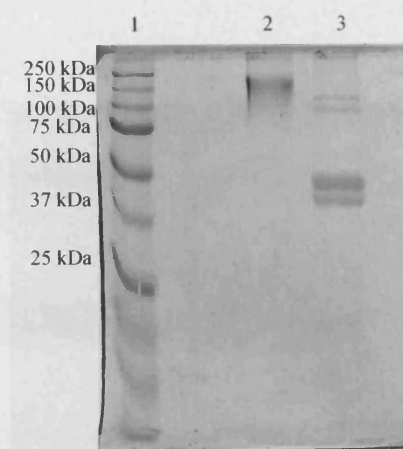
2.3.6 Deglycosylation of Decorin and Biglycan

Chondroitinase ABC was used to remove the GAG chain(s) from decorin and biglycan, as described in section 2.2.3. The GAGs chondroitin sulphate and dermatan sulphate can be digested by this enzyme. The glycosylation state of both proteoglycans was analysed by SDS-PAGE and Western blotting. Samples were separated by SDS-PAGE on 10% polyacrylamide gels; approximately 2 μ g of protein/per well was loaded onto the gels.

Coomassie staining, figure 2.6 (a) shows decorin in lane 2 appearing as a smear at around 150 kDa before deglycosylation. Lane 3 shows the deglycosylation of decorin results in a doublet which is between the 37 and 50 kDa molecular weight markers. The monoclonal antibody 28.4 was used in Western blot analysis of decorin. Figure 2.6 (b) shows a faint smear in lane 2 corresponding to decorin with its GAG chain intact, the decorin doublet in lane 3 appears as a large band due to merging of the two bands.

The biglycan samples were reduced prior to SDS-PAGE and Western blot analysis. Coomassie staining, figure 2.7 (a) shows biglycan in lane 2 appearing as a band between the 150 and 250 kDa molecular weight markers before deglycosylation. After deglycosylation the biglycan band in lane 3 shifts down to between the 37 and 50 kDa molecular weight markers. Western blot analysis of biglycan used the monoclonal antibody PR-1. Figure 2.7 (b) reveals a band which corresponds to lane 3 of the Coomassie stained gel, the band appears between the 37 and 50 kDa molecular weight markers. No band is detected in the biglycan sample which has not been deglycosylated, lane 2. This could be due to the presence of the GAG chains sterically hindering binding of the antibody to the protein core. Whole and deglycosylated decorin and biglycan were used in interaction analysis with type X collagen.

(a)



(b)

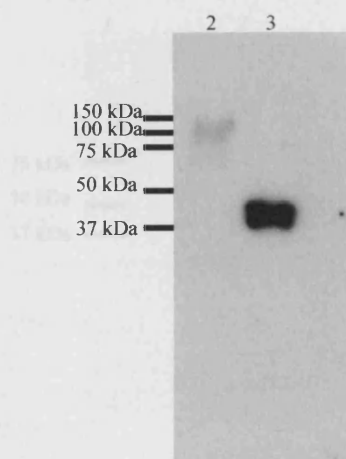
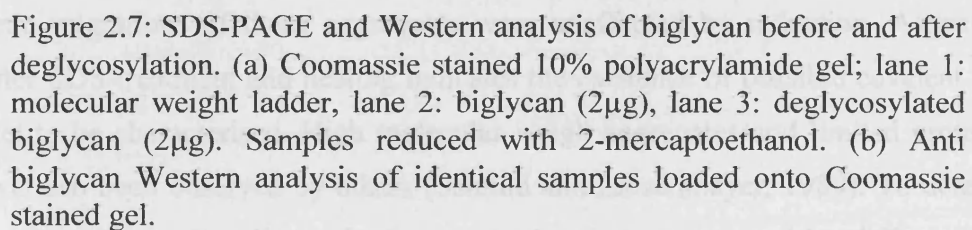


Figure 2.6 : SDS-PAGE and Western analysis of decorin before and after deglycosylation. (a) Coomassie stained 10% polyacrylamide gel; lane 1: molecular weight ladder, lane 2: decorin (2 μ g), lane 3: deglycosylated decorin (2 μ g). Samples are non-reduced. (b) Anti decorin Western analysis of identical samples loaded onto Coomassie stained gel.



2.4 DISCUSSION

Epiphyseal plates of 17-day old embryonic chick tibiae were dissected and used as a source of hypertrophic chondrocytes. Following isolation of hypertrophic chondrocytes from the tissue the cells were maintained in culture. Light microscopy was used to assess the morphology and viability of the cells during the culture period. Culture medium containing all the proteins synthesised and secreted by the cells during culture was collected over a four week period, protease inhibitors were added to the medium to minimise any protein degradation during storage.

Type X collagen was purified from the collected culture medium, using well established techniques. Differential salt fractionation was used to separate type X collagen from other collagen types and proteins synthesised by hypertrophic chondrocytes. The salt fractions were de-salted by dialysing against a large volume of 0.5 M acetic acid, the samples were subsequently freeze dried and resuspended in a small volume of acetic acid. SDS-PAGE and Western blotting were used to detect and confirm the presence of type X collagen and other collagen types in the samples generated by differential salt fractionation. Type X collagen was found in all salt fractions generated; however, the 2 M precipitate was used as the source of type X collagen because of type X collagens predominance and the lack of other collagen types in this fraction. Western blot analysis confirmed there was no type II collagen in the 2 M precipitate. Other minor collagen types produced by chondrocytes, such as type IX collagen are unlikely to be present in the 2 M precipitate in significant quantities, the expression of type X collagen is up-regulated and the expression of other collagen types is down-regulated in hypertrophic chondrocytes.

High molecular weight aggregates of type X collagen were detected in the samples, electrophoretic migrations of these aggregates were unaffected by reduction. Aggregation persisting after SDS-treatment and heating indicates the existence of possible covalent bonds which are yet to be characterised. High molecular weigh aggregates and limited proteolytic products have also been observed by others (Schmid and Linsenmayer, 1989). To determine the concentration of type X collagen in the prepared samples generated by differential salt fractionation, a hydroxyproline assay was performed. The type X collagen preparation was qualitative, cell numbers and medium volume were not closely monitored and there was intra-batch variation in the yields of type X collagen produced. Large quantities of type X collagen

was successfully prepared using this method, contamination from other collagen types was minimal and was monitored by SDS-PAGE and Western blotting. Other potential techniques which could have been utilised to ensure that the type X collagen was pure include immunoprecipitation, however this would not have been efficient for preparative scale work.

Pepsin digestion of the chick native type X collagen was performed to isolate the triple helical domain of type X collagen, a change in molecular weight from 59 kDa for whole type X collagen to 45 kDa for the triple helical domain, was visualised by SDS-PAGE and Western blotting. This was the method of choice for preparing the triple helical domain, as the stability of the triple helix is not compromised and the procedure is simple. Pepsin digestion results in the loss of the high molecular weight aggregates seen in the whole type X collagen sample, indicating the covalent cross-links mentioned above are located in the non helical region. This is consistent with the putative role of NC1 in the aggregation of individual type X collagen molecules to form a hexagonal lattice structure (Kwan et al., 1991). Previous studies have characterised cross-links found in the triple-helical domain. Type X collagen contains the non-reducible lysylpyridinoline cross-link which is frequently associated with type I collagen (Orth et al., 1996).

The NC1 domain of type X collagen was produced recombinantly in XL-1 Blue *E. Coli* cells, a vector with a human NC1 construct was expressed by the cells, the vector also contained a 6x His tag which was utilised to purify type X collagen from all other bacterial proteins. The NC1 was prepared from the cell lysate under non-denaturing conditions. Trimeric NC1 which is heat stable can be seen on the Coomassie stained gel and its identification was confirmed using a 6x His-tag antibody in Western blot analysis. NC1 was also prepared from the native chick whole type X collagen by collagenase digestion. Trimeric, dimeric and monomeric NC1 were separated on a Sephacryl 300 gel filtration column. Characterisation of the NC1 prepared in this way, was not possible due to the lack of availability of an antibody to the NC1 domain. Native chick type X collagen, pepsinised type X collagen and the recombinant NC1 domain were all used in subsequent interaction analysis.

Decorin and biglycan were deglycosylated enzymatically with chondroitinase ABC, which can remove chondroitin and dermatan sulphate chains. As with the type X collagen material, SDS-PAGE and Western blotting were used before and after enzyme treatment to ensure that deglycosylation was complete. Both decorin and biglycan appeared as a diffuse band at ~ 100

– 150 kDa on gels before deglycosylation but became discrete bands of ~ 40 kDa after enzyme treatment. Decorin and biglycan with and without their respective GAG chains were used in interaction analysis with type X collagen.

In summary, the materials required for in vitro interaction analysis have been prepared. Type X collagen was purified from the medium of hypertrophic chondrocyte cultures. Methods used to purify type X collagen included an ammonium sulphate precipitation and a differential salt fractionation. To isolate the triple helical domain type X collagen was subjected to pepsin digestion. Recombinant NC1 domain which contains a 6x His-tag was expressed in *E. Coli*, a Nickel affinity column was used to purify the NC1 domain from an *E. Coli* lysate. Decorin and biglycan were bought from commercial sources and were deglycosylated using chondroitinase ABC. SDS-PAGE and Western blot analysis were used to assess the molecular weights and to confirm the identity of type X collagen, decorin and biglycan.

Chapter 3: Interaction Studies of Type X Collagen with Decorin and Biglycan

3.1 BACKGROUND

A variety of in vitro methods were employed to study interactions of type X collagen with decorin and biglycan.

3.1.1 Molecular Interactions in a Solid Phase Assay

Immunoassays fall within the class of analytic techniques – frequently described as binding, or ligand assays – which rely on observation of the reaction between the target substance (analyte) and a specific binding substance, the latter being generally of biologic origin and typically comprising a specific binding protein (Ekins and Chu, 1997). A solid phase assay based on an immunoassay was developed to study type X collagen interactions with decorin and biglycan. Enzymatic manipulations of the proteins allowed the likely domains involved in the interaction to be elucidated. Solid phase assay systems have been utilised in the past to study the interactions of many extracellular matrix molecules. Examples include COMP with fibronectin (Di Cesare et al., 2002), decorin and biglycan with collagen type VI, collagen types I, II and IX with COMP (Holden et al., 2001; Rosenberg et al., 1998).

In brief, one of the interacting proteins, (A) is bound to a solid support, usually a well in a microtiter plate. Any unoccupied sites on the support are blocked, before the other interacting protein, (B), is incubated with the solid phase immobilised protein A and allowed to bind. An antibody specific for protein B, followed by a secondary antibody, which is enzyme linked, is used to detect protein B. Enzyme linked antibodies are detected and quantitated using a soluble chromogenic substrate which is converted to a soluble coloured product. Enzyme levels are determined by monitoring colour development in a spectrophotometer. Any unbound proteins and antibodies are removed and washed away during the procedure; therefore the colour development at the end is directly related to the interaction occurring between proteins A and B.

Complexity may be added to the assay by incubating protein B with protein A or a different protein C, before incubation with the solid phase protein A. Thus, the interaction between A in the solid phase and B in the liquid phase is being competitively inhibited by the presence of

A or C in the liquid phase. This leads to a decrease in the absorbance readings as a result of less protein B being bound to protein A in the solid phase.

In the assay used to investigate type X collagens interaction with decorin and biglycan, protein A was either decorin or biglycan, protein B was always type X collagen and protein C was either decorin or biglycan. The arrangement of the molecules in a well of a microtitre plate are demonstrated in figure 3.1

3.1.2. Bioluminescence Interaction Analysis (BIA) Technology

Protein A is a protein that binds to the Fc region of antibodies. It is commonly used in immunology to purify antibodies or to immobilize them on a solid support. One of the interactions (the binding of the antibody to the antigen) is detected with additional components. One of the interactions (the binding of the antibody to the antigen) is detected with additional components. One of the interactions (the binding of the antibody to the antigen) is detected with additional components.

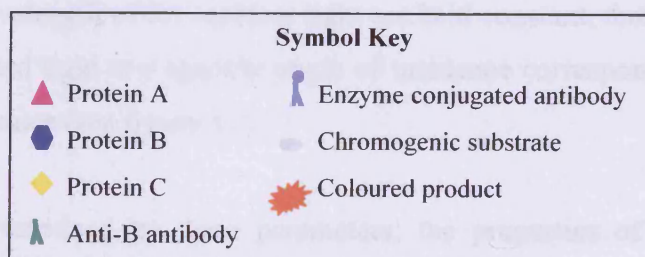
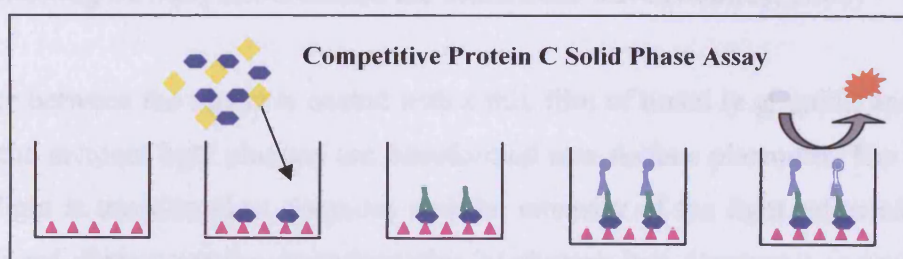
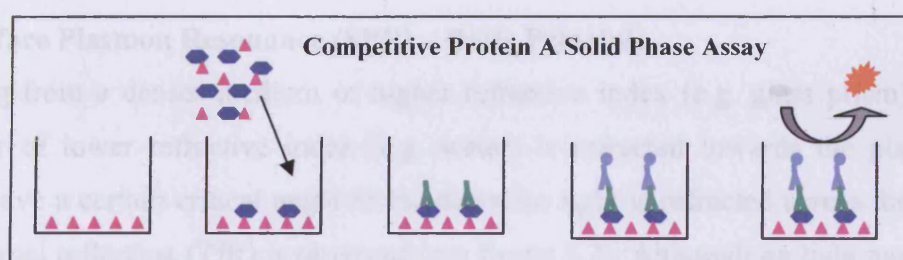
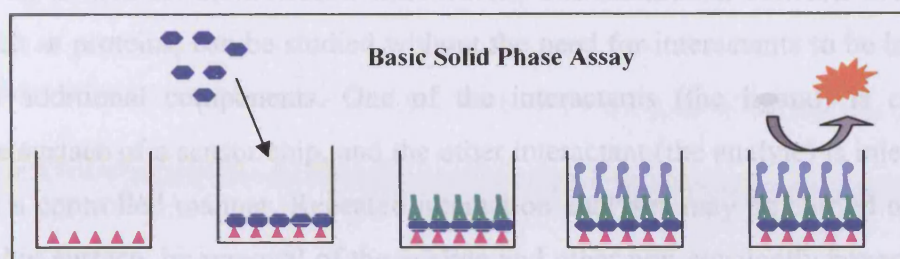


Figure 3.1: Interaction analysis using solid phase assays. Arrangement of protein molecules in a well during basic and competitive solid phase assays.

3.1.2 Biomolecular Interaction Analysis (BIA) Technology

Real-time BIA from Biacore AB, Sweden uses the optical phenomenon of surface plasmon resonance (SPR) to monitor biomolecular interactions. The interaction between two or more molecules, such as proteins, can be studied without the need for interactants to be labelled or detected with additional components. One of the interactants (the ligand) is covalently attached to the surface of a sensor chip, and the other interactant (the analyte) is injected over the surface in a controlled manner. Repeated interaction analyses may be carried out on the same sensor chip surface, by removal of the analyte and other non-covalently bound material with a regeneration step.

3.1.2.1 Surface Plasmon Resonance (SPR) – Basic Principle

Light passing from a denser medium or higher refractive index (e.g. glass prism) to a less dense one or of lower refractive index (e.g. water) is refracted towards the plane of the interface. Above a certain critical angle of incidence no light is refracted across the interface and total internal reflection (TIR) is observed (see figure 3.2). Although no light passes out of the prism, the electric field of the photons extends a short distance (about one wavelength) beyond the reflecting surface; this is termed the evanescent wave (Markey, 2000)

If the interface between the media is coated with a thin film of metal (e.g. gold), and the light is polarized, the incident light photons are transformed into surface plasmons. The energy of the incident light is transferred to plasmons and the intensity of the light reflected from the surface is reduced. Resonance (i.e. transformation of photons into plasmons) occurs when the momentum of the incoming photons is equal to the plasmon momentum. If the metal surface conditions and the wavelength of the incident light are held constant, there will be a dip in the intensity of the reflected light at a specific angle of incidence corresponding to the angle for surface plasmon resonance (see figure 3.3).

The SPR angle is determined by three parameters; the properties of the metal film, the wavelength of the incident light and the refractive index of the media on the other side of the metal film. In BIAcore systems, the metal film properties, wavelength and refractive index of the denser medium (glass) are kept constant, and SPR is used to probe the refractive index of the aqueous layer immediately adjacent to the metal (gold) surface.

The monochromatic light source is focused on the TIR / glass-gold interface of the sensor chip in a wedge shaped beam, giving a fixed range of incident angles. Reflected light is monitored by a two-dimensional diode array. Changes such as biomolecular interactions occurring at the sensor surface change the solute concentration and thus the refractive index within the evanescent wave penetration angle. The alteration in the angle of incidence required to create the SPR phenomenon is measured as a response signal. Plotting the response against time during the course of an interaction provides a quantitative measure of the progress of the interaction – this plot is called a sensogram. SPR response values are expressed in resonance units (RU). One RU represents a change of 0.0001° in the angle of the intensity medium.

3.1.2.2 Sensor Chip Technology

The sensor chip consists of a glass surface, coated with a thin layer of gold. The sensor surface in BIAcore forms one wall of a flow cell, and measurements are made under conditions of continuous liquid flow over the surface. Each sensor chip has 4 flow cells on its surface. The gold surface can be modified with a range of derivatives. The most commonly used sensor chip, CM5, is modified with a carboxymethylated dextran layer. This dextran hydrogel layer forms a hydrophilic environment for attached biomolecules, preserving them in a native state. The most common method for direct immobilisation of ligands is covalent coupling to amino groups in the ligand molecule. The immobilisation procedure is carried out in four steps: 1) activation of carboxyl groups on the sensor surface; 2) attachment of ligand; 3) inactivation of residual active groups; and 4) conditioning of the sensor surface with the regeneration solution.

Other sensor chips include surfaces modified with streptavidin for capture of biotinylated ligands, surfaces modified for capture of ligand via metal chelation and some sensor chips have a matrix free planar surface rather than a dextran matrix. Planar chip surfaces allow interactions to take place closer to the chip surface therefore maintaining sensitivity when large molecules like some of the ECM proteins are being studied. The choice of which interacting component to immobilise depends on whether the investigation involves comparing the interaction of several molecules with a common species, the stability of the molecules – which would be more able to withstand regeneration conditions, the purity of the sample and the size of the molecules involved.



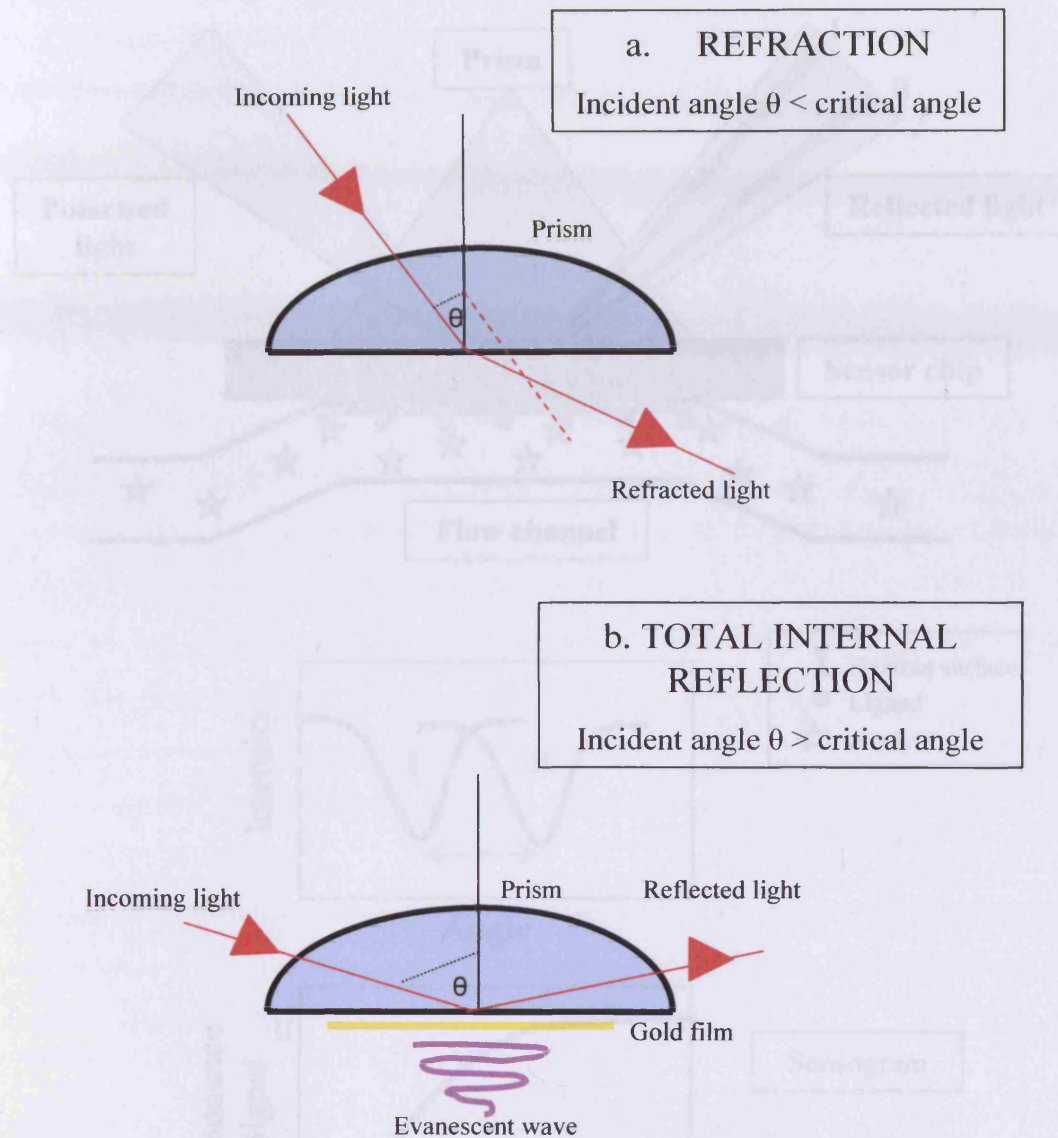


Figure 3.2: Schematic diagram of refraction and total internal reflection.

- a. Light passing from a denser medium to a less dense one is refracted towards the plane of the interface.
- b. Above a critical angle of incidence, total internal reflection occurs and no light passes into the less dense medium.

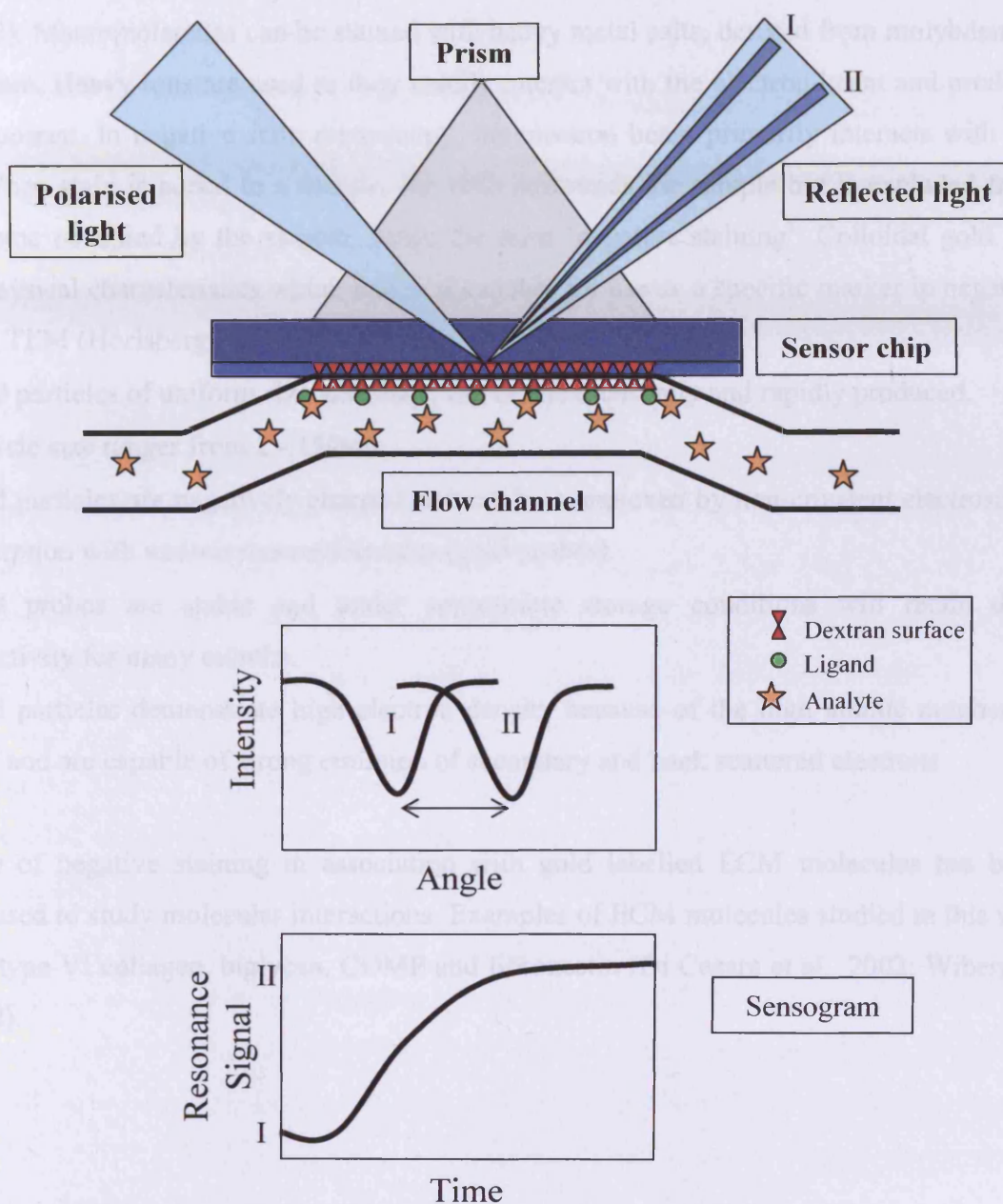


Figure 3.3: Applying SPR to biomolecular analysis. The SPR angle is sensitive to the mass concentration of molecules close to the sensor chip surface. As analyte binds to the ligand on the chip surface, the SPR angle shifts from I to II. The changes in the SPR angle are monitored over time and displayed as a sensogram.

3.1.3 Visualising Interacting Molecules Using Negative Staining

The examination of ECM macromolecules by transmission electron microscopy (TEM) can provide important information on macromolecular organisation and interactions (Sherratt et al., 2000). Macromolecules can be stained with heavy metal salts, derived from molybdenum or uranium. Heavy ions are used as they readily interact with the electron beam and produce phase contrast. In negative stain microscopy, the electron beam primarily interacts with the stain. When stain is added to a sample, the stain surrounds the sample but is excluded from the volume occupied by the sample, hence the term 'negative staining'. Colloidal gold has many physical characteristics which makes it suitable for use as a specific marker in negative staining TEM (Horisberger, 1992), these include:

- * Gold particles of uniform size and shape can be inexpensively and rapidly produced.
- * Particle size ranges from 2 - 150nm.
- * Gold particles are negatively charged and can be complexed by non-covalent electrostatic adsorption with various macromolecules (gold probes).
- * Gold probes are stable and under appropriate storage conditions will retain their bioactivity for many months.
- * Gold particles demonstrate high electron density because of the high atomic number of gold and are capable of strong emission of secondary and back scattered electrons.

The use of negative staining in association with gold labelled ECM molecules has been widely used to study molecular interactions. Examples of ECM molecules studied in this way include type VI collagen, biglycan, COMP and fibronectin (Di Cesare et al., 2002; Wiberg et al., 2002).

3.2 MATERIALS AND METHODS

All materials and reagents for the solid phase assay were obtained from Sigma (UK), reagents used during the SPR interaction studies were obtained from BIAcore AB (Sweden), reagents used for negative staining analysis were obtained from Agar Scientific Ltd (UK), unless otherwise stated.

3.2.1 Basic Solid Phase Assay

96 well microtiter plates (ICN Biomedicals, UK) were coated with 100 μ l of 5 μ g/ml human recombinant decorin (EMP Genetech, Germany) or bovine biglycan, in Phosphate Buffered Saline (PBS), 0.14 M NaCl pH 7.4, 2.7 mM KCl, 1.8 mM KH_2PO_4 , 10 mM Na_2HPO_4 . In control experiments wells were coated with 100 μ l of 3% (w/v) skimmed milk powder (Co-op, UK) in PBS. Plates were coated overnight at 37°C, all following incubations were carried out at 37°C. Wells were washed three times with 200 μ l of PBS containing 0.05% (v/v) Tween-20 (PBS-T), this washing step was repeated after each subsequent incubation. To avoid nonspecific interactions, wells were blocked for 1 hour with 200 μ l of 3% (w/v) skimmed milk powder in PBS-T. Coated wells were incubated for 2 hours with 100 μ l of 0-10 μ g/ml of type X collagen in PBS. The amount of bound type X collagen was determined by incubation for 2 hours with 100 μ l of a monoclonal anti-type X collagen antibody, MA3, diluted 1:1000 with PBS-T. Bound IgG was detected with a sheep anti-mouse horse radish peroxidase (HRP) secondary antibody, diluted 1:1000 with PBS-T, 100 μ l per well of the secondary antibody was incubated for 2 hours. Enzyme activity was measured with o-phenylenediamine (OPD) as the substrate, 100 μ l of 1 mg/ml OPD in 0.5 M sodium citrate, pH 5.5, containing 0.125% (v/v) hydrogen peroxide was incubated in wells for 5-15 minutes after which the reaction was stopped by addition of 50 μ l of 1 M H_2SO_4 . The absorbance was read at 492 nm on a multiwell plate reader (Philips PU8675 UV/VIS Spectrophotometer). Experiments were repeated on separate plates three times.

3.2.1.1 Competitive Solid Phase Assay

Coating and blocking followed the basic solid phase assay method. When type X collagen was applied as a ligand, varying amounts of decorin or biglycan 0-10 μ g/ml in PBS were mixed with the type X collagen before being applied to the plate. The total volume remained 100 μ l. All subsequent steps were the same as the basic solid phase assay. Experiments were repeated on separate plates three times.

3.2.2 Biomolecular Interaction Analysis

Protein-protein interaction studies were carried out on the BIAcore 3000 system (BIAcore AB, Sweden). The running buffer HBS-EP (0.01 M HEPES pH 7.4, 0.15 M NaCl, 3mM EDTA, 0.005% (v/v) surfactant P20) was used for diluting all the ligands and analytes in BIAcore experiments.

3.2.2.1 Immobilisation of Ligands on CM5 Sensor Chips

Whole and pepsin treated type X collagen purified from chick hypertrophic chondrocyte cultures and purified recombinant NC1 domain were used as ligands. Amine coupling chemistry was used at 25°C to immobilise ligands onto the CM5 sensor chip surface. The chip surface was activated by injection of a 1:1 mixture of 0.05 M N-hydroxysuccinimide and 0.2 M N-ethyl-N'-(dimethylaminopropyl) carbodiimide. Ligands whole type X collagen (100µg/ml), pepsinised type X collagen (90 µg/ml) and recombinant NC1 domain were immobilised at a flow rate of 5 µl/min. A maximum target of 400 RU was aimed for during immobilisation to ensure accumulation of data suitable for kinetic analysis, as recommended by BIAcore. The remaining active groups were blocked with 1 M ethanolamine hydrochloride, pH 8.5. Additional flow cells were prepared as blanks by activation and blocking of the carboxymethyl dextran surface.

3.2.2.2 Kinetic Assays on the BIAcore

All the kinetic experiments were carried out at 25°C at a flow rate of 30 µl/min. Analytes decorin and biglycan were injected for 3 minutes and 15 minutes was allowed for dissociation. Different concentrations of decorin and biglycan (0-200 µg/ml) were injected in duplicate over the three different type X collagen chip surfaces and blank surfaces. The sensor chip surface was regenerated with a 30 second injection of 50 mM NaOH, the surface was stabilised for 15 minutes before the next cycle of analyte injection was started.

3.2.2.3 Data Preparation and Analysis using BIAevaluation 3.0

BIAevaluation was used to analyse BIAcore data, and apparent kinetic rate constants were estimated directly from response curves using non-linear least squares regression. Each data set, which consists of sensograms of analyte at varying concentrations over the same surface, were analysed using different kinetic binding models

3.2.3 Negative Staining Electron Microscopy

3.2.3.1 Preparation of Gold Colloids

Gold colloid was prepared as previously described with some modifications (Slot and Geuze, 1985). This method produces homodisperse gold sols having particle sizes between 3 nm and 15 nm, depending on the amount of tannic acid used. Briefly; solution A – the Au^{3+} solution contained 0.5 ml 1% (w/v) AuCl_4 and 79.5 ml of dH_2O , solution B – the reducing solution, consisted of 4 ml 1% (w/v) sodium citrate, 2 ml 1% (v/v) tannic acid, 5 ml 25 mM K_2CO_3 and 9 ml of dH_2O . Solutions A and B were heated to 30°C in clean glassware, mixed and then boiled for 5 minutes or until a brown-red colour develops, indicating formation of gold colloid. The solution was allowed to cool to room temperature.

3.2.3.2 Preparation of Decorin and Biglycan Gold Probes

The necessary amount of decorin and biglycan required for colloid stabilisation was determined by titrating increasing amount of proteoglycan to the gold sol. To 5 ml of the colloidal gold solution, 2 – 100 μl of decorin or biglycan solution (250 $\mu\text{g/ml}$) was added. Successful stabilisation against electrolyte-induced precipitation was achieved when, upon the addition of 10% (w/v) NaCl conjugate formation was not observed as assessed by electron microscopy. Gold probe preparations were examined for the presence of fused particles, chains and aggregates.

3.2.3.3 Concentration of Gold Particle Populations by Centrifugation

Gold decorin and gold biglycan probes were concentrated and differentiated according to gold particle size by centrifugation. Colloidal gold solutions, 5 ml, containing decorin and biglycan were centrifuged at 20,000 rpm at 4°C for 10 minutes. The pellets were retained and the supernatants were centrifuged at 30,000 rpm at 4°C for 15 minutes. The pellets were retained and the supernatants were centrifuged at 40,000 rpm at 4°C for 30 minutes. The pellets were resuspended in 500 μl of 20 mM Tris, pH 8, containing 0.025% (v/v) polyethyleneglycol,

20% (v/v) glycerol and 0.1% (w/v) BSA. Aliquots of the resuspended decorin and biglycan gold probes were stored at -20°C .

3.2.3.4 Estimation of Gold Particle Sizes

A line grating grid with known dimensions (in nm) was recorded at all magnifications. Electron micrographs of the line grating were scanned and scaled up to A4 paper. The line grating was measured (in mm) with a ruler. Calculation of $\chi \text{ nm} = 1 \text{ mm}$ were subsequently carried out for each magnification. Decorin and biglycan gold particles were adsorbed onto pioloform coated grids and were analysed by electron microscopy. Electron micrographs were scaled up to A4 size and the diameter of at least 50 decorin and biglycan labelled particles on three separate micrographs were measured. Grids were examined by TEM (Phillips EM208). Images were recorded at variable magnifications and were scanned using an Epson GT-7000 scanner.

3.2.3.5 Grid Preparation and TEM

Decorin and biglycan gold probes obtained from the pellet after the 40,000 rpm centrifugation step, were diluted 1:20 and were mixed with equal volumes of whole type X collagen (10 $\mu\text{g/ml}$). Following incubation for 15 minutes a 50 μl aliquot of the mixture was pipetted onto nescofilm. A 400-mesh pioloform coated copper grid was floated onto the droplet and incubated for 30 seconds, the grid was subsequently placed on a droplet of 0.5% (w/v) uranyl formate for 30 seconds and on two water droplets for approximately 10 seconds each. The grid was blotted on filter paper and allowed to air dry. Grids were examined by TEM (Phillips EM208). Images were recorded at variable magnifications and were scanned using an Epson GT-7000 scanner.

3.3 RESULTS

3.3.1 Solid Phase Assays

Using the solid phase assay developed; interactions of type X collagen with decorin and biglycan were characterised. Experiments were performed in triplicate, a single data set representative of the findings are shown.

3.3.1.1 *Decorin interacts with type X collagen in a solid phase assay*

A 96 well plate was coated with 5 µg/ml of decorin in PBS, 3% (w/v) skimmed milk powder in PBS coated wells were used as controls. Type X collagen was applied to the experimental and control wells in triplicate as a ligand, varying concentrations from 0 to 10 µg/ml were used. OPD was used as the substrate for antibody conjugated with HRP, optical densities were measured at 492 nm. Absorbance readings for the control 3% (w/v) milk coated wells were averaged and subtracted from triplicate absorbance values gained from the corresponding decorin coated wells. The absorbance values have been plotted against the concentration of type X collagen (figure 3.4). As the concentration of type X collagen increases the absorbance values increase until binding saturation is reached at around 5 µg/ml. Absorbance readings reach a plateau as excess type X collagen is unable to bind decorin and is consequently removed during the washing procedure.

3.3.1.2 *Interaction of decorin with type X collagen can be competitively inhibited by decorin*

A 96 well plate was coated with 5 µg/ml of decorin in PBS, 3% skimmed milk powder in PBS coated wells were used as controls. Type X collagen was pre-incubated with decorin before being applied to the experimental and control wells in triplicate as a ligand. The concentration of type X collagen was kept constant at 5 µg/ml, while decorin was used at a range from 0 to 10 µg/ml. OPD was used as the substrate for antibody conjugated with HRP, optical densities were measured at 492 nm. Absorbance readings for the control 3% (w/v) milk coated wells were averaged and subtracted from triplicate absorbance values gained from the corresponding decorin coated wells. The absorbance values have been plotted against the concentration of competing decorin (figure 3.5). The data was analysed using non-linear regression and a sigmoidal dose response curve was generated. As the concentration of competing decorin increases the absorbance values decrease until binding is abolished. All the

type X collagen in the liquid phase is bound to competing decorin and is therefore unable to bind to decorin in the solid phase. 50% inhibition is reached between 4.4 $\mu\text{g/ml}$ and 5.2 $\mu\text{g/ml}$ of competing decorin. An R^2 value (correlation coefficient) of 0.87 was calculated for the curves goodness of fit.

3.3.1.3 Interaction of decorin with type X collagen can be competitively inhibited by biglycan

A 96 well plate was coated with 5 $\mu\text{g/ml}$ of decorin in PBS, 3% (w/v) skimmed milk powder in PBS coated wells were used as controls. Type X collagen was pre-incubated with biglycan before being applied to the experimental and control wells in triplicate as a ligand. The concentration of type X collagen was kept constant at 5 $\mu\text{g/ml}$, while biglycan was used at a range from 0 to 10 $\mu\text{g/ml}$. OPD was used as the substrate for antibody conjugated with HRP, optical densities were measured at 492 nm. Absorbance readings for the control 3% (w/v) milk coated wells were averaged and subtracted from triplicate absorbance values gained from the corresponding decorin coated wells. The absorbance values have been plotted against the concentration of competing biglycan (figure 3.6). The data was analysed using non-linear regression and a sigmoidal dose response curve was generated. As the concentration of competing biglycan increases the absorbance values decrease until binding is abolished. All the type X collagen in the liquid phase is bound to competing biglycan and is therefore unable to bind to decorin in the solid phase. 50% inhibition is reached between 5.8 $\mu\text{g/ml}$ and 6.2 $\mu\text{g/ml}$ of competing biglycan. An R^2 value of 0.97 was calculated for the curves goodness of fit.

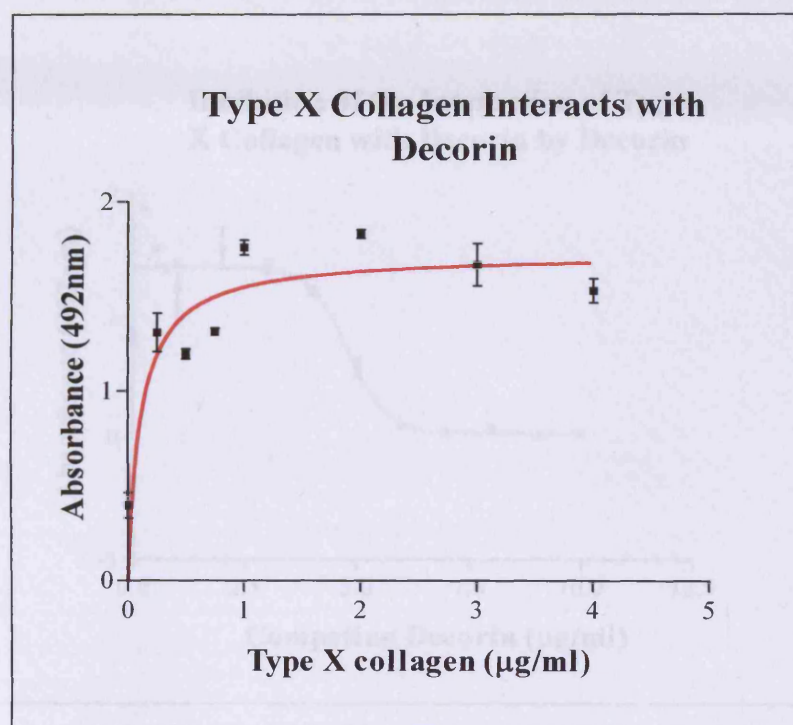


Figure 3.4: Type X collagen interacts with decorin in a solid phase assay. A plot of absorbance at 492nm against concentration of type X collagen applied as a ligand, to a plate coated with 5 $\mu\text{g/ml}$ of decorin.

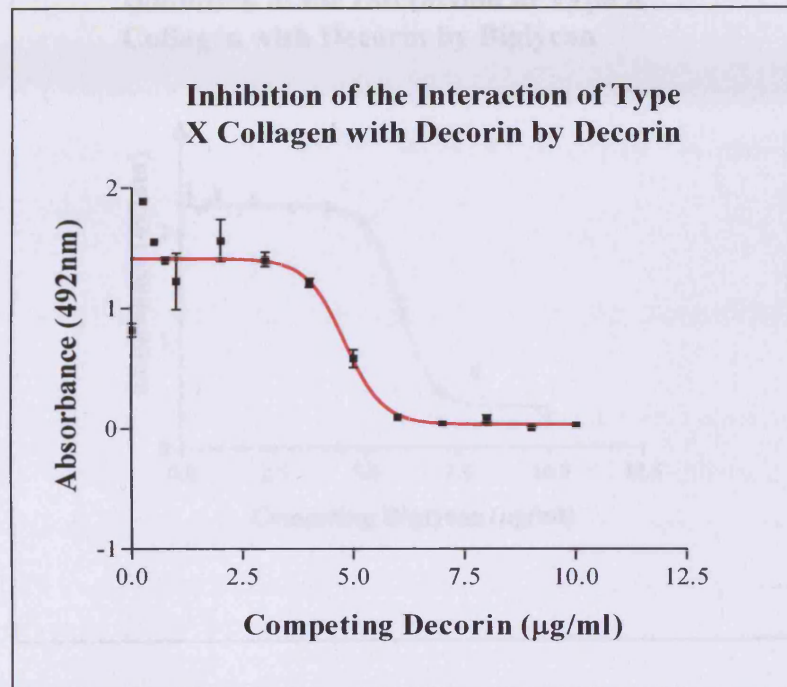


Figure 3.5: The interaction of type X collagen with decorin can be competitively inhibited by decorin. A plot of absorbance at 492nm against concentration of competing decorin applied as a ligand with 5 $\mu\text{g/ml}$ of type X collagen, to a plate coated with 5 $\mu\text{g/ml}$ of decorin.

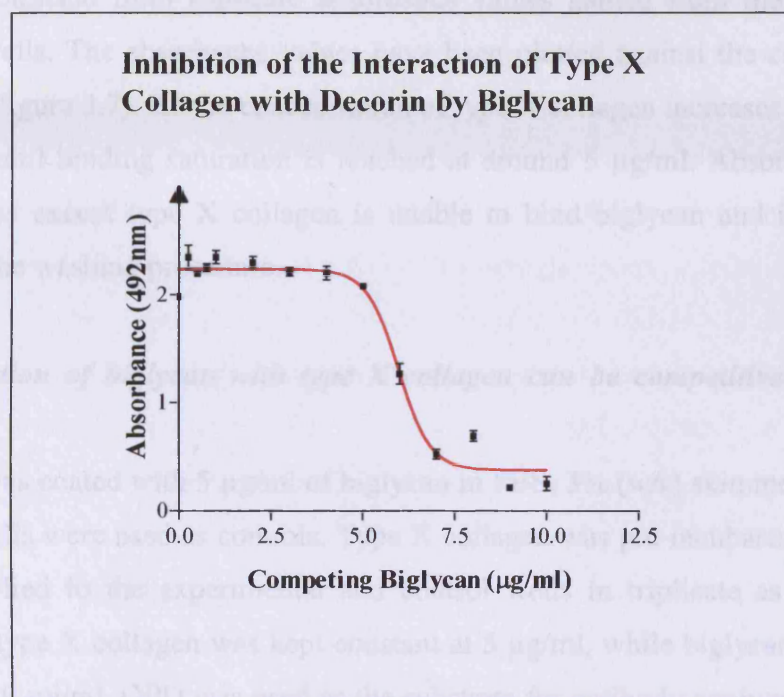


Figure 3.6: The interaction of type X collagen with decorin can be competitively inhibited by biglycan. A plot of absorbance at 492nm against concentration of competing biglycan applied as a ligand with 5µg/ml of type X collagen, to a plate coated with 5µg/ml of decorin.

3.3.1.4 *Biglycan interacts with type X collagen in a solid phase assay*

A 96 well plate was coated with 5 µg/ml of biglycan in PBS, 3% (w/v) skimmed milk powder in PBS coated wells were used as controls. Type X collagen was applied to the experimental and control wells in triplicate as a ligand, varying concentrations from 0 to 10 µg/ml were used. OPD was used as the substrate for antibody conjugated with HRP, optical densities were measured at 492 nm. Absorbance readings for the control 3% (w/v) milk coated wells were averaged and subtracted from triplicate absorbance values gained from the corresponding decorin coated wells. The absorbance values have been plotted against the concentration of type X collagen (figure 3.7). As the concentration of type X collagen increases the absorbance values increase until binding saturation is reached at around 5 µg/ml. Absorbance readings reach a plateau as excess type X collagen is unable to bind biglycan and is consequently removed during the washing procedure.

3.3.1.5 *Interaction of biglycan with type X collagen can be competitively inhibited by biglycan*

A 96 well plate was coated with 5 µg/ml of biglycan in PBS, 3% (w/v) skimmed milk powder in PBS coated wells were used as controls. Type X collagen was pre-incubated with biglycan before being applied to the experimental and control wells in triplicate as a ligand. The concentration of type X collagen was kept constant at 5 µg/ml, while biglycan was used at a range from 0 to 10 µg/ml. OPD was used as the substrate for antibody conjugated with HRP, optical densities were measured at 492 nm. Absorbance readings for the control 3% (w/v) milk coated wells were averaged and subtracted from triplicate absorbance values gained from the corresponding decorin coated wells. The absorbance values have been plotted against the concentration of competing biglycan (figure 3.8). The data was analysed using non-linear regression and a sigmoidal dose response curve was generated. As the concentration of competing biglycan increases the absorbance values decrease indicating binding is abolished. All the type X collagen in the liquid phase is bound to competing biglycan and is therefore unable to bind to biglycan in the solid phase. 50% inhibition is reached between 3.1 µg/ml and 3.6 µg/ml of competing biglycan. An R^2 value of 0.94 was calculated for the curves goodness of fit.

3.3.1.6 Interaction of biglycan with type X collagen can be competitively inhibited by decorin

A 96 well plate was coated with 5 µg/ml of biglycan in PBS, 3% (w/v) skimmed milk powder in PBS coated wells were used as controls. Type X collagen was pre-incubated with biglycan before being applied to the experimental and control wells in triplicate as a ligand. The concentration of type X collagen was kept constant at 5 µg/ml, while decorin was used at a range from 0 to 10 µg/ml. OPD was used as the substrate for antibody conjugated with HRP, optical densities were measured at 492 nm. Absorbance readings for the control 3% (w/v) milk coated wells were averaged and subtracted from triplicate absorbance values gained from the corresponding biglycan coated wells. The absorbance values have been plotted against the concentration of competing decorin (figure 3.9). The data was analysed using non-linear regression and a sigmoidal dose response curve was generated. As the concentration of competing decorin increases the absorbance values decrease until binding is abolished. All the type X collagen in the liquid phase is bound to competing decorin and is therefore unable to bind to biglycan in the solid phase. 50% inhibition is reached between 6.6 µg/ml and 7.7 µg/ml of competing decorin. An R^2 value of 0.73 was calculated for the curves goodness of fit.

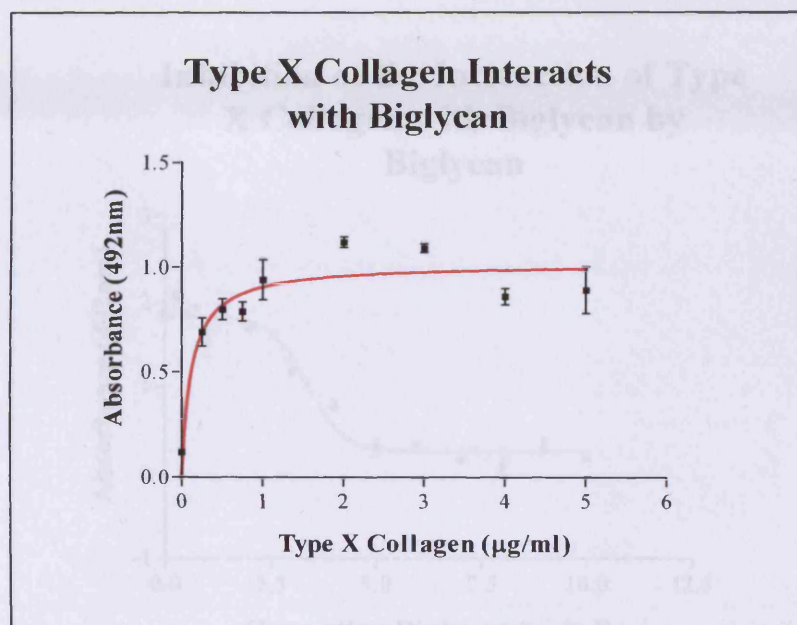


Figure 3.7: Type X collagen interacts with biglycan in a solid phase assay. A plot of absorbance at 492nm against concentration of type X collagen applied as a ligand to a plate coated with $5\mu\text{g/ml}$ of biglycan.

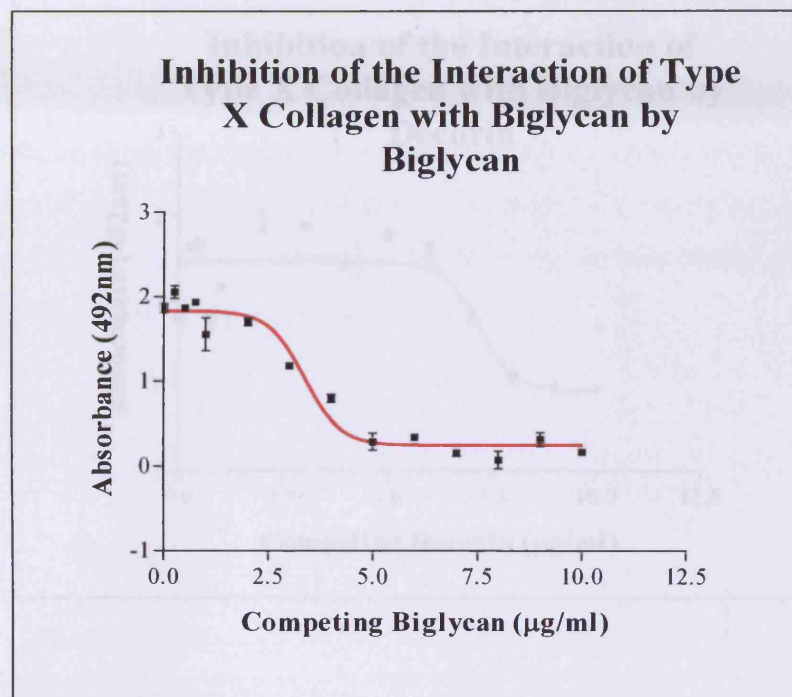


Figure 3.8: The interaction of type X collagen with biglycan can be competitively inhibited by biglycan. A plot of absorbance at 492nm against concentration of competing biglycan applied as a ligand with $5\mu\text{g/ml}$ of type X collagen, to a plate coated with $5\mu\text{g/ml}$ of biglycan.

3.3.1.7. *Pepsinised Type X Collagen Does Not Interact With Decorin or Biglycan*

96 well microtitre plates were coated with 5µg/ml of decorin or biglycan in PBS, 3% (w/v) bovine serum albumin powder in PBS coated wells were used as controls. Type X collagen, before or after pepsin digestion was applied to the coated wells as a ligand, varying concentrations from 0 to 5µg/ml were used. OPD was used as the substrate for antibody conjugated with anti- $\alpha 1(\text{I})$ collagen antibody. Absorbance readings for the control wells were subtracted from the experimental wells to give the net absorbance values.

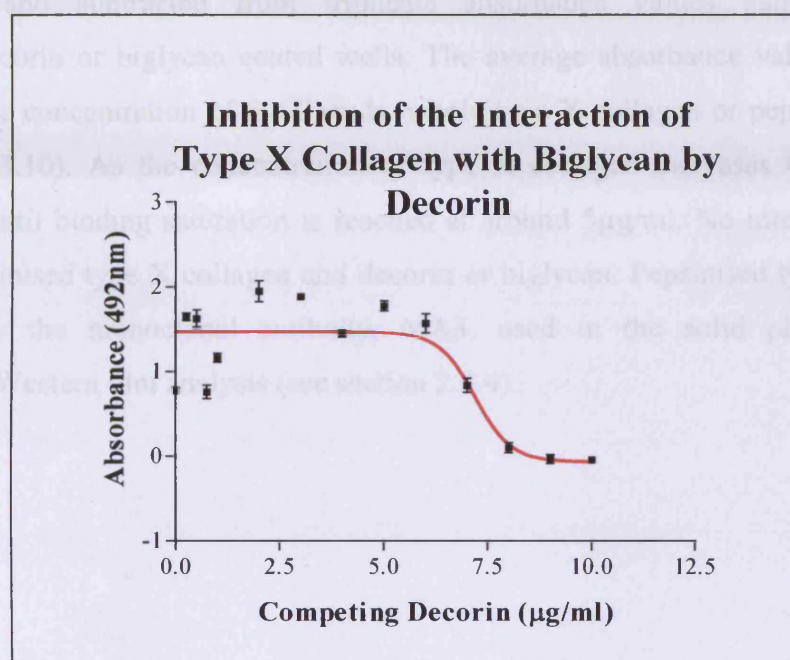


Figure 3.9: The interaction of type X collagen with biglycan can be competitively inhibited by decorin. A plot of absorbance at 492nm against concentration of competing decorin applied as a ligand with 5µg/ml of type X collagen, to a plate coated with 5µg/ml of biglycan.

3.3.1.7 Pepsinised Type X Collagen Does Not Interact With Decorin or Biglycan

96 well microtitre plates were coated with 5µg/ml of decorin or biglycan in PBS, 3% (w/v) skimmed milk powder in PBS coated wells were used as controls. Type X collagen, before and after pepsin digestion was applied to the coated wells as a ligand, varying concentrations from 0 to 5µg/ml were used. OPD was used as the substrate for antibody conjugated with HRP, optical densities were measured at 492nm. Absorbance readings for the control wells were averaged and subtracted from triplicate absorbance values gained from the corresponding decorin or biglycan coated wells. The average absorbance values have been plotted against the concentration of the ligands, whole type X collagen or pepsinised type X collagen (figure 3.10). As the concentration of type X collagen increases the absorbance values increase until binding saturation is reached at around 5µg/ml. No interaction is seen between the pepsinised type X collagen and decorin or biglycan. Pepsinised type X collagen is recognised by the monoclonal antibody, MA3, used in the solid phase assay, as demonstrated by Western blot analysis (see section 2.3.4).

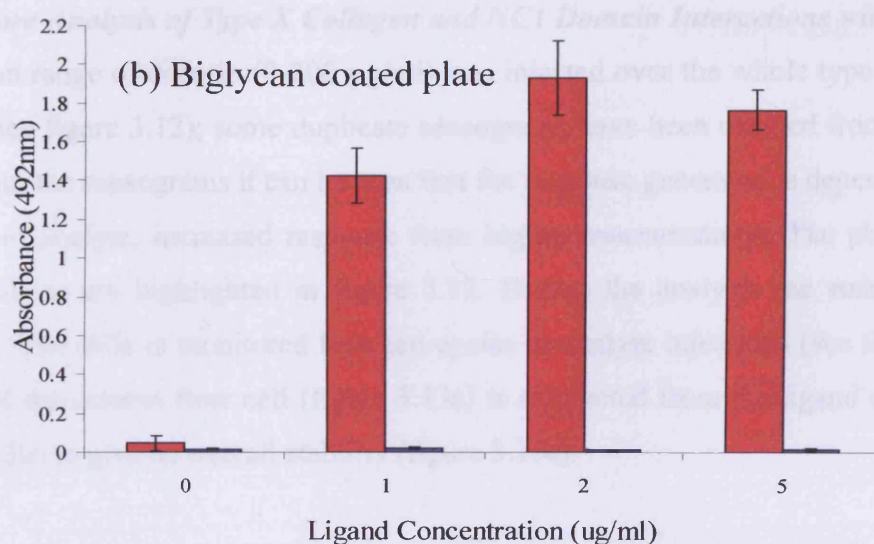
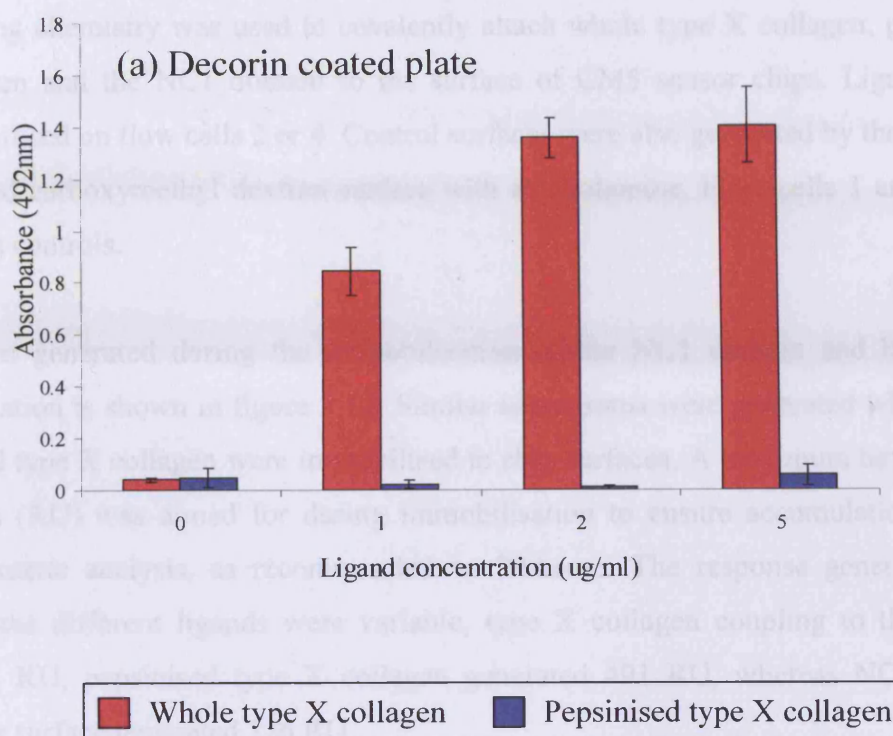


Figure 3.10: Solid phase assay demonstrating interactions of decorin and biglycan with whole type X collagen but not with pepsinised type X collagen. Graph of absorbance at 492nm against concentration of whole and pepsinised type X collagen applied as a ligand to plates coated with (a) decorin and (b) biglycan.

3.3.2 Biomolecular Interaction Analysis Results

3.3.2.1 *Immobilisation of Ligands to the Sensor Chip Surface*

Amine coupling chemistry was used to covalently attach whole type X collagen, pepsinised type X collagen and the NC1 domain to the surface of CM5 sensor chips. Ligands were always immobilised on flow cells 2 or 4. Control surfaces were also generated by the blocking of the activated carboxymethyl dextran surface with ethanolamine. Flow cells 1 and 3 were always used as controls.

The sensogram generated during the immobilisation of the NC1 domain and blank chip surface preparation is shown in figure 3.11. Similar sensograms were generated when whole and pepsinised type X collagen were immobilised to chip surfaces. A maximum target of 400 response units (RU) was aimed for during immobilisation to ensure accumulation of data suitable for kinetic analysis, as recommended by BIAcore. The response generated from immobilising the different ligands were variable, type X collagen coupling to the surface generated 264 RU, pepsinised type X collagen generated 491 RU, whereas NC1 domain coupling to the surface generated 226 RU.

3.3.2.2 *BIAcore Analysis of Type X Collagen and NC1 Domain Interactions with Decorin*

A concentration range of decorin (0-200 $\mu\text{g/ml}$) was injected over the whole type X collagen chip surface (see figure 3.12); some duplicate sensograms have been omitted from the figure for clarity. From the sensograms it can be seen that the response generated is dependant on the concentration of analyte, increased response from higher concentrations. The phases of the interaction analysis are highlighted in figure 3.12. During the analysis the stability of the baseline in all flow cells is monitored between cycles or analyte injections (see figure 3.13). The stability of the control flow cell (figure 3.13a) is subtracted from the ligand coated flow cell (figure 3.13b) to give an overall stability (figure 3.13c).

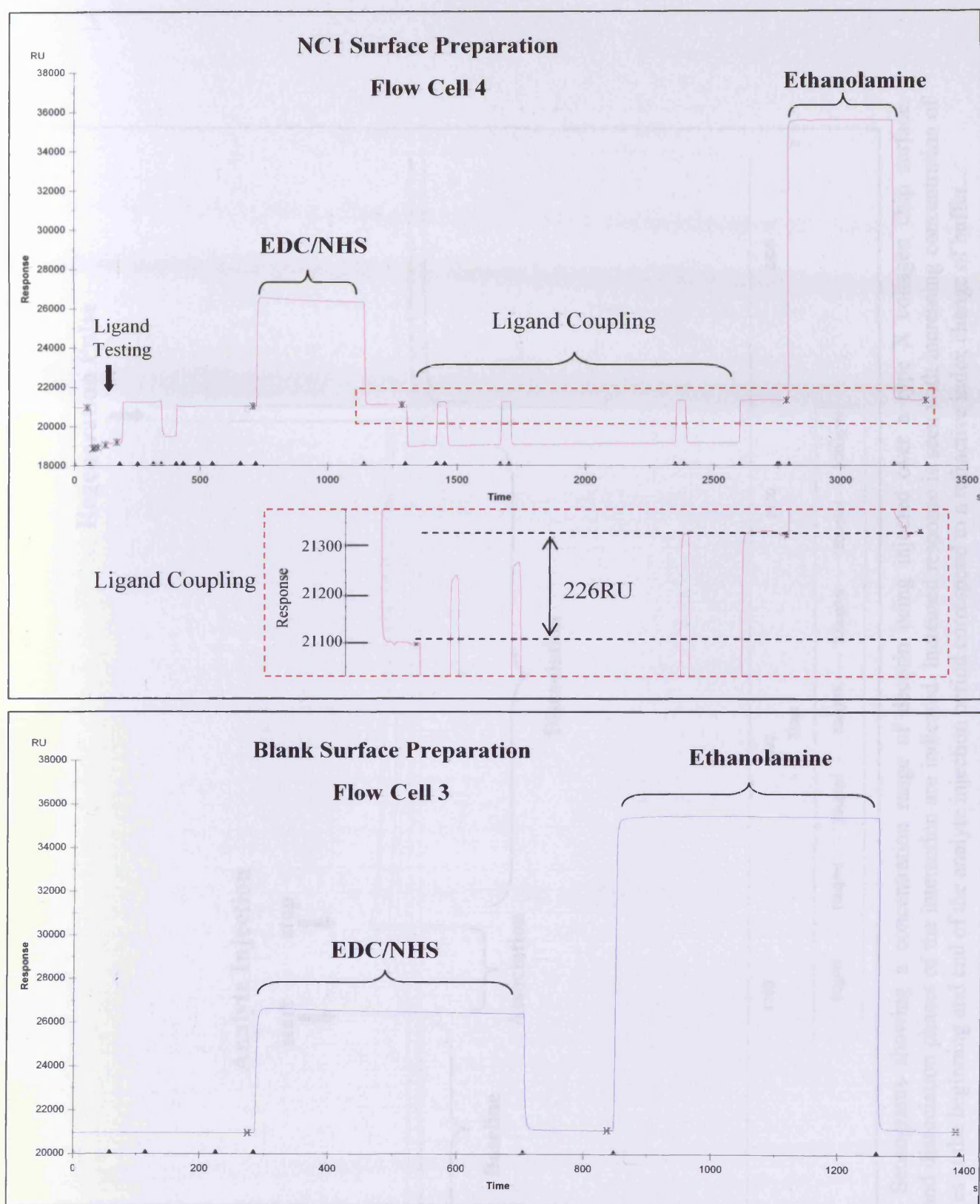


Figure 3.11: An example of sensogram responses during the process of ligand immobilisation and control flow cell preparation. The ligand coupling region of the NC1 surface preparation graph has been expanded to demonstrate the 226 RU of NC1 immobilised on the chip surface.

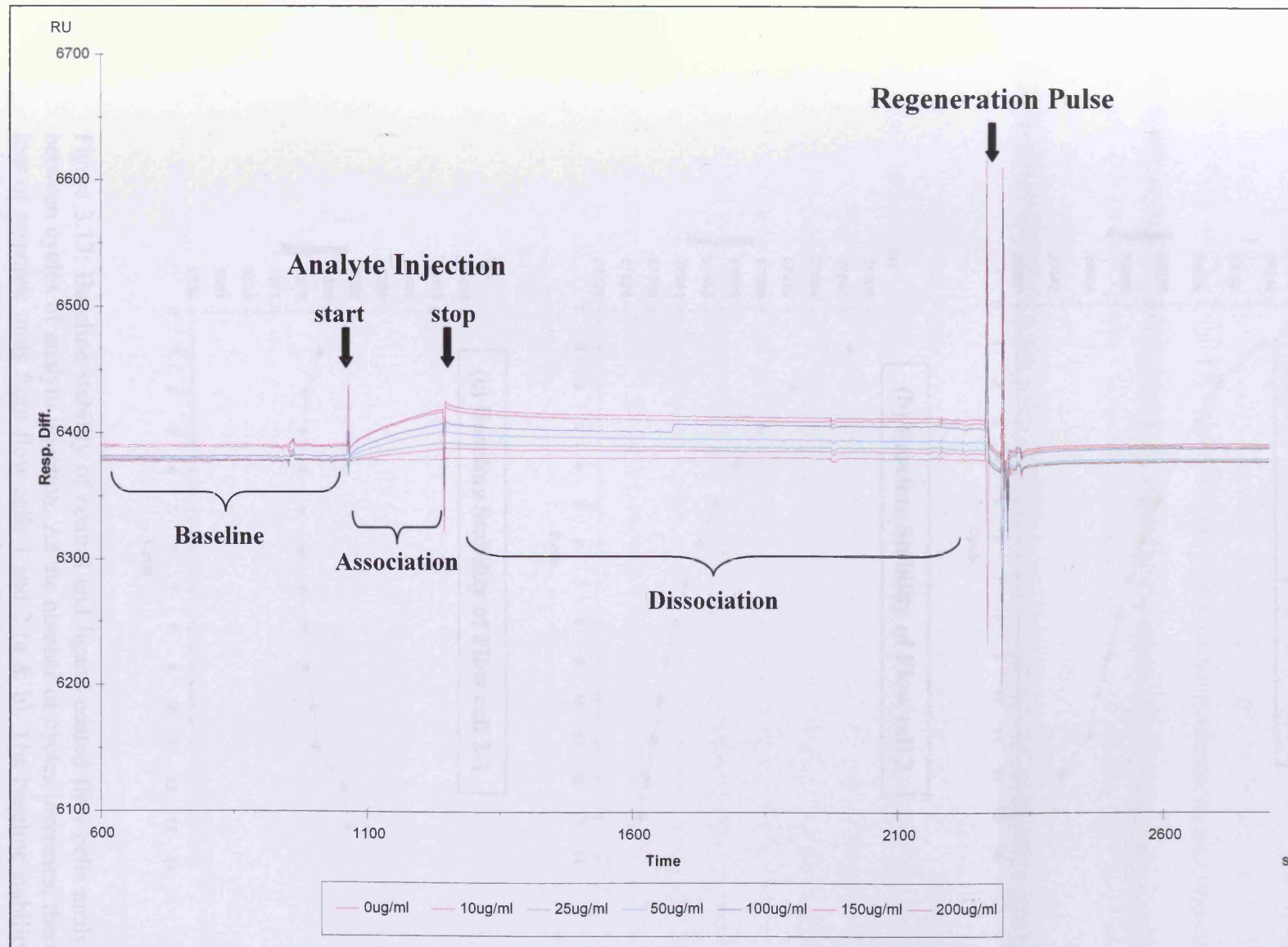


Figure 3.12: Sensograms showing a concentration range of decorin being injected over a type X collagen chip surface. Association and dissociation phases of the interaction are indicated. Increased response is seen with increasing concentration of decorin. Spikes at the beginning and end of the analyte injection period correspond to a refractive index change of buffer.

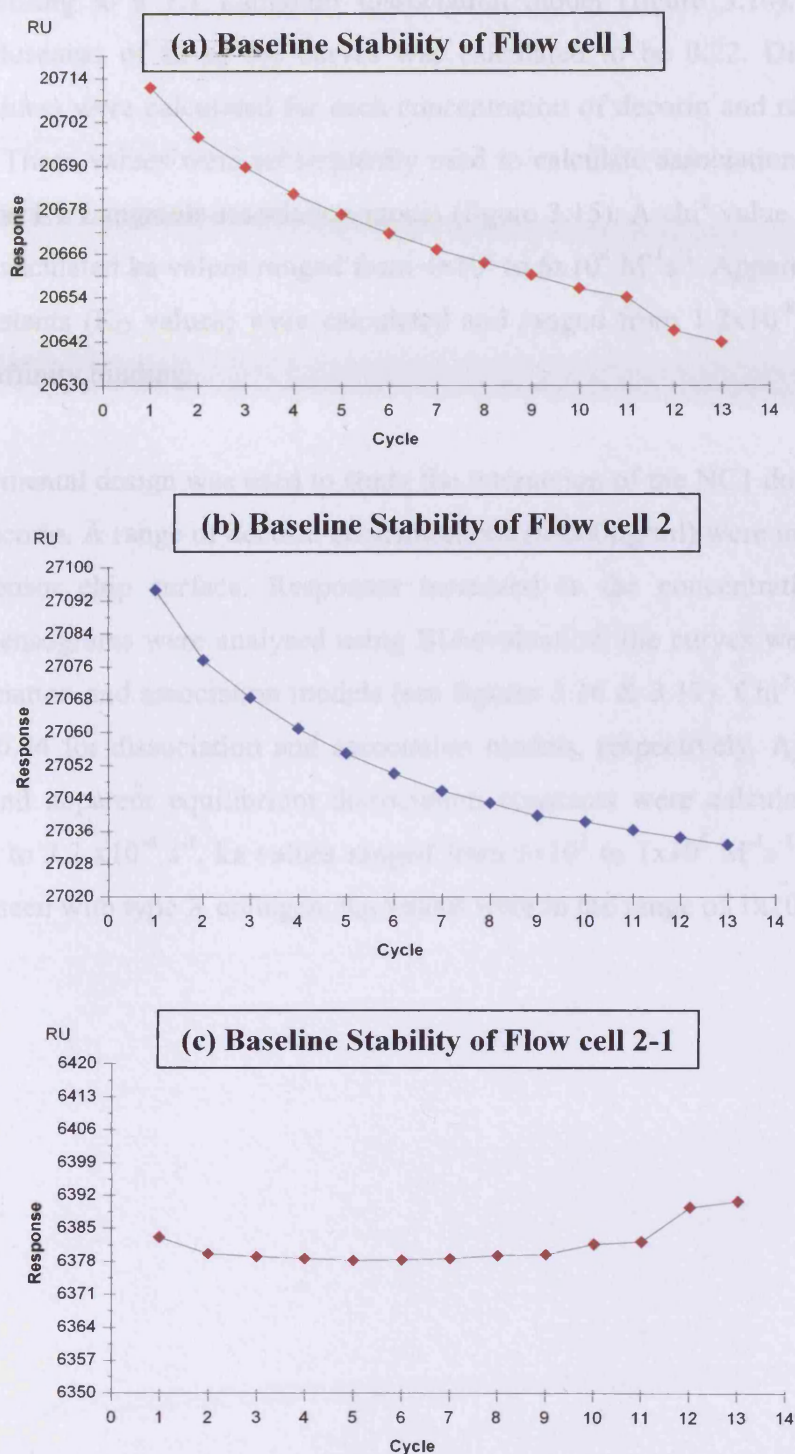


Figure 3.13: Baseline stability of control and ligand coated flow cells analysed between cycles of analyte injection. As the number of cycles increases, there is loss of response units from flow cells 1 and 2 (a & b). The baseline stability is relatively constant as cycles progress when flow cell 2-1 is assessed (c).

3.3.2.2 *BIAcore Analysis of Type X Collagen and NC1 Domain Interactions with Decorin*

The sensograms were manipulated and analysed using the BIAevaluation software. Curves were fitted according to a 1:1 Langmuir dissociation model (figure 3.14). A χ^2 value indicating the closeness of fit of the curves was calculated to be 0.22. Dissociation rate constants (k_d values) were calculated for each concentration of decorin and ranged from 3.2 to $3.8 \times 10^{-4} \text{ s}^{-1}$. These values were subsequently used to calculate association rate constants (k_a values), in the 1:1 Langmuir association model (figure 3.15). A χ^2 value was calculated to be 0.07. The calculated k_a values ranged from 4×10^3 to $6 \times 10^4 \text{ M}^{-1} \text{ s}^{-1}$. Apparent equilibrium dissociation constants (K_D values) were calculated and ranged from 1.2×10^{-8} to $8.3 \times 10^{-9} \text{ M}$, indicating high affinity binding.

The same experimental design was used to study the interaction of the NC1 domain of type X collagen with decorin. A range of decorin concentrations (0-200 $\mu\text{g/ml}$) were injected over the NC1 domain sensor chip surface. Responses increased as the concentration of decorin increased. The sensograms were analysed using BIAevaluation, the curves were fitted to 1:1 Langmuir dissociation and association models (see figures 3.16 & 3.17). χ^2 was calculated to be 0.06 and 0.04 for dissociation and association models, respectively. Apparent kinetic rate constants and apparent equilibrium dissociation constants were calculated. k_d values ranged from 1.1 to $2.2 \times 10^{-4} \text{ s}^{-1}$, k_a values ranged from 5×10^3 to $1 \times 10^5 \text{ M}^{-1} \text{ s}^{-1}$. Like the high affinity binding seen with type X collagen, K_D values were in the range of 1×10^{-8} to $1 \times 10^{-9} \text{ M}$.

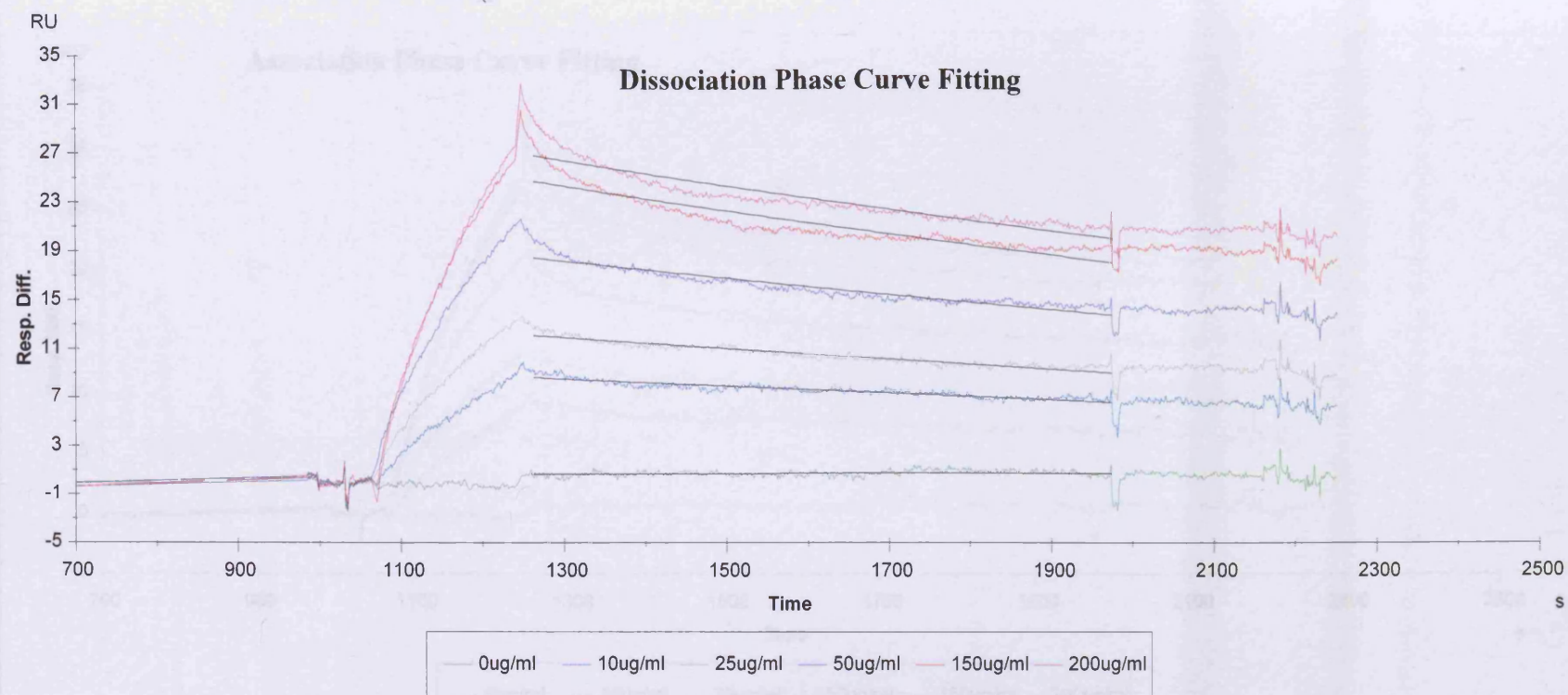


Figure 3.14: Sensogram showing a concentration range of the analyte decorin, being injected over a type X collagen chip surface. The dissociation phase curves have been fitted to a 1:1 Langmuir dissociation model.

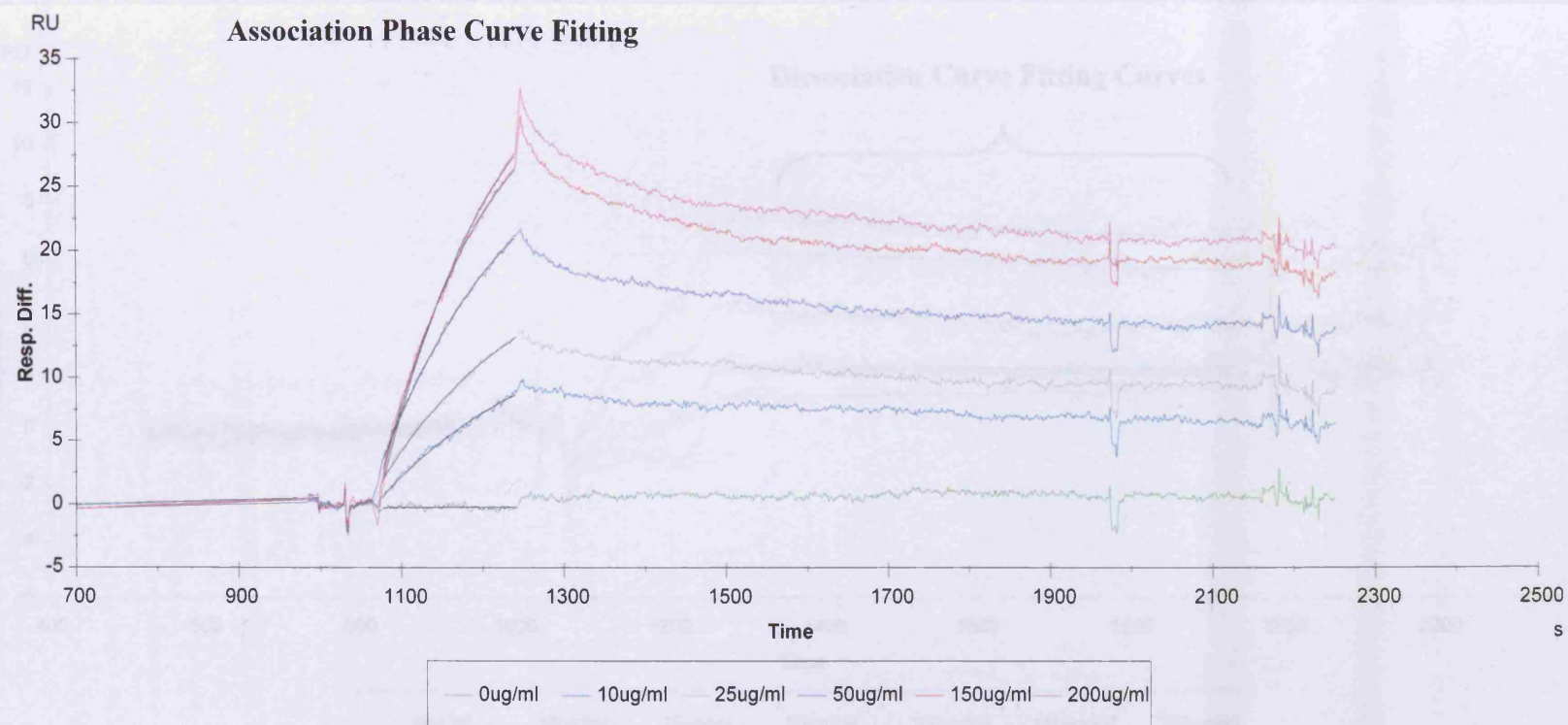
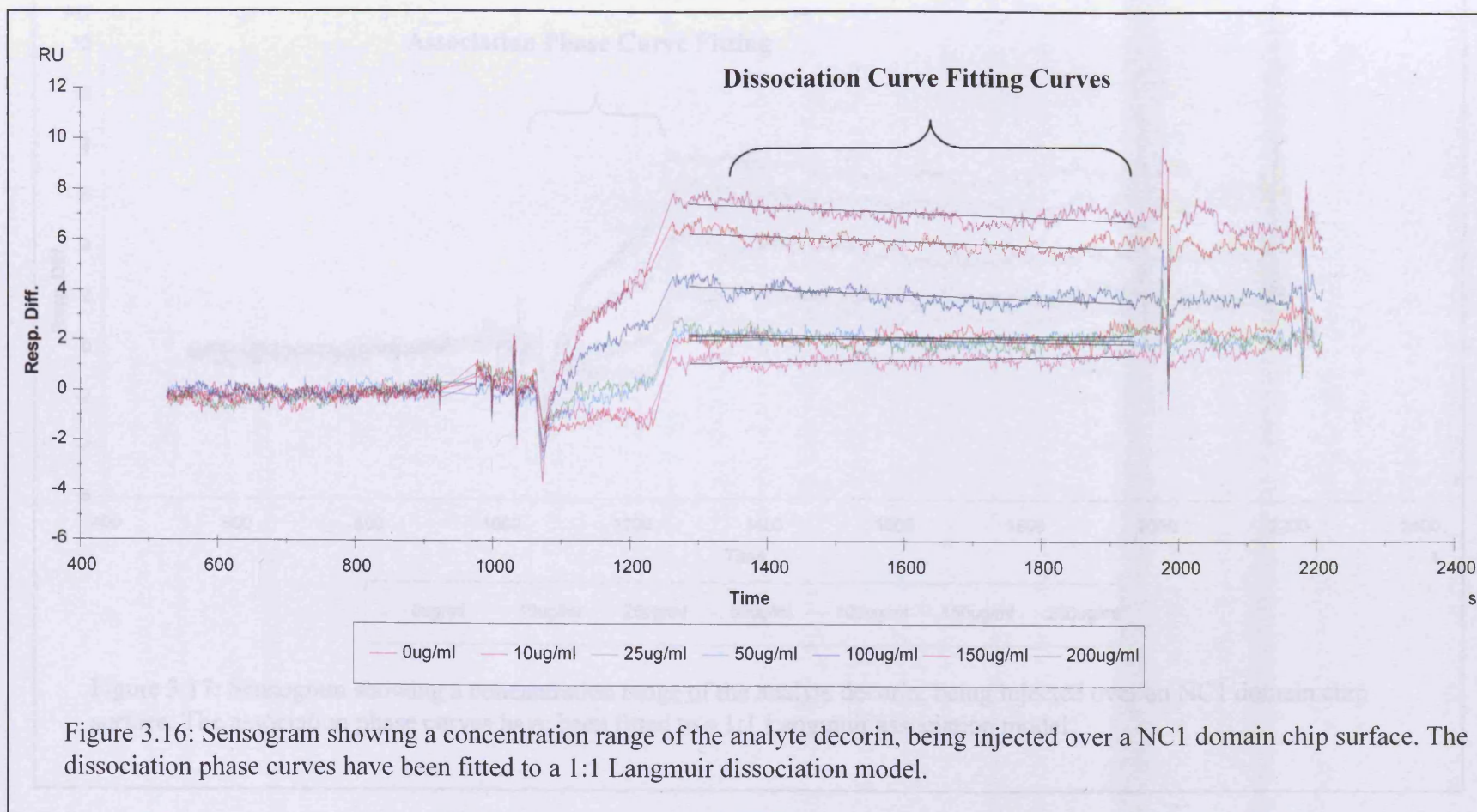


Figure 3.15: Sensogram showing a concentration range of the analyte decorin, being injected over a type X collagen chip surface. The association phase curves have been fitted to a 1:1 Langmuir association model.



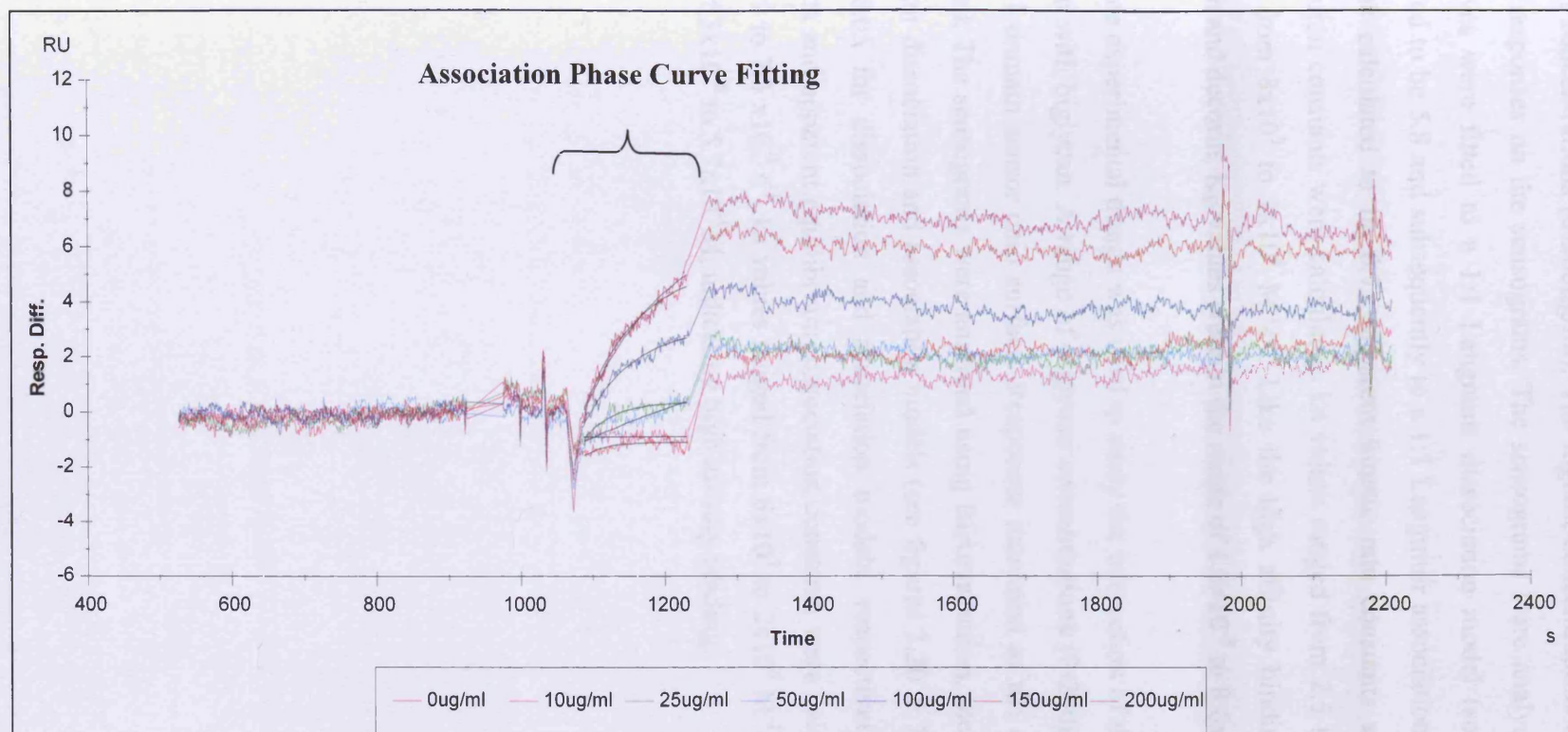


Figure 3.17: Sensogram showing a concentration range of the analyte decorin, being injected over an NC1 domain chip surface. The association phase curves have been fitted to a 1:1 Langmuir association model.

3.3.2.3 *BIAcore Analysis of Type X Collagen and NC1 Domain Interactions with Biglycan*

Biglycan was used as the analyte and was injected over a type X collagen chip surface at a range of concentrations (0-200 μ g/ml). The highest concentrations of biglycan generated the biggest responses on the sensograms. The sensograms were analysed using BIAevaluation, the curves were fitted to a 1:1 Langmuir dissociation model (see figure 3.18), χ^2 was calculated to be 5.8 and subsequently to a 1:1 Langmuir association model (see figure 3.19); χ^2 was calculated to be 0.7. Apparent kinetic rate constants and apparent equilibrium dissociation constants were calculated. k_d values ranged from 2.5 to 7.9 $\times 10^{-4}$ s $^{-1}$, k_a values ranged from 8 $\times 10^3$ to 2 $\times 10^5$ M $^{-1}$ s $^{-1}$. Like the high affinity binding seen between type X collagen and decorin, K_D values were in the range of 1.8 $\times 10^{-8}$ to 8.6 $\times 10^{-8}$ M.

The same experimental design was used to study the interaction of the NC1 domain of type X collagen with biglycan. A range of biglycan concentrations (0-200 μ g/ml) were injected over the NC1 domain sensor chip surface. Responses increased as the concentration of biglycan increased. The sensograms were analysed using BIAevaluation, the curves were fitted to 1:1 Langmuir dissociation and association models (see figures 3.20 & 3.21). χ^2 was calculated to be 0.05 for dissociation and association models, respectively. Apparent kinetic rate constants and apparent equilibrium dissociation constants were calculated. k_d values ranged from 2.9 to 7.3 $\times 10^{-4}$ s $^{-1}$, k_a values ranged from 6 $\times 10^3$ to 2 $\times 10^5$ M $^{-1}$ s $^{-1}$. K_D values were in the range of 3 $\times 10^{-8}$ to 5.7 $\times 10^{-9}$ M, indicating high affinity binding.

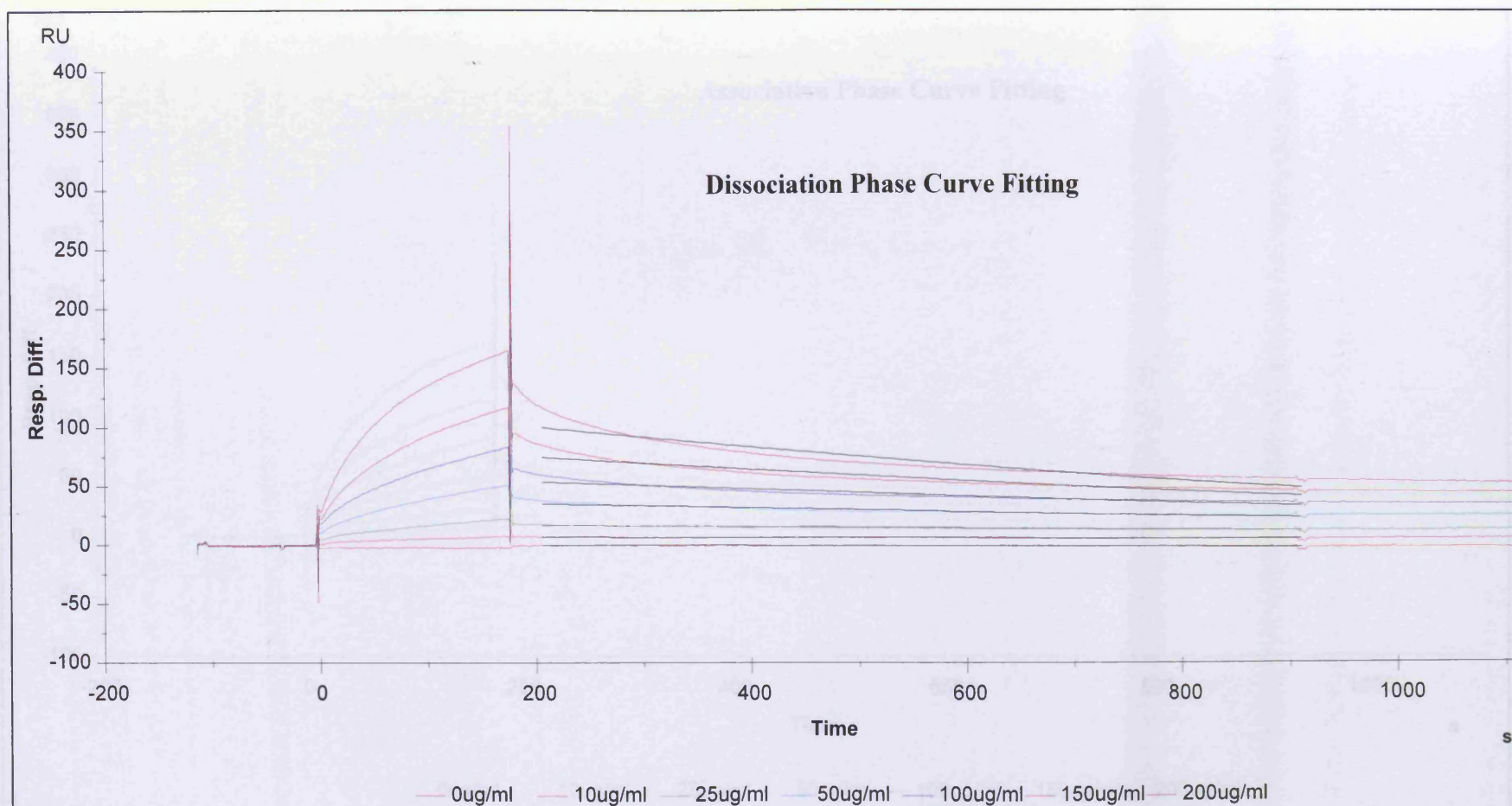


Figure 3.18: Sensogram showing a concentration range of the analyte biglycan, being injected over a type X collagen chip surface. The dissociation phase curves have been fitted to a 1:1 Langmuir dissociation model.

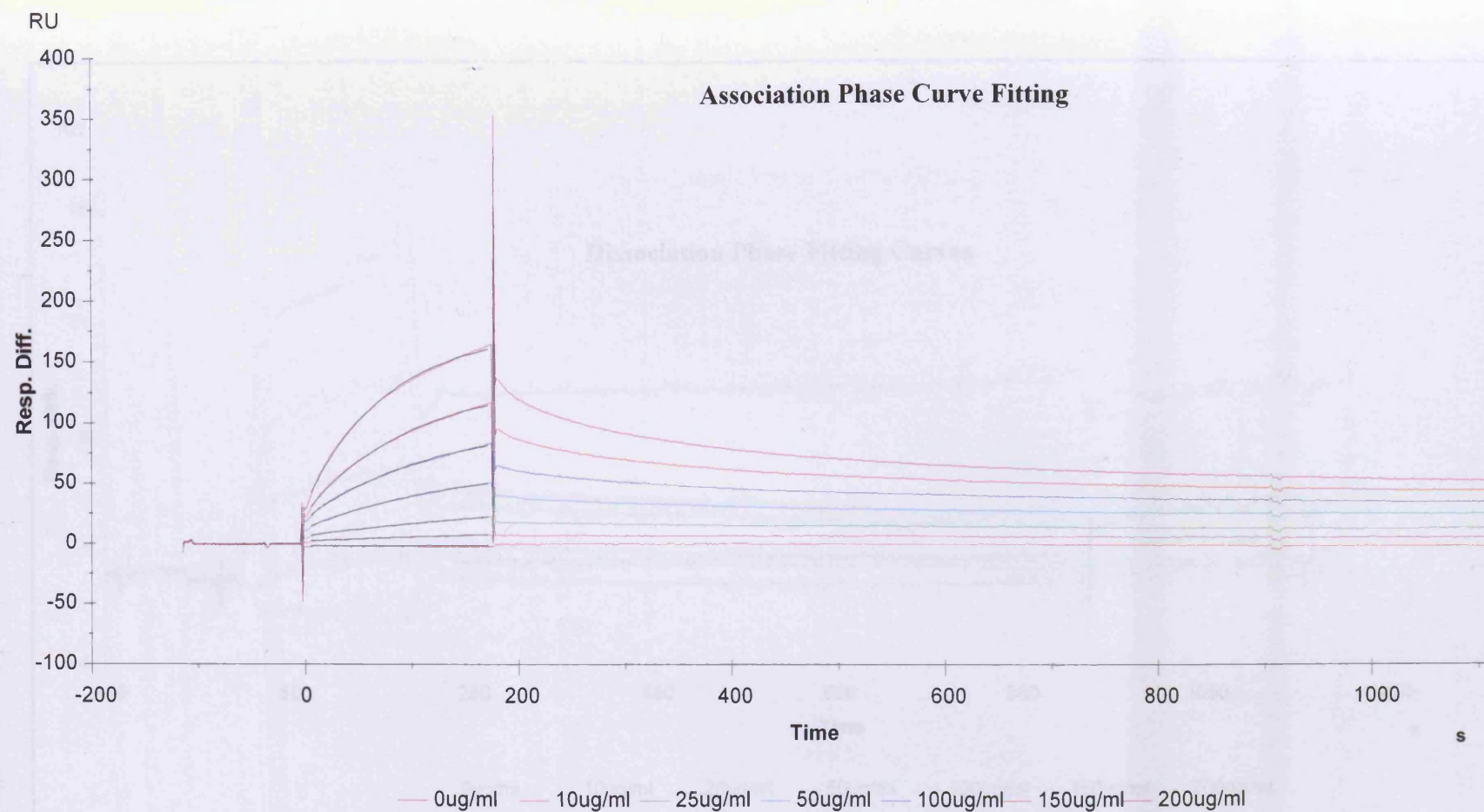


Figure 3.19. Sensogram showing a concentration range of the analyte biglycan, being injected over a type X collagen chip surface. The association phase curves have been fitted to a 1:1 Langmuir association model.

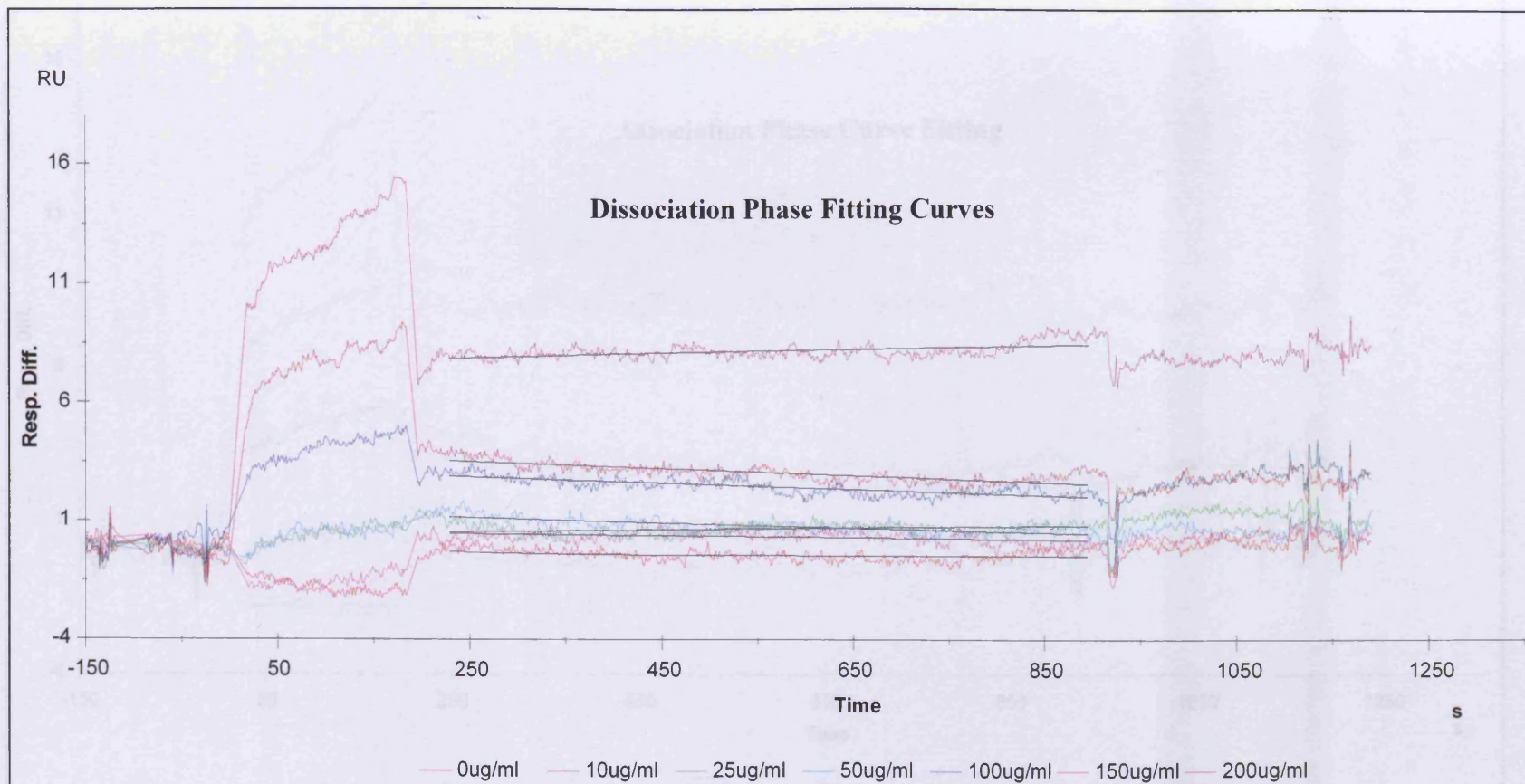


Figure 3.20: Sensogram showing a concentration range of the analyte biglycan, being injected over a NC1 domain chip surface. The dissociation phase curves have been fitted to a 1:1 Langmuir dissociation model.

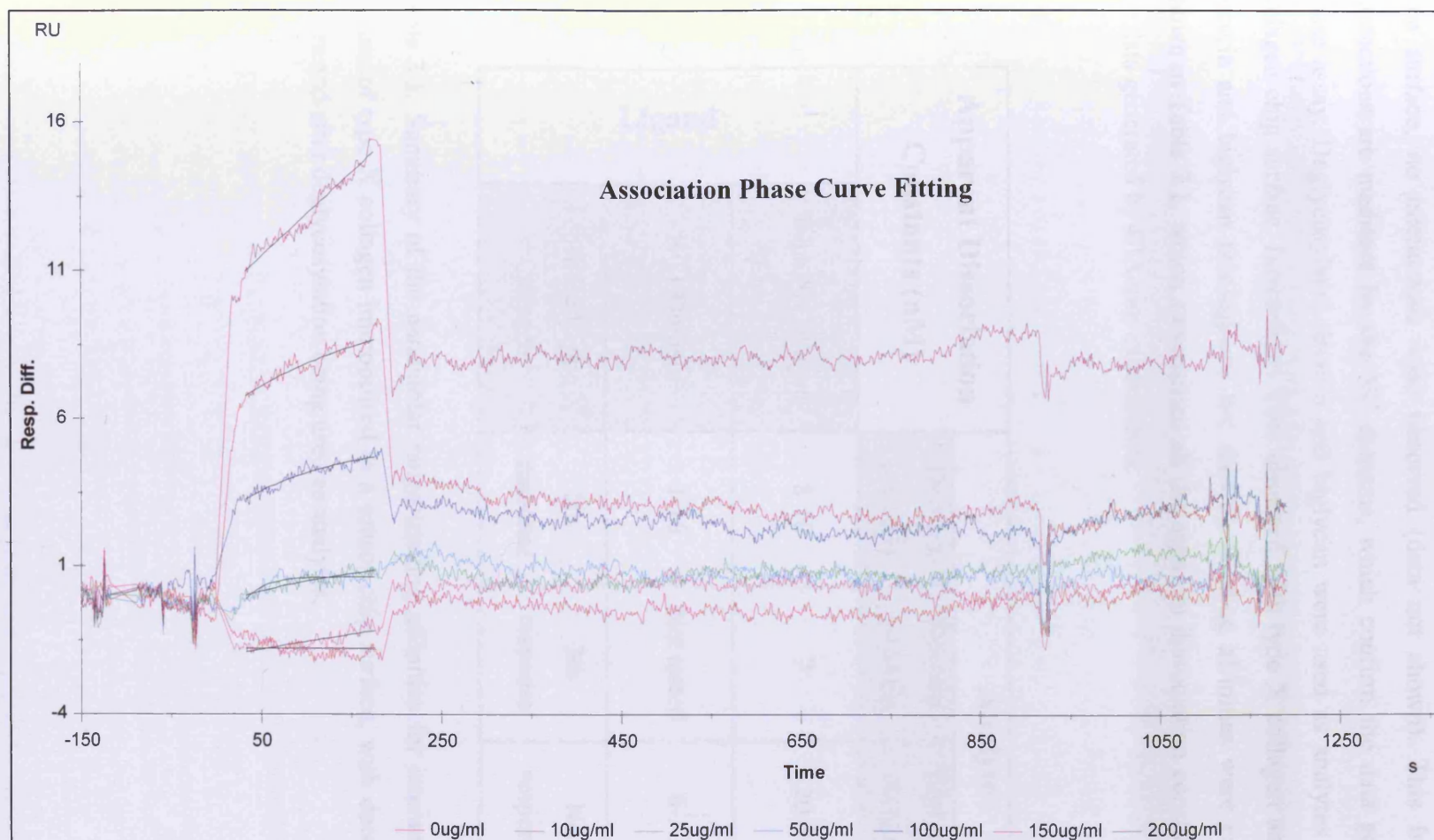


Figure 3.21: Sensogram showing a concentration range of the analyte biglycan, being injected over an NC1 domain chip surface. The association phase curves have been fitted to a 1:1 Langmuir association model.

3.3.2.4 Interactions of Type X Collagen with Decorin and Biglycan are Mediated Via The NC1 Domain and are Independent of the Presence of GAG Chains

When decorin and biglycan were used as analytes over the pepsinised type X collagen ligand chip surface, no interactions were observed (data not shown). This indicated that the interactions are mediated by the NC domains, which confirm the data generated by solid phase assay. Deglycosylated decorin and biglycan were used as analytes over the type X collagen chip surface. Interactions were observed with type X collagen and deglycosylated decorin and biglycan (sensograms not shown). Binding affinities were calculated and are shown in Table 3.1, which summarises all the apparent dissociation constants calculated for the data generated by BIAcore experiments.

| Apparent Dissociation Constants (nM) | | Analyte | | | |
|--------------------------------------|----------------------------|----------------|----------------|-----------------|-----------------|
| | | Decorin (+GAG) | Decorin (-GAG) | Biglycan (+GAG) | Biglycan (-GAG) |
| Ligand | Type X Collagen | 8-10 | 7 | 20-90 | 20 |
| | NC1 Domain | 1-10 | Not tested | 6-30 | Not tested |
| | Pepsinised Type X Collagen | No response | No response | No response | No response |

Table 3.1: Summary of the nanomolar range binding affinities for interactions of different regions of type X collagen immobilised to a sensor chip surface, with decorin and biglycan before and after deglycosylation being used as analytes.

3.3.3 Interactions Visualised by Negative Staining

3.3.3.1 *Production of Decorin and Biglycan Labelled Gold Particles (4 – 5nm diameter)*

Using the reduction of HAuCl_4 by tannic acid method gold sols were prepared. Decorin and biglycan were used to label the gold particles; chemical methods were used to ensure the gold particles were completely adsorbed. Different sized labelled gold particles were fractionated by centrifugation. The pelleted gold particles after the 40,000 rpm centrifugation step were used for interaction analysis. The sizes of the labelled particles were estimated by using a line grating grid of known dimensions. The line grating was photographed at a variety of magnifications (figure 3.22 a – d). The arrow in figure 3.22d corresponds to approximately 400nm. By measuring this distance in mm after each electron micrograph is scaled up to A4 paper size, it was possible to estimate how many nm's in each mm on a scaled up electron micrograph at all magnifications. On examination using electron microscopy the gold particles appeared spherical. Three separate electron micrographs were used to estimate the sizes of the decorin and biglycan labelled gold particles, the diameter of at least 150 gold particles were measure for each label. Decorin labelled gold particles were estimated to be approximately 4nm in size (figure 3.23), while the biglycan labelled gold particles were estimated to be approximately 5nm in diameter (figure 3.24).

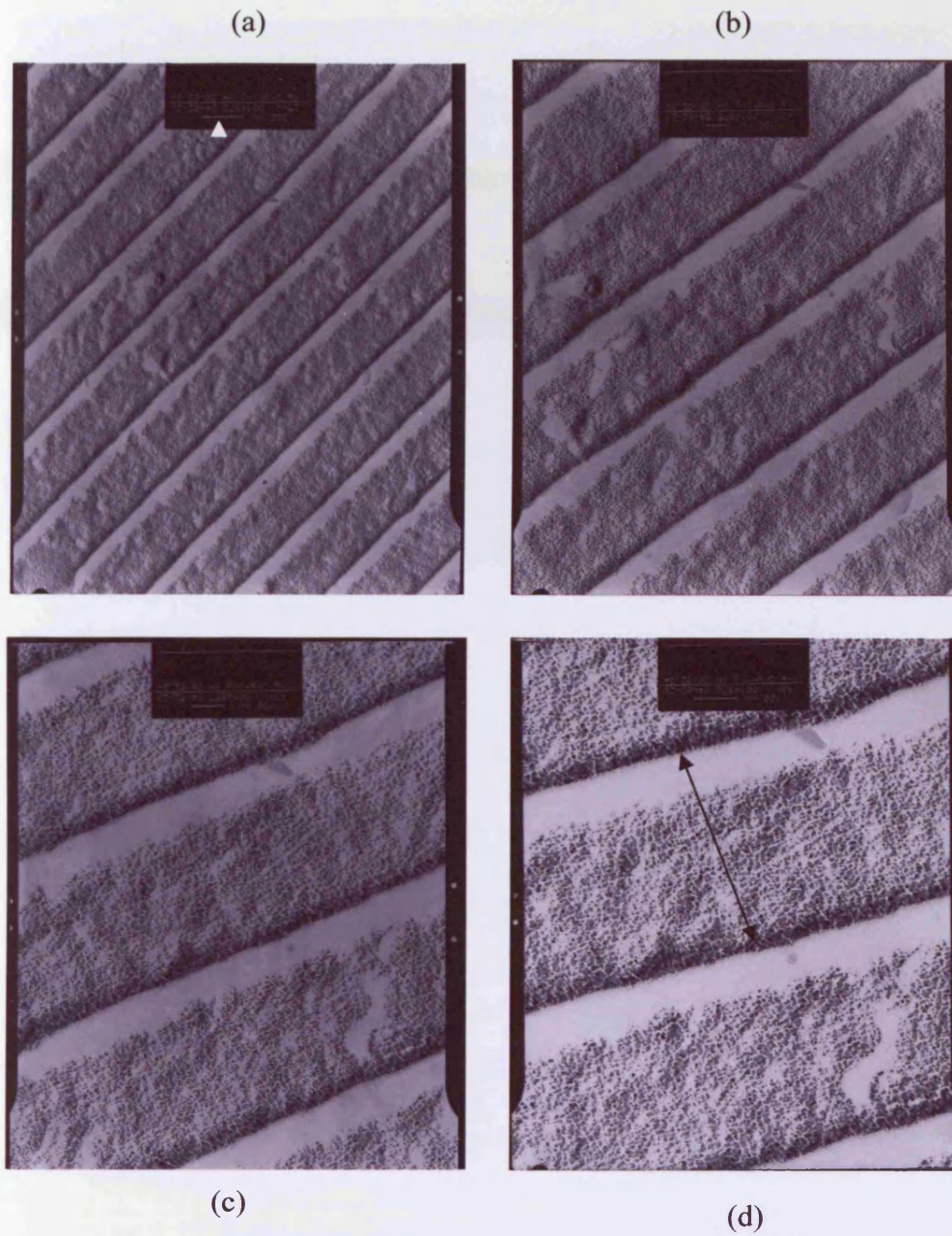


Figure 3.22: Electron micrographs of the line grating grid used for measuring and size estimation purposes. The scale bar provided by the electron microscope and one line grating are highlighted in (a) & (d), respectively. Line grating grid recorded at (a) 25,000x (b) 40,000x (c) 63,000x (d) 80,000x.

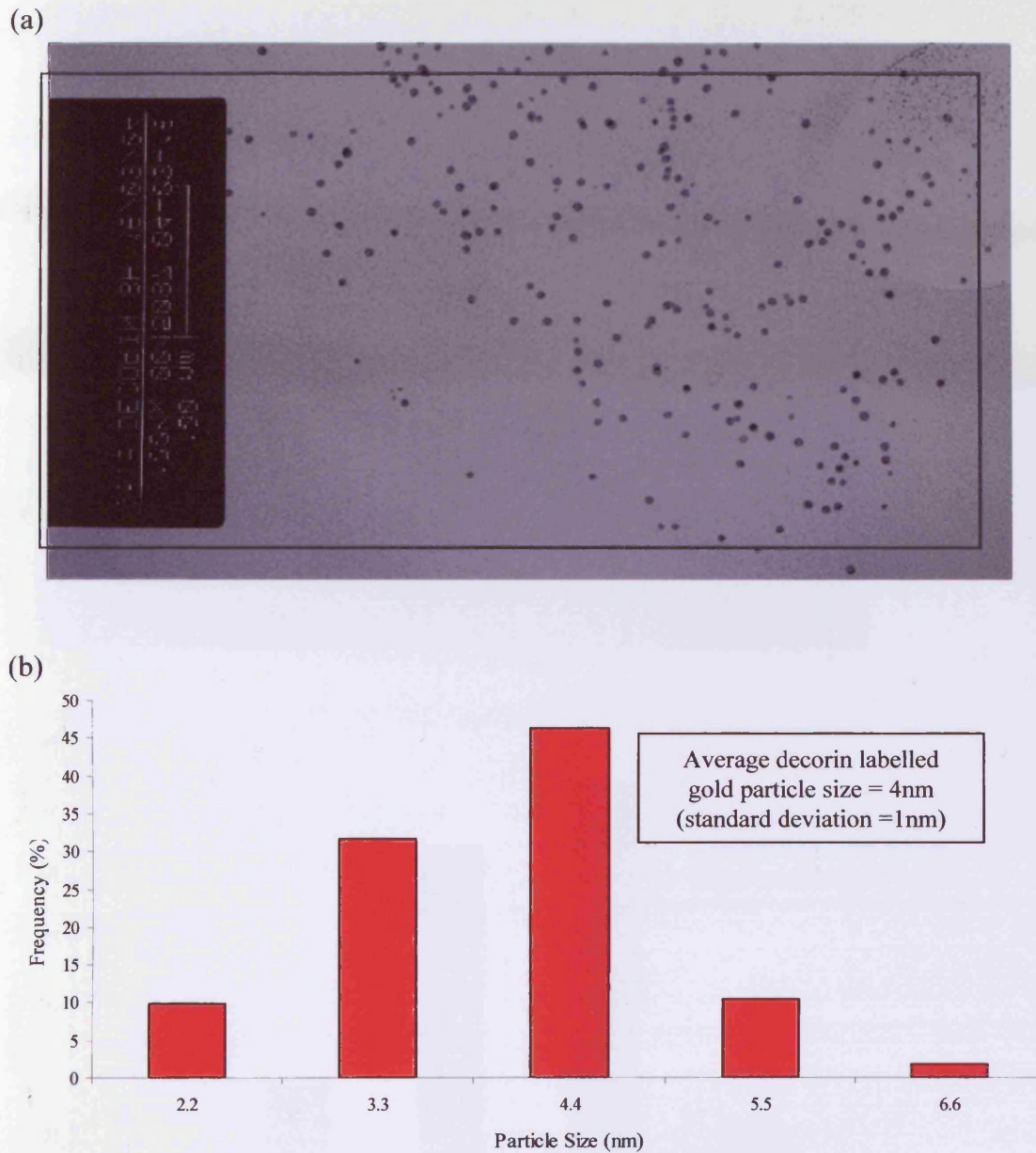


Figure 3.23: Estimation of decorin labelled gold particle diameter.

(a) Electron micrograph of decorin labelled gold particles adsorbed onto pioloform coated copper grids (100,000x magnification).

(b) Frequency distribution bar chart of different sized decorin labelled gold particles, derived from the 40,000rpm centrifuge fraction.

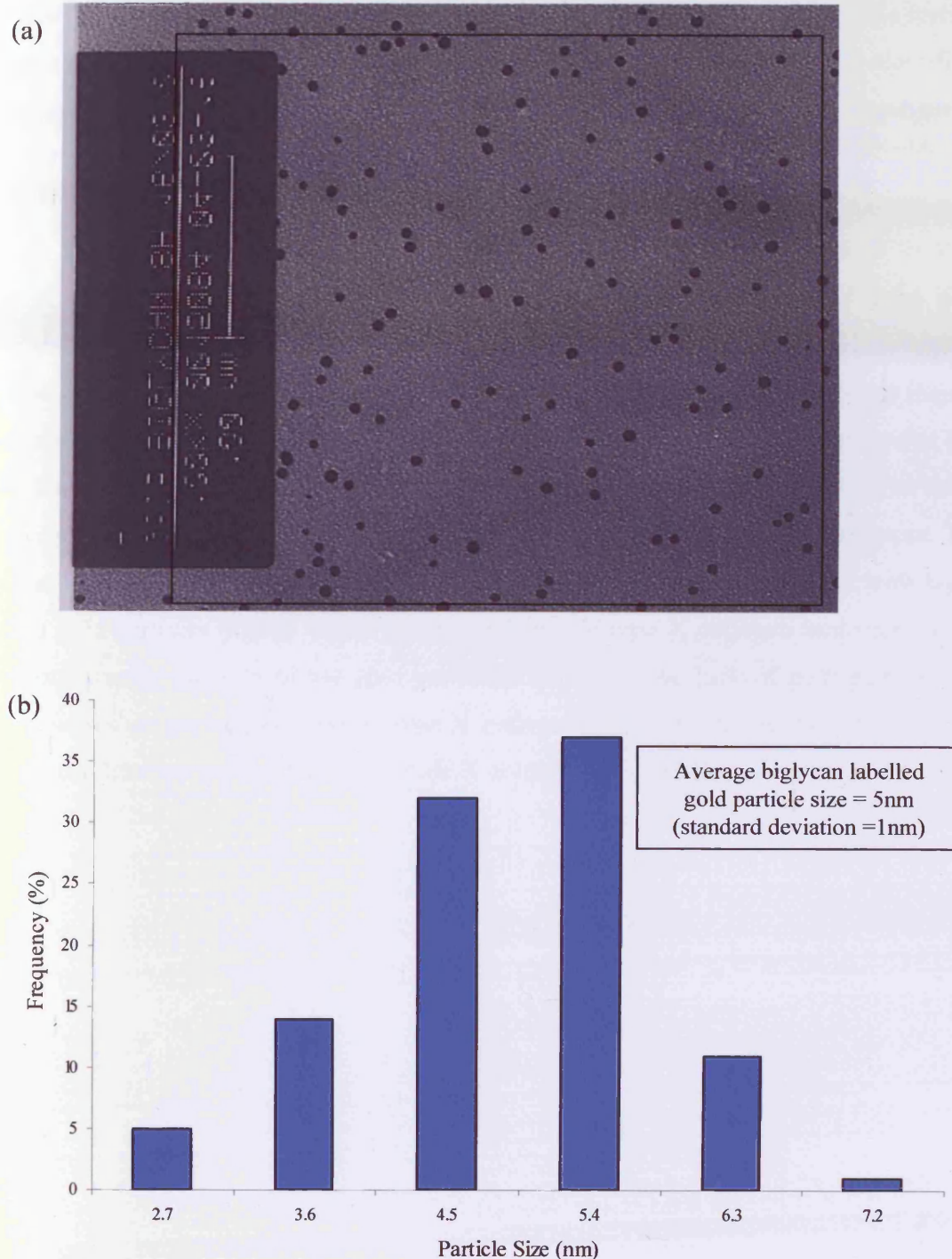


Figure 3.24: Estimation of biglycan labelled gold particle diameter.

(a) Electron micrograph of biglycan labelled gold particles adsorbed onto pioloform coated copper grids (100,000x magnification).

(b) Frequency distribution bar chart of different sized biglycan labelled gold particles, derived from the 40,000rpm centrifuge fraction.

3.3.3.2 Type X Collagen in, Multimeric and Aggregated Forms

A grid was prepared with type X collagen only and stained with 1% uranyl formate. At moderately high magnification it was possible to see type X collagen as multimeric forms and in aggregates (figure 3.25a). Isolated type X collagen molecules were not easily identified. At low magnification the distribution of stain indicated that type X collagen had aggregated into a regular pattern (figure 3.25b).

3.3.3.3 Type X Collagen Interacts with Decorin and Biglycan

Type X collagen was incubated with the decorin and biglycan labelled gold particle preparations and grids were prepared, as described in section 3.2.3. Type X collagen was found to associate with the decorin labelled gold particles (figure 3.26). On closer inspection these interactions appear to be localised to the end of the type X collagen molecules (figure 3.27). Unfortunately, the stoichiometry of interactions can not be commented on as there are not many type X collagen molecules in isolation, there is a tendency for aggregation. This is also true for the electron micrograph showing type X collagens interaction with biglycan labelled gold particles (figure 3.28). The aggregation of type X collagen molecules does not allow any precise location of the gold particles. However, the lack of gold particles in the regions which do not contain stained type X collagen suggests that the interactions between the biglycan labelled gold particles and type X collagen are specific.

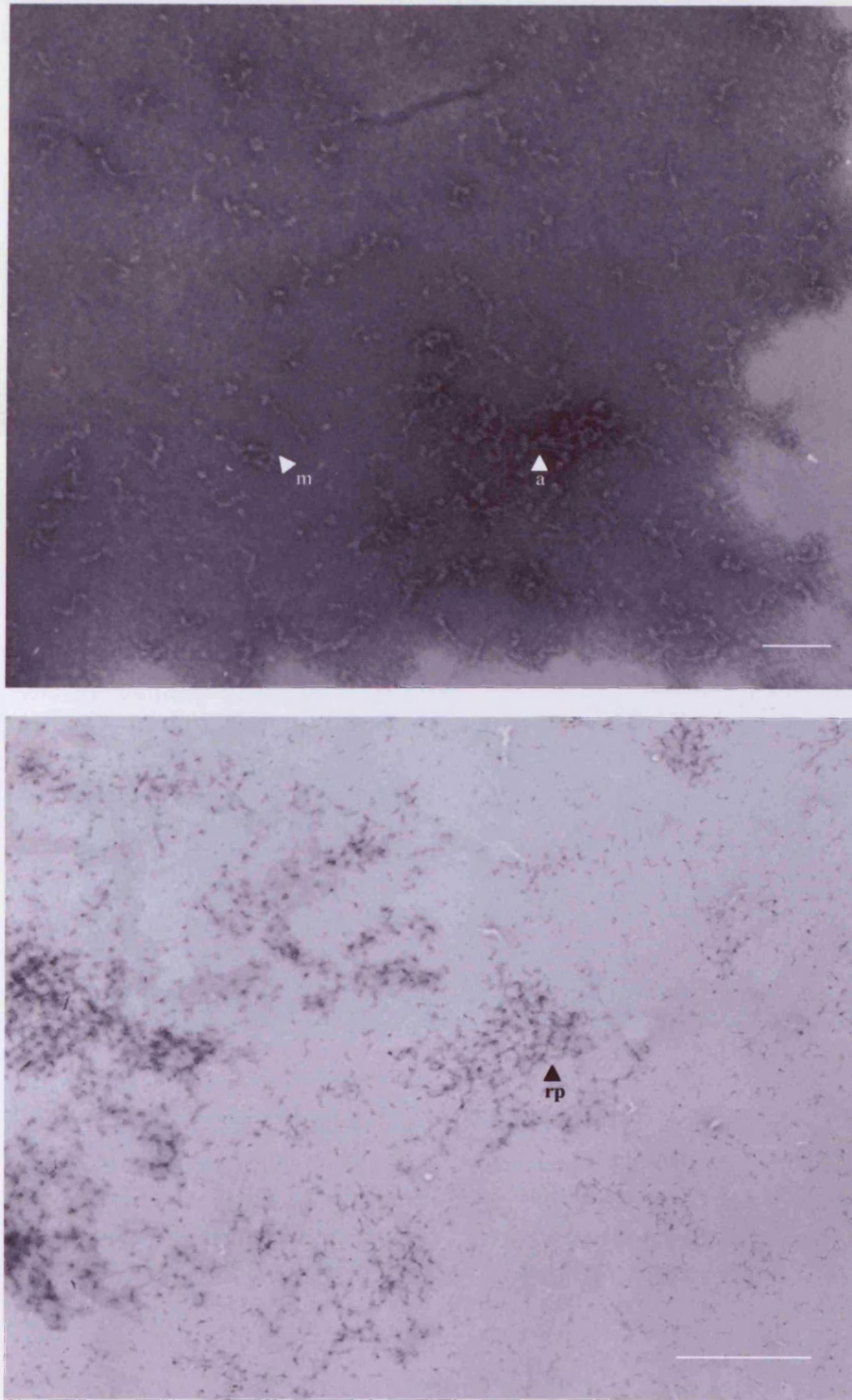


Figure 3.25: Electron micrographs of type X collagen stained with 1% uranyl formate.

- (a) Type X collagen multimers (m) and aggregates (a). Bar = 86nm, 40,000x magnification.
- (b) Aggregated type X collagen staining forming a regular pattern (rp). Bar = 900nm, 8000x magnification.

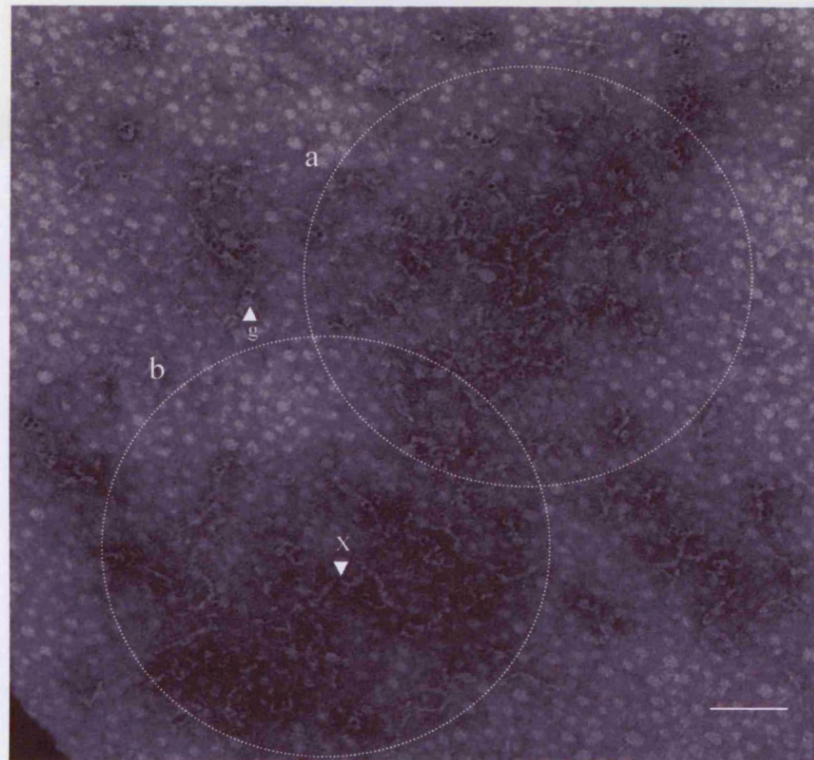


Figure 3.26: Electron micrograph after negative staining with 1% uranyl formate of type X collagen (X) interacting with decorin labelled gold particles (g). Circled areas are shown at higher magnification in figure 3.27. Bar = 86nm approx, 40,000x magnification.

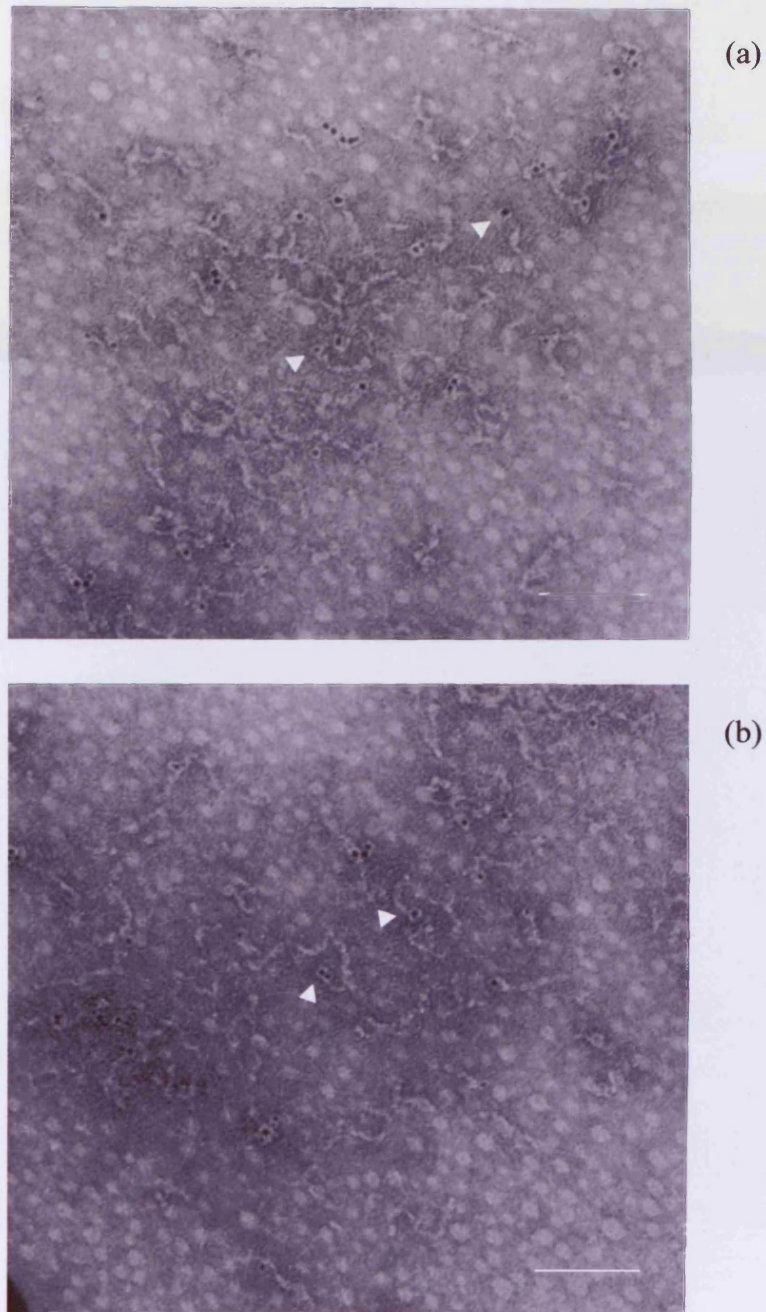


Figure 3.27: Electron micrograph after negative staining with 1% uranyl formate of type X collagen interacting with decorin labelled gold particles. Bar = 90nm approx. 63,000x magnification.

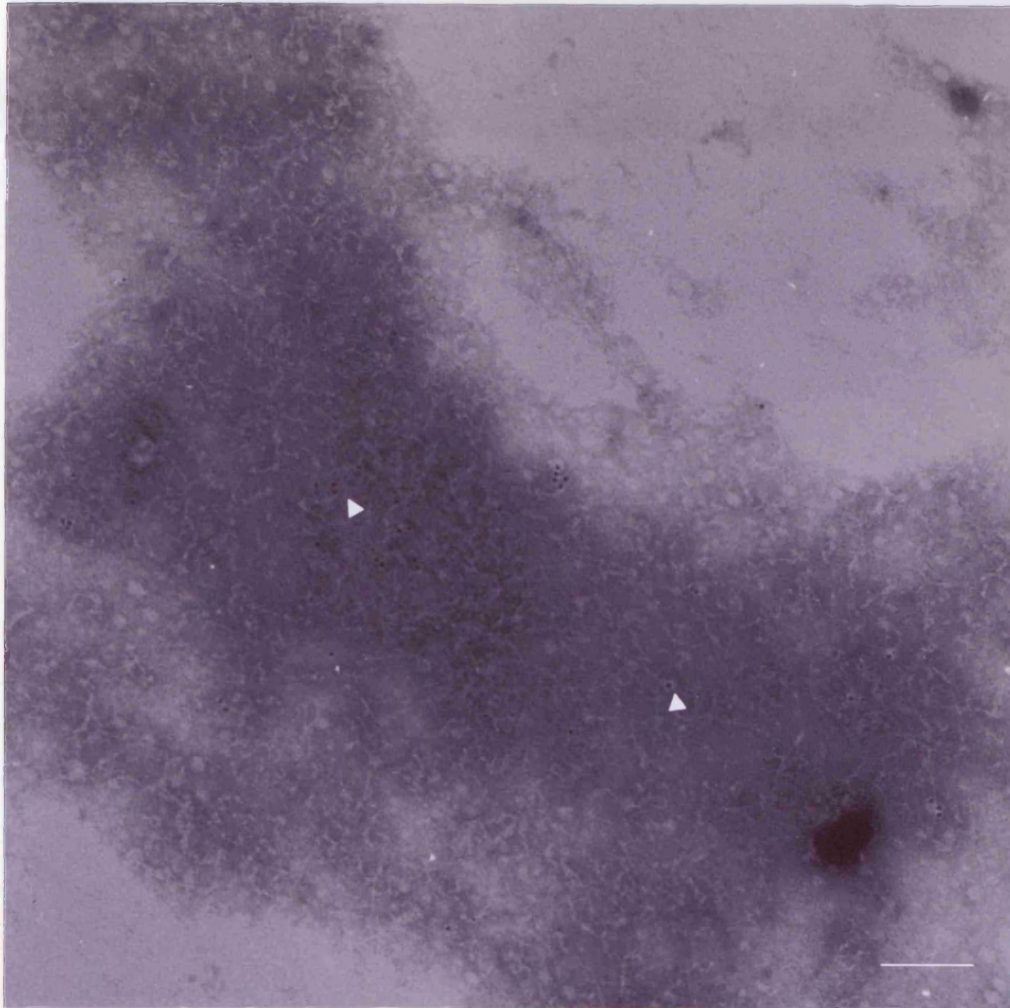


Figure 3.28: Electron micrograph of type X collagen interacting with biglycan labelled gold particles; negatively stained with 1% uranyl formate. Bar = 92nm approx. 50,000x magnification.

3.4 DISCUSSION

Type X collagen was shown to interact with decorin and biglycan in a solid phase assay system. Decorin and biglycan were used to coat multi-well plates and type X collagen was applied as a ligand. Binding saturation was reached at around 5 $\mu\text{g/ml}$ of type X collagen (figures 3.4 & 3.7).

Interaction of type X collagen with decorin can be competitively inhibited by the addition of decorin (figure 3.5) or biglycan (figure 3.6) in the liquid phase with type X. The competing proteins are mixed with type X collagen before being applied to the plate. The absorbance readings decrease as the concentration of the competing proteins increase. The type X collagen in the liquid phase is prevented from binding to the protein in the solid phase. Thus the type X collagen antibody, and subsequently the enzyme conjugated antibody have nothing to bind to, when the chromogenic substrate is applied to the wells minimal coloured product is seen and the absorbance readings are low.

When decorin is used as a competitor with decorin coated wells, 50% inhibition is reached between 4.4 and 5.2 $\mu\text{g/ml}$ of competing decorin. When biglycan is used competitively, 50% inhibition is reached between 5.8 and 6.2 $\mu\text{g/ml}$ of competing biglycan. These results indicate that decorin and biglycan may bind to the same sites on type X collagen. However, decorin is slightly more efficient at inhibiting the decorin–type X interaction than biglycan is.

Interaction of type X collagen with biglycan can be competitively inhibited by the addition of biglycan (figure 3.8) or decorin (figure 3.9) in the liquid phase with type X. The competing proteins are mixed with type X collagen before being applied to the plate. As with the decorin data, as the concentration of competing protein increases the absorbance values decrease.

When biglycan is used as a competitor with biglycan coated wells, 50% inhibition is reached between 3.2 and 3.6 $\mu\text{g/ml}$ of competing biglycan. When competitive decorin is used, 50% inhibition is reached between 6.7 and 7.7 $\mu\text{g/ml}$ of competing decorin. These results indicate that decorin and biglycan may bind to the same sites on type X collagen. However, biglycan is slightly more efficient at inhibiting the biglycan–type X interaction than decorin is.

In the reported experiments type X collagen interacts with decorin and biglycan with apparently similar affinity. The inhibition experiments performed suggests that decorin and biglycan have a common site of interaction on the type X collagen molecule. The finding that 100% inhibition could be produced in the inhibition experiments is evidence for this. Pepsinised type X collagen which is the triple helical domain of type X collagen was used as a ligand and its binding was compared to that of whole type X collagen. Decorin and biglycan coated plates were allowed to interact with whole and pepsinised type X collagen. No interaction was observed between the proteoglycans and pepsinised type X collagen (figure 3.10). This indicates that the NC domains of type X collagen mediate the interactions of type X collagen with decorin and biglycan. Solid phase assays are a popular in vitro method for studying protein-protein interactions, many ECM molecular interactions have been demonstrated with this method (Di Cesare et al., 2002; Holden et al., 2001; Rosenberg et al., 1998).

In the reported experiments, purified chick type X collagen, recombinant human decorin and bovine biglycan were used in solid phase assays. The proteins being from a variety of species is not ideal for interaction analysis, however, the conserved homologies across species of all the proteins involved has proven strong enough to be able to perform interaction analysis successfully. Ideally recombinant human proteins should have been used, but the construction of expression vectors, transfections and purification of expressed proteins can be very time consuming and the yields may not be great.

The BIAcore system monitors biomolecular interactions in real time, using a non-invasive optical detection principle based on SPR. The SPR response reflects a change in mass concentration at the detector surface as molecules bind or dissociate. Since real-time BIA monitors interactions directly as they happen, the technique is well suited for the determination of kinetic parameters. Comparative affinity ranking is simple to perform, and both kinetic and affinity constants can be derived from the sensogram data. SPR has been widely used for studying interactions of ECM proteins (Holden et al., 2001; Wiberg et al., 2001).

Type X collagen was shown to interact with decorin and biglycan using SPR (figures 3.12, 3.18 & 3.19). The sensogram data was fitted to 1:1 Langmuir association (figure 3.15 & 3.19) and dissociation (figures 3.14 & 3.18) binding models, figures show the sensogram curves in

colour with the fitted curves in black. χ^2 values are a statistical measure of the closeness of the fit of the curves. For good fitting, χ^2 is of the same order as the noise in RU (typically <2). The χ^2 values ranged from 0.07 to 5.8, indicating the fitting was adequate. K_D values were calculated and were in the nanomolar range, indicating that the interaction between type X collagen and decorin and biglycan was high affinity binding.

The lack of binding of decorin and biglycan to pepsin digested type X collagen in the solid phase assays indicated that the NC domains were involved. This could not be investigated in the solid phase system as the available antibody to type X collagen, MA3, recognises a collagenous domain. However, the availability of recombinant NC1 enabled direct interactions of NC1 with decorin and biglycan to be investigated using the BIAcore system. The NC1 domain of type X collagen was shown to bind to decorin and biglycan. The sensogram data was fitted to 1:1 association (figure 3.17 & 3.21) and dissociation (figures 3.16 & 3.20) binding models, figures show the sensogram curves in colour with the fitted curves in black. χ^2 values ranged from 0.04 to 0.06, indicating good curve fitting. K_D values were calculated and were in the nanomolar range indicating high affinity binding between the NC1 domain of type X collagen and decorin and biglycan.

The data indicates that the interaction between type X collagen and the proteoglycans is mediated by the NC1 domain. The sensograms and the K_D values indicate that the binding to NC1 is comparable to whole type X. Experiments using pepsinised type X collagen as a ligand on the chip surface, have confirmed this finding with no responses being seen when the analytes decorin and biglycan are injected over its surface. These findings have led to the conclusion that the NC2 domain of type X collagen is unlikely to be involved in the interaction of type X collagen with decorin and biglycan. However, this has not been investigated in the solid phase assay or BIAcore system directly to confirm its exclusion. Interactions were also observed between type X collagen and deglycosylated decorin and biglycan. The similar binding affinities (Table 3.1) found before and after deglycosylation indicate that the interactions are occurring independently of the presence or absence of the GAG chains on the proteoglycans, therefore are mediated by the protein cores of decorin and biglycan.

When the data for the type X-decorin/biglycan interactions and the NC1 domain-decorin/biglycan interactions was fitted to simultaneous k_a/k_d binding models the fitted

curves did not appear to fit the sensograms well and the χ^2 value was often very large. This is why the association and dissociation phases were fitted separately. A possible explanation of why this was necessary is that different conditions apply during association and dissociation.

Kinetic data is always interpreted in terms of a model of the interaction process, and the kinetic constants obtained from the analysis are apparent constants which are valid in the context of the model. The simplest model for interaction on the sensor chip surface is a homogeneous 1:1 binding, treating the immobilised ligand as a solid phase component. Analysing data in terms of this model is done by non-linear curve fitting procedures. The results of model fitting do not reveal what is actually happening at the sensor chip surface. The apparent constants which are derived are valid within the context of the model and are sufficient for purposes such as indicating high affinity binding (Markey, 2000)

Negative staining can be used as a tool to capture images of interacting proteins. Such images can be considered as powerful evidence of an interaction, and are an ideal complement to data generated from other interaction studies such as solid phase assays or SPR. Decorin and biglycan labelled gold particles were prepared for utilisation in negative staining experiments. The gold particles were relatively spherical and uniformly sized at around 4 -5nm (figures 3.23 & 3.24).

Prior to interaction with decorin and biglycan analysis, type X collagen samples were negatively stained (figure 3.25). The images captured demonstrate the tendency for type X collagen to aggregate, and highlight the lack of single molecules in isolation. Changes to the concentration or the ionic conditions of the solution that type X collagen is dissolved in are probably necessary to prevent such aggregation. However, this was not optimised and interaction analysis was performed.

Preliminary negative staining experiments of type X collagen utilising decorin and biglycan labelled gold particles have proved promising. Type X collagen can be seen interacting with decorin and biglycan gold probes, figures 3.26 & 3.27 and 3.28, respectively. Due to the problems associated with the aggregation of type X collagen described above, isolated molecules have not been photographed and the precise stoichiometry of the interactions can not be commented on. The gold probes appear to be localised to the end of some of the type X

collagen molecules, possibly indicating interactions with the NC1 domain. The lack of decorin and biglycan gold particles in areas of the electron micrographs which do not contain type X collagen are suggestive that the interactions seen are specific.

In summary, type X collagen interacts with decorin and biglycan as demonstrated by solid phase assays and SPR. The interactions are likely to be mediated by the NC1 domain of type X collagen; as pepsinised type X collagen was found not to interact with decorin or biglycan by solid phase assays or by SPR and the binding affinities of interactions with decorin and biglycan are comparable between whole type X collagen and the NC1 domain. The high affinity binding interactions were found to be independent of the presence or absence of the GAG chain(s) on decorin and biglycan, indicating that the protein cores of decorin and biglycan mediate the interactions. The interaction of type X collagen with decorin and biglycan labelled gold particles was investigated by negative staining and TEM. Interactions were visualised on electron micrographs, no additional information regarding the interactions was generated using this method.

Chapter 4: Construction of Expression Clones, Expression and Purification of Recombinant Proteins and Interaction Analysis of NC1 Fragments with Decorin and Biglycan

4.1 BACKGROUND

The identified interactions involving the NC1 domain of type X collagen with decorin and biglycan require further characterisation, fragments of the NC1 domain of type X collagen could be used in interaction studies to localise the site of interaction on the NC1 domain. Subsequent comparisons of interacting NC1 fragments with the resolved crystal structure of the NC1 domain could potentially pinpoint key regions important for the interaction of type X collagen with these SLRP's.

4.1.1 Bacterial Expression of NC1 Recombinant Fragments

Recombinant fragments of the NC1 domain were produced and used in interaction studies, to further characterise the interactions with decorin and biglycan. *Escherichia coli* (*E. coli*) was used as a host system for production of recombinant proteins; factors such as ease of genetic manipulation, availability of optimised expression plasmids and ease of growth were among the reasons that this system was chosen (Wingfield, 1997).

The QIAexpress system (Qiagen) was the method of choice for expression, purification and detection of recombinant proteins. The vectors are designed to place an affinity tag of 6 consecutive histidine residues (6xHis-tag) at the N-terminus of the protein of interest. The 6xHis-tag rarely interferes with the secretion or the structure and functions of fusion proteins, and can be used for purification purposes. Other features of the vectors such as the T5 promoter, *lac* operator sequences and the multiple cloning site are highlighted in figure 4.1. Three different versions of the pQE expression vector used were available; pQE -30, -31 and -32, which allowed cloning of the gene of interest in different open reading frames, figure 4.2 (QIAGEN, 2003).

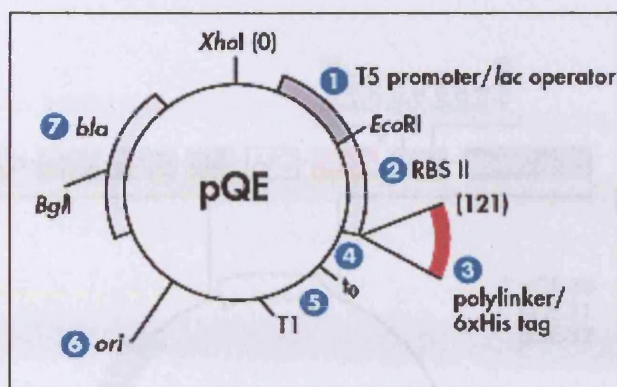
4.1.2 Regulation of Expression: pREP4 plasmid

Transcription at the T5 promoter of pQE vectors can be regulated and repressed by high levels of the *lac* repressor protein. The *E. coli* strain M15[pREP4] contains the low-copy plasmid

pREP4 which confers kanamycin resistance and constitutively expresses the *lac* repressor protein encoded by the *lac* I gene. Recombinant proteins expressed by pQE vectors can be induced by the addition of isopropyl- β -D-thiogalactoside (IPTG) which binds to the *lac* repressor protein and inactivates it. RNA polymerase then transcribes the sequences downstream from the promoter, and translation of the recombinant protein follows.

4.1.3 Purification of 6xHis-tagged proteins by Ni-NTA affinity chromatography

Nitrilotriacetic acid (NTA) is a tetradentate chelating agent, which occupies four of the six ligand binding sites in the coordination sphere of the nickel ion, leaving two sites free to interact with the 6x-His-tag (figure 4.3). Ni-NTA agarose is composed of Ni-NTA coupled to Sepharose®CL-6B and offers high binding capacity and minimal non-specific binding, it can be used to purify 6xHis-tagged proteins in a variety of ways including; on a column, or by centrifugation.



Elements Present in QIAexpress pQE -30, -31 & -32 Vectors

- 1 Optimised promoter / operator element consisting of the phage T5 promoter and two lac operator sequences which increase lac repressor binding and ensure efficient repression of the powerful T5 promoter.
- 2 Synthetic ribosomal binding site, RBSII, for efficient translation.
- 3 6 x His-tag coding sequence 5' to the polylinker cloning region.
- 4 Multiple cloning site and translational stop codons in all reading frames for convenient preparation of expression constructs.
- 5 Two strong transcriptional terminators: t_0 from phage lamda and T1 from the *rrnB* operon of *E. Coli*, to prevent read-through transcription and ensure stability of the expression construct.
- 6 ColE1 origin of replication from pBR322.
- 7 Beta-lactamase gene (*bla*) conferring resistance to ampicillin at 100 μ g/ml.

Figure 4.1: pQE vector map with characteristics required for protein expression highlighted. (Taken from QIAGEN 2003).

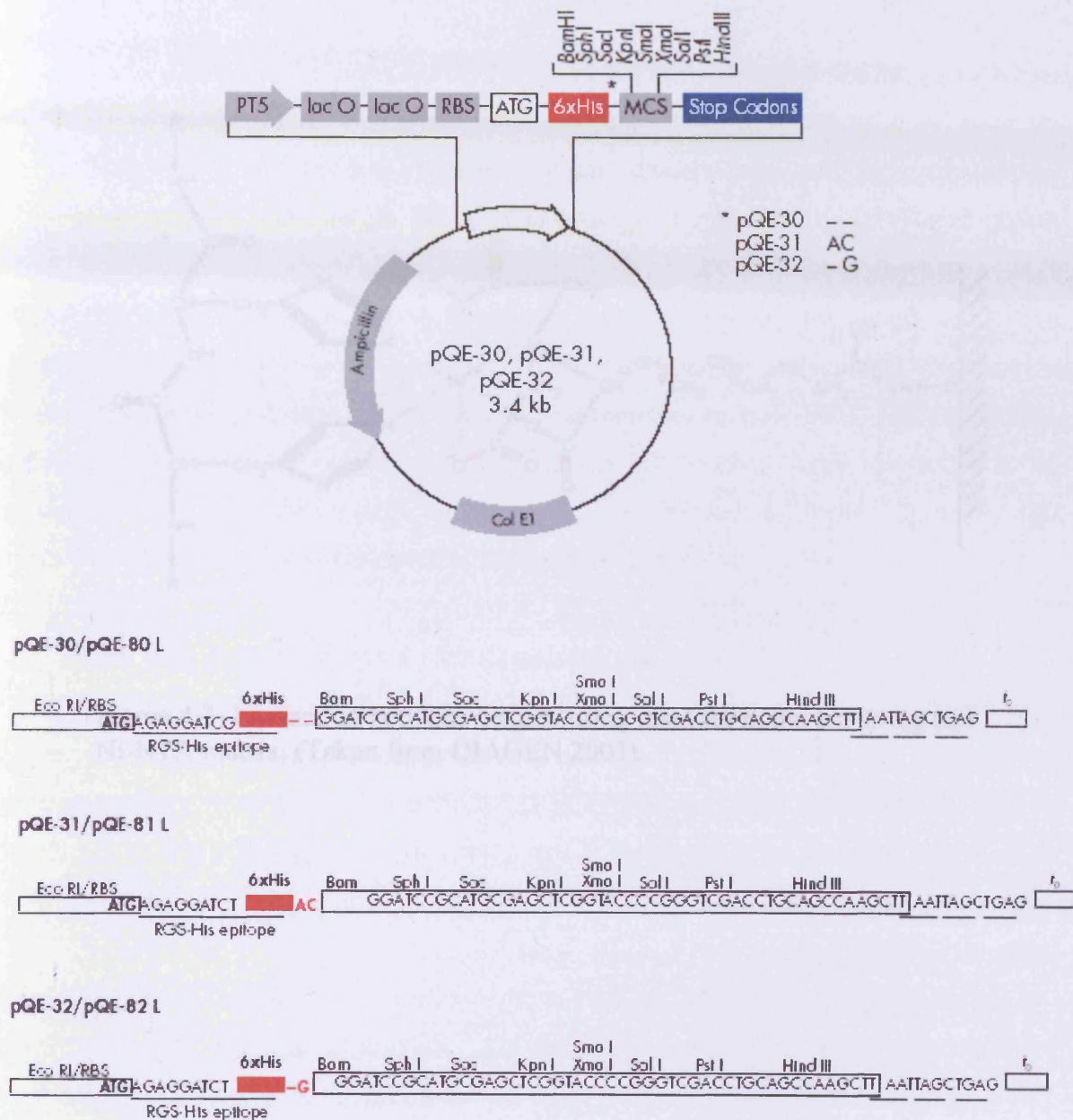


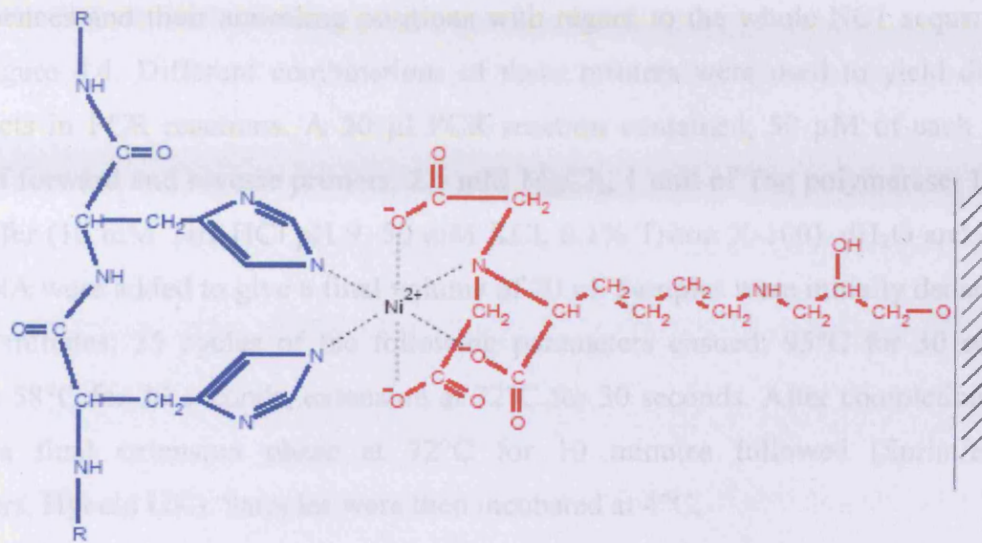
Figure 4.2: Vector map showing positions of features important for protein expression and diagram detailing sequence of restriction sites present in the multiple cloning sites of vectors pQE -30, -31 and -32. (Taken from QIAGEN 2003).

4.2 MATERIALS AND METHODS

All reagents for protein biochemistry were purchased from Sigma, all molecular biology reagents were purchased from Pierce and all reagents used for protein expression were purchased from Qiagen, unless otherwise stated.

4.2.1 Amplification of NCI Fragment by Polymerase Chain Reaction (PCR)

Primer sequences and their associated position with respect to the whole NCI sequence are shown in Figure 4.3. Different combinations of these primers were used to yield different sized products in 1.5 reactions. A 20 µl PCR reaction contained: 50 mM of each dNTP, 0.125 µM of forward and reverse primers, 1 unit of Taq polymerase, 1 µl of Taq polymerase PCR reaction buffer (Qiagen), and 1.5 µl of template DNA. The PCR was performed at 95°C for 30 seconds, followed by 30 cycles of 94°C for 30 seconds, 58°C for 30 seconds, 72°C for 1 minute, followed by a final extension at 72°C for 10 minutes (Hyundai Express thermocycler, Hybrid UK). Samples were stored at 4°C.



4.2.1.1 PCR Using Primers Adaptor with Restriction Sequences

PCR using primers adaptor with restriction sequences was performed as follows. A PCR reaction contained: 2 µl of 10x Acc Buffer (600 mM Tris-Cl, 60 mM (NH₄)₂SO₄, 100 mM KCl, 20 mM MgSO₄, pH 8.3), 50 µM of each dNTP, 0.125 µM of forward and reverse primer, 1 unit of Accuscript DNA polymerase, 1 µl of template DNA diluted 1:100 and 1:1000 and filled up to a final volume of 20 µl. Samples were subjected to an isogenic restriction step: 30 minutes at 95°C, followed by 30 cycles of 94°C for 30 seconds, 58°C for 30 seconds, 72°C for 1 minute, followed by a final extension at 72°C for 10 minutes (Hyundai Express thermocycler, Hybrid UK). Samples were stored at 4°C.

4.2 MATERIALS AND METHODS

All reagents for protein biochemistry were purchased from Sigma, all molecular biology reagents were purchased from Promega and all reagents used for protein expression were purchased from Qiagen, unless otherwise stated.

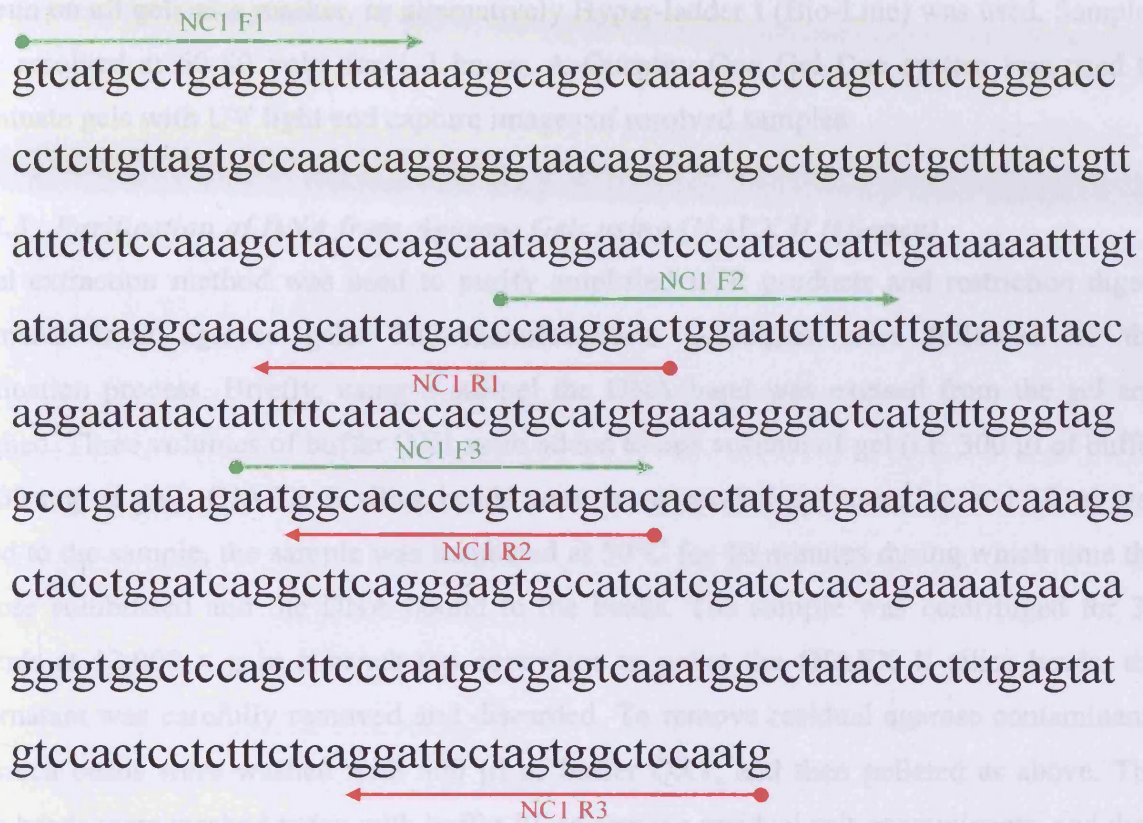
4.2.1 Amplification of NC1 Fragments by Polymerase Chain Reaction (PCR)

Primer sequences and their annealing positions with regard to the whole NC1 sequence are shown in figure 4.4. Different combinations of these primers were used to yield different sized products in PCR reactions. A 20 µl PCR reaction contained, 50 µM of each dNTP, 0.125 µM of forward and reverse primers, 2.5 mM MgCl₂, 1 unit of Taq polymerase, 1x PCR reaction buffer (10 mM Tris-HCl pH 9, 50 mM KCl, 0.1% Triton X-100). dH₂O and 1 µl of template DNA were added to give a final volume of 20 µl. Samples were initially denatured at 95°C for 5 minutes, 35 cycles of the following parameters ensued; 95°C for 30 seconds, annealing at 58°C for 30 seconds, extension at 72°C for 30 seconds. After completion of the 35 cycles a final extension phase at 72°C for 10 minutes followed (Sprint/Express thermocyclers, Hybaid UK). Samples were then incubated at 4°C.

4.2.1.1 PCR Using Primers Adapted with Restriction Sequences

The enzyme Accusure DNA polymerase (Bioline, UK) was used for its high fidelity feature, it possesses 3'-5' proof-reading activities which prevents mis-incorporations during DNA polymerase activity. A PCR reaction included; 2 µl of 10x Acc Buffer (600 mM Tris-Cl, 60 mM (NH₄)₂SO₄, 100 mM KCl, 20 mM MgSO₄, pH 8.3), 50 µM of each dNTP, 0.125 µM of forward and reverse primer, 1 unit of Accusure DNA polymerase, 1 µl of template DNA (plasmid DNA diluted 1:100 and 1:1000) and dH₂O up to a final volume of 20 µl. Samples were subjected to an enzyme activation step; 10 minutes at 95°C, followed by 30 cycles of : 95°C for 30 seconds, 58°C for 30 seconds, 72°C for 1 minute, followed by a final extension at 72°C for 10 minutes (Sprint/Express thermocyclers, Hybaid UK). Samples were stored at 4°C.

NC1 Nucleotide Sequence and Primer Positions



Forward Primers: ● →

NCI F1. gtcatgcctgagggtttata

NCI F2. ccaaggactggaatctttact

NCI F3. aatggcaccctgtaatgtac

Reverse Primers: ← ●

NCI R1. agtccttgggtcataatgctg

NCI R2. gtacattacaggggtgcc

NCI R3. cattggagccactaggaatcc

Figure 4.4. Sequence of the NC1 domain of human type X collagen COL10A1 mRNA (gi:18105031). Positions and sequences of forward primers (in green) and reverse primers (in red) are shown.

4.2.1.2 Agarose Gel Electrophoresis

PCR products were analysed by electrophoresis in agarose gels. 1% gels containing 10 µg/ml ethidium bromide (Sigma) in Tris borate EDTA buffer (80 mM Tris borate, 2 mM EDTA, pH 8.3) were prepared. 10 µl of sample was mixed with 1 µl of loading dye (10 mM Tris-Cl, pH 7.5, 50 mM EDTA, 10% Ficoll 400, 0.255% Bromophenol blue, 0.25% Xylene Cyanol FF, 0.4% orange G) prior to loading on the gel. A 100bp DNA ladder was mixed with loading dye and run on all gels as a marker, or alternatively Hyper-ladder I (Bio-Line) was used. Samples were resolved at 60-80 volts for 1-2 hours. A Quantity One Gel Doc system was used to illuminate gels with UV light and capture images of resolved samples.

4.2.1.3 Purification of DNA from Agarose Gels using QIAEX II (Qiagen)

A gel extraction method was used to purify amplified PCR products and restriction digest fragments from agarose gels. The manufacturer's guidelines were followed for the purification process. Briefly, using a scalpel the DNA band was excised from the gel and weighed. Three volumes of buffer QX1 were added to one volume of gel (i.e. 300 µl of buffer to 100 mg of gel). QIAEX II silica beads were re-suspended by vortexing and 10 µl was added to the sample, the sample was incubated at 50°C for 10 minutes during which time the agarose solubilised and the DNA bound to the beads. The sample was centrifuged for 30 seconds at 12,000 x g in a bench top centrifuge to pellet the QIAEX II silica beads, the supernatant was carefully removed and discarded. To remove residual agarose contaminants the silica beads were washed with 500 µl of buffer QX1, and then pelleted as above. The silica beads were washed twice with buffer PE to remove residual salt contaminants, and then pelleted as above. The silica beads were air-dried for 10-15 minutes and were resuspended by adding 20 µl of 10 mM Tris-HCl, pH 8, and vortexing. The eluted DNA was obtained by pelleting the silica beads as above, and by carefully removing the supernatant which contained the DNA.

4.2.2 Cloning NC1 Fragments into the Cloning Vector pGEM®-T

Purified PCR products were 'TA-cloned' into the cloning vector pGEM®-T (figure 4.5). Cloning using this method, utilises the single deoxyadenosine that polymerases often add to the 3' end of amplified products during PCR and the single 3' terminal thymidine overhang present on the linearised pGEM®-T. Insertional inactivation of the α -peptide coding region of the enzyme β -galactosidase allows recombinant clones to be directly identified by colour screening on selective agar plates. Clones that contain PCR products usually produce white

colonies, while those that do not produce blue colonies. When the β -galactosidase gene is not inactivated by the insertion of a PCR product, the presence of isopropyl β -D-thiogalactopyranoside (IPTG) and 5-bromo-4-chloro-3-indolyl- β -D-galactopyranoside (x-gal) in the agar plates induces expression of the enzyme which then converts the substrate x-gal into a blue product.

4.2.2.1 Ligating PCR Products into the pGEM®-T Vector

The 5 μ l reaction mixture included; 2.5 μ l of 2x rapid ligation buffer (60 mM Tris-HCl pH 7.8, 20 mM MgCl_2 , 20 mM DTT, 2 mM ATP, 10% polyethylene glycol), 0.5 μ l of pGEM®-T vector (50 ng μl^{-1}), 1 μ l of purified PCR product, 0.5 μ l of T4 DNA ligase (3 units μl^{-1}) and 0.5 μ l dH_2O . Ligation reactions were mixed by gentle pipetting and incubated overnight at 4°C.

4.2.2.2 Transformation of Competent *E. coli* (JM109) with pGEM®-T.

Plasmid DNA was used to transform high efficiency competent JM109 cells. From ligation reactions 2 μ l of DNA was removed and added to sterile Falcon 2059 polypropylene tubes (Becton Dickinson, UK), 25 μ l of just thawed JM109 cells was mixed with the DNA and incubated on ice for 20 minutes. Cells were heat-shocked at 42°C for 45-50 seconds in a water bath and then returned to ice for 2 minutes. To the cells, 475 μ l of SOC medium (Gibco Life Sciences, UK) was added, and incubated at 37°C with shaking at 150 rpm for 1.5 hours. 100 μ l of each transformation culture was plated onto LB agar plates containing 100 $\mu\text{g/ml}$ ampicillin, 0.5 mM IPTG, 50 $\mu\text{g/ml}$ x-gal. Plates were inverted and incubated at 37°C overnight.

White colonies were selected using a sterile tip and used to inoculate 5 ml of LB broth containing 100 $\mu\text{g/ml}$ ampicillin, cells were incubated at 37°C shaking at 225 rpm overnight. Glycerol stocks of each clone were prepared in LB broth with 20% (v/v) glycerol and stored at -80°C. The remaining cells were used to prepare plasmid DNA.

4.2.2.3 DNA purification using the Wizard® Plus SV Miniprep System (Promega)

Plasmid DNA was isolated from 1-10 ml of overnight *E. coli* cultures using the above system according to manufacturer's protocol, the method is summarised in figure 4.6. Briefly, cells were harvested by centrifugation at 10,000 x g for 5 minutes. Cells were resuspended in 250 μ l of cell resuspension solution (50 mM Tris-Cl pH 7.5, 10 mM EDTA, 100 $\mu\text{g ml}^{-1}$ RNase

A) and transferred to 1.5 ml microcentrifuge tubes. Cells were lysed using 250 μ l of cell lysis solution (0.2 M NaOH, 1% SDS), tubes were inverted 4 times to ensure mixing and incubated for no longer than 5 minutes. To inactivate endonucleases and to non-specifically degrade protein contaminants, 10 μ l of alkaline protease solution was added to the cleared cell lysate, mixed by inverting the tube 4 times and incubated for 5 minutes. The mixture was neutralised by the addition of 350 μ l of neutralisation solution, tubes were inverted 4 times to ensure thorough mixing. The bacterial lysate was centrifuged at 14,000 x g for 10 minutes at room temperature.

The supernatant was decanted into a spin column inserted into a 2 ml collection tube. The supernatant was centrifuged at 14,000 x g for 1 minute, the flow-through was discarded from the collection tube. The column was washed using 750 μ l of wash solution (60 mM potassium acetate, 8.3 mM Tris-HCl pH 7.5, 40 μ M EDTA, 60% ethanol), centrifuged at 14,000xg for 1 minute, the flow-through was discarded as before. This wash step was repeated using 250 μ l of wash solution and a 2 minute centrifugation step. The columns were transferred to sterile 1.5 ml microcentrifuge tubes, plasmid DNA was eluted from the column by the addition of 100 μ l of nuclease-free water, followed by centrifugation at 14, 000 x g for 1 minute. Plasmid DNA was stored at -20°C.

4.2.2.4 Sequencing Reaction

Sequence analysis was performed using the ABI Prism® 3100 Genetic Analyser (Applied Biosystems, UK). The Big Dye Terminator Ready Reaction Cycle Sequencing Kit (Applied Biosystems, UK) was used and includes: dye terminators, dNTPs, AmpliTaq DNA polymerase and MgCl₂. Sequencing was performed by a Cardiff University support facility. In brief, DNA plasmid template was prepared as described in 4.2.2.3 to concentrations of around 100 μ g ml⁻¹. 250-500 ng of plasmid DNA was combined with 8 μ l of terminator ready reaction mix, 3.2 pmol forward or reverse primer and was made up to 20 μ l with dH₂O. Details of sequencing primers are shown in table 4.1. The sequencing reactions were subjected to 25 cycles of: 96°C for 20 seconds, 50°C for 10 seconds and 60°C for 4 minutes (Express Thermocycler, Hybaid).

Prior to electrophoresis unincorporated Big Dye terminators were removed by precipitation. To each 20 μ l sequencing reaction, 80 μ l of 70% (v/v) iso-propanol was added and briefly vortexed. Extension products were precipitated by incubation at room temperature for 15

minutes; they were collected by centrifugation at 12,000 x g for 30 minutes. The supernatant was discarded and the sample pellets were washed twice in 250 μ l of 70% (v/v) ethanol to remove traces of residual salts. The sample pellets were air-dried for 15 minutes, and then resuspended in 15 μ l of HiDi® Formamide (Applied Biosystems, UK) before being run on the ABI Prism® 3100 Genetic Analyser. Sequence chromatograms were analysed using Chromas, version 1.43 (Conor McCarthy, Griffith University, Brisbane, Australia), the sequence data was copied into text format and analysed using the BLAST search engine for homology with sequences on the EMBL database.

| Vector | Primer | Primer Sequence |
|--------|-------------|---------------------------------|
| pGEM-T | M13 Forward | 5'-CGCCAGGGTTTTCCCAGTCACGAC-3' |
| | M13 Reverse | 5'-AGCGGATAACAATTTTCACACAGGA-3' |
| pQE-30 | pQE Forward | 5'-CCCGAAAAGTGCCACCTG-3' |
| | pQE Reverse | 5'-GTTCTGAGGTCATTACTGG-3' |

Table 4.1: Oligonucleotide sequences of primers used in sequencing reactions.

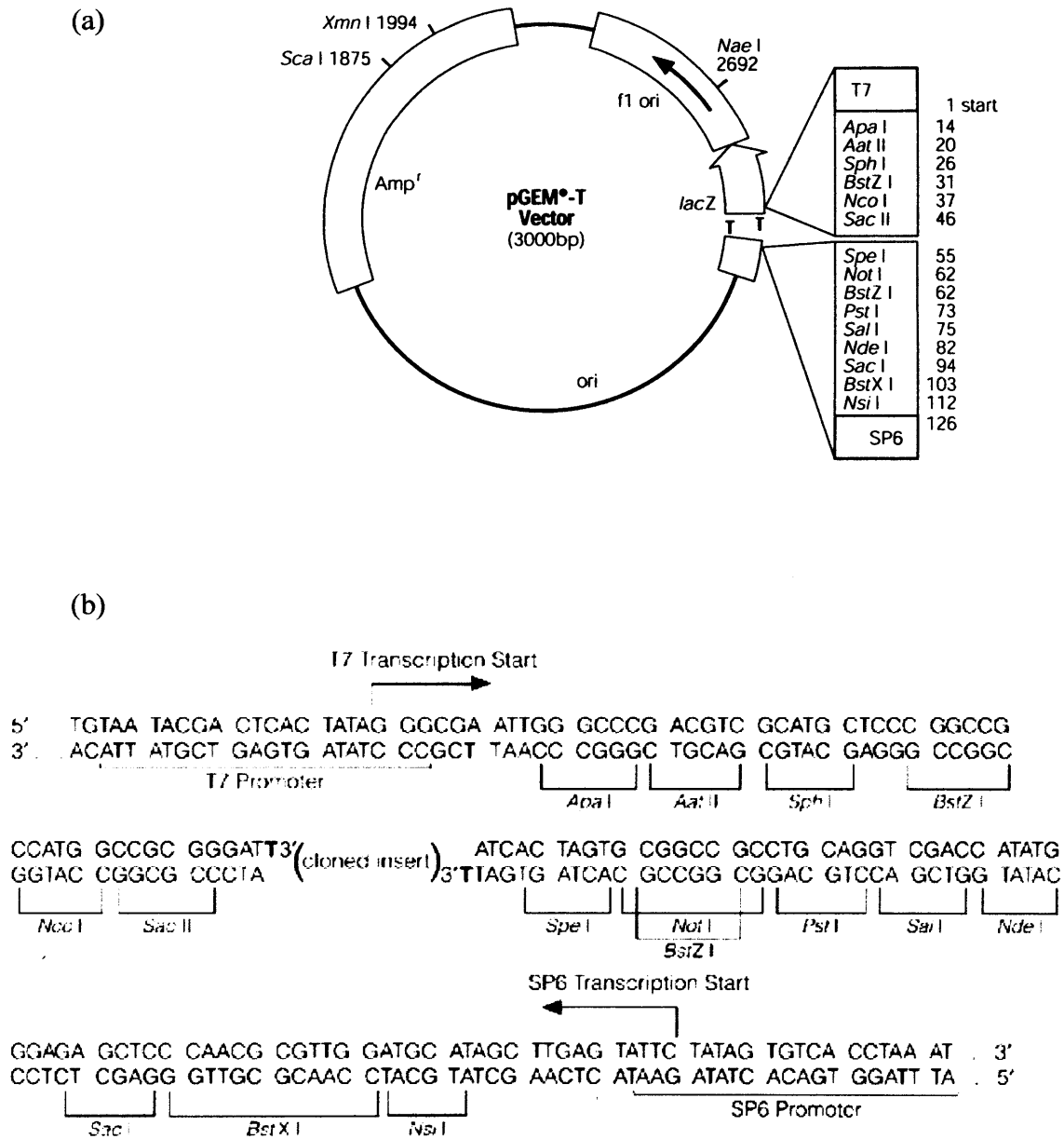


Figure 4.5: (a) pGEM®-T vector circle map and sequence reference points. (b) The promoter and multiple cloning sequence of the pGEM®-T vector. (Taken from Promega 2003).

Overnight culture



Centrifuge.



Remove culture media.

Resuspend cells.

Lyse cells.

Neutralise.



Clear lysate by centrifugation.



Transfer lysate.



Insert column in collection tube. Transfer cleared lysate and bind DNA



Wash, removing solution by centrifugation.



Elute plasmid DNA.

Figure 4.6: Protocol for the Wizard® Plus SV Minipreps DNA purification system. (Adapted from Promega 2001).

4.2.3 Restriction Digestion of NC1 PCR Products

PCR products generated from reactions using primers that had been adapted with restriction sites were digested with *Bam* H I and *Pst* I. Restriction digestion reactions included, 5 µl of buffer H (90 mM Tris-HCl, 10m M MgCl₂, 50 mM NaCl, pH 7.5) which is compatible for both enzymes, 0.1 µg/µl BSA, 10 units of enzymes *Bam* H I and *Pst* I, 50-250 ng of DNA, and H₂O up to 50 µl. Samples were incubated at 37°C for 3 hours and resolved by agarose gel electrophoresis.

4.2.3.1 Linearisation of pQE-30 Expression Vector

The pQE-30 expression vector from the QIAexpress Kit was prepared by dissolving 5µg of plasmid DNA in 10µl of 10mM Tris-HCl, pH 8. A 2µl aliquot was linearised using restriction enzymes *Bam* H I and *Pst* I in buffer H (90mM Tris-HCl, 10mM MgCl₂, 50mM NaCl, pH 7.5). The 20µl restriction digestion reaction contained 1µg DNA template, 2µl of 10x digest buffer H, 10 units of each enzyme, 0.1µg/µl BSA made up to 20µl with H₂O. Samples were incubated at 37°C for 1-4 hours and resolved by agarose gel electrophoresis.

4.2.3.2 Ligation of NC1 Fragments into pQE-30 Expression Vector

T4 DNA ligase was used to catalyse the joining of the NC1 fragments to the linearised pQE-30 expression vector. A 1:3 molar ratio of vector : insert DNA was used for cloning NC1 fragments into the pQE-30 expression vector. The following calculation was used to convert molar ratios to mass ratios:

$$\frac{\text{ng of vector} \times \text{kb size of insert}}{\text{kb size of vector}} \times \text{molar ratio of } \frac{\text{insert}}{\text{vector}} = \text{ng of insert}$$

The ligation reactions contained 3 units of T4 DNA ligase, 3 µl of ligase 10 x buffer (300 mM Tris-HCl pH 7.8, 100 mM MgCl₂, 100 mM DTT and 10 mM ATP), 400 ng of pQE-30 vector DNA, 40–110 ng of insert DNA, made up to a total volume of 30 µl with H₂O. Initially, vector DNA, insert DNA and H₂O were combined and heated at 45°C for 5 minutes, to melt cohesive termini that had re-annealed. The DNA was placed on ice and the ligase buffer and enzyme were added. The ligations were incubated overnight at 4°C.

4.2.4 Preparation of Competent *E. Coli* Cells:

4.2.4.1 M15[Prep4] Cells

A sterile inoculating loop was used to remove a trace of M15[Prep4] cells and to streak the cells onto LB agar plates containing 25 µg/ml kanamycin. Plates were incubated at 37°C overnight. A single colony was picked and inoculated in 10 ml of LB broth containing 25 µg/ml kanamycin, cells were incubated at 37°C overnight in a shaking incubator at 225 rpm. From the overnight culture 1 ml was taken and added to a flask of 100 ml of pre-warmed LB broth containing 25 µg/ml kanamycin, the flask was incubated at 37°C at 225 rpm, until an optical density of 0.5 was reached at a wavelength of 600 nm. The culture was cooled on ice for 5 minutes and then centrifuged at 4°C at 4000 x g for 5 minutes. The supernatant was discarded and the cells were kept on ice. The cells were resuspended in 30 ml of 100 mM RbCl, 50 mM MnCl₂, 30 mM potassium acetate, 10 mM CaCl₂, 15% glycerol, pH 5.8. The cell suspension was incubated on ice for 90 minutes. The cells were centrifuged at 4°C at 4000 x g for 5 minutes. The supernatant was discarded and the cells were kept on ice. Cells were resuspended in 4 ml of ice cold 10 mM MOPS, 10 mM RbCl, 75 mM CaCl₂, 15% glycerol, pH 6.8 with KOH. Aliquots of 200 µl were prepared in cryovials and frozen in liquid nitrogen, cryovials were stored at -80°C for long term storage.

4.2.4.2 XL-1 Blue Cells

A sterile inoculating loop was used to remove a trace of XL-1 Blue cells from glycerol stocks and to streak the cells onto LB agar plates containing 25 µg/ml kanamycin. Plates were incubated at 37°C overnight. A single colony was picked and inoculated in 10 ml of LB broth containing 25 µg/ml ampicillin, cells were incubated at 37°C overnight in a shaking incubator at 225 rpm. From the overnight culture 5 ml was taken and added to a flask of 250 ml of pre-warmed SOB broth (2% w/v bactotryptone, 0.5% w/v yeast extract, 10 mM NaCl, 2.5 mM KCl, 10 mM MgCl₂, 10 mM MgSO₄, pH 6.7). The flask was incubated at 37°C at 225 rpm, until an optical density of 0.5 was reached at a wavelength of 600 nm. The culture was cooled on ice for 10 minutes and then centrifuged at 4°C at 2500 x g for 10 minutes. The supernatant was discarded and the cells were kept on ice. The cells were resuspended in 80 ml of transformation buffer (10 mM Pipes, 55 mM MnCl₂, 15 mM CaCl₂, 250 mM KCl, pH 6.7) and incubated on ice for 10 minutes. The cells were centrifuged at 4°C at 2500 x g for 10 minutes. The supernatant was discarded and the cells resuspended in 20 ml of transformation buffer. DMSO was added to a final concentration of 7% (v/v). Cells were incubated on ice for 10

minutes before aliquots of 200 μ l were prepared in cryovials and frozen in liquid nitrogen, cryovials were stored at -80°C for long term storage.

4.2.4.3 Transformation of Competent M15 and XL-1 Cells

A 5 μ l aliquot of ligation reaction containing NC1 inserts in the pQE-30 expression vector was aliquoted into a cold sterile transformation tube (Falcon) and kept on ice. The control expression plasmid pQE-40 (2 ng) was also used to transform *E. coli*. An aliquot of frozen M15 or XL-1 cells was removed from -80°C storage and thawed on ice, 100 μ l of cell suspension was added to the ligation mix. The cells were kept on ice for 20 minutes and then transferred to a water bath at 42°C for 90 seconds. Psi broth 500 μ l (LB medium containing 4mM MgSO_4 , 10 mM KCl) was added to the cells, which were then incubated at 37°C shaking at 225 rpm for 90 minutes. Aliquots of 100 μ l of M15 and XL-1 cells were then plated onto LB-agar plates containing either 25 $\mu\text{g/ml}$ kanamycin and 100 $\mu\text{g/ml}$ ampicillin or 100 $\mu\text{g/ml}$ ampicillin, respectively. Plates were incubated at 37°C overnight. Colonies were selected using a sterile tip and used to inoculate 5ml of LB broth containing 25 $\mu\text{g/ml}$ kanamycin and 100 $\mu\text{g/ml}$ ampicillin for M15[prep4] cells or 100 $\mu\text{g/ml}$ ampicillin for XL-1 cells. Cultures were incubated at 37°C shaking at 225 rpm overnight. Glycerol stocks of each clone were prepared in LB broth with 20% [v/v] glycerol and stored at -80°C . The remaining cells were used to prepare plasmid DNA.

4.2.5 *E. coli* Culture Growth for Preparative Purification

Glycerol stocks of M15[pREP4] cells containing pQE-30 / NC1 fragment expression vector and the control expression plasmid pQE-40 were streaked onto LB agar plates containing 25 $\mu\text{g/ml}$ kanamycin and 100 $\mu\text{g/ml}$ ampicillin and incubated at 37°C overnight. Single colonies were then used to inoculate 10 ml of LB broth containing 25 $\mu\text{g/ml}$ kanamycin and 100 $\mu\text{g/ml}$ ampicillin. Liquid cultures were incubated overnight at 37°C with vigorous shaking. A 500 ml pre-warmed culture containing 25 $\mu\text{g/ml}$ kanamycin and 100 $\mu\text{g/ml}$ ampicillin, was then inoculated 1:50 with the non-induced overnight culture. The 500 ml culture was grown at 37°C with vigorous shaking until an OD_{600} of 0.6 was reached. A 1 ml non-induced control sample was taken immediately before induction, the cells were pelleted and resuspended in 50 μ l of 5x SDS-PAGE sample buffer. Expression was induced in the 500 ml culture by adding IPTG to a final concentration of 1 mM. The culture was incubated for a further 4-5 hours. A 1 ml induced control sample was taken, the cells were pelleted and resuspended in 100 μ l of 5x

SDS-PAGE sample buffer. The cells in the 500 ml culture were harvested by centrifugation at 4000 x g for 20 minutes. The cell pellets were stored at -20°C overnight.

4.2.5.1 Preparation of Cleared *E. coli* Lysates Under Native Conditions

The cell pellet was thawed on ice for 15 minutes and was then resuspended in lysis buffer (50 mM NaH₂PO₄, 300 mM NaCl, 10 mM imidazole, pH 8) at 2-5 ml per gram of wet weight. A 100 x protease inhibitor cocktail (Calbiochem, UK) was added to the cell lysate suspension, to yield a final concentration of 500 µM AEBSF-HCl, 150 nM aprotinin, 1 µM E-64, 0.5 mM EDTA disodium salt, and 1 µM leupeptin hemisulphate. Lysozyme to 1 mg/ml was added and incubated on ice for 30 minutes. Cells were sonicated with a microtip at 40% amplitude using a Sonics Vibra-Cell™, six pulses of 9 seconds with a 9 second cooling period between each burst was used. To the cell lysate RNase A at 10 µg/ml and DNase I at 5 µg/ml were added along with MgCl₂ to a final concentration of 1 mM, the lysate was incubated on ice for 15 minutes. The lysate was centrifuged at 10,000 x g for 30 minutes at 4°C to pellet the cellular debris. A small sample of the native supernatant was mixed with an equal volume of 2x sample buffer for analysis by SDS-PAGE, the remainder of the native supernatant was stored at -20°C. The cellular debris pellet was then prepared under denaturing conditions.

4.2.5.2 Preparation of *E. coli* Cellular Debris Under Denaturing Conditions

The cellular debris pellet was resuspended in denaturing lysis buffer (50 mM NaH₂PO₄, 10 mM Tris-Cl, 8 M urea, pH 8) at 5 ml per gram of wet weight. The cell debris suspension was stirred for 1 hour at room temperature. The suspension was centrifuged at 10,000 x g for 30 minutes at room temperature to pellet the cellular debris. A small sample of the denatured supernatant was mixed with an equal volume of 2x sample buffer for analysis by SDS-PAGE, the remainder of the denatured supernatant was stored at -20°C.

4.2.5.3 Purification of 6xHis-tagged Proteins from *E. coli* Lysate Under Native Conditions

To 4ml of the native supernatant, 1 ml of a 50% Ni-NTA slurry was added and mixed gently on a rotary shaker at 4°C for 60 minutes. The mixture was centrifuged at 1000 x g for 10 seconds to pellet the resin. The supernatant was carefully taken off the resin, a 100µl aliquot of the supernatant was mixed with 5x sample buffer for analysis by SDS-PAGE as the unbound fraction, and the remainder of the supernatant was stored at -20°C. The resin was then washed twice with 5 ml of wash buffer (50 mM NaH₂PO₄, 300 mM NaCl, 20 mM

imidazole, pH 8), the suspension was centrifuged at 1000 x g for 30 seconds after each wash, the supernatant was carefully removed from the resin and a 100 µl aliquot of the supernatant mixed with 5x sample buffer for analysis by SDS-PAGE as the first and second wash fractions, respectively, the remainder of the supernatant was stored at -20°C. Proteins were eluted from the resin 4 times by the addition of 1 ml of elution buffer (50 mM NaH₂PO₄, 300 mM NaCl, 250 mM imidazole, pH 8), the suspension was centrifuged at 1000 x g for 1 minute after each elution step, the supernatant was carefully removed from the resin and a 100 µl aliquot of the supernatant mixed with 5x sample buffer for analysis by SDS-PAGE and labelled as eluates 1-4, respectively, the remainder of the supernatant was stored at -20°C.

4.2.5.4 Purification of 6xHis-tagged Proteins from *E. coli* Cellular Debris Under Denaturing Conditions

The procedure for preparing 6xHis-tagged proteins from *E. coli* cellular debris under denaturing conditions is as described in 4.2.5.3. With the following exceptions wash buffer (50 mM NaH₂PO₄, 10 mM Tris-Cl, 8 M urea, pH 6.3) and elution buffer (50 mM NaH₂PO₄, 10 mM Tris-Cl, 8 M urea, pH 5.9). A further 4 elutions were carried out by the addition of 1 ml of elution buffer (50 mM NaH₂PO₄, 10 mM Tris-Cl, 8 M urea, pH 4.5) the suspension was centrifuged at 1000xg for 1 minute after each elution step, the supernatant was carefully removed from the resin and a 100 µl aliquot of the supernatant mixed with 5x sample buffer for analysis by SDS-PAGE and labelled as eluates 5-8, respectively, the remainder of the supernatants were stored at -20°C.

4.2.6 SDS-PAGE and Western Blot Analysis

SDS-PAGE and Western blot analysis was carried out as previously described in section 2.2.4 of Chapter 2.

4.2.6.1 Western Blotting using Specialised Membrane

Immobilon-P^{SQ} transfer membrane (Millipore) was used to maximise protein binding, this membrane is well-suited for immunodetection of proteins that are less than 20 kDa following electroblotting from electrophoresis gels. SDS-PAGE gels were equilibrated for 20 minutes in transfer buffer P^{SQ} (Laemmli buffer containing 35% methanol). The Immobilon-P^{SQ} transfer membrane was prepared by wetting the membrane in 100% methanol for 1-3 seconds,

transferring to H₂O for 2 minutes to displace the methanol, finally the membrane was equilibrated in transfer buffer P^{SQ} prior to Western blotting as detailed in section 2.2.4.

4.2.6.2 *Immuno-detection Using Qiagen's Penta-His Antibody*

PVDF filters were removed from the blotting apparatus; washed twice for 10 minutes with TBS, and then incubated in 3% (w/v) BSA in TBS for 1 hour to saturate protein binding sites on the filters. The filters were again washed twice for 10 minutes with TBS containing 0.05% (v/v) Tween 20 and once for 10 minutes with TBS. Filters were incubated in penta-His antibody diluted to 0.2 µg/ml in 3% (w/v) BSA in TBS for 1 hour. The filters were washed again twice for 10 minutes with TBS containing 0.05% (v/v) Tween 20 and once for 10 minutes with TBS. Filters were incubated with a sheep anti-mouse HRP conjugated secondary antibody, diluted 1:20,000 with TBS containing 0.05% (v/v) Tween 20 for 45 minutes. Filters were washed four times with TBS containing 0.05% (v/v) Tween 20 for 10 minutes each time. ECL reagent was applied to the filters and the filters were exposed to ECL hyperfilm for 1 hour.

4.2.7 **Determination of Protein Concentration**

A protein assay kit based on bicinchoninic acid (BCA) was used to estimate the concentration of protein samples. The BCA protein assay kit (Pierce) was used according to manufacturer's instructions. Briefly, the BCA working reagent was prepared by mixing 50 parts of BCA reagent A (containing sodium carbonate, sodium bicarbonate, bicinchoninic acid and sodium tartate in 0.1M sodium hydroxide) with 1 part of BCA reagent B (containing 4% cupric sulphate). A range of BSA standards from 0 to 2000 µg/ml were prepared to generate a standard curve for determining concentrations of unknown protein samples. 25 µl of BSA standards or unknown samples were applied to wells of a 96-well microplate in triplicate, 200 µl of the working reagent was added to each well and was mixed thoroughly using a plate shaker for 30 seconds. The plate was covered and incubated for 30 minutes at 37°C, the plate was cooled to room temperature and the absorbance was measured at 590nm. The BSA standard curve was then used to estimate the protein concentration in samples prepared using the Ni-NTA agarose.

4.2.8 **Optimisation of Antibody Dilutions Required for Interaction Analysis**

The His-tagged mouse recombinant DHFR protein (5 µg/ml) in PBS was used to coat the wells of a 96-well microtitre plate, as a control 3% (w/v) BSA in PBS was also used to coat

wells, 100 μ l of each coating was applied. The plate was incubated at 37°C overnight, all subsequent incubations were carried out at 37°C. The wells were washed three times with 200 μ l of PBS containing 0.05% (v/v) Tween 20. Un-occupied binding sites on the wells were then blocked with 200 μ l of 3% (w/v) BSA in PBS for 1 hour. The wells were washed as above. The Qiagen penta-His antibody was applied down the plate in doubling dilutions, from 1 μ g/ml to 0.0625 μ g/ml, the antibody was diluted in PBS and 100 μ l was applied to DHFR and 3% (w/v) BSA coated wells. The antibody was incubated for 2 hours, before the wells were washed as above. A HRP conjugated sheep anti-mouse secondary antibody (Sigma) was then applied 100 μ l/well across the plate in doubling dilutions in PBS, from 1:1000 to 1:16,000. The wells were washed as above. The chromogenic substrate OPD was then applied to the wells, 100 μ l of 1 mg/ml OPD in 0.5M sodium citrate, pH 5.5, containing 0.125% (v/v) hydrogen peroxide was incubated in wells from 5-15 minutes after which the reaction was stopped by addition of 50 μ l of 1 M H₂SO₄. The absorbance was read at 492 nm on a multiwell plate reader.

4.2.8.1 Interaction Analysis using Basic Solid Phase Assay

96 well microtiter plates (ICN Biomedicals, UK) were coated with 100 μ l of 5 μ g/ml human recombinant decorin (EMP Genetech, Germany) or bovine biglycan, in PBS, (0.14 M NaCl, 2.7 mM KCl, 1.8 mM KH₂PO₄, 10 mM Na₂HPO₄, pH 7.4). In control experiments wells were coated with 100 μ l of 3% (w/v) BSA in PBS. Plates were coated overnight at 37°C, all following incubations were carried out at 37°C. Wells were washed three times with 200 μ l of PBS containing 0.05% (v/v) Tween-20 (PBS-T), this washing step was repeated after each subsequent incubation. To avoid non-specific interactions, wells were blocked for 1 hour with 200 μ l of 3% (w/v) BSA in PBS. Coated wells were incubated for 2 hours with 100 μ l of 0-5 μ g/ml of the recombinant NC1 fragments (F1/R1, F1/R2, F2/R2, F2/R3) and DHFR in PBS. The amount of bound protein was determined by incubation for 2 hours with 100 μ l of a monoclonal penta-His antibody diluted with PBS to 0.125 μ g/ml. Bound IgG was detected with a sheep anti-mouse horse radish peroxidase (HRP) secondary antibody, diluted 1:1000 with PBS, 100 μ l per well of the secondary antibody was incubated for 2 hours. Enzyme activity was measured with OPD as the substrate, 100 μ l of 1 mg/ml OPD in 0.5 M sodium citrate, pH 5.5, containing 0.125% (v/v) hydrogen peroxide was incubated in wells for 5-15 minutes and the reaction was stopped with 50 μ l of 1 M H₂SO₄. The absorbance was read at 492 nm on a multiwell plate reader.

4.3 RESULTS

4.3.1 Amplification, TA Cloning and DNA Sequencing of NC1 Fragments

Primers which had been previously designed by Dr Alvin Kwan (Cardiff University, UK) were utilised to amplify different regions of the NC1 sequence from a plasmid DNA preparation which contained the entire NC1 sequence (supplied by Dr Alvin Kwan). Primer sequences and their annealing positions with regard to the whole NC1 sequence are shown in figure 4.4. The primer pair combinations displayed in table 4.2 were used to yield five different products:

| Forward Primer | Reverse Primer | Size of Product (bp) |
|----------------|----------------|----------------------|
| NC1 F1 | NC1 R1 | 201 |
| NC1 F1 | NC1 R2 | 312 |
| NC1 F2 | NC1 R2 | 120 |
| NC1 F2 | NC1 R3 | 291 |
| NC1 F3 | NC1 R3 | 192 |

Table 4.2: Summary of primer pair combinations used and expected product sizes generated.

PCR was performed as previously described and products were visualised using ethidium bromide staining in a 1% agarose gel after electrophoresis (figure 4.7). Products of 201bp generated by F1/R1, 312bp generated by F1/R2, 120bp generated by F2/R2, 291bp generated by F2/R3 and 192bp generated by F3/R3 can be seen in lanes 2, 4, 6, 8 and 10, respectively. The H₂O controls for each PCR reaction were negative, lanes 3, 5, 7, 9 and 11.

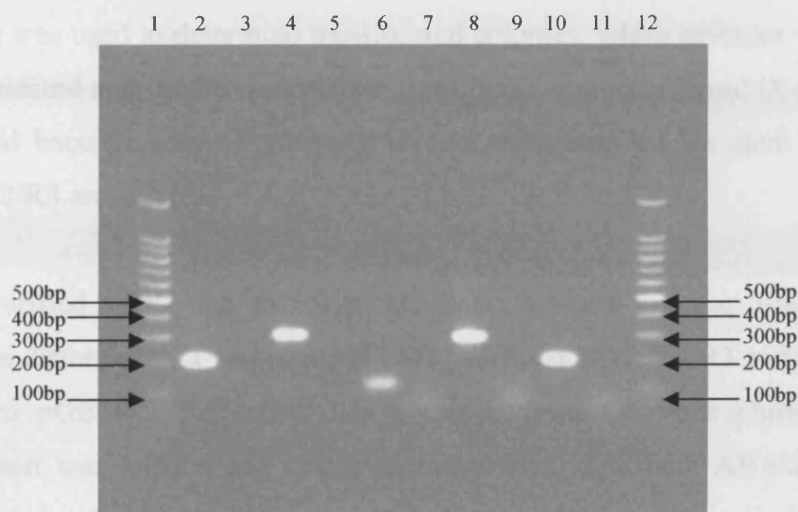


Figure 4.7: PCR products generated using different combinations of the NC1 primers. 1% agarose gel electrophoresis of PCR amplified products from a plasmid DNA template containing the NC1 sequence (diluted 1:100) and a H₂O control:

- | | | |
|----------------------|----------------|-------------------------------|
| 1. 100 bp ladder | | |
| 2. Plasmid DNA | 201 bp product | } Primed with NC1 F1 – NC1 R1 |
| 3. H ₂ O | | |
| 4. Plasmid DNA | 312bp product | } Primed with NC1 F1 – NC1 R2 |
| 5. H ₂ O | | |
| 6. Plasmid DNA | 120bp product | } Primed with NC1 F2 – NC1 R2 |
| 7. H ₂ O | | |
| 8. Plasmid DNA | 291bp product | } Primed with NC1 F2 – NC1 R3 |
| 9. H ₂ O | | |
| 10. Plasmid DNA | 192bp product | } Primed with NC1 F3 – NC1 R3 |
| 11. H ₂ O | | |
| 12. 100bp ladder | | |

PCR products F1/R1, F1/R2, F2/R2, F2/R3 and F3/R3 were excised from the agarose gel and purified using Qiagen's QIAEX II gel extraction kit. Purified PCR product was then used in a ligation reaction with the cloning vector pGEM-T, these ligations were subsequently used to transform competent *E. coli* JM109 cells. Transformed bacteria were plated onto LB agar plates containing IPTG, X-gal and 100µg/ml ampicillin. Following overnight incubations colour screening was used to determine transformed colonies, white colonies which contained an insert were selected and used to inoculate a 10ml liquid culture. Plasmid DNA was prepared from transformed bacteria using Promega's Wizard mini-prep kit for each product F1/R1, F1/R2, F2/R2, F2/R3 and F3/R3.

Plasmid DNA purified using the Promega Miniprep Wizard kit was used to determine sequences for the different NC1 fragments (F1/R1, F1/R2, F2/R2, F2/R3 and F3/R3) that had been cloned into pGEM-T. Sequence data obtained from Chromas chromatograms was analysed, the insert was located and vector sequence was identified. All the sequence data from the different clones was aligned to the COL10A1 mRNA sequence (gi:18105031) using the sequence alignment programme BLAST2, only clones that contained a 100% sequence homology were selected for sub-cloning into the expression vector. The NC1 fragment clones F1/R1 (figure 4.8), F1/R2 (figure 4.9), F2/R2 (figure 4.10) and F2/R3 (figure 4.11) all contained 100% homology to the COL10A1 mRNA sequence. Unfortunately none of the F3/R3 containing clones selected had 100% homology to the COL10A1 mRNA, all F3/R3 clones selected containing the 192bp product contained mismatches in the sequence. These clones were therefore not used for subsequent sub-cloning and were excluded from the remainder of the study.

```

Query: 1      gtcatgcctgaggggtttataaaggcaggccaaaggcccagtcctttctgggacccctctt 60
             |||
Sbjct: 1654   gtcatgcctgaggggtttataaaggcaggccaaaggcccagtcctttctgggacccctctt 1713

Query: 61      gttagtccaaccagggggtaacaggaatgcctgtgtctgcttttactgttattctctcc 120
             |||
Sbjct: 1714   gttagtccaaccagggggtaacaggaatgcctgtgtctgcttttactgttattctctcc 1773

Query: 121     aaagcttaccagcaataggaactcccataccatttgataaaattttgtataacaggcaa 180
             |||
Sbjct: 1774   aaagcttaccagcaataggaactcccataccatttgataaaattttgtataacaggcaa 1833

Query: 181     cagcattatgacccaaggact 201
             |||
Sbjct: 1834   cagcattatgacccaaggact 1854

```

Figure 4.8: 100% sequence identity of NC1 clone F1/R1, the query, with the COL10A1 mRNA, the subject, sequence alignment was performed using nucleotide-nucleotide BLAST. Positions of forward primers (in green) and reverse primers (in red) are highlighted. All 201bp are 100% homologous to the COL10A1 subject.

```

Query: 1      gtcatgcctgaggggtttataaaggcaggccaaaggcccagtcctttctgggacccctctt 60
             ||||||||||||||||||||||||||||||||||||||||||||||||||||
Sbjct: 1654   gtcatgcctgaggggtttataaaggcaggccaaaggcccagtcctttctgggacccctctt 1713

Query: 61      gttagtgcccaaccagggggtaacaggaatgcctgtgtctgcttttactgttattctctcc 120
             ||||||||||||||||||||||||||||||||||||||||||||||||||||
Sbjct: 1714   gttagtgcccaaccagggggtaacaggaatgcctgtgtctgcttttactgttattctctcc 1773

Query: 121     aaagcttaccagcaataggaactcccataccatttgataaaattttgtataacaggcaa 180
             ||||||||||||||||||||||||||||||||||||||||||||||||||||
Sbjct: 1774   aaagcttaccagcaataggaactcccataccatttgataaaattttgtataacaggcaa 1833

Query: 181     cagcattatgacccaaggactggaatctttacttgtcagataccaggaatatactatttt 240
             ||||||||||||||||||||||||||||||||||||||||||||||||||||
Sbjct: 1834   cagcattatgacccaaggactggaatctttacttgtcagataccaggaatatactatttt 1893

Query: 241     tcataccacgtgcatgtgaaagggactcatgtttgggtaggcctgtataagaatggcacc 300
             ||||||||||||||||||||||||||||||||||||||||||||||||||||
Sbjct: 1894   tcataccacgtgcatgtgaaagggactcatgtttgggtaggcctgtataagaatggcacc 1953

Query: 301     cctgtaatgtac 312
             ||||||||||||
Sbjct 1954   cctgtaatgtac 1965

```

Figure 4.9: 100% sequence identity of NC1 clone F1/R2, the query, with the COL10A1 mRNA, the subject, sequence alignment was performed using nucleotide-nucleotide BLAST. Positions of forward primers (in green) and reverse primers (in red) are highlighted. All 312bp are 100% homologous to the COL10A1 subject.

```

Query: 1      ccaaggactggaatctttacttgtcagataccaggaatatactatttttcataccacgtg 60
             ||||||||||||||||||||||||||||||||||||||||||||||||||||
Sbjct: 1846   ccaaggactggaatctttacttgtcagataccaggaatatactatttttcataccacgtg 1905

Query: 61      catgtgaaagggactcatgtttgggtaggcctgtataagaatggcaccctgtaatgtac 120
             ||||||||||||||||||||||||||||||||||||||||||||||||||||
Sbjct: 1906   catgtgaaagggactcatgtttgggtaggcctgtataagaatggcaccctgtaatgtac 1965

```

Figure 4.10: 100% sequence identity of NC1 clone F2/R2, the query, with the COL10A1 mRNA, the subject, sequence alignment was performed using nucleotide-nucleotide BLAST. Positions of forward primers (in green) and reverse primers (in red) are highlighted. All 120bp are 100% homologous to the COL10A1 subject.

```

Query: 1      ccaaggactggaatctttacttggcagataaccaggaatatactatTTTTcataccacgtg 60
              |||
Sbjct: 1846   ccaaggactggaatctttacttggcagataaccaggaatatactatTTTTcataccacgtg 1905

Query: 61      catgtgaaagggactcatgtttgggtaggcctgtataagaatggcaccctgtaatgtac 120
              |||
Sbjct: 1906   catgtgaaagggactcatgtttgggtaggcctgtataagaatggcaccctgtaatgtac 1965

Query: 121     acctatgatgaatacaccaaaggctacctggatcaggcttcagggagtgccatcatcgat 180
              |||
Sbjct: 1966   acctatgatgaatacaccaaaggctacctggatcaggcttcagggagtgccatcatcgat 2025

Query: 181     ctcacagaaaatgaccaggtgtggctccagcttcccaatgccgagtgcaaatggcctatac 240
              |||
Sbjct: 2026   ctcacagaaaatgaccaggtgtggctccagcttcccaatgccgagtgcaaatggcctatac 2085

Query: 241     tcctctgagtatgtccactcctctttctcaggattcctagtggctccaatg 291
              |||
Sbjct: 2086   tcctctgagtatgtccactcctctttctcaggattcctagtggctccaatg 2136

```

Figure 4.11: 100% sequence identity of NC1 clone F2/R3, the query, with the COL10A1 mRNA, the subject, sequence alignment was performed using nucleotide-nucleotide BLAST. Positions of forward primers (in green) and reverse primers (in red) are highlighted. All 291bp are 100% homologous to the COL10A1 subject.

4.3.2 Sub-cloning into the pQE-30 expression vector

Plasmid DNA containing NC1 inserts F1/R1, F1/R2, F2/R2 and F2/R3; which were confirmed to have a 100% homology with the COL10A1 mRNA, were used as templates for subsequent PCR reactions. All of the NC1 fragments: F1/R1, F1/R2, F2/R2 and F2/R3 were generated using primers designed to be 'in-frame', no additional base pairs were therefore required in the expression vector to ensure that the correct in-frame protein would be produced. The expression vector pQE-30 was therefore selected as the expression vector (figure 4.2)

The NC1 primers previously described were adapted to contain 5' restriction sites, which would allow directional sub-cloning into the pQE-30 expression vector. Analysing the pQE-30 expression vectors multiple cloning site (MCS) (figure 4.2); showed that cleaving the expression vector with *Bam* H I and *Hind* III, would be beneficial with regards to removing the largest amount of sequence from the MCS and hence having least number of additional

amino acids when the protein is expressed. However, following analysis of the NC1 domain sequence for restriction sites, a *Hind* III restriction site was identified. The enzymes used for directional sub-cloning should not have recognition sequences within the insert to be cloned. Therefore, *Bam* H I and *Pst* I were determined as the enzymes of choice for linearising the pQE-30 expression vector and were the recognition sequences used to adapt the NC1 primers (figure 4.12). The *Bam* H I recognition sequence GGA TCC was placed 5' of the forward primers and the *Pst* I recognition sequence CTG CAG was placed 5' of the reverse primers. Three additional nucleotides; CCA, were placed 5' of the restriction enzyme recognition sequences, this was to ensure there were enough nucleotides for stable binding of the restriction enzyme to the DNA.

Forward Primers

Bam H I–NC1 F1 5'CCA GGA TCC GTC ATG CCT GAG GGT TTT ATA

Bam H I–NC1 F2 5'CCA GGA TCC CCA AGG ACT GGA ATC TTT ACT

Reverse Primers

Pst I–NC1 R1 5'CCA CTG CAG AGT CCT TGG GTC ATA ATG CTG

Pst I–NC1 R2 5'CCA CTG CAG GTA CAT TAC AGG GGT GCC

Pst I–NC1 R3 5'CCA CTG CAG CAT TGG AGC CAC TAG GAA TCC

Figure 4.12: Sequences of the restriction site adapted NC1-F and NC1-R primers, restriction sites are highlighted in blue.

These restriction site adapted primers were then used in PCR reactions with the F1/R1, F1/R2, F2/R2 and F2/R3 pGEM–T plasmid DNA preparations. Plasmid DNA was used as a template at different dilutions and using a DNA polymerase containing proof-reading activity. PCR was performed as previously described and products were visualised using ethidium bromide staining in a 1% agarose gel after electrophoresis (figure 4.13). All of the products were expected to be 18bp larger than the previous product size in figure 4.7, due to the additional restriction sequences on the primers.

Products in lanes 2 and 3 of figure 4.13(a) are approximately 309bp, generated from the F2/R3 template using the primers *Bam* H I–NC1 F2 and *Pst* I–NC1 R3. Products in lanes 2 and 3 of figure 4.13(b) are approximately 330bp, generated from the F1/R2 template using the

primers *Bam* H I–NC1 F1 and *Pst* I–NC1 R2. Products in lanes 2 and 3 of figure 4.13(c) are approximately 138bp, generated from the F2/R2 template using the primers *Bam* H I–NC1 F2 and *Pst* I–NC1 R2. Products in lanes 2 and 3 of figure 4.13(d) are approximately 218bp, generated from the F1/R1 template using the primers *Bam* H I–NC1 F1 and *Pst* I–NC1 R1. Water controls for each PCR reaction in lane 4 (figure 4.13 (a), (b), (c), (d)) were all negative. Products were run on separate gels to prevent cross-contamination during extraction of the bands from the gels. The PCR products were purified using Qiagen’s QIAex II purification kit.

The purified PCR products from figure 4.13 and the pQE–30 expression vector were digested with restriction enzymes *Bam* H I and *Pst* I. The restricted products and the linearised p QE-30 expression vector (figure 4.14) were then ligated using the enzyme T4 DNA ligase. Figure 4.15 summarises the sub-cloning procedure.

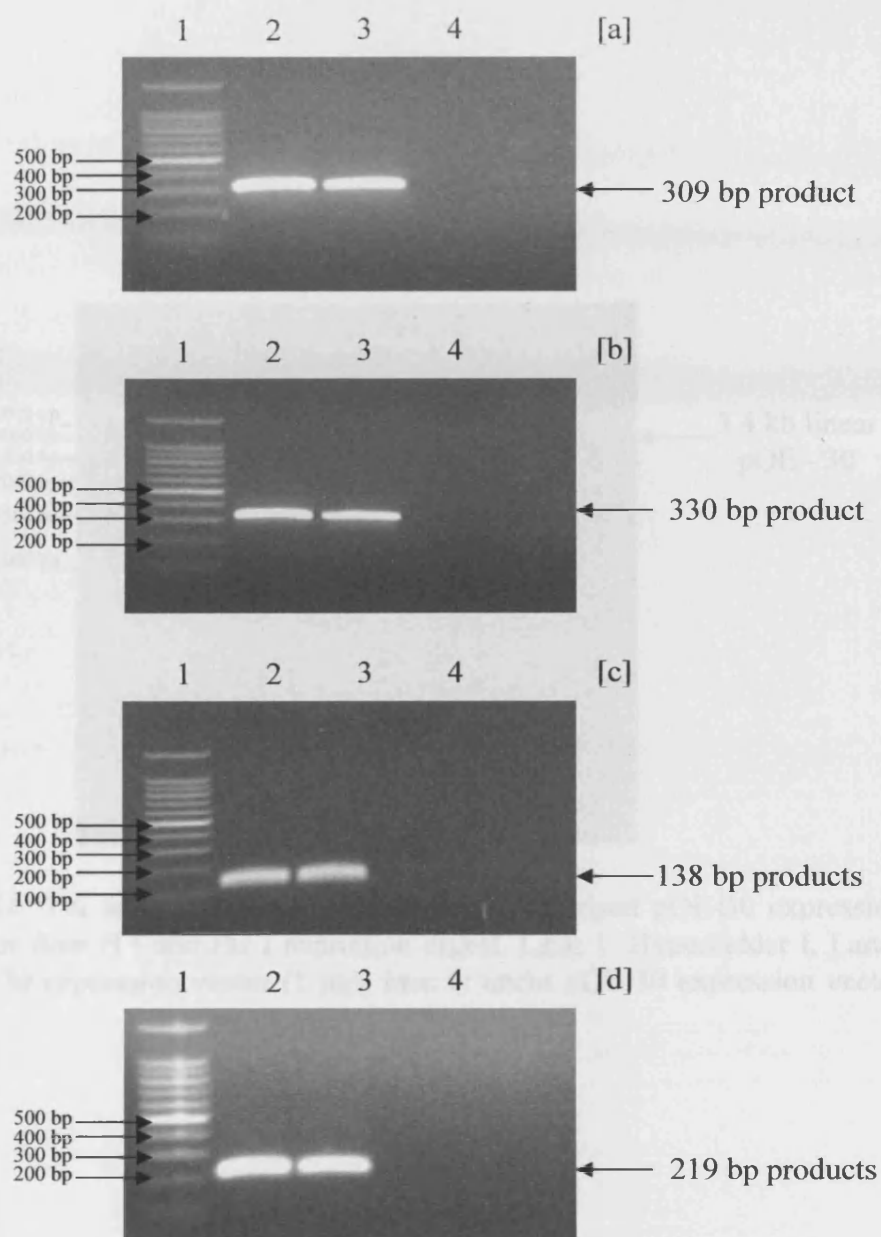


Figure 4.13: 1% agarose gel electrophoresis of PCR amplified products with NC1 primers containing 5' restriction sites from plasmid DNA. Lane 1: 100 bp ladder, lane 2: plasmid DNA diluted 1:1000, lane 3: plasmid DNA diluted 1:100, lane 4: H₂O control.

[a] Amplification with *Bam* H I NC1 F2 and *Pst* I NC1 R3

[b] Amplification with *Bam* H I NC1 F1 and *Pst* I NC1 R2

[c] Amplification with *Bam* H I NC1 F2 and *Pst* I NC1 R2

[d] Amplification with *Bam* H I NC1 F1 and *Pst* I NC1 R1

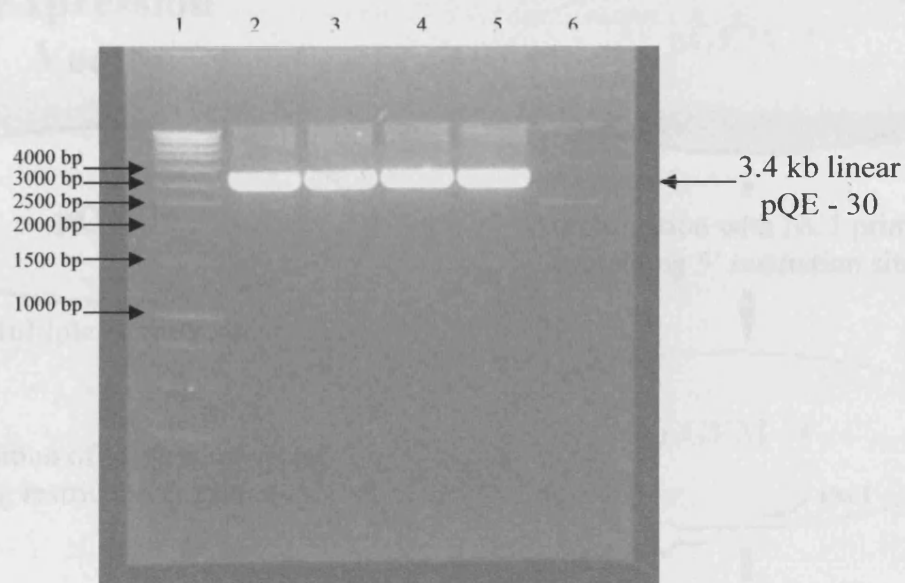


Figure 4.14: 1% agarose gel electrophoresis of linearised pQE-30 expression vector after *Bam* H I and *Pst* I restriction digest. Lane 1: Hyperladder I, Lanes 2-5: pQE-30 expression vector (1 µg), lane 6: uncut pQE-30 expression vector (0.2 µg).

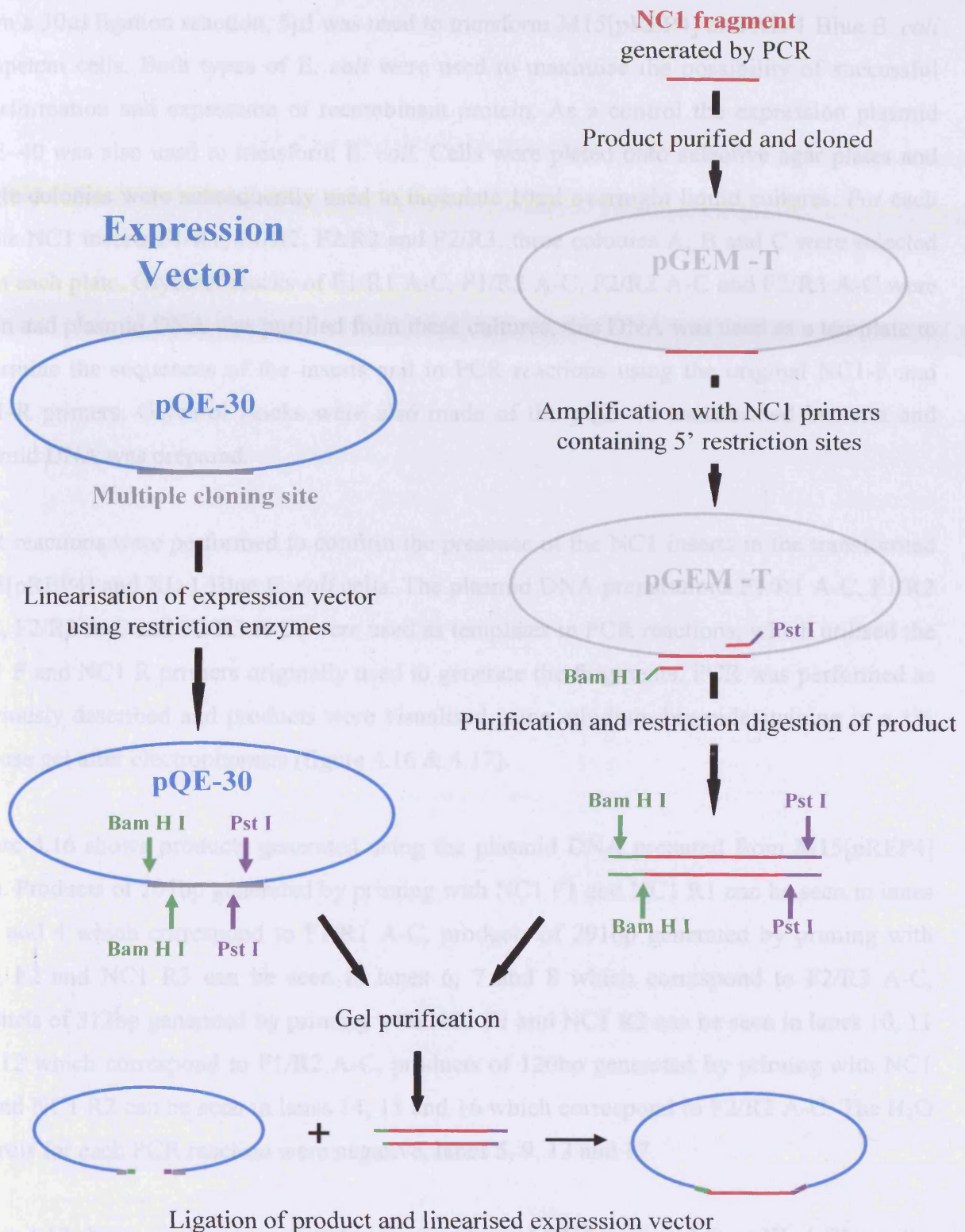


Figure 4.15: Sub-cloning steps used to generate NC1 fragment expression vectors.

4.3.3 Confirming the presence of NC1 Fragments in the pQE-30 expression vector in transformed *E. coli*

From a 30µl ligation reaction, 5µl was used to transform M15[pREP4] and XL-1 Blue *E. coli* competent cells. Both types of *E. coli* were used to maximise the possibility of successful transformation and expression of recombinant protein. As a control the expression plasmid pQE-40 was also used to transform *E. coli*. Cells were plated onto selective agar plates and single colonies were subsequently used to inoculate 10ml overnight liquid cultures. For each of the NC1 inserts F1/R1, F1/R2, F2/R2 and F2/R3, three colonies A, B and C were selected from each plate. Glycerol stocks of F1/R1 A-C, F1/R2 A-C, F2/R2 A-C and F2/R3 A-C were taken and plasmid DNA was purified from these cultures, this DNA was used as a template to determine the sequences of the inserts and in PCR reactions using the original NC1-F and NC1-R primers. Glycerol stocks were also made of the pQE-40 transformed bacteria and plasmid DNA was prepared.

PCR reactions were performed to confirm the presence of the NC1 inserts in the transformed M15[pREP4] and XL-1 Blue *E. coli* cells. The plasmid DNA preparations F1/R1 A-C, F1/R2 A-C, F2/R2 A-C and F2/R3 A-C; were used as templates in PCR reactions, which utilised the NC1 F and NC1 R primers originally used to generate the fragments. PCR was performed as previously described and products were visualised using ethidium bromide staining in a 1% agarose gel after electrophoresis (figure 4.16 & 4.17).

Figure 4.16 shows products generated using the plasmid DNA prepared from M15[pREP4] cells. Products of 201bp generated by priming with NC1 F1 and NC1 R1 can be seen in lanes 2, 3 and 4 which correspond to F1/R1 A-C, products of 291bp generated by priming with NC1 F2 and NC1 R3 can be seen in lanes 6, 7 and 8 which correspond to F2/R3 A-C, products of 312bp generated by priming with NC1 F1 and NC1 R2 can be seen in lanes 10, 11 and 12 which correspond to F1/R2 A-C, products of 120bp generated by priming with NC1 F2 and NC1 R2 can be seen in lanes 14, 15 and 16 which correspond to F2/R2 A-C. The H₂O controls for each PCR reaction were negative, lanes 5, 9, 13 and 17.

Figure 4.17 shows products generated using the plasmid DNA prepared from XL-1 Blue cells. Products of 201bp generated by priming with NC1 F1 and NC1 R1 can be seen in lanes 2 and 4 which correspond to F1/R1 A and C, no product was generated using the F1/R1 B DNA as a template, products of 291bp generated by priming with NC1 F2 and NC1 R3 can be seen in

lanes 6, 7 and 8 which correspond to F2/R3 A-C, products of 312bp generated by priming with NC1 F1 and NC1 R2 can be seen in lanes 10, 11 and 12 which correspond to F1/R2 A-C, products of 120bp generated by priming with NC1 F2 and NC1 R2 can be seen in lanes 14, 15 and 16 which correspond to F2/R2 A-C. The H₂O controls for each PCR reaction were negative, lanes 5, 9, 13 and 17.

Plasmid DNA F1/R1 A-C, F1/R2 A-C, F2/R2 A-C and F2/R3 A-C from M15[pREP4] cells was used as templates for sequencing the inserts in the pQE-30 expression vector using the Qiagen sequencing primers. Sequence data obtained from Chromas chromatograms was analysed, the insert was located and vector sequence was identified. All the sequence data from the different clones was aligned to the COL10A1 mRNA sequence (gi:18105031) using the sequence alignment programme BLAST2. Sequencing was carried out to ensure that no errors had been incorporated into the inserts during the sub-cloning procedure. 100% homology was found in all clones sequenced, figures 4.18, 4.19, 4.20 and 4.21 show the nucleotide sequence of the inserts, the predicted protein sequence and the sizes expected when the recombinant proteins are expressed.

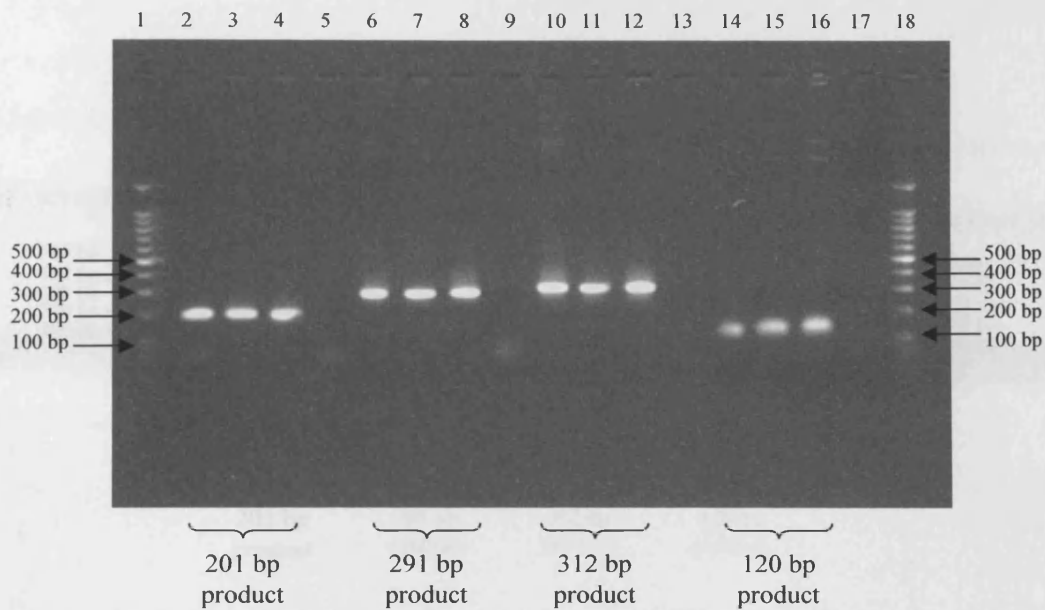


Figure 4.16: 1% agarose gel electrophoresis of PCR amplified products from plasmid DNA samples diluted 1:100; from different colonies of M15[pREP4] cells transformed with different NC1 fragments, using combinations of NC1 F and NC1 R primers:

- | | | | |
|-----|------------------|-----------------|----------------|
| 1. | 100 bp ladder | | |
| 2. | Colony A | NC1 F1 – NC1 R1 | 201 bp product |
| 3. | Colony B | | |
| 4. | Colony C | | |
| 5. | H ₂ O | | |
| 6. | Colony A | NC1 F2 – NC1 R3 | 291 bp product |
| 7. | Colony B | | |
| 8. | Colony C | | |
| 9. | H ₂ O | | |
| 10. | Colony A | NC1 F1 – NC1 R2 | 312 bp product |
| 11. | Colony B | | |
| 12. | Colony C | | |
| 13. | H ₂ O | | |
| 14. | Colony A | NC1 F2 – NC1 R2 | 120 bp product |
| 15. | Colony B | | |
| 16. | Colony C | | |
| 17. | H ₂ O | | |
| 18. | 100 bp ladder | | |

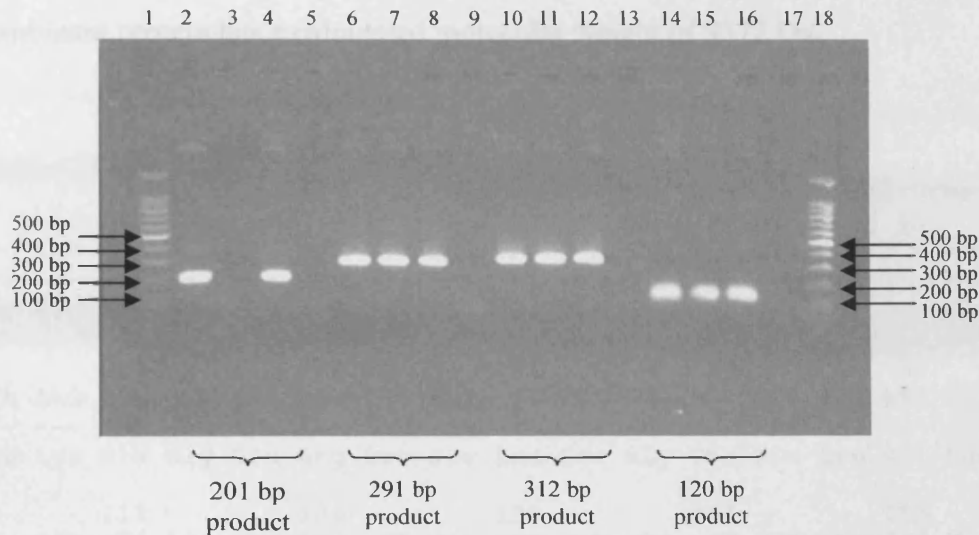


Figure 4.17: 1% agarose gel electrophoresis of PCR amplified products from plasmid DNA samples diluted 1:100; from different colonies of XL-1 Blue cells transformed with different NC1 fragments, using combinations of NC1 F and NC1 R primers:

- | | | | |
|-----|------------------|-----------------|----------------|
| 1. | 100 bp ladder | | |
| 2. | Colony A | NC1 F1 – NC1 R1 | 201 bp product |
| 3. | Colony B | | |
| 4. | Colony C | | |
| 5. | H ₂ O | | |
| 6. | Colony A | NC1 F2 – NC1 R3 | 291 bp product |
| 7. | Colony B | | |
| 8. | Colony C | | |
| 9. | H ₂ O | | |
| 10. | Colony A | NC1 F1 – NC1 R2 | 312 bp product |
| 11. | Colony B | | |
| 12. | Colony C | | |
| 13. | H ₂ O | | |
| 14. | Colony A | NC1 F2 – NC1 R2 | 120 bp product |
| 15. | Colony B | | |
| 16. | Colony C | | |
| 17. | H ₂ O | | |
| 18. | 100 bp ladder | | |

Below is shown the nucleotide and protein sequences for the F1/R1 NC1 fragment, the 201 bp insert codes for 67 amino acids, however the recombinant protein will contain 19 additional amino acids due to the presence of the MCS of the pQE-30 expression vector. This 86 amino acid recombinant protein has a calculated molecular weight of 9372 Da.

```

5'   9       18       27       36       45       54
    ATG AGA GGA TCG CAT CAC CAT CAC CAT CAC GGA TCC GTC ATG CCT GAG GGT TTT
    --- --- --- --- --- --- --- --- --- --- --- --- --- --- ---
    Met Arg Gly Ser His His His His His His Gly Ser Val Met Pro Glu Gly Phe

       63       72       81       90       99       108
    ATA AAG GCA GGC CAA AGG CCC AGT CTT TCT GGG ACC CCT CTT GTT AGT GCC AAC
    --- --- --- --- --- --- --- --- --- --- --- --- --- --- ---
    Ile Lys Ala Gly Gln Arg Pro Ser Leu Ser Gly Thr Pro Leu Val Ser Ala Asn

      117      126      135      144      153      162
    CAG GGG GTA ACA GGA ATG CCT GTG TCT GCT TTT ACT GTT ATT CTC TCC AAA GCT
    --- --- --- --- --- --- --- --- --- --- --- --- --- --- ---
    Gln Gly Val Thr Gly Met Pro Val Ser Ala Phe Thr Val Ile Leu Ser Lys Ala

      171      180      189      198      207      216
    TAC CCA GCA ATA GGA ACT CCC ATA CCA TTT GAT AAA ATT TTG TAT AAC AGG CAA
    --- --- --- --- --- --- --- --- --- --- --- --- --- --- ---
    Tyr Pro Ala Ile Gly Thr Pro Ile Pro Phe Asp Lys Ile Leu Tyr Asn Arg Gln

      225      234      243      252      261
    CAG CAT TAT GAC CCA AGG ACT CTG CAG CCA AGC TTA ATT AGC TGA 3'
    --- --- --- --- --- --- --- --- --- --- --- --- --- ---
    Gln His Tyr Asp Pro Arg Thr Leu Gln Pro Ser Leu Ile Ser ***
  
```

Figure 4.18: Sequence data of NC1 fragment F1/R1, showing multiple cloning site of pQE-30 expression vector (in red) and the NC1 insert (in black), the protein sequence is displayed below the corresponding nucleotide sequence.

Below is shown the nucleotide and protein sequences for the F2/R3 NC1 fragment, the 291 bp insert codes for 97 amino acids, however the recombinant protein will contain 19 additional amino acids due to the presence of the MCS of the pQE-30 expression vector. This 116 amino acid recombinant protein has a calculated molecular weight of 13,075 Da.

```

5'  ATG  AGA  GGA  TCG  CAT  CAC  CAT  CAC  CAT  CAC  GGA  TCC  CCA  AGG  ACT  GGA  ATC  TTT
    ---  ---  ---  ---  ---  ---  ---  ---  ---  ---  ---  ---  ---  ---  ---  ---  ---
    Met  Arg  Gly  Ser  His  His  His  His  His  His  Gly  Ser  Pro  Arg  Thr  Gly  Ile  Phe

      63      72      81      90      99      108
    ACT  TGT  CAG  ATA  CCA  GGA  ATA  TAC  TAT  TTT  TCA  TAC  CAC  GTG  CAT  GTG  AAA  GGG
    ---  ---  ---  ---  ---  ---  ---  ---  ---  ---  ---  ---  ---  ---  ---  ---  ---
    Thr  Cys  Gln  Ile  Pro  Gly  Ile  Tyr  Tyr  Phe  Ser  Tyr  His  Val  His  Val  Lys  Gly

      117      126      135      144      153      162
    ACT  CAT  GTT  TGG  GTA  GGC  CTG  TAT  AAG  AAT  GGC  ACC  CCT  GTA  ATG  TAC  ACC  TAT
    ---  ---  ---  ---  ---  ---  ---  ---  ---  ---  ---  ---  ---  ---  ---  ---  ---
    Thr  His  Val  Trp  Val  Gly  Leu  Tyr  Lys  Asn  Gly  Thr  Pro  Val  Met  Tyr  Thr  Tyr

      171      180      189      198      207      216
    GAT  GAA  TAC  ACC  AAA  GGC  TAC  CTG  GAT  CAG  GCT  TCA  GGG  AGT  GCC  ATC  ATC  GAT
    ---  ---  ---  ---  ---  ---  ---  ---  ---  ---  ---  ---  ---  ---  ---  ---  ---
    Asp  Glu  Tyr  Thr  Lys  Gly  Tyr  Leu  Asp  Gln  Ala  Ser  Gly  Ser  Ala  Ile  Ile  Asp

      225      234      243      252      261      270
    CTC  ACA  GAA  AAT  GAC  CAG  GTG  TGG  CTC  CAG  CTT  CCC  AAT  GCC  GAG  TCA  AAT  GGC
    ---  ---  ---  ---  ---  ---  ---  ---  ---  ---  ---  ---  ---  ---  ---  ---  ---
    Leu  Thr  Glu  Asn  Asp  Gln  Val  Trp  Leu  Gln  Leu  Pro  Asn  Ala  Glu  Ser  Asn  Gly

      279      288      297      306      315      324
    CTA  TAC  TCC  TCT  GAG  TAT  GTC  CAC  TCC  TCT  TTC  TCA  GGA  TTC  CTA  GTG  GCT  CCA
    ---  ---  ---  ---  ---  ---  ---  ---  ---  ---  ---  ---  ---  ---  ---  ---  ---
    Leu  Tyr  Ser  Ser  Glu  Tyr  Val  His  Ser  Ser  Phe  Ser  Gly  Phe  Leu  Val  Ala  Pro

      333      342      351
    ATG  CTG  CAG  CCA  AGC  TTA  ATT  AGC  TGA  3'
    ---  ---  ---  ---  ---  ---  ---  ---  ---
    Met  Leu  Gln  Pro  Ser  Leu  Ile  Ser  ***
  
```

Figure 4.19: Sequence data of NC1 fragment F2/R3, showing multiple cloning site of pQE-30 expression vector (in red) and the NC1 insert (in black), the protein sequence is displayed below the corresponding nucleotide sequence.

Below is shown the nucleotide and protein sequences for the F1/R2 NC1 fragment, the 312 bp insert codes for 104 amino acids, however the recombinant protein will contain 19 additional amino acids due to the presence of the MCS of the pQE-30 expression vector. This 123 amino acid recombinant protein has a calculated molecular weight of 13,632 Da.

```

5'   9      18      27      36      45      54
    ATG AGA GGA TCG CAT CAC CAT CAC CAT CAC GGA TCC GTC ATG CCT GAG GGT TTT
    --- --- --- --- --- --- --- --- --- --- --- --- --- --- --- ---
    Met Arg Gly Ser His His His His His His Gly Ser Val Met Pro Glu Gly Phe

      63      72      81      90      99      108
    ATA AAG GCA GGC CAA AGG CCC AGT CTT TCT GGG ACC CCT CTT GTT AGT GCC AAC
    --- --- --- --- --- --- --- --- --- --- --- --- --- --- --- ---
    Ile Lys Ala Gly Gln Arg Pro Ser Leu Ser Gly Thr Pro Leu Val Ser Ala Asn

     117     126     135     144     153     162
    CAG GGG GTA ACA GGA ATG CCT GTG TCT GCT TTT ACT GTT ATT CTC TCC AAA GCT
    --- --- --- --- --- --- --- --- --- --- --- --- --- --- --- ---
    Gln Gly Val Thr Gly Met Pro Val Ser Ala Phe Thr Val Ile Leu Ser Lys Ala

     171     180     189     198     207     216
    TAC CCA GCA ATA GGA ACT CCC ATA CCA TTT GAT AAA ATT TTG TAT AAC AGG CAA
    --- --- --- --- --- --- --- --- --- --- --- --- --- --- --- ---
    Tyr Pro Ala Ile Gly Thr Pro Ile Pro Phe Asp Lys Ile Leu Tyr Asn Arg Gln

     225     234     243     252     261     270
    CAG CAT TAT GAC CCA AGG ACT GGA ATC TTT ACT TGT CAG ATA CCA GGA ATA TAC
    --- --- --- --- --- --- --- --- --- --- --- --- --- --- --- ---
    Gln His Tyr Asp Pro Arg Thr Gly Ile Phe Thr Cys Gln Ile Pro Gly Ile Tyr

     279     288     297     306     315     324
    TAT TTT TCA TAC CAC GTG CAT GTG AAA GGG ACT CAT GTT TGG GTA GGC CTG TAT
    --- --- --- --- --- --- --- --- --- --- --- --- --- --- --- ---
    Tyr Phe Ser Tyr His Val His Val Lys Gly Thr His Val Trp Val Gly Leu Tyr

     333     342     351     360     369
    AAG AAT GGC ACC CCT GTA ATG TAC CTG CAG CCA AGC TTA ATT AGC TGA 3'
    --- --- --- --- --- --- --- --- --- --- --- --- --- --- ---
    Lys Asn Gly Thr Pro Val Met Tyr Leu Gln Pro Ser Leu Ile Ser ***
  
```

Figure 4.20: Sequence data of NC1 fragment F1/R2, showing multiple cloning site of pQE-30 expression vector (in red) and the NC1 insert (in black), the protein sequence is displayed below the corresponding nucleotide sequence.

Below is shown the nucleotide and protein sequences for the F2/R2 NC1 fragment, the 120 bp insert codes for 40 amino acids, however the recombinant protein will contain 19 additional amino acids due to the presence of the MCS of the pQE-30 expression vector. This 59 amino acid recombinant protein has a calculated molecular weight of 6770 Da.

```

5'   9       18       27       36       45       54
    ATG AGA GGA TCG CAT CAC CAT CAC CAT CAC GGA TCC CCA AGG ACT GGA ATC TTT
    ---
    Met Arg Gly Ser His His His His His His Gly Ser Pro Arg Thr Gly Ile Phe

        63       72       81       90       99       108
    ACT TGT CAG ATA CCA GGA ATA TAC TAT TTT TCA TAC CAC GTG CAT GTG AAA GGG
    ---
    Thr Cys Gln Ile Pro Gly Ile Tyr Tyr Phe Ser Tyr His Val His Val Lys Gly

        117       126       135       144       153       162
    ACT CAT GTT TGG GTA GGC CTG TAT AAG AAT GGC ACC CCT GTA ATG TAC CTG CAG
    ---
    Thr His Val Trp Val Gly Leu Tyr Lys Asn Gly Thr Pro Val Met Tyr Leu Gln

        171       180
    CCA AGC TTA ATT AGC TGA 3'
    ---
    Pro Ser Leu Ile Ser ***
  
```

Figure 4.21: Sequence data of NC1 fragment F2/R2, showing multiple cloning site of pQE-30 expression vector (in red) and the NC1 insert (in black), the protein sequence is displayed below the corresponding nucleotide sequence.

4.3.4 Recombinant Protein Production and Purification

Bacteria were grown from glycerol stocks, up to a 500ml culture for each of the NC1 fragments F1/R1, F1/R2, F2/R2 and F2/R3, and also for the control plasmid pQE-40 which encodes for the mouse recombinant DHFR protein. The bacterial cultures were induced to begin recombinant protein transcription and translation by addition of IPTG (as detailed in section 4.2.5). Cells were harvested after 5 hours, *E. coli* lysates were prepared under native conditions; (see section 4.2.5.1) and the cellular debris was prepared under denaturing conditions (see section 4.2.5.2). Proteins from the native and denatured preparations were purified using Ni-NTA agarose.

During the native purification process using Ni-NTA agarose; a total of ten samples were removed for analysis, these included: a non-induced culture control, an induced control culture, an *E. coli* native lysate, an un-bound protein fraction, the first Ni-NTA agarose wash (wash 1), the second Ni-NTA agarose wash (wash 2), and four Ni-NTA agarose elution fractions (Eluates 1-4). During the denaturing purification process using Ni-NTA agarose; a total of twelve samples were removed for analysis, these included: an *E. coli* denatured lysate, an un-bound protein fraction, the first Ni-NTA agarose wash (wash 1), the second Ni-NTA agarose wash (wash 2), and eight Ni-NTA agarose elution fractions (Eluates 1-8).

To determine the purity and the fraction which contained most of the recombinant proteins, all of the above samples were subsequently analysed by SDS-PAGE and Western blot analysis using the Qiagen penta-His antibody. Samples were separated on 12.5 or 15% polyacrylamide gels.

The mouse recombinant DHFR protein encoded by the pQE-40 expression plasmid is optimised for high level expression producing up to 40 mg/litre in culture. It is an ideal control for cell growth, expression and purification. Approximately, 10% of the 26 kDa recombinant protein is soluble and can be purified under native conditions the remaining 90% of protein accumulates as an insoluble form in inclusion bodies, purification under denaturing conditions is therefore required. The DHFR recombinant protein produced by M15[pREP4] cells and purified as a positive control in this study, was largely found in the insoluble inclusion bodies as expected.

4.3.4.1 Analysis of the Positive Control Protein, DHFR

The 26 kDa DHFR recombinant protein purified under native conditions can be seen in figure 4.22. On the Coomassie stained polyacrylamide gel, figure 4.22(a), a band which is slightly lower than the 29 kDa molecular weight marker can be seen in the induced control sample (lane 3), the native *E. coli* lysate (lane 4) and in eluates 1-4 (lanes 8-11). These bands (lanes 3, 4, 8, 9 & 10) were confirmed to be the his-tagged DHFR recombinant protein by Western blot analysis, figure 4.22(b). The faint band seen in lane 11 in figure 4.22(a) was not detected by Western blot.

The samples which were purified under denaturing conditions, contained far more of the DHFR recombinant protein, as expected. On the Coomassie stained polyacrylamide gel, figure 4.23(a), a band which is around the same position as the 29 kDa molecular weight marker can be seen in all lanes. The intensity of this band varies in the samples with the most intense being found in the *E. coli* denatured lysate (lane 2) and in eluates 5-8 (lanes 10-13). The high level of DHFR in this preparation is highlighted by the fact that there are bands present in the un-bound protein fraction (lane 3), indicative that all the his-tagged binding sites on the Ni-NTA agarose were occupied and there are also bands present in wash fractions 1 and 2 (lanes 4 & 5).

These bands were confirmed to be the His-tagged DHFR recombinant protein by Western blot analysis, figure 4.23(b). A band around the same level as the 29 kDa molecular weight marker can be seen in all lanes. A higher molecular weight band has also been detected in the Western blot, this band is positioned around the 49 kDa molecular weight marker, this band is most prominent in the samples which have the most intense band at 29 kDa in the Coomassie stained gels (lanes 2 & 10-13). This band could potentially be a dimer of the 26 kDa DHFR protein.

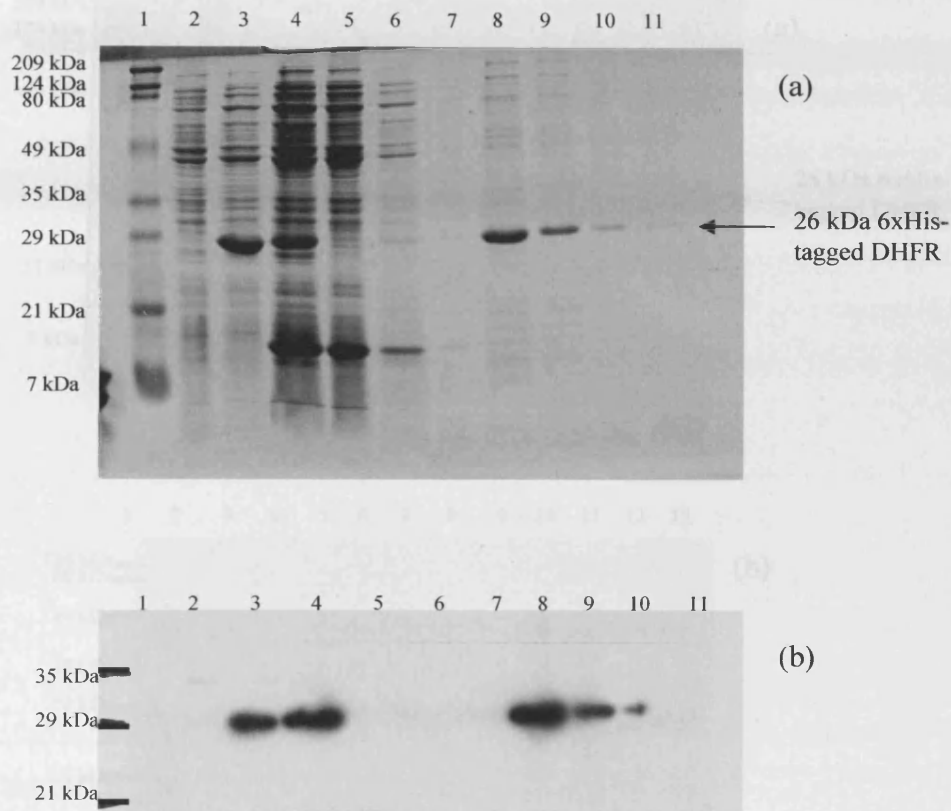


Figure 4.22: SDS-PAGE and Western blot analysis of samples generated under native conditions using the Ni-NTA agarose to purify 6xHis-tagged DHFR. (a) Coomassie stained 12.5% polyacrylamide gel, 10µl of each sample loaded, lane 1: molecular weight ladder, lane 2: non-induced control, lane 3: induced control, lane 4: native lysate, lane 5: un-bound protein, lane 6: wash 1, lane 7: wash 2, lane 8: eluate 1, lane 9: eluate 2, lane 10: eluate 3, lane 11: eluate 4. (b) Anti penta-His antibody used in Western analysis of the samples detailed in (a).

4.2 Analysis of the Ni-NTA Fractions, P1 R1

series of bands from the purification of the P1 R1 recombinant protein under native and denaturing conditions was analysed by SDS-PAGE and Western blot analysis. The P1 R1 recombinant protein is reported to have a molecular weight of 95.75 kDa, therefore the region between 7 and 21 kDa molecular weight markers for the Coomassie stained

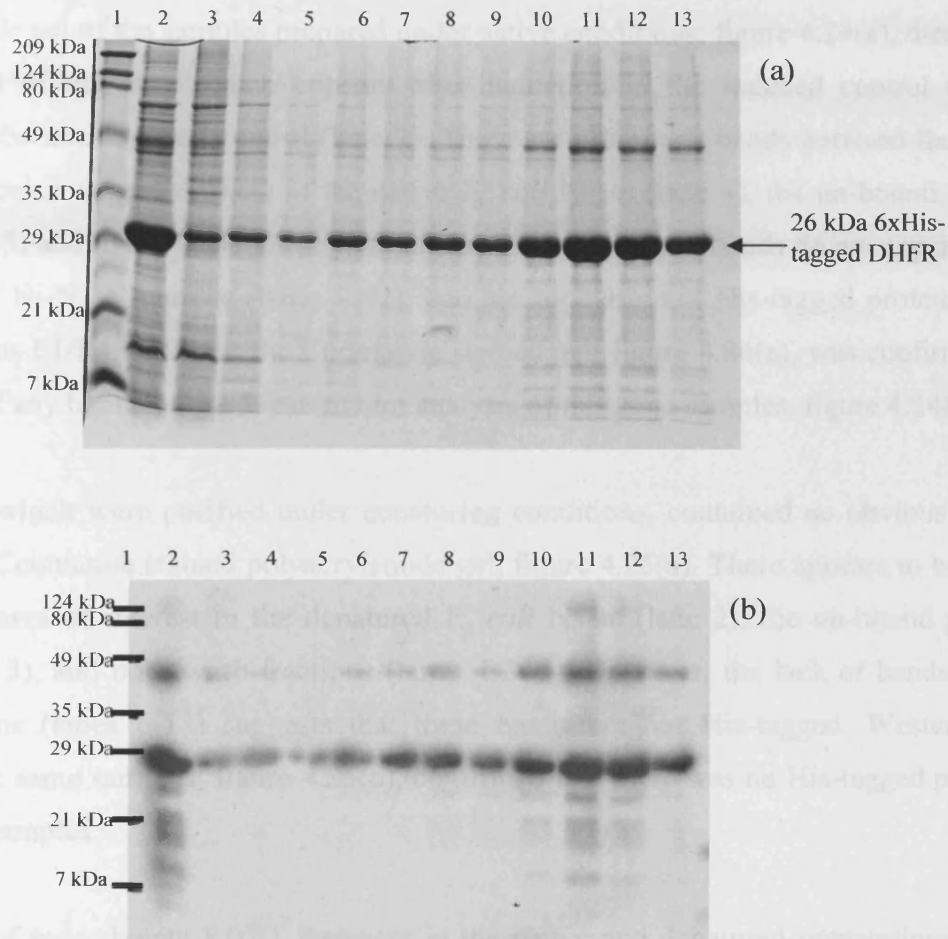


Figure 4.23: SDS-PAGE and Western blot analysis of samples generated under denaturing conditions using the Ni-NTA agarose to purify 6xHis-tagged DHFR. (a) Coomassie stained 12.5% polyacrylamide gel, 10µl of each sample loaded, lane 1: molecular weight ladder, lane 2: denatured lysate, lane 3: un-bound protein, lane 4: wash 1, lane 5: wash 2, lane 6: eluate 1, lane 7: eluate 2, lane 8: eluate 3, lane 9: eluate 4, lane 10: eluate 5, lane 11: eluate 6, lane 12: eluate 7, lane 13: eluate 8, (b) Anti penta-His antibody used in Western analysis of the samples detailed in (a).

4.3.4.2 Analysis of the NCI Fragment, F1/R1

Samples obtained from the purification of the F1/R1 recombinant protein under native and denaturing conditions were analysed by SDS-PAGE and Western blot analysis. The F1/R1 recombinant protein is expected to have a molecular weight of 9372 Da, therefore the region of interest lay between the 7 and 21 kDa molecular weight markers. On the Coomassie stained polyacrylamide gel of the samples prepared under native conditions; figure 4.24(a), there is no obvious band of this size which appears after induction in the induced control (lane 3) compared to the non-induced control (lane 2). There are prominent bands between the 7 and 21 kDa molecular weight markers in the native *E. coli* lysate (lane 4), the un-bound protein fraction (lane 5) and in the wash 1 fraction (lane 6). However, these bands do not appear to be eluted off the Ni-NTA agarose (lanes 8-11), and are probably not His-tagged proteins. The lack of obvious F1/R1 bands on the Coomassie stained gel; figure 4.24(a), was confirmed by the absence of any bands on the Western blot analysis of the same samples, figure 4.24(b).

The samples which were purified under denaturing conditions, contained no obvious F1/R1 bands on the Coomassie stained polyacrylamide gel, figure 4.25(a). There appears to be some bands in the area of interest in the denatured *E. coli* lysate (lane 2), the un-bound protein fraction (lane 3), and both wash fractions (lanes 4 & 5). However, the lack of bands in the eluate fractions (lanes 6-13) suggests that these bands are not His-tagged. Western blot analysis of the same samples; figure 4.25(b), confirmed that there was no His-tagged proteins in any of the samples.

The absence of recombinant F1/R1 fragment in the native and denatured preparations could be caused by many factors which will be discussed later.

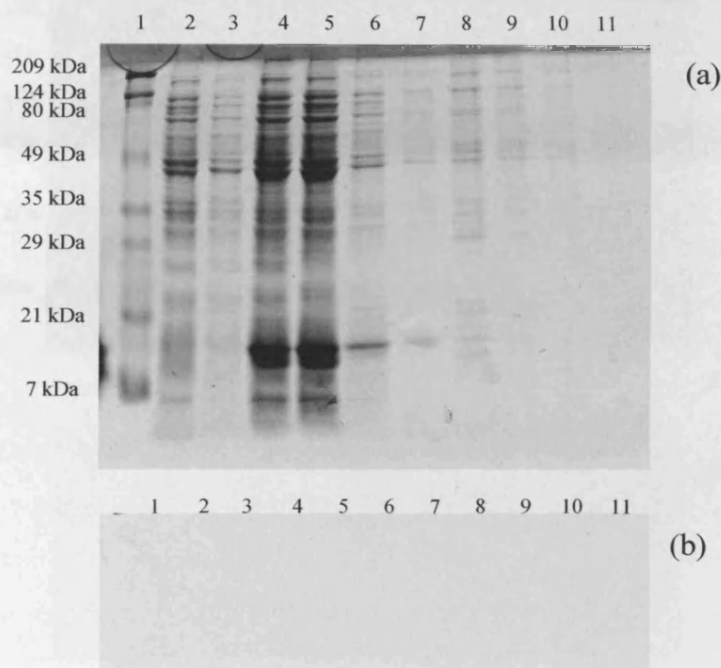


Figure 4.24: SDS-PAGE and Western blot analysis of samples generated under native conditions using the Ni-NTA agarose to purify 6xHis-tagged F1/R1 recombinant fragment. (a) Coomassie stained 12.5% polyacrylamide gel, 10 μ l of each sample loaded, lane 1: molecular weight ladder, lane 2: non-induced control, lane 3: induced control, lane 4: native lysate, lane 5: un-bound protein, lane 6: wash 1, lane 7: wash 2, lane 8: eluate 1, lane 9: eluate 2, lane 10: eluate 3, lane 11: eluate 4. (b) Anti penta-His antibody used in Western analysis of the samples detailed in (a).

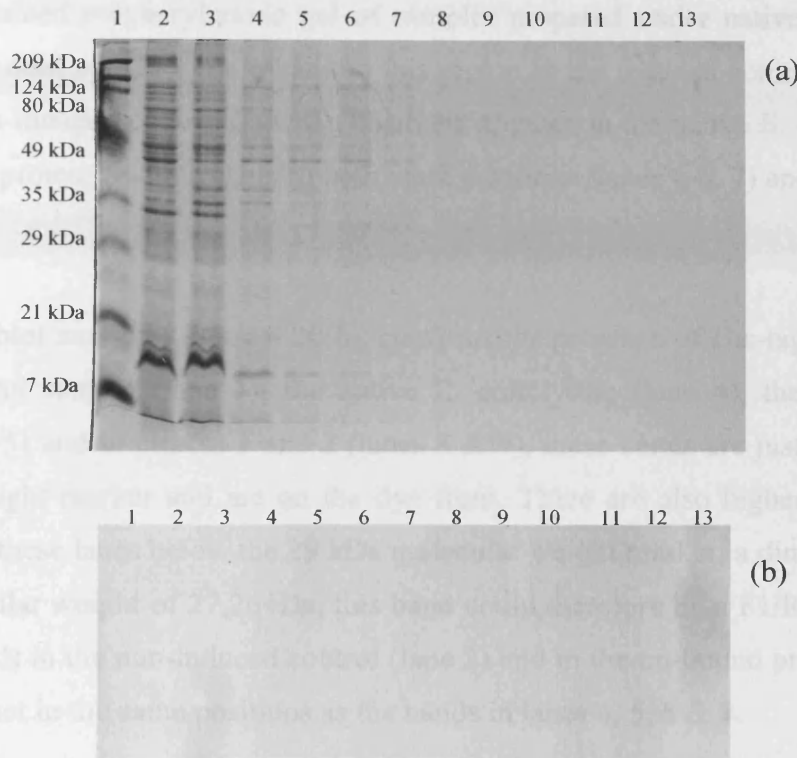


Figure 4.25: SDS-PAGE and Western blot analysis of samples generated under denaturing conditions using the Ni-NTA agarose to purify 6xHis-tagged F1/R1 recombinant fragment. (a) Coomassie stained 12.5% polyacrylamide gel, 10µl of each sample loaded, lane 1: molecular weight ladder, lane 2: denatured lysate, lane 3: un-bound protein, lane 4: wash 1, lane 5: wash 2, lane 6: eluate 1, lane 7: eluate 2, lane 8: eluate 3, lane 9: eluate 4, lane 10: eluate 5, lane 11: eluate 6, lane 12: eluate 7, lane 13: eluate 8, (b) Anti penta-His antibody used in Western analysis of the samples detailed in (a).

4.3.4.3 Analysis of the NC1 Fragment, F1/R2

SDS-PAGE and Western blot analysis were used to analyse samples obtained from the purification of the F1/R2 recombinant protein under native and denaturing conditions. The F1/R2 recombinant protein was expected to have a molecular weight of 13,632 Da, therefore the region of interest lay between the 7 and 21 kDa molecular weight markers. On the Coomassie stained polyacrylamide gel of samples prepared under native conditions; figure 4.26(a), there does appear to be a band in this region in the induced control (lane 3), which is not in the non-induced control (lane 2), this band appears in the native *E. coli* lysate (lane 4), the un-bound protein fraction (lane 5) both wash fractions (lanes 6 & 7) and in eluates 1 and 2 (lanes 8 & 9).

The Western blot analysis; figure 4.26(b), confirms the presence of His-tagged proteins in the induced control sample (lane 3), the native *E. coli* lysate (lane 4), the un-bound protein fraction (lane 5) and in eluates 1 and 2 (lanes 8 & 9), these bands are just below the 21 kDa molecular weight marker and are on the dye front. There are also higher molecular weight aggregates in these lanes below the 29 kDa molecular weight marker, a dimer of F1/R2 would have a molecular weight of 27,264Da, this band could therefore be a F1/R2 dimer. There are also faint bands in the non-induced control (lane 2) and in the un-bound protein fraction (lane 5) which are not in the same positions as the bands in lanes 4, 5, 8 & 9.

The samples which were purified under denaturing conditions, contained far more of F1/R2 recombinant protein. On the Coomassie stained polyacrylamide gel, figure 4.27(a), a band which is between the 7 and 21 kDa molecular weight marker can be seen in all lanes. The intensity of this band varies in the samples with the most intense being found in the *E. coli* denatured lysate (lane 2), the un-bound protein fraction (lane 3) and in eluates 5-8 (lanes 10-13). The high level of F1/R2 in this preparation is highlighted by the fact that there are bands present in the un-bound protein fraction (lane 3), indicative that all the His-tagged binding sites on the Ni-NTA agarose were occupied and there are also bands present in wash fractions 1 and 2 (lanes 4 & 5). These bands were confirmed to be the His-tagged F1/R2 recombinant protein by Western blot analysis, figure 4.27(b). A band between the 7 and 21 kDa molecular weight marker can be seen in all lanes.

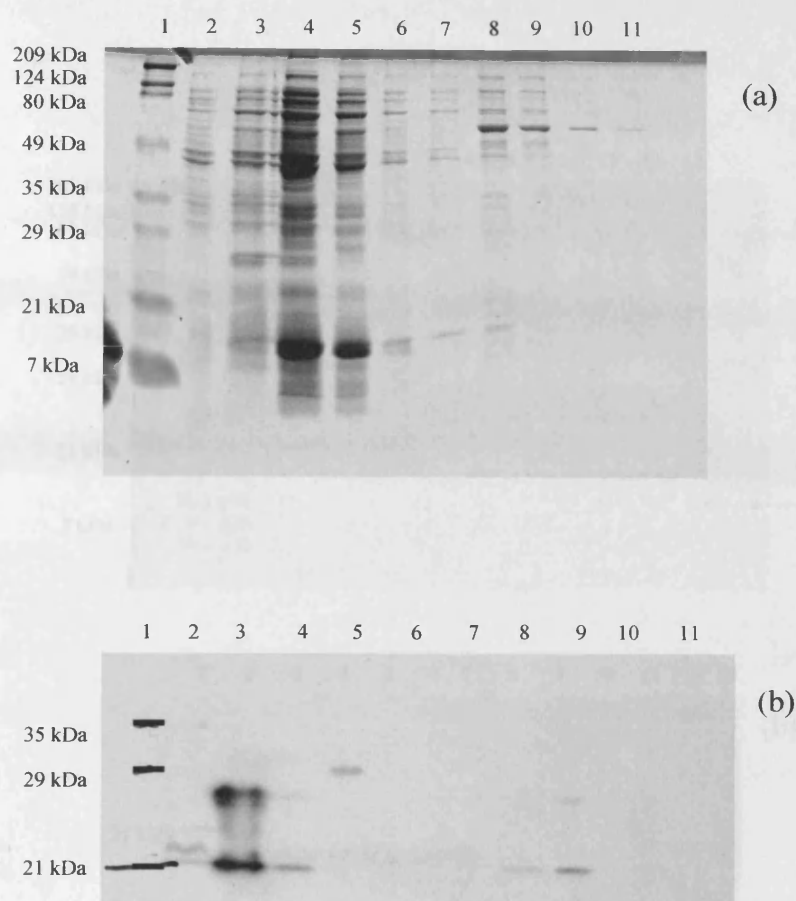


Figure 4.26: SDS-PAGE and Western blot analysis of samples generated under native conditions using the Ni-NTA agarose to purify 6xHis-tagged F1/R2 recombinant fragment. (a) Coomassie stained 12.5% polyacrylamide gel, 10µl of each sample loaded, lane 1: molecular weight ladder, lane 2: non-induced control, lane 3: induced control, lane 4: native lysate, lane 5: un-bound protein, lane 6: wash 1, lane 7: wash 2, lane 8: eluate 1, lane 9: eluate 2, lane 10: eluate 3, lane 11: eluate 4. (b) Anti penta-His antibody used in Western analysis of the samples detailed in (a).

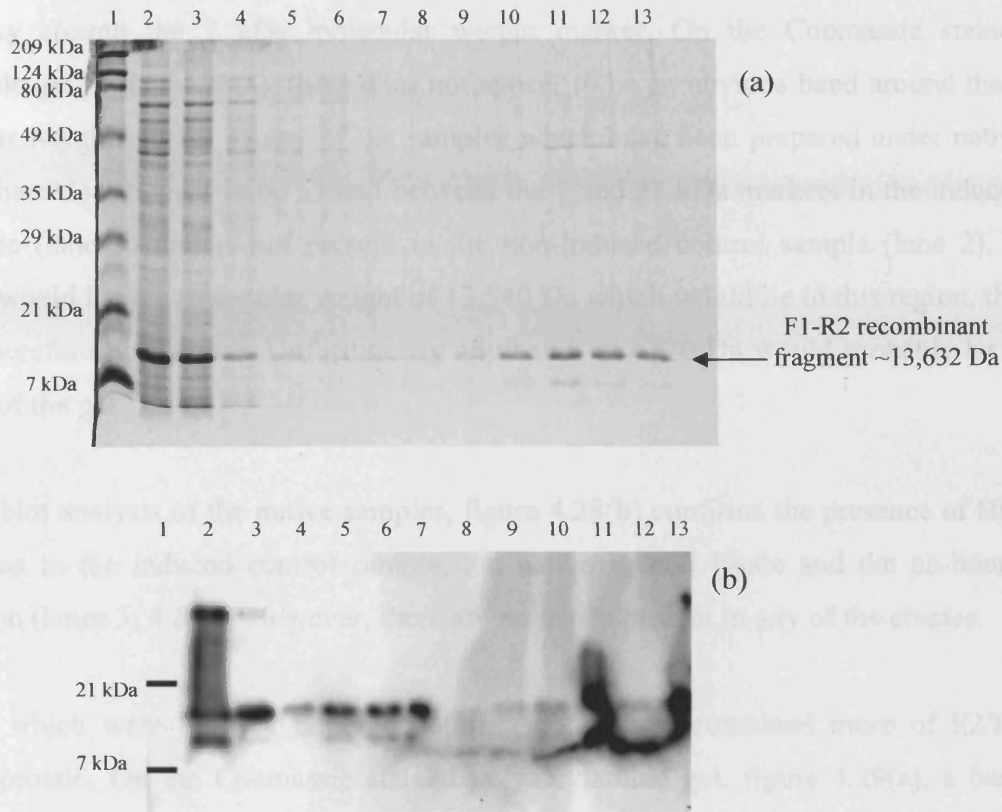


Figure 4.27: SDS-PAGE and Western blot analysis of samples generated under denaturing conditions using the Ni-NTA agarose to purify 6xHis-tagged F1/R2 recombinant fragment. (a) Coomassie stained 12.5% polyacrylamide gel, 10µl of each sample loaded, lane 1: molecular weight ladder, lane 2: denatured lysate, lane 3: un-bound protein, lane 4: wash 1, lane 5: wash 2, lane 6: eluate 1, lane 7: eluate 2, lane 8: eluate 3, lane 9: eluate 4, lane 10: eluate 5, lane 11: eluate 6, lane 12: eluate 7, lane 13: eluate 8, (b) Anti penta-His antibody used in Western analysis of the samples detailed in (a).

4.3.4.4 Analysis of the NC1 Fragment, F2/R2

Samples obtained from the purification of the F2/R2 recombinant protein under native and denaturing conditions were analysed by SDS-PAGE and Western blot analysis. The F2/R2 recombinant protein is expected to have a molecular weight of 6770 Da, therefore the region of interest lay around the 7 kDa molecular weight marker. On the Coomassie stained polyacrylamide gel, figure 4.28(a), there does not appear to be an obvious band around the 7 kDa molecular weight marker in any of the samples which have been prepared under native conditions. There does appear to be a band between the 7 and 21 kDa markers in the induced control sample (lane 3) that is not present in the non-induced control sample (lane 2). A F2/R2 dimer would have a molecular weight of 13,540 Da which would lie in this region, this band could therefore be a dimer. Unfortunately any bands at 6770 Da would probably be in the dye front of the gel.

The Western blot analysis of the native samples, figure 4.28(b) confirms the presence of His-tagged proteins in the induced control sample, the native *E. coli* lysate and the un-bound protein fraction (lanes 3, 4 & 5). However, there are no bands present in any of the eluates.

The samples which were purified under denaturing conditions, contained more of F2/R2 recombinant protein. On the Coomassie stained polyacrylamide gel, figure 4.29(a), a band which is around the 7 kDa molecular weight marker can be seen in the denatured *E. coli* lysate (lane 2), the un-bound protein fraction (lane 3), wash 1 fraction (lane 4) and in eluates 5-7 (lanes 10-12). The Western blot analysis of the denatured samples, figure 4.29(b) confirms the presence of His-tagged proteins in most of the above samples (lanes 2, 3, 10, 11 & 12).

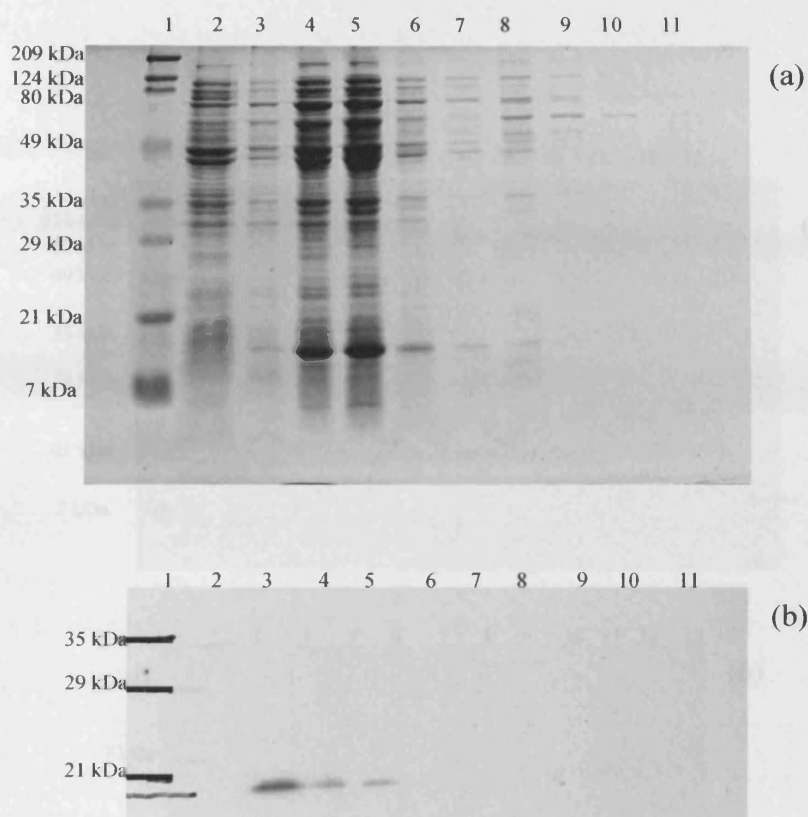


Figure 4.28: SDS-PAGE and Western blot analysis of samples generated under native conditions using the Ni-NTA agarose to purify 6xHis-tagged F2/R2 recombinant fragment. (a) Coomassie stained 12.5% polyacrylamide gel, 10µl of each sample loaded, lane 1: molecular weight ladder, lane 2: non-induced control, lane 3: induced control, lane 4: native lysate, lane 5: un-bound protein, lane 6: wash 1, lane 7: wash 2, lane 8: eluate 1, lane 9: eluate 2, lane 10: eluate 3, lane 11: eluate 4. (b) Anti penta-His antibody used in Western analysis of the samples detailed in (a).

4.3.4.3 Analysis of the NCI Fragment, F2/R2

SDS-PAGE and Western blot analysis were used to analyse samples obtained from the purification of the F2/R2 recombinant protein under native and denaturing conditions. The F2/R2 recombinant protein is expected to have a molecular weight of 13.075 kDa, therefore the region of interest lay between the 7 and 21 kDa molecular weight markers. On the Coomassie stained polyacrylamide gel (Figure 4.29a), there

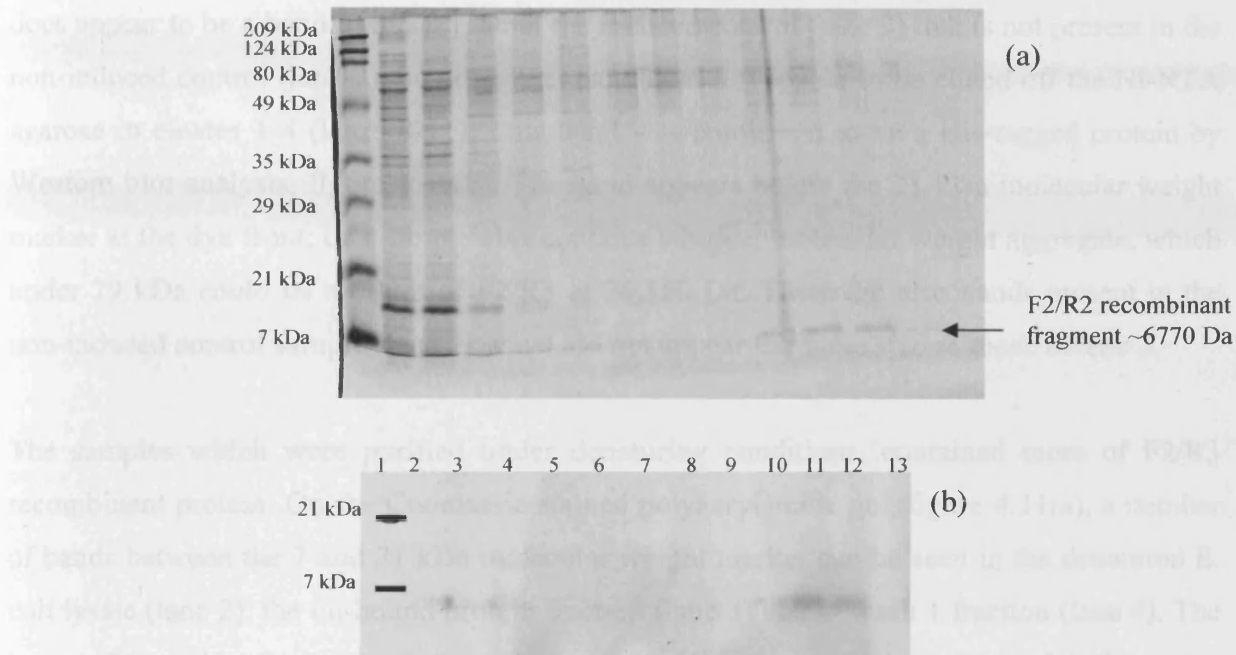


Figure 4.29: SDS-PAGE and Western blot analysis of samples generated under denaturing conditions using the Ni-NTA agarose to purify 6xHis-tagged F2/R2 recombinant fragment. (a) Coomassie stained 12.5% polyacrylamide gel, 10µl of each sample loaded, lane 1: molecular weight ladder, lane 2: denatured lysate, lane 3: un-bound protein, lane 4: wash 1, lane 5: wash 2, lane 6: eluate 1, lane 7: eluate 2, lane 8: eluate 3, lane 9: eluate 4, lane 10: eluate 5, lane 11: eluate 6, lane 12: eluate 7, lane 13: eluate 8, (b) Anti penta-His antibody used in Western analysis of the samples detailed in (a).

4.3.4.5 Analysis of the NC1 Fragment, F2/R3

SDS-PAGE and Western blot analysis were used to analyse samples obtained from the purification of the F2/R3 recombinant protein under native and denaturing conditions. The F2/R3 recombinant protein is expected to have a molecular weight of 13,075 Da, therefore the region of interest lay between the 7 and 21 kDa molecular weight markers. On the Coomassie stained polyacrylamide gel of samples prepared under native conditions figure 4.30(a), there does appear to be a band in this region in the induced control (lane 3) that is not present in the non-induced control (lane 2), however this band does not appear to be eluted off the Ni-NTA agarose in eluates 1-4 (lanes 8-11). This band was confirmed to be a His-tagged protein by Western blot analysis, figure 4.30(b). The band appears below the 21 kDa molecular weight marker at the dye front; this sample also contains a higher molecular weight aggregate, which under 29 kDa could be a dimer of F2/R3 at 26,150 Da. There are also bands present in the non-induced control sample (lane 2) which do not appear the same size as those in lane 3.

The samples which were purified under denaturing conditions, contained more of F2/R3 recombinant protein. On the Coomassie stained polyacrylamide gel, figure 4.31(a), a number of bands between the 7 and 21 kDa molecular weight marker can be seen in the denatured *E. coli* lysate (lane 2), the un-bound protein fraction (lane 3) and in wash 1 fraction (lane 4). The lower of these bands appears to be eluting off the Ni-NTA agarose in eluates 5-8 (lanes 10-13).

The Western blot analysis figure 4.31(b); of these denatured samples confirmed the presence of a His-tagged protein between the 7 and 21 kDa molecular weight markers in all of the samples. There also appears to be a higher molecular weight aggregate; below the 29 kDa molecular weight marker in the following samples, the denature *E. coli* lysate (lane 2), the un-bound protein fraction (lane 3) and in eluates 5-8 (lanes 10-13). This could be a dimer of F2/R3 which would have a molecular weight of 26,150 Da.

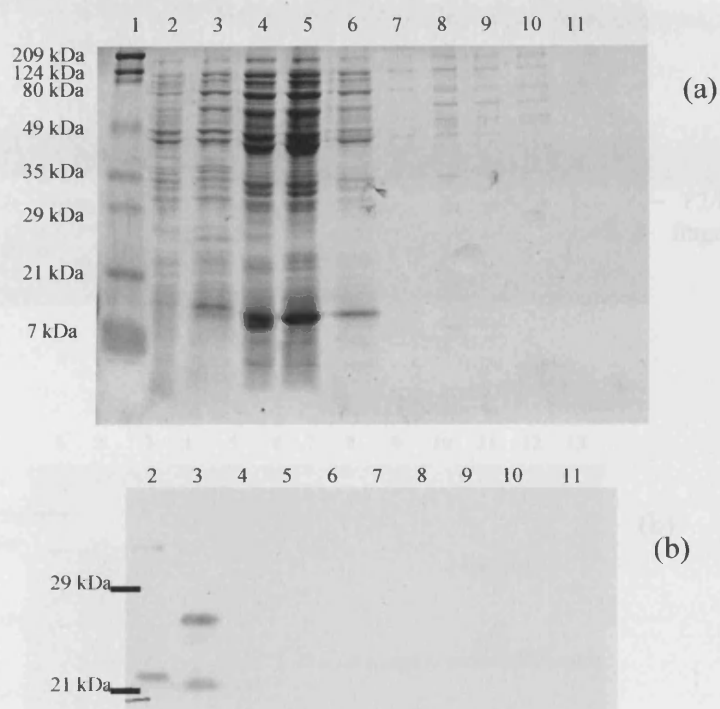


Figure 4.30: SDS-PAGE and Western blot analysis of samples generated under native conditions using the Ni-NTA agarose to purify 6xHis-tagged F2/R3 recombinant fragment. (a) Coomassie stained 12.5% polyacrylamide gel, 10µl of each sample loaded, lane 1: molecular weight ladder, lane 2: non-induced control, lane 3: induced control, lane 4: native lysate, lane 5: un-bound protein, lane 6: wash 1, lane 7: wash 2, lane 8: eluate 1, lane 9: eluate 2, lane 10: eluate 3, lane 11: eluate 4. (b) Anti penta-His antibody used in Western analysis of the samples detailed in (a).

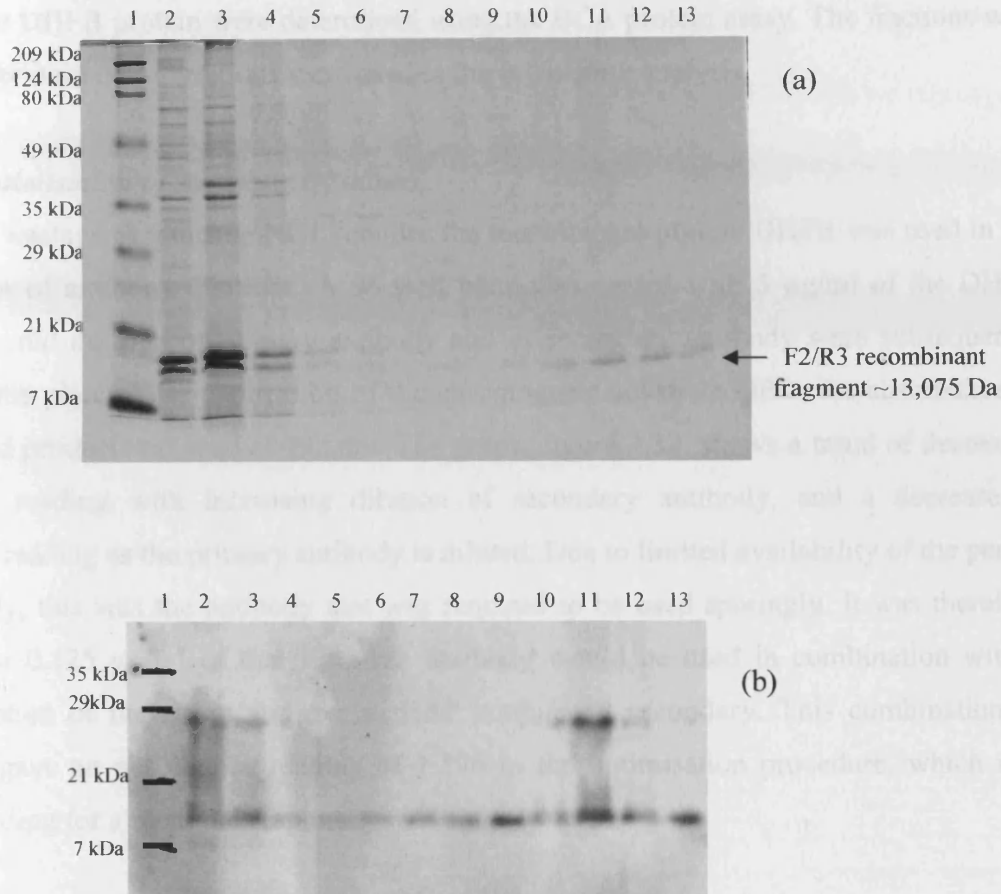


Figure 4.31: SDS-PAGE and Western blot analysis of samples generated under denaturing conditions using the Ni-NTA agarose to purify 6xHis-tagged F2/R3 recombinant fragment. (a) Coomassie stained 12.5% polyacrylamide gel, 10µl of each sample loaded, lane 1: molecular weight ladder, lane 2: denatured lysate, lane 3: un-bound protein, lane 4: wash 1, lane 5: wash 2, lane 6: eluate 1, lane 7: eluate 2, lane 8: eluate 3, lane 9: eluate 4, lane 10: eluate 5, lane 11: eluate 6, lane 12: eluate 7, lane 13: eluate 8, (b) Anti penta-His antibody used in Western analysis of the samples detailed in (a).

4.3.5 Interaction Analysis

For subsequent interaction analysis the samples from the purification procedures which were deemed to have most of the purest recombinant protein, were the denatured eluates 5-8. The protein concentrations of these samples; NC1 fragments F1/R2, F2/R2 and F2/R3; and the recombinant DHFR protein were determined using the BCA protein assay. The fractions with the highest protein concentrations were used in the interaction analysis.

4.3.5.1 Optimisation of Antibody Dilutions

To prevent wastage of valuable NC1 samples the recombinant protein DHFR was used in the optimisation of antibody dilutions. A 96-well plate was coated with 5 µg/ml of the DHFR protein, a serial dilution of primary antibody and of secondary antibody were subsequently applied to the plate. After application of the chromogenic substrate OPD, the absorbance of the coloured product was read at 492 nm. The graph; figure 4.32, shows a trend of decreased absorbance reading with increasing dilution of secondary antibody, and a decrease in absorbance reading as the primary antibody is diluted. Due to limited availability of the penta-His antibody, this was the antibody that was required to be used sparingly. It was therefore decided that 0.125 µg/ml of the penta-His antibody would be used in combination with a 1:1000 dilution of the sheep anti-mouse HRP conjugated secondary. This combination of antibodies gave an absorbance reading of 1.196 in the optimisation procedure, which is a suitable reading for a maximal response.

4.3.5.2 Interaction Analysis using NC1 Recombinant fragments F1/R2, F2/R2 and F2/R3

A 96-well plate was coated with 5 µg/ml of the proteoglycans decorin or biglycan. After washing and blocking the wells as detailed in the methods section; the NC1 Recombinant fragments (F1/R2, F2/R2 and F2/R3), were applied to the wells in triplicate at a range of concentration from 0 to 2.5 µg/ml. After incubation and washing steps, 0.125 µg/ml of the penta-His antibody was used in combination with a 1:1000 dilution of the sheep anti-mouse HRP conjugated secondary. After application of the chromogenic substrate OPD the absorbance of the coloured product was read at 492 nm.

Unfortunately the absorbance readings were not above the background absorbance for empty wells, or the control wells which had been coated with 3% (w/v) BSA in PBS. The solid phase assay was repeated with increased concentrations of the NC1 recombinant fragments F1/R2,

F2/R2 and F2/R3, up to 5 $\mu\text{g/ml}$. Once again the absorbance readings were not above background absorbance. These results will be deliberated in the discussion.

Optimisation of Antibody Dilutions for Interaction Analysis

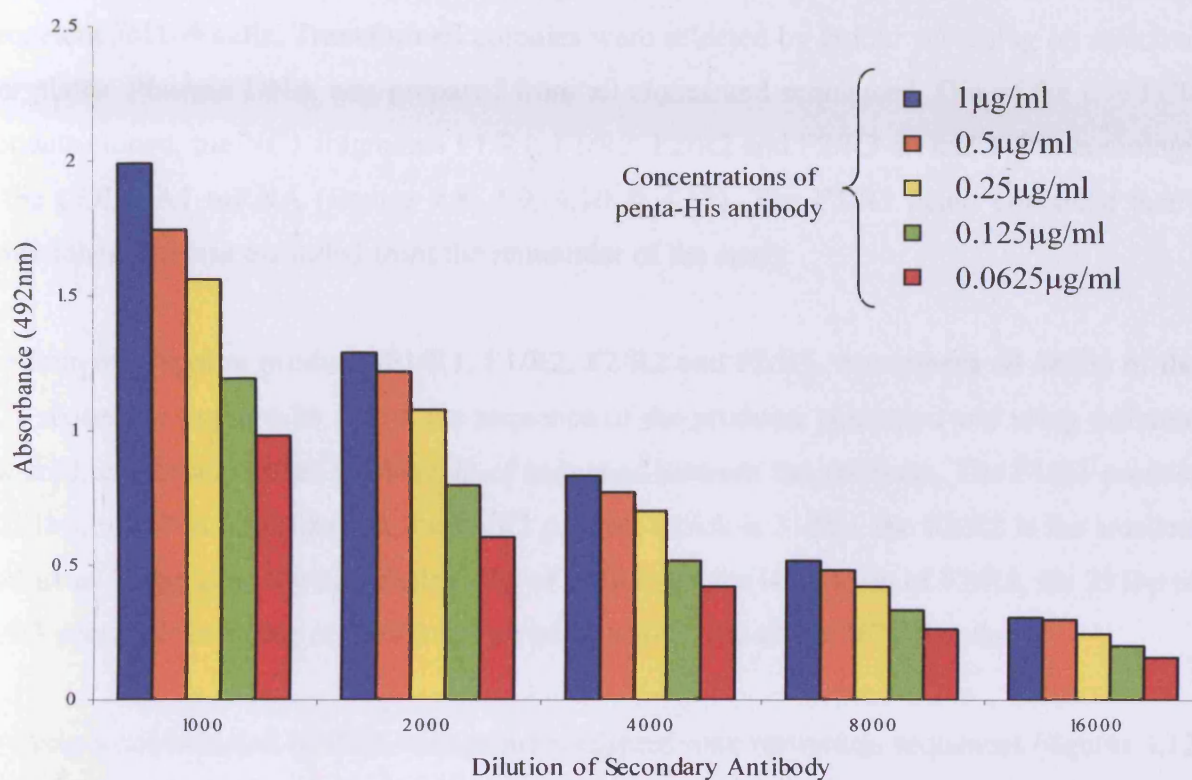


Figure 4.32: Graph of absorbance at 492 nm versus a range of dilutions for the sheep anti-mouse HRP secondary antibody for five different concentrations of the penta-His antibody, on a 96-well plate coated with the His-tagged recombinant DHFR protein.

4.4 DISCUSSION

The NC1 domain of type X collagen contains 161 amino acids which is encoded for by 483 bp. Plasmid DNA which contained the entire NC1 sequence was used as a template in PCR reactions, using primers designed to produce products that were 'in-frame' with regards to the translated protein sequence. PCR was used to generate five overlapping products which encompassed all 483 bp (figure 4.7)

These products were cloned into the cloning vector pGEM-T, which was used to transform competent JM109 cells. Transformed colonies were selected by colour screening on selective agar plates. Plasmid DNA was prepared from all clones and sequenced. Out of the five PCR products cloned, the NC1 fragments F1/R1, F1/R2, F2/R2 and F2/R3 all had 100% homology to the COL10A1 mRNA (figures 4.8, 4.9, 4.10 & 4.11). The F3/R3 insert contained many mismatches and was excluded from the remainder of the study.

The four overlapping products F1/R1, F1/R2, F2/R2 and F2/R3, encompass all 483bp of the NC1 sequence, figure 4.33 shows the sequence of the products generated and using different coloured text demonstrates the overlap of sequence between the products. The F1/R1 product is 201bp, which is all present in the F1/R2 product which is 312bp, the F2/R2 is the smallest product at 120bp and contains the last 9bp of F1/R1 and the last 111bp of F1/R2, the 291bp of F2/R3 contains the whole of F2/R2 and an additional 171bp of the NC1 sequence.

By using a combination of PCR with primers adapted with restriction sequences (figures 4.12 & 4.13), restriction digestions (figure 4.14) and ligation, the products were directionally sub-cloned into the expression vector pQE-30 (summarised in figure 4.15). These expression constructs and the control expression plasmid pQE-40 were used to transform two different strains of *E. coli*, M15 and XL-1 Blue. M15 carries the pREP4 repressor plasmid, while XL-1 Blue contains an episomal copy of lacI^q , which is a mutation of lacI that produces high levels of the lac repressor. Both strains were used because clone analysis can sometimes be difficult using the M15 strain due to the presence of the p REP4 plasmid. However, for the most stable propagation of expression constructs, the M15 strain was recommended by the manufacturer's (Qiagen) because of higher repressor levels.

F1/R1

```
gtcatgcctgagggtttataaaggcaggccaaaggcccagtccttctgggacccctcttgttagtgccaa
ccagggggtaacaggaatgcctgtgtctgcttttactgttattctctccaaagcttaccagcaataggaac
tccataccatttgataaaattttgtataacaggcaacagcattatgaccaaggact
```

F1/R2

```
gtcatgcctgagggtttataaaggcaggccaaaggcccagtccttctgggacccctcttgttagtgccaa
ccagggggtaacaggaatgcctgtgtctgcttttactgttattctctccaaagcttaccagcaataggaac
tccataccatttgataaaattttgtataacaggcaacagcattatgaccaaggactggaatctttactgtc
agataccaggaatatactattttcataccacgtgcatgtgaaagggactcatgttgggtaggcctgtataa
gaatggcaccctgtaatgtac
```

F2/R2

```
ccaaggactggaatctttactgtcagataccaggaatatactattttcataccacgtgcatgtgaaaggg
actcatgtttgggtaggcctgtataagaatggcaccctgtaatgtac
```

F2/R3

```
ccaaggactggaatctttactgtcagataccaggaatatactattttcataccacgtgcatgtgaaaggg
actcatgtttgggtaggcctgtataagaatggcaccctgtaatgtacacctatgatgaatacaccaaagg
ctacctggatcaggcttcaggagtgccatcatcgatctcacagaaaatgaccaggttggtccagctt
cccaatgccgagtcaaattggcctatactcctctgagtatgtccactcctcttctcaggattcctagtggctc
caatg
```

Figure 4.33: The nucleotide sequence of the NC1 products generated by PCR. The overlap of nucleotide sequence between the products is highlighted by coloured text.

The presence of the inserts in the bacteria was confirmed by PCR (figures 4.16 & 4.17), and sequence analysis was used to confirm the inserts had 100% homology to the COL10A1 mRNA. The creation of expression constructs utilising the expression vector pQE-30, and four different fragments of the in frame human NC1 sequence with 100% homology to the COL10A1 mRNA was successful (figures 4.18, 4.19, 4.20 & 4.21).

The production of recombinant protein on a small scale was attempted at first (data not shown), a 10 ml culture was induced to produce recombinant proteins, the cells were harvested, resuspended in sample buffer and subsequently analysed by SDS-PAGE and Western blot analysis. The recombinant proteins DHFR (translation product of the control pQE-40 expression plasmid), F1/R2, F2/R2 and F2/R3 were all visualised on Coomassie stained polyacrylamide gels and confirmed to be present by Western blot analysis. However, the F1/R1 recombinant protein was not observed. It was assumed that the protein was insoluble and was therefore not loaded onto the gel or may have been unstable and was degraded.

A large scale production of recombinant protein was performed. Cells were harvested and were subjected to preparation under native and denaturing conditions, purification of His-tagged proteins using Ni-NTA agarose was also performed under native and denaturing conditions. Small samples which were taken during these procedures were analysed by SDS-PAGE and Western blotting. The recombinant proteins DHFR, F1/R2, F2/R2 and F2/R3 were all successfully expressed and were purified under denaturing conditions (figures 4.23, 4.27, 4.29 & 4.31, respectively). The F1/R1 recombinant fragment was not observed (figures 4.24 & 4.25), under native or denaturing conditions. This result was similar to that found in the preliminary small scale purification. The possibility that the F1/R1 recombinant protein was insoluble however was disproved by its absence in samples prepared under denaturing conditions.

Proteins that are smaller than 10 kDa are not stable in *E. coli* and may be rapidly degraded. Two out of the four NC1 recombinant fragments are smaller than 10 kDa, F1/R1 has an expected molecular weight of 9372 Da, F2/R2 has an expected molecular weight of 6770 Da, F1/R2 has an expected molecular weight of 13,632 Da and F2/R3 has an expected molecular weight of 13,075 Da. For this reason during the preparation procedure, protease inhibitors were present, as detailed in the methods section. However, having successfully produced the

F2/R2 recombinant protein that is smaller than F1/R1 this complication is probably not an issue.

There are a number of possibilities; including culture conditions, reading frame and secretion, as to why the F1/R1 recombinant protein was not successfully synthesised. The culture conditions for expression and the host cells for all recombinant proteins were the same, and obviously were adequate for the positive control DHFR, as well as the NC1 fragments F1/R2, F2/R2 and F2/R3. These are examples of things that can be easily altered in the future for the F1/R1 fragment. The coding sequence was ligated in the correct reading frame, as this was checked before recombinant proteins were produced this is not the reason why recombinant protein F1/R1 was not produced.

Another potential problem as far as synthesis of recombinant proteins is concerned; is the stability of the expression construct. During this study this aspect was not explored, all of the bacterial cultures were maintained with 100 µg/ml of ampicillin and 25 µg/ml of kanamycin. Plasmid levels can be checked by plating cells from the expression culture on agar plates with and without ampicillin. Bacteria containing the expression construct will be resistant to ampicillin, if there are only a few or even no colonies on the plate containing ampicillin, this is indicative that there are not many expression construct containing cells in the culture. Ampicillin resistant bacteria produce the enzyme β -lactamase; this in turn rapidly depletes the ampicillin which is an unstable antibiotic in the growing cultures. This allows bacteria without ampicillin resistance and hence the expression construct to grow. The stability of the expression construct could possibly have been different for F1/R1; if this expression construct is unstable then cultures should have been grown in the presence of 200 µg/ml ampicillin.

Freshly transformed bacterial colonies often express recombinant proteins at different levels. Three colonies were selected for all the recombinant proteins; this is a small number of colonies to screen. A better way of screening, in light of the unsuccessful F1/R1 recombinant protein would be to perform a colony-blot procedure. Comparison of the signals produced after colony blotting could identify high-expressing colonies which would significantly aid establishing expression cultures.

Lastly, the F1/R1 recombinant protein contains 29 hydrophobic amino acids which accounts for 34% of the total amino acids. Hydrophobic proteins can be incorporated into membrane

systems of the host cells during protein synthesis, thus having a toxic effect on the cells and ceasing recombinant protein production. However, the hydrophobicity of the other NC1 fragments are not markedly different to F1/R1, ranging from 27 to 33%, therefore this is unlikely to be the cause of problematic F1/R1 production

The recombinant proteins F1/R2, F2/R2 and F2/R3 from the denatured purification eluates were used in interaction analysis with decorin and biglycan, as detailed in the methods section. Unfortunately, no interactions were observed in the solid phase assay between the recombinant proteins and the proteoglycans. Due to the conditions required for purification of the recombinant proteins, it is reasonable to assume that the proteins may have been part of insoluble aggregates known as inclusion bodies. It is well characterised that many eukaryotic gene products expressed intracellularly in *E. coli* that accumulate as insoluble aggregates lack functional activity. Further optimisation of the culture conditions could ensure the expression of soluble functionally active protein, which when purified under native conditions may demonstrate interactions with the proteoglycans in a solid phase assay.

In summary, four recombinant fragments of the NC1 domain have been cloned into the cloning vector pGEM-T, sequence analysis was performed and these fragments were directionally sub-cloned into the expression vector pQE-30. *E. coli* was used as a host to synthesise the recombinant proteins. Three of the four NC1 fragments were purified using metal affinity chromatography from *E. coli* lysates under native and denaturing conditions. They were subsequently used in interaction analysis with decorin and biglycan. No additional information about the interaction of NC1 with decorin and biglycan was generated using these fragments.

Chapter 5: Expression and Localisation of Interacting Components Type X Collagen, Decorin and Biglycan in Hypertrophic Cartilage.

5.1 BACKGROUND

Identification and characterisation of novel interactions in vitro, such as interaction of type X collagen with decorin and biglycan need to be substantiated by other methods which indicate the interaction may have some physiological importance, in vivo. Examples of such methods are expression by the same cell types, localisation of protein to the same region or using chemical cross-linking agents to covalently bridge molecules that are close enough to interact in the tissue.

5.1.1 Confirming Hypertrophic Chondrocyte Expression

During expression studies, RNA isolated from different regions of embryonic chick sternal cartilage was used. The sternum can be easily divided into caudal and cephalic regions, the chondrocyte populations within these regions have been extensively studied and are well characterised (Gibson et al., 1984; LuValle et al., 1992). Type X collagen is expressed by hypertrophic chondrocytes which are only found in the cephalic region of the sternum. Isolation of hypertrophic and non-hypertrophic chondrocyte populations from the sternum is much easier than isolating them from the epiphyseal growth plate due to the size of the tissues involved.

5.1.2 Confirming Localisation of Interacting Components Type X Collagen, Decorin and Biglycan in Epiphyseal Growth Plate Cartilage

The localisation of type X collagen in hypertrophic cartilage of the growth plate has been well studied utilising immunohistochemical methods (Schmid and Linsenmayer, 1985). The precise localisation of decorin and biglycan within the epiphyseal growth plate is however more controversial. Contrasting studies have been reported in species such as bovine and rat (Alini and Roughley, 2001; Takagi et al., 2000), while no studies of decorin and biglycan localisation in the mouse growth plate have been reported.

5.2 MATERIALS AND METHODS

Molecular biology reagents were obtained from Promega (UK) unless otherwise stated. Tissue samples from the caudal and cephalic regions of 17 day embryonic chick sterna were a kind donation from Mr. Wael Al-Amoudi (Cardiff University, UK). Tissue samples from 6 week old C57 black mice were obtained from Dr. Elaine Rees (Cardiff University, UK).

5.2.1 RNA Preparation

5.2.1.1 *Homogenisation of Cartilage in Trizol®*

Embryonic chick sternal cartilage samples; approximately 50 mg wet weight, were snap frozen in liquid nitrogen. Frozen tissue samples were placed in liquid nitrogen cooled dismembrator chambers (B. Braun Biotech International, Germany) with 200 µl Trizol® reagent (Gibco, UK), and the tissue was homogenised for 1.5 minutes at 2000 rpm. The chamber was cooled in liquid nitrogen and a further 200 µl Trizol® reagent was added to the homogenate. The homogenisation step described above was repeated twice. The homogenised tissue was scraped from the chamber into a sterile micro-centrifuge tube containing 600 µl Trizol® reagent. In total 1 ml of Trizol® reagent was used.

5.2.1.2 *Phase Separation*

The homogenised samples were incubated at room temperature for 5 minutes to permit the complete dissociation of nucleoprotein complexes. To the sample in 1 ml of Trizol® reagent, 0.2 volumes (200 µl) of chloroform was added, it was mixed by inverting the tube for 15 seconds, and then samples were incubated at room temperature for 2 minutes. Samples were centrifuged at 12,000 x g for 15 minutes at 4°C. The RNA present in the aqueous phase was then carefully removed from the organic phase and the interphase; and transferred to a fresh tube.

5.2.1.3 *RNA Precipitation, Washing and Re-dissolving*

RNA was precipitated by the addition of an equal volume of isopropanol to the aqueous phase containing the RNA, the sample was briefly vortexed and then incubated at -20°C for 1 hour. The RNA precipitate was obtained by centrifugation at 12,000 x g for 10 minutes at 4°C. The supernatant was removed and the gel-like pellet washed with 75% ethanol, the sample was vortexed briefly and then centrifuged at 7500 x g for 5 minutes at 4°C. The washing and

centrifugation step was repeated once again. The RNA pellet was air dried for 15 minutes and resuspended in 86 µl of RNase-free sterile water.

5.2.1.4 DNase Treatment of Isolated RNA

Contaminating DNA in RNA samples was removed by DNase treatment. To 86 µl of RNA; the following were added: 2 units of RQ1 RNase-free DNase (deoxyribonuclease), 80 units of recombinant RNasin® ribonuclease inhibitor, 10µl of 10x reaction buffer, yielding a final concentration in 100 µl of 40 mM Tris-HCl pH 8, 10 mM MgSO₄ and 10 mM CaCl₂. The samples were vortexed and incubated at 37°C for 15-30 minutes.

5.2.1.5 Re-Extraction of RNA Post-DNase Treatment

The RNA was re-extracted after DNase treatment by the addition of 3 volumes of Trizol® reagent, i.e. 300 µl Trizol® reagent added to 100 µl. The phase separation, precipitation, washing and redissolving was carried out as described in sections 5.2.1.2 & 5.2.1.3. The RNA pellet harvested after re-extraction was dissolved in 50 µl RNase-free sterile water. The concentration of RNA was estimated by analysis on 1% agarose gel with mass molecular weight markers. RNA samples were stored at -80°C.

5.2.2 cDNA Synthesis by Reverse Transcription of RNA (RT-PCR)

For each RNA sample cDNA was generated in a 20 µl reaction by RT-PCR. Approximately 1 µg of total RNA was made up to 11 µl with nuclease-free water, 1 µl of Oligo (dT)15 (500 µg/ml) and 1 µl of 10 mM dNTPs were added to a nuclease free 0.2 ml tube. The mixture was incubated at 65°C for 5 minutes and chilled quickly on ice. 4 µl of the 5x first-strand buffer (250 mM Tris-HCl, pH 8.3, 375 mM KCl, 15m M MgCl₂) (Invitrogen, UK), 2 µl of 0.1 M DTT (Invitrogen, UK) and 1 µl of nuclease free water were added to the tubes and were incubated at 42°C for 2 minutes. 200 units/1 µl of Superscript II (Invitrogen, UK) was added to each tube and was incubated at 42°C for 50 minutes. The reaction was then inactivated by heating to 70°C for 15 minutes. cDNA samples were stored at -20°C until required for PCR reactions.

5.2.3 Primer Design

Decorin and biglycan oligonucleotide primers were designed using the Primer Express programme and were synthesised by MWG (UK). Decorin primers were designed using the chick mRNA sequence (Accession number X63797). Due to there being no sequence data for chick biglycan; the biglycan primers were designed to regions that were homologous across species using the mRNA sequences for mouse, human and rat (Accession numbers NM0007542, NM001711 and NM017087, respectively). Dr. Alvin Kwan provided the primers for type X collagen and the house-keeping gene glyceraldehyde-3-phosphate dehydrogenase (GAPDH) (Accession number AF047874).

| Gene | Primer Sequence & Direction (F – forward & R – reverse) | Annealing Temp (°C) | Product Size (bp) |
|-----------------|--|------------------------|----------------------|
| Type X Collagen | F 5' agc agg agc aaa tca agc | 56 | 379 |
| | R 5' atg gtc tct att cct ctg | | |
| Decorin | F 5' tcc gca tcg cag aca cc | 58 | 493 |
| | R 5' ata caa cca aac ccc gcc t | | |
| Biglycan | F 5' cca aga tcc at gaga agg cc | 58 | 690 |
| | R 5' tca gta acg cag cgg aag g | | |
| GAPDH | F 5' aag gct gag aac ggg aaa ctt g | 57 | 551 |
| | R 5' tca aca aca gag aca ttg ggg g | | |

Table 5.1: Oligonucleotide primer pair sequences used for PCR are shown, along with their annealing temperature and expected product sizes.

5.2.4 Polymerase Chain Reaction (PCR)

PCR was carried out as detailed in section 4.2.1. 1 µl of cDNA generated from the cephalic and caudal regions of 17 day embryonic chick sterna, was used as DNA template for PCR reactions which utilised primers for decorin, biglycan, type X collagen and GAPDH detailed in Table 5.1. PCR products were separated by agarose gel electrophoresis and visualized using ethidium bromide as detailed in section 4.2.1.2.

5.2.4.1 *PCR product Cloning & Sequencing*

PCR products were extracted from the agarose gel, cloned in to the TA cloning vector pGEM-T and sequenced as detailed in sections 4.2.1.3, 4.2.2 & 4.2.2.4, respectively.

5.2.5 Preparation of Tissue for Histology and Immunohistochemistry

5.2.5.1 *Dissection and Preparation of Cryosections*

The knee joint with the femoral and tibial heads intact were dissected from 6 week old C57 black mice. Tissue was snap frozen by immersion into liquid nitrogen. Chucks were cooled in isopentane cooled in liquid nitrogen, and the tissue was mounted on to the chucks using Tissue-Tek (Sakura, Finetek, Netherlands). The mounted tissue and chuck were then immersed into liquid nitrogen. Sections, 10-15 μm , were cut using a cryostat (Bright, UK) and were adhered to poly-lysine coated slides (BDH Laboratory Supplies). The sections were allowed to air-dry before being wrapped and stored at -20°C . Cryosections were brought to room temperature prior to staining.

5.2.5.2 *Dissection, Fixation and Decalcification Prior to Paraffin Wax Sectioning*

The knee joint with the femoral and tibial heads intact were dissected from 6 week old C57 black mice. The tissue was fixed in 10% neutral buffered formal saline (25 mM NaH_2PO_4 , 45 mM Na_2HPO_4 , 155 mM NaCl , pH 7.2, containing 10% (v/v) formaldehyde) for 48 hours at 4°C . The fixative was removed and the tissue was rinsed with dH_2O . The tissue was then decalcified in a 10% (w/v) EDTA solution pH 7.2, over 5 days at 4°C . The decalcifying solution was changed twice during the five days, the tissue was rinsed with dH_2O after decalcification.

5.2.5.3 *Paraffin Wax Sectioning*

Tissue samples were processed on a Leica TP1050 automatic tissue processor using the following schedule: 70% alcohol for 1.5 hr, 90% alcohol for 1.5 hr, 100% alcohol for 2 hr, 100% alcohol for 2 hr, 100% alcohol for 2 hr, xylene for 0.5 hr, xylene for 0.5 hr, paraffin wax for 1.5 hr under vacuum, paraffin wax for 2 hr under vacuum, paraffin wax for 2 hr under vacuum. After processing, the samples were embedded in paraffin wax using a Leica EG1140H Embedding Centre. Sections were cut using a Leica 2040 rotary microtome at a thickness of 8 μm , sections were floated on warm water and mounted on Histobond slides. The sections were dried in an oven at 45°C overnight.

5.2.5.4 *Pre-staining treatment*

Paraffin wax sections were re-hydrated by being taken through a series of solvents: xylene for 2 minutes, xylene for 2 minutes, 100% ethanol for 2 minutes, 100% ethanol for 2 minutes, 95% ethanol for 2 minutes, 70% ethanol for 2 minutes. Sections were then washed in running tap water for 5 minutes before being stained.

5.2.5.5 *Masson's Trichrome Staining*

Cryosections and wax embedded sections were stained with Celestine Blue B for 10 minutes and then rinsed in running water until excess dye was removed. Slides were then stained with Mayers' Haematoxylin for 10 minutes followed by another wash in running water for 10 minutes. Staining with Ponceau acid / Fushin acid followed for a further 5 minutes, before a brief 30 second wash in running water. Slides were immersed in 1% Phosphomolybdic acid for 5 minutes and then transferred directly to light green stain for 2 minutes before being rinsed with running water until excess dye was removed. Slides were washed in 1% acetic acid for 2 minutes and then rinsed in running water for 15 seconds. Finally slides were immersed in 95% alcohol for 1 minute, 100% alcohol for 1 minute, 100% alcohol for a further 2 minutes, xylene for 2 minutes and xylene for a further 2 minutes. Slides were then covered using DPX mountant and coverslips. Slides were observed under a light microscope (Laborlux 12, Leitz) and images were recorded using a digital camera.

5.2.5.6 *Haematoxylin and Eosin Staining*

Cryosections and wax embedded sections were stained with Mayers' Haematoxylin for 1 minute followed by a wash in running water for 5 minutes. Slides were stained in 1% Eosin for 5 minutes and then briefly washed in running water for 20 seconds. Finally slides were immersed in 70% alcohol for 20 seconds, 95% alcohol for 45 seconds, 100% alcohol for 1 minute, 100% alcohol for a further 2 minutes, xylene for 2 minutes and xylene for a further 2 minutes. Slides were then covered using DPX mountant and coverslips. Slides were observed under a light microscope (Laborlux 12, Leitz) and images were recorded using a digital camera.

5.2.6 Immunohistochemistry

5.2.6.1 *Type X Collagen Staining*

Paraffin wax sections were treated with a 100 μ l of 2 mg/ml hyaluronidase in PBS, and incubated at 4°C for 16–24 hours. Sections were washed thoroughly with PBS five times. 2% normal goat serum (Sigma) in PBS was applied to the sections, and incubated for 1 hour at room temperature, all subsequent incubations were carried out at room temperature. Sections were washed thoroughly with PBS five times. Monoclonal antibody MA3 was used to detect type X collagen, this antibody was diluted 1:100 and 1:500 with PBS and incubated for 2 hours. Primary negative control sections were incubated in PBS only for 2 hours. Sections were washed thoroughly with PBS five times. An anti-mouse FITC conjugated antibody raised in goat (Sigma), was used as a secondary antibody, it was diluted 1:64 with PBS and incubated on the sections for 1 hour. Sections were washed thoroughly with PBS five times. Coverslips were mounted onto the slides with Vectashield without probidium iodide. Sections were viewed using a fluorescence microscope (Laborlux 12, Leitz) and images were recorded on a digital camera.

5.2.6.2 *Decorin and Biglycan Staining*

Paraffin wax sections were treated with a 100 μ l of 0.5 Units/ml of Chondroitinase ABC in 0.1 M Tris-acetate, pH 6.5, for 16-24 hours at 4°C. Sections were washed thoroughly with PBS five times. 2% normal goat serum in PBS was applied to the sections, and incubated for 1 hour at room temperature; all subsequent incubations were carried out at room temperature. Sections were washed thoroughly with PBS five times. Polyclonal antibody LF-113 which was raised against murine decorin, was used to detect decorin, and the polyclonal antibody LF-159 which was raised against murine biglycan was used to detect biglycan (polyclonal antibodies were a kind gift from Dr. Larry Fisher, National Institute of Health, NIDCR, CSDB, Bethesda, Maryland). The polyclonal antibodies were diluted 1:100 to 1:300 with PBS, and were incubated on the sections for 2 hours. Primary negative control sections were incubated in PBS only for 2 hours. Sections were washed thoroughly with PBS five times. An anti-rabbit FITC conjugated antibody raised in goat (Sigma), was used as a secondary it was diluted 1:160 with PBS and incubated on the sections for 1 hour. Sections were washed thoroughly with PBS five times. Coverslips were mounted onto the slides with Vectashield.

Sections were viewed using a fluorescence microscope (Laborlux 12, Leitz) and images were recorded on a digital camera.

5.3 RESULTS

5.3.1 Generation of cDNA for PCR Analysis

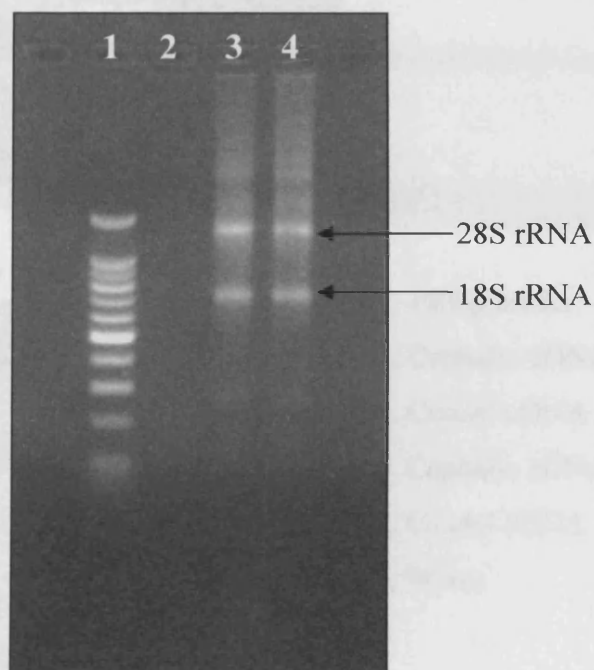
The caudal and cephalic regions of 17 day embryonic chick sternae were used as a tissue source of non-hypertrophic and hypertrophic cells, respectively. The RNA was isolated from the cells in these tissues using Trizol reagent, the integrity of the RNA was assessed by agarose gel electrophoresis. The RNA prepared, figure 5.1 is of good quality with minimal degradation, 28S and 18S rRNA bands are visible and are highlighted. The RNA was subsequently used in a RT reaction as described in the methods section to generate caudal and cephalic cDNA. As controls RT-PCR reactions were carried out as described except the reverse transcriptase enzyme was omitted and substituted with water. This is referred to as the No RT control.

5.3.2 Type X Collagen and Decorin are Expressed by Hypertrophic Chondrocytes

The cDNA generated was used in PCR reactions with primers designed to GAPDH, type X collagen, decorin and biglycan. Products from PCR reactions were run on 1% agarose gels and the results are shown in figure 5.2 a-c. GAPDH expression is seen in cDNA generated from both cephalic and caudal RNA, as is decorin (figure 5.2 a & b, lanes 2 & 3). Type X collagen expression however is found only in the cDNA generated from the cephalic region of the sternum, the region that contains hypertrophic chondrocytes (figure 5.2 c, lane 2). All controls were negative, demonstrating the specificity of the PCR amplification. This confirms that type X collagen and decorin are co-expressed by the same cell type, namely hypertrophic chondrocytes.

The PCR products were cloned into pGEM-T, the vector was used to transform competent E. Coli JM109 cells. Following overnight incubation on selective agar plates, colour screening was used to determine transformed colonies. Using Promega's Wizard mini-prep kit; plasmid DNA was prepared from a 5ml liquid culture which had been inoculated with a transformed colony. Sequence analysis of the plasmid DNA allowed identification of the PCR products. The PCR product sequences were analysed using the NCBI Blast search engine. The PCR product generated using the type X collagen primers was found to be 100% homologous to the chick type X collagen gene sequence (gi:211699) present in the EMBL database, figure

5.3. While the product generated with the decorin primers was 100% homologous to the mRNA sequence for chicken decorin (Accession number: X63797.1), figure 5.4.



1. 100bp ladder
2. -
3. Caudal RNA
4. Cephalic RNA

Figure 5.1: RNA samples isolated from the caudal (lane 3) and cephalic (lane 4) regions of embryonic chick sternae run on a 1% agarose gel containing ethidium bromide.

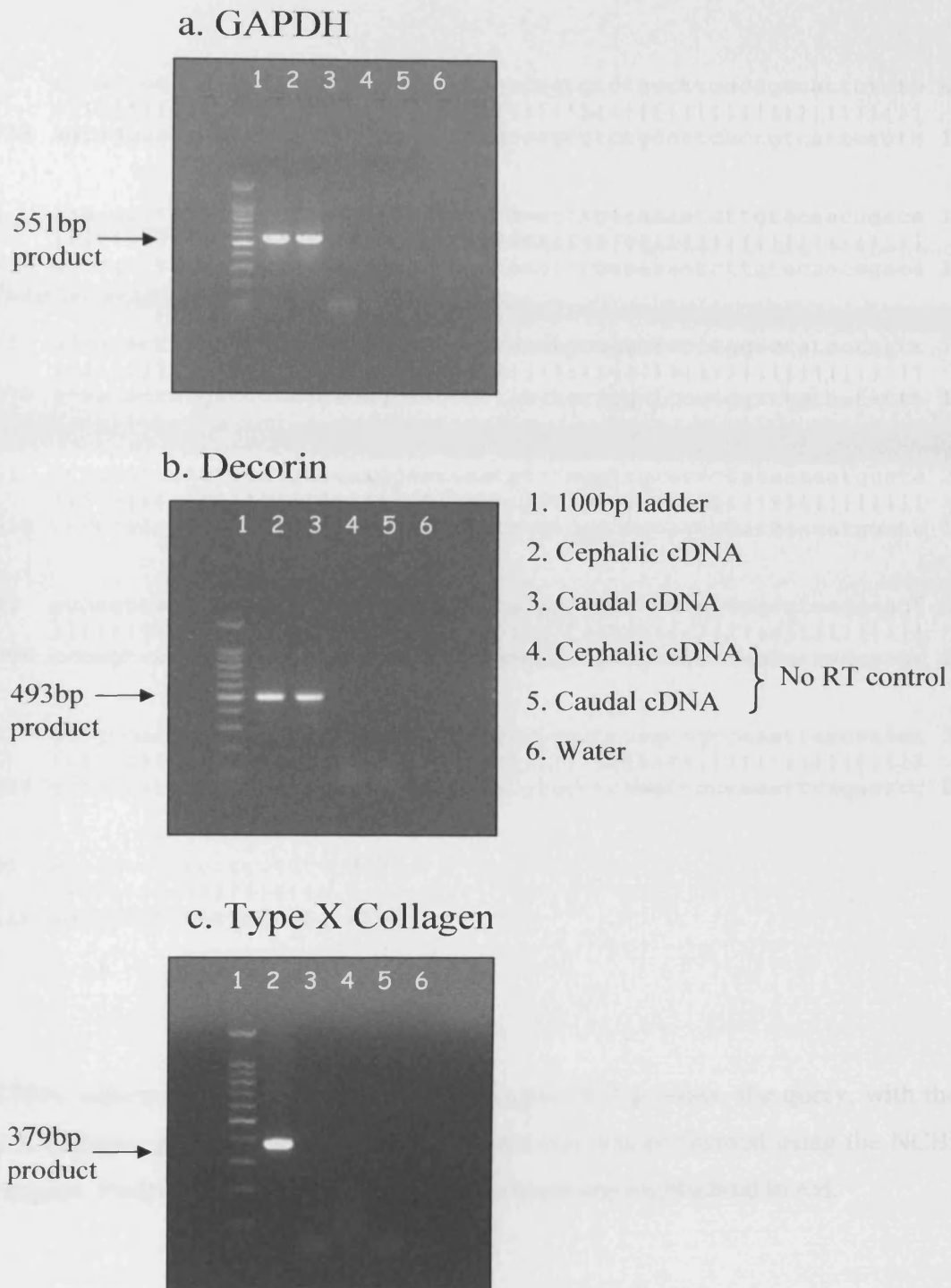


Figure 5.2: PCR products run on an ethidium bromide containing 1% agarose gel.

(a) GAPDH expression in both cephalic and caudal regions.

(b) Decorin expression in both cephalic and caudal regions.

(c) Type X collagen expressed in cephalic region only.

```

Query: 1      agcaggagcaaataaagctctcacaggaatgccagtgtctgccttcactgtcattctctc 60
            |||
Sbjct: 1758   agcaggagcaaataaagctctcacaggaatgccagtgtctgccttcactgtcattctctc 1817

Query: 61      aaaagcctaccctggggcaacagtcctcatcaaatttgacaaaatcttgataacagaca 120
            |||
Sbjct: 1818   aaaagcctaccctggggcaacagtcctcatcaaatttgacaaaatcttgataacagaca 1877

Query: 121     gcaacactatgaccccaggacaggaatctttacctgcaggatccctgggtctatactatct 180
            |||
Sbjct: 1878   gcaacactatgaccccaggacaggaatctttacctgcaggatccctgggtctatactatct 1937

Query: 181     ctctatcatgtacatgcaaaaggaacaaatgtttgggtgcactctataaaaatggctc 240
            |||
Sbjct: 1938   ctctatcatgtacatgcaaaaggaacaaatgtttgggtgcactctataaaaatggctc 1997

Query: 241     ccagtcatgtacacttatgatgaataccagaaaggataccttgaccagcctcaggcagt 300
            |||
Sbjct: 1998   ccagtcatgtacacttatgatgaataccagaaaggataccttgaccagcctcaggcagt 2057

Query: 301     gctgtcattgatctcatggagaacgatcaagtgtggctccagctgccaattcagaatcc 360
            |||
Sbjct: 2058   gctgtcattgatctcatggagaacgatcaagtgtggctccagctgccaattcagaatcc 2117

Query: 361     aatggctctctattcctctg 379
            |||
Sbjct: 2118   aatggctctctattcctctg 2136

```

Figure 5.3: 100% sequence identity of the type X collagen PCR product, the query, with the chicken type X collagen gene, the subject, sequence analysis was performed using the NCBI Blast search engine. Positions of forward and reverse primers are highlighted in red.

```

Query: 1      tccgcatcgagacaccaacattactagcatccctaaagggtcttctccatcccttactg 60
             |||
Sbjct: 743    tccgcatcgagacaccaacattactagcatccctaaagggtcttctccatcccttactg 802

Query: 61     agcttcaccttgatggcaacaaaattagcaaaattgatgcggaagggtctgtctggactca 120
             |||
Sbjct: 803    agcttcaccttgatggcaacaaaattagcaaaattgatgcggaagggtctgtctggactca 862

Query: 121     ccaacttggctaaaattgggtctcagcttcaacagtatttcttctgttgaaaatggctctc 180
             |||
Sbjct: 863    ccaacttggctaaaattgggtctcagcttcaacagtatttcttctgttgaaaatggctctc 922

Query: 181     tgaacaatgtacctcatctgagagaacttcatctgaataacaacgaacttgtcagagtac 240
             |||
Sbjct: 923     tgaacaatgtacctcatctgagagaacttcatctgaataacaacgaacttgtcagagtac 982

Query: 241     ctagtgggttgggtgaacacaaatacatccaggtgggtctatcttcataacaacaagattg 300
             |||
Sbjct: 983     ctagtgggttgggtgaacacaaatacatccaggtgggtctatcttcataacaacaagattg 1042

Query: 301     cttcaattggtatcaacgacttttgcctcttgggtacaacacacaaaaaggcaacctatt 360
             |||
Sbjct: 1043    cttcaattggtatcaacgacttttgcctcttgggtacaacacacaaaaaggcaacctatt 1102

Query: 361     ctggtgtgagtctcttcagcaaccccggtgcagtactgggaaatccagccctctgctttcc 420
             |||
Sbjct: 1103    ctggtgtgagtctcttcagcaaccccggtgcagtactgggaaatccagccctctgctttcc 1162

Query: 421     gatgtatccatgaacgctctgcagtacagatcggaattacaaatagatttctaaaggcg 480
             |||
Sbjct: 1163    gatgtatccatgaacgctctgcagtacagatcggaattacaaatagatttctaaaggcg 1222

Query: 481     gggtttggttgat 494
             |||
Sbjct: 1223    gggtttggttgat 1236

```

Figure 5.4: 100% sequence identity of the decorin PCR product, the query, with the chicken decorin mRNA sequence, the subject, analysis was performed using the NCBI Blast search engine. Positions of forward and reverse primers are highlighted in red.

5.3.3 Expression of Biglycan by Hypertrophic Chondrocytes Not Confirmed

Using primers designed to homologous regions in the human, mouse and rat biglycan sequences, numerous PCR products were generated using the chick cDNA as template. Despite numerous successful cloning attempts, the products were not identified as biglycan by sequence analysis. Therefore, expression of biglycan by chick hypertrophic chondrocytes was not confirmed.

5.3.4 Cellular Morphology of the Growth Plate

Using histological staining of cryosections and wax sections of 6 week old mouse tibia, the cellular morphology of the growth plate was studied. H & E staining was used to demonstrate cellular morphology, it is designed to show basophilic structures such as nucleic acids in the nucleus blue, black or purple and acidophilic structures such as the more basic proteins within cells and in the extracellular matrix shades of pink and red. Masson's Trichrome Stain was used to distinguish cellular from extracellular components, collagen fibres stain an intense green while the nuclei stain blue or black.

The epiphyseal growth plate is highly cellular with little inter-territorial matrix. Figure 5.5 shows a 6 week mouse tibia cryosection stained with H & E, the different zones of the growth plate are highlighted; which reflect the differentiation state of the chondrocytes within them. The smallest chondrocytes are observed in the resting zone, the proliferating chondrocytes appear slightly flattened and are arranged in columns, the hypertrophic chondrocytes increased volume is evident as is the paucity of the ECM in the hypertrophic zone when compared to the other zones.

The general morphology of the growth plate described above is also evident in the wax sections of 6 week old mouse growth plate which are stained with Masson's trichrome, figure 5.6 a & b. The intensity of the green stain on the sections decreases as the ECM surrounding the chondrocytes becomes less abundant from the resting zone through to the hypertrophic zone. For comparison the articular cartilage of the 6 week old mouse is also shown, figure 5.6 c. The intensity of the green stain in the ECM of the articular cartilage highlights the cellularity of the growth plate as well as the less abundant ECM.

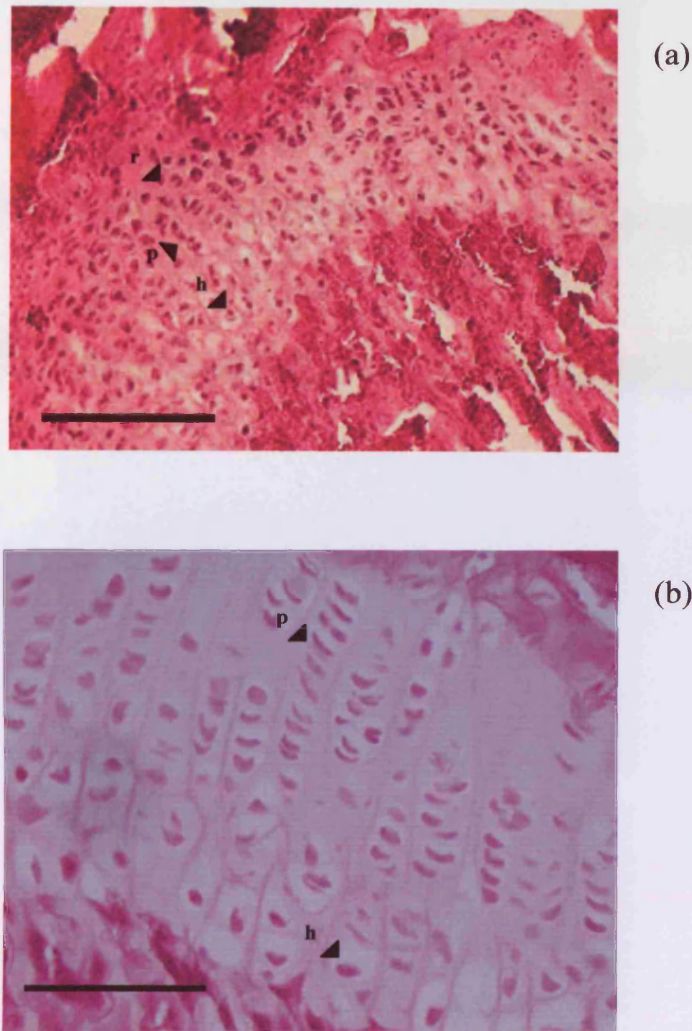


Figure 5.5: Six week old mouse tibia unfixed and decalcified 15 μ m cryosections stained with H & E. Bar = 100 μ m.

(a) Chondrocytes of the epiphyseal growth plate at different stages of differentiation are highlighted within their respective zones, (**r**) resting chondrocytes, (**p**) proliferating chondrocytes, (**h**) hypertrophic chondrocytes.

(b) Growth plate image at higher magnification.

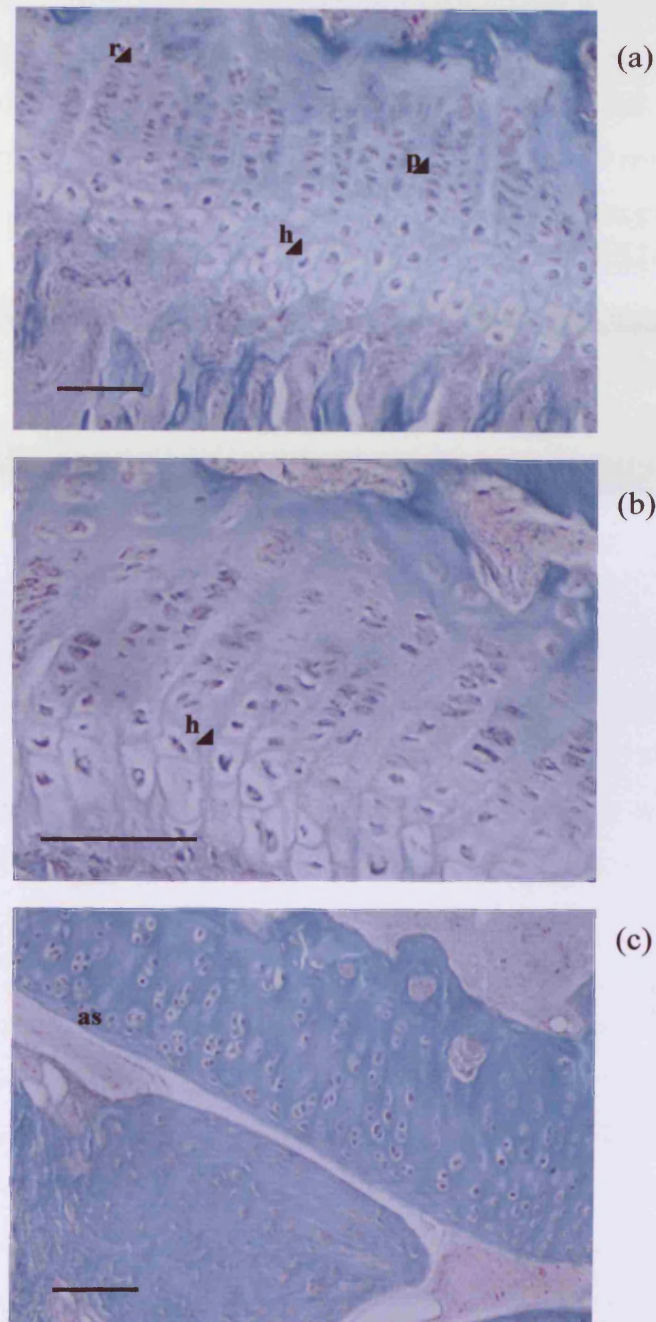


Figure 5.6: Histological staining with Masson's Trichrome of 10µm wax sections of 6 week old mouse fixed and decalcified tibia. Bar = 100µm

- (a) Chondrocytes of the epiphyseal growth plate at different stages of differentiation are highlighted within their respective zones, (r) resting chondrocytes, (p) proliferating chondrocytes, (h) hypertrophic chondrocytes.
- (b) Growth plate image at higher magnification.
- (c) Articular cartilage, (as) articular surface.

5.3.5 Localisation of Type X Collagen in the Hypertrophic Zone of the Growth Plate

The monoclonal antibody MA3 was used in immunohistological analyses of the 6 week old mouse knee joint. Type X collagen staining can be seen in the hypertrophic zone of the growth plate and in cartilaginous remnants at the ossification front, figure 5.7 a. White arrowheads indicate type X collagen staining, lack of staining in the resting and proliferating zones is also highlighted. Higher magnification images of the hypertrophic zone figures 5.7 b & c, reveal intense extracellular staining of type X collagen surrounding the hypertrophic chondrocytes and in cartilaginous remnants at the ossification front. Type X collagen staining was not observed in the other zones of the growth plate. The primary negative control sections; figure 5.7 d & e, are diffusely stained by the secondary FITC conjugated antibody. The staining appears to be cellular rather than in the extracellular matrix.

5.3.6 Localisation of Type X Collagen in Articular Cartilage

Type X collagen staining can be seen around chondrocytes in the articular cartilage, figure 5.8 a. The staining is not as intense as the staining seen in the hypertrophic zone of the growth plate, but is markedly different when compared to the primary negative control. The pericellular staining in the articular cartilage is highlighted with white arrowheads and appears to be specific for chondrocytes in the deep zone, figure 5.8 b.

5.3.7 Localisation of Decorin and Biglycan in the Growth Plate

The localisation of decorin and biglycan within the tibial growth plates of 6 week old mice were studied using the polyclonal antibodies LF-113 and LF-159, respectively. Diffuse decorin staining can be seen around the chondrocytes of the proliferating and hypertrophic zones, figure 5.9 a. Biglycan staining can be seen around resting and hypertrophic chondrocytes; as well as in the cartilaginous remnants of the ossification front, figure 5.10 a & b. The biglycan staining appears more intense and less diffuse than the decorin staining. The staining of sections incubated with the LF-113 and LF-159 is markedly different to the background cellular fluorescence seen in the primary negative control sections, figure 5.9 b and 5.10 c.

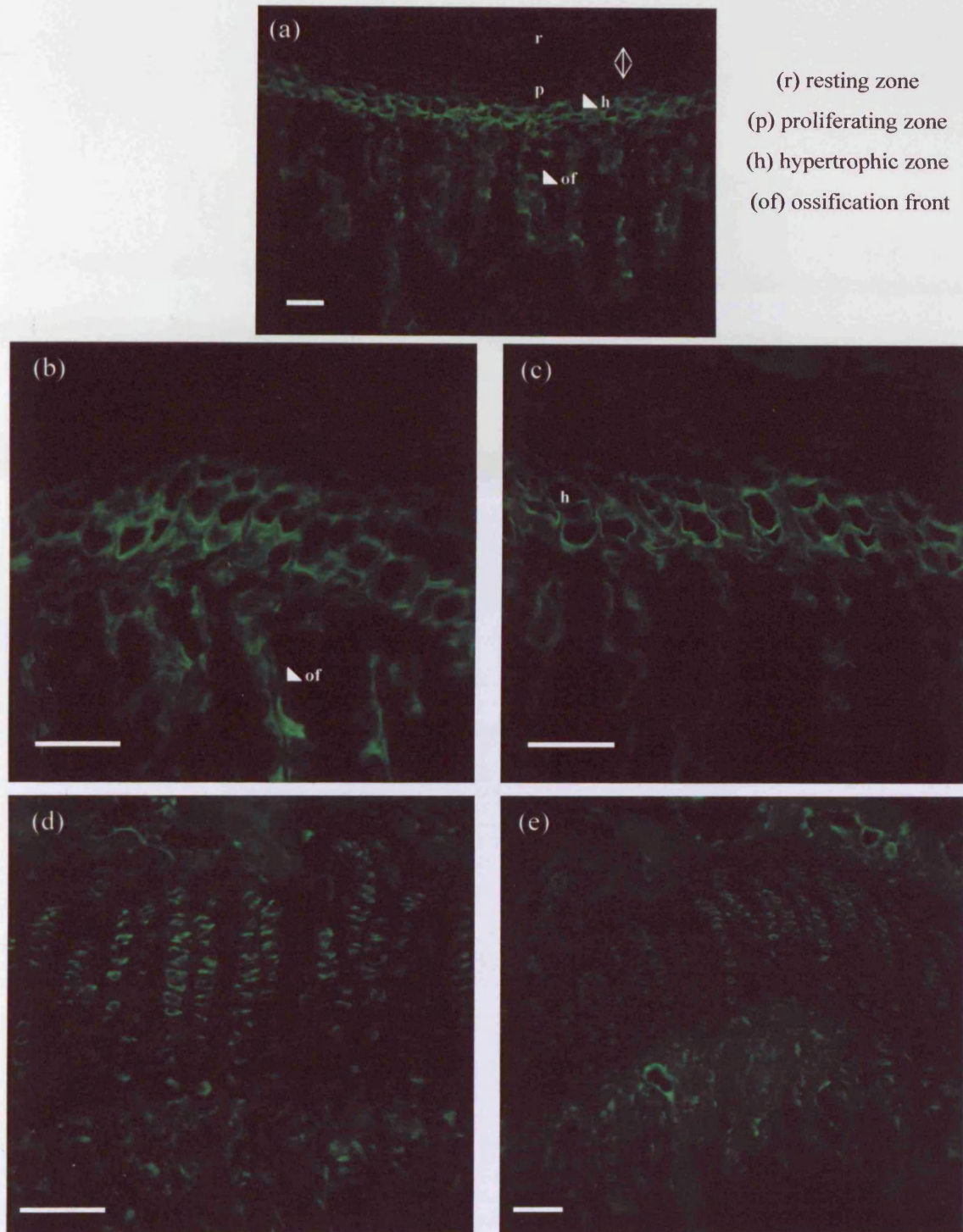


Figure 5.7: Immunolocalisation of type X collagen in the tibial growth plate of 6 week old C57 black mice. Tissue was fixed, decalcified, wax embedded and 10 μ m sections cut. Bar = 50 μ m.

(a) Staining of the hypertrophic zone and the ossification front.

(b) & (c) Higher magnification images of staining in the hypertrophic zone.

(d) & (e) Two different magnifications of the primary negative control sections, no staining is visible in the extracellular matrix.

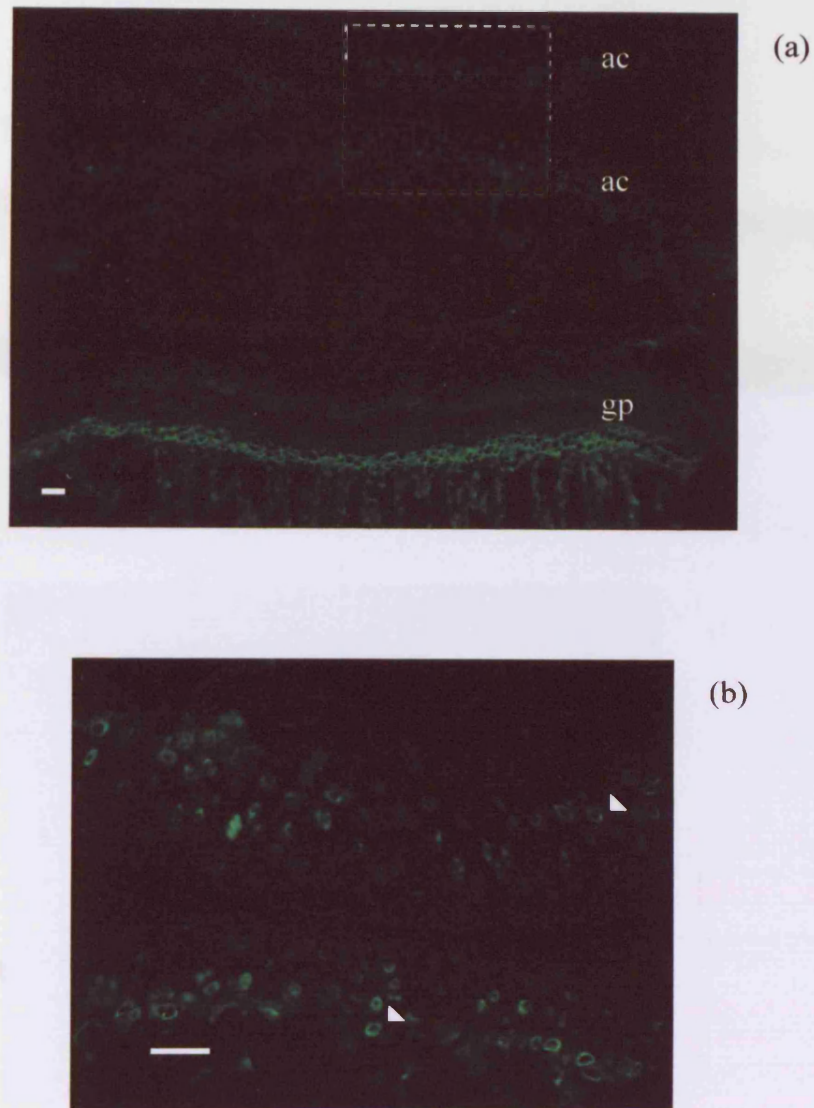


Figure 5.8: Immunolocalisation of type X collagen in the knee joint of 6 week old C57 black mice. Tissue was fixed, decalcified, wax embedded and 10 μ m sections cut. Bar = 50 μ m.

- (a) Type X collagen staining in the growth plate (gp) and in articular cartilage (ac).
- (b) Higher magnification image of the articular surface, with pericellular type X collagen staining.

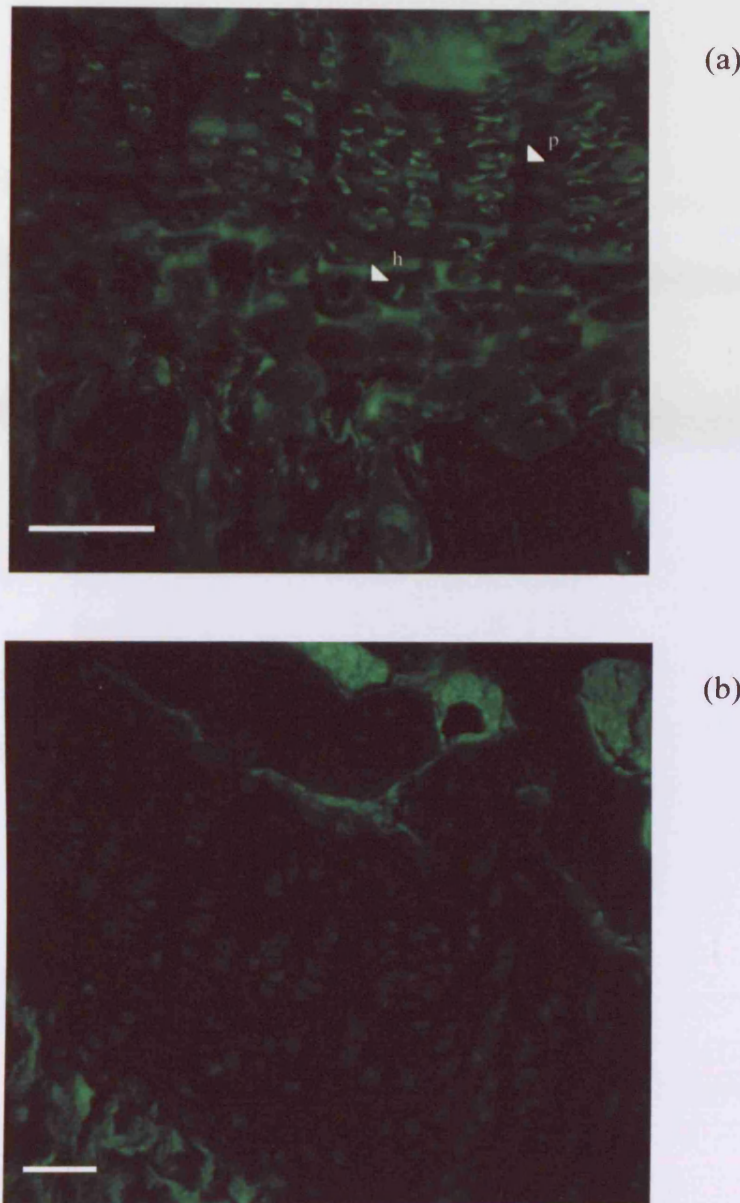


Figure 5.9: Immunolocalisation of decorin in the growth plate of 6 week old C57 black mice. Tissue was fixed, decalcified, wax embedded and 10 μ m sections cut. Bar = 50 μ m.

- (a) Diffuse pericellular staining around chondrocytes in the proliferating (p) and hypertrophic (h) zones.
- (b) Negative control section showing no staining in the matrix of the growth plate.

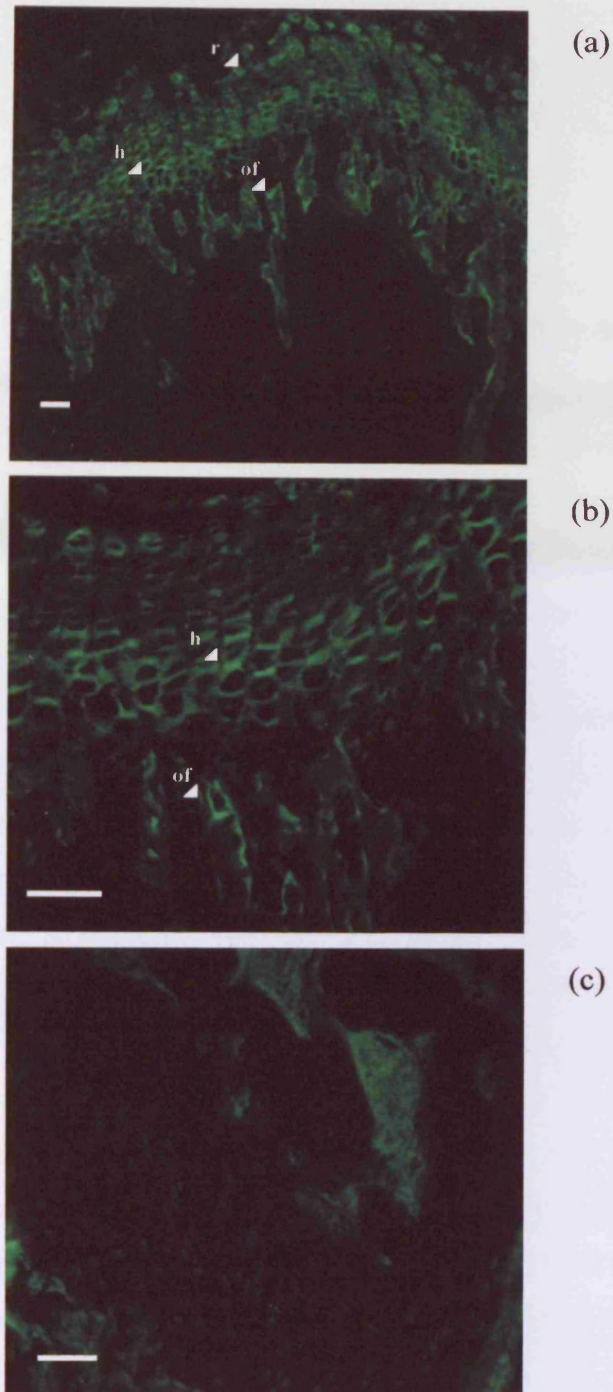


Figure 5.10: Immunolocalisation of biglycan in the growth plate of 6 week old C57 black mice. Tissue was fixed, decalcified, wax embedded and 10µm sections cut. Bar = 50µm.

- (a) Pericellular staining around resting (r) chondrocytes, staining in the hypertrophic (h) zone and in the cartilaginous remnants of the ossification front (of).
- (b) Higher magnification image of the hypertrophic zone and ossification front staining.
- (c) Negative control section showing no staining in the matrix of the growth plate.

5.4 DISCUSSION

Expression studies were carried out to determine whether decorin and biglycan were expressed by the same cell type as type X collagen, namely hypertrophic chondrocytes. mRNA was purified from the cephalic and caudal regions of 17 day embryonic chick sterna, and was subsequently used to generate cDNA. Hypertrophic chondrocytes are found in the cephalic region of the sternum but not in the caudal region. Using primers designed against the chick sequence for type X collagen and decorin, PCR products of the expected sizes were produced (see table 5.1 & figure 5.2). These PCR products were purified and ligated into the cloning vector pGEM-T, sequence analysis of the plasmid DNA confirmed the identification of the products. It was therefore concluded that decorin is expressed by hypertrophic chondrocytes. Type X collagen would have an opportunity to interact with decorin in the ECM after synthesis and export out of the hypertrophic chondrocytes.

Expression of biglycan by hypertrophic chondrocytes was not demonstrated using the primers designed against the human, mouse and rat biglycan sequences. There are a number of possible reasons as to why the biglycan expression study was not successful. Biglycan may not be expressed by hypertrophic chondrocytes; this does not exclude / disprove interactions occurring between type X collagen and biglycan in the ECM surrounding hypertrophic chondrocytes, as there have been reports of molecules diffusing through the ECM to locations remote from their site of synthesis (Polgar et al., 2003). A likely cause of the unsuccessful PCR is primer design; differences of a few base pairs in the chick sequence at the site where the primers anneal would affect the PCR reaction. The chicken genome has since been sequenced and the primers used during this study have been analysed against the database. No matches with significant similarity were found when the biglycan primers sequences were Blasted against chicken specific sequences in the Blast chicken genome.

During histological analyses both cryosections and decalcified wax sections of 6 week old mouse tibiae were used. Initially it was thought that unfixed calcified cryosections would yield good histological results and would be preferable for the immunohistochemical analyses. However sectioning proved difficult, often only part of the section would adhere to the slide despite using a variety of coated slides including poly-lysine and APES. It was almost always the calcified bony regions of the section that did not adhere to the slide; during washing procedures this region would cause the detachment of all or part of the section from

the slide resulting in a fragmented section. For this reason wax sections of decalcified bone were used as an alternative.

Histological staining using Masson's Trichrome and Haematoxylin & Eosin revealed the cellular nature of the tibial epiphyseal growth plate. Comparisons were made between the abundant ECM found surrounding chondrocytes of articular cartilage and the sparse ECM surrounding chondrocytes of the growth plate. The morphology of the small flattened chondrocytes of the resting zone, the columnar arrangement of the chondrocytes in the proliferating zone and the increased volume of the hypertrophic chondrocytes in the hypertrophic zone was well demonstrated. Analysis of the sections which had been histologically stained assisted in the orientation and interpretation of the immunohistochemistry which followed. Analysis of the mineralisation status of the sections of 6 week old mouse epiphyseal plates was desirable, but was not performed because the sections were decalcified. Previous studies in the growth plates of Wistar rats have shown the presence of mineralized chondrocytes ghosts, which were demonstrated to contain biglycan by immunohistochemistry (Takagi et al., 2000).

Immunohistochemistry showed that type X collagen co-localised with decorin and biglycan in the epiphyseal growth plate of 6 week old mouse tibiae. This indicates that the interactions of type X collagen with decorin and biglycan demonstrated in vitro may be functionally significant in vivo. Localisation to the same region of the growth plate indicates that the molecules are in the correct vicinity to interact. However, immunohistochemistry at the light microscope level does not provide any information regarding the exact proximity of the molecules. Electron microscopy studies using antibodies and gold labels would offer higher resolution, and would provide more detailed information regarding the proximity of interacting molecules. The differences in the intensity and diffuse nature of staining by the type X collagen, decorin and biglycan antibodies may be due to different affinities for their binding epitopes in fixed wax sections. Immunohistochemistry using unfixed cryosections would complement the data generated with the fixed wax sections.

In summary, RT-PCR analysis was used to demonstrate that type X collagen and decorin are co-expressed by hypertrophic chondrocytes, derived from the sternum of 17-day-old embryonic chicks. Analysis of biglycan expression by hypertrophic chondrocytes was inconclusive due to the lack of biglycan primers designed against the chick sequence.

Immunohistochemistry was performed using antibodies raised against type X collagen, decorin and biglycan on paraffin wax sections of the knee joint of 6 week old C57 black mice. Type X collagen, decorin and biglycan were demonstrated to co-localise in the hypertrophic cartilage matrix.

Chapter 6: General Discussion

6.1 Background

Type X collagen is produced by hypertrophic chondrocytes of the epiphyseal growth plate and has been proposed to be important for endochondral ossification (EO). A precise functional role for type X collagen has not been defined although a number of potential roles have been suggested (Shen, 2005). These include:

- * being involved in regulating the calcification process during EO
- * providing support as the cartilage matrix is degraded during EO
- * providing an easily resorbed matrix for the deposition of bone matrix during EO.

Decorin and biglycan have been demonstrated to be important for collagen biology. They have been linked to the mineralisation process; interact with numerous collagen types, non-collagenous proteins and growth factors. This led to the hypothesis that type X collagen interacts with decorin and biglycan in the hypertrophic cartilage extracellular matrix. The aim of this study was to characterise these molecular interactions.

6.2 Summary of Findings

Interactions of type X collagen with decorin and biglycan have been studied *in vitro* using material from a variety of sources. Type X collagen was purified from culture medium of hypertrophic chondrocytes which were derived from the tibial epiphyseal growth plates of 17 day old embryonic chicks. The culture medium was subjected to ammonium sulphate precipitation and differential salt fractionation, which allowed type X collagen to be isolated from the other proteins and collagen types synthesised by cultured hypertrophic chondrocytes. This procedure for preparation of type X collagen is well established (Barber and Kwan, 1996). Human recombinant decorin produced in a human cell line and bovine cartilage biglycan were obtained from commercial sources for use in the *in vitro* studies.

A solid phase microtitre plate assay was developed to study the interactions of type X collagen with decorin and biglycan. Optimisation of conditions such as antibody dilutions, incubation times and temperatures were performed. Decorin and biglycan were used to coat wells and type X collagen was applied as a ligand. The assay utilised a monoclonal antibody, MA3, which recognises a triple helical epitope on type X collagen, a HRP conjugated secondary antibody and the chromogenic substrate o-phenylenediamine. Binding saturation

was reached in decorin and biglycan coated wells when type X collagen reached a concentration of around 5 μ g/ml. Competitive inhibition experiments have demonstrated that type X collagen probably has a common site of interaction for decorin and biglycan. Assays which were performed with pepsinised type X collagen indicated that the triple helical region of type X collagen was not involved in the interaction with decorin and biglycan, and the interactions were therefore likely to be mediated by the NC domains. Solid phase assays are a popular in vitro method for studying protein-protein interactions, many ECM proteins have been studied in this way, examples include collagens, fibronectin, COMP, decorin and biglycan (Di Cesare et al., 2002; Holden et al., 2001; Rosenberg et al., 1998).

The interaction of type X collagen with decorin and biglycan was shown to be of high affinity using SPR. Equilibrium constants were calculated and were in the nanomolar range. The hypothesis that the interaction is probably mediated via the NC domains was also studied using SPR. Interactions of whole type X collagen and the NC1 domain with the proteoglycans produced similar results indicating that the interaction was probably mediated via the NC1 domain. This was further confirmed, when the sensor chip with immobilised pepsinised type X collagen was used in experiments with decorin and biglycan and produced no interaction. Using decorin and biglycan as analytes before and after deglycosylation, over the type X collagen chip surface produced similar results. This indicates that the interactions of type X collagen with decorin and biglycan involve the core protein and are independent of the presence or absence of the GAG chain(s).

SPR has become one of the most predominant methods for studying in vitro interactions. The kinetic data that can be generated offers advantages over other in vitro interaction analysis methods and can be very informative. However, there are limitations with studying interactions of isolated molecules. This is especially true when these molecules are normally found in a complex three dimensional matrix. The method does not resemble the physiological environment of the molecules. Despite these drawbacks SPR has been widely used for studying interactions of ECM proteins, examples include interactions of type IX collagen with COMP (Holden et al., 2001) and interactions of decorin and biglycan with type VI collagen (Wiberg et al., 2001).

Following the identification of the involvement of NC1 in the interactions with decorin and biglycan, further characterisation of the region of the NC1 domain involved was required. The

crystal structure of the NC1 domain has been resolved (Bogin et al., 2002), details of the amino acid residues on the surface of the domain and potential residues that could be involved in interactions have been identified. Recombinant fragments of the NC1 domain were cloned into an expression vector and were produced in *E. Coli*. Recombinant proteins with a 6xHis-tag were purified from other bacterial proteins using a nickel chelate column and were subsequently used in interaction analysis. Due to reasons discussed in Chapter 4, the attempt at further determining more specifically the region of the NC1 domain involved in interactions with decorin or biglycan were at present unsuccessful. Differences in folding of small fragments of the NC1 domain compared with folding of the whole domain could be a perceived problem. Previous studies however, using regions of ECM proteins such as the collagen binding domain of fibronectin have been produced in *E. Coli* and have been used successfully in interaction analysis with a variety of collagen types, including type X collagen (Steffensen et al., 2002). This indicated that post-translational folding of recombinant proteins in *E. Coli* does not have to be a complication.

Preliminary studies using decorin and biglycan labelled gold particles and type X collagen in negative staining experiments have been encouraging. They have provided limited morphological evidence of the interactions of type X collagen with decorin and biglycan. The positioning of the gold particles appear to be at the end of the type X collagen molecules, however due to aggregation and to the condensed nature of the molecules on the electron micrographs they have proved difficult to interpret. Further optimisation of the method for the negative staining of type X collagen and decorin and biglycan labelled gold particles is required. Negative staining utilising gold labelled particles has been widely used previously to identify domains of ECM proteins involved in interactions, examples include decorin and biglycan labelled gold particles with type VI collagen (Wiberg et al., 2001; Wiberg et al., 2002).

To substantiate data gained from interaction studies, expression and localisation studies have been carried out. The co-expression of decorin and type X collagen by hypertrophic chondrocytes has been demonstrated using RT-PCR analysis. Due to the lack of chick biglycan sequence, primers for biglycan were designed to regions of sequence that are homologous across mouse, rat and human. Despite this the cloning and sequence analysis of PCR products generated using the biglycan primers proved not to be biglycan.

Immunohistochemical analysis of 6 week old C57 black mice growth plates revealed that type X collagen co-localises with decorin and biglycan in the hypertrophic cartilage ECM. Staining for decorin and biglycan appeared more diffuse than that of type X collagen; this may be due to differences in the antibody affinities for their epitopes in paraffin wax sections. Expression and co-localisation studies suggest that interactions of type X collagen with decorin and biglycan may have some physiological relevance and could be occurring *in vivo*. Previous studies of the expression of decorin and biglycan message by cells of the epiphyseal growth plate and their localisation to the ECM of the growth plate have demonstrated variable results. A study of the formation of bone in the rat mandible found expression of decorin and biglycan at the gene and protein level by newly differentiated osteoblasts before the onset of matrix mineralisation and concluded that they could play a role in the earliest stages of bone formation (Kamiya et al., 2001). Decorin and biglycan have been localised in bovine growth plates but their abundance in the hypertrophic zone was minimal (Alini and Roughley, 2001), in contrast biglycan was found in the hypertrophic zone of developing epiphyseal cartilage of Wistar rats (Takagi et al., 2000).

6.3 Proposed Biological Significance of the Identified Interactions

6.3.1 Involvement in Endochondral Ossification

Molecular interactions that contribute to the molecular assembly of the matrix in the growth plate are fundamental to its functions. Molecules form a macromolecular complex, and do not act in isolation, the structure and function is dependent on the matrix as a whole. The interaction between type X collagen and other matrix components, such as the small leucine rich proteoglycans, decorin and biglycan, may have a role in matrix assembly or maintaining the integrity and mechanical stability of the matrix in the hypertrophic region of the growth plate.

A number of different roles have been postulated for the interaction of type X collagen with decorin and biglycan in the growth plate (figure 6.1). Type X collagen has been shown to form a hexagonal lattice *in vitro* (Kwan et al., 1991), lattice formation is mediated via interactions of the NC1 domain. Whether this lattice like structure occurs *in vivo* is unclear. Interactions of type X collagen with decorin or biglycan could potentially organise the assembly of this lattice or any other supramolecular assembly of type X collagen. Binding of the proteoglycans could regulate the assembly or final dimensions of the type X collagen

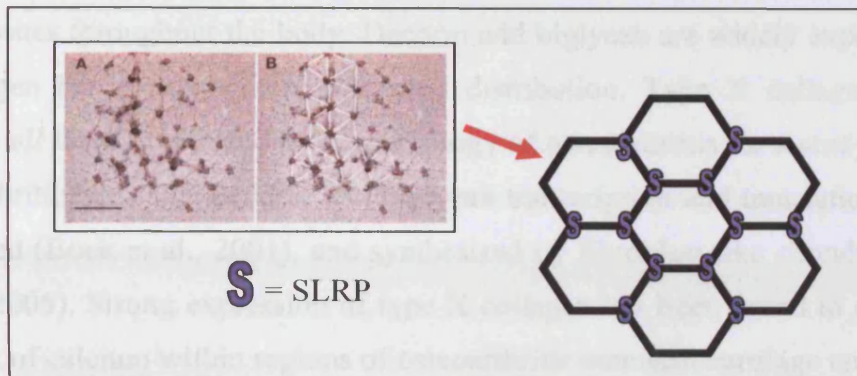
pericellular lattice in hypertrophic cartilage (figure 6.1a). Decorin and biglycan are known to regulate the fibril diameter of fibrillar collagens (Scott and Orford, 1981) and have been shown to organise collagen VI into hexagonal-like networks (Wiberg et al., 2002). Their importance in collagen biology has been demonstrated by the abnormal ultrastructural effects of fibrillar collagens seen in transgenic mice lacking decorin and biglycan. The effect of abnormal ultrastructure is enhanced in mice that are deficient in both proteoglycans. The shorter limbs that double deficient animals have (Corsi et al., 2002) suggests that decorin and biglycan may have roles in the growth plate, possibly in regulating some of the processes involved in EO, however this has not been investigated and is speculative. Changes in the ECM architecture of epiphyseal cartilage in these animals may alter the mechanical stability of the growth plate and could lead to abnormal long bone formation and shortened limbs.

The interactions may serve purely a structural role; proteoglycans may act as a bridge between type X collagen in the hypertrophic zone of the growth plate; and the fibrillar collagens in the proliferative zone, or the fibrillar collagens being turned over in the hypertrophic region (figure 6.1b). Such structural interactions will be important for maintaining the stability of the matrix during a dynamic remodelling period. Type X collagen has been linked to the compartmentalisation of matrix components to the hypertrophic zone of growth cartilage, providing the proper environment for mineralisation and remodeling (Kwan et al., 1997). The identified interactions with decorin and biglycan would be consistent with a role in compartmentalisation. Type X collagen may bind to and retain these molecules in the hypertrophic zone promoting the mineralisation process. Biglycan has been linked with growth plate mineralisation after being found in clusters of hydroxyapatite (HAP) crystals or in the crystal ghosts within the ossifying region of the epiphyseal plates of Wistar rats (Takagi et al., 2000). While both decorin and biglycan have been demonstrated to be able to bind to HAP (Sugars et al., 2003).

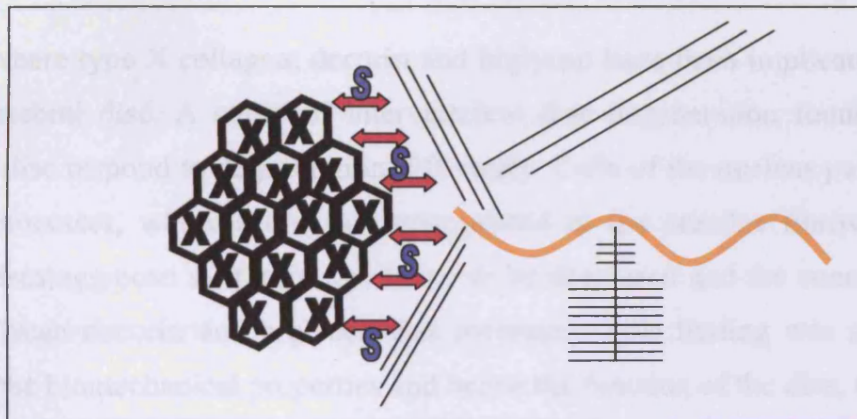
The interaction between type X collagen and the proteoglycans may have important implications in the process of endochondral ossification, possibly via the actions of TGF- β (figure 6.1c). The proteoglycans are known to bind to the growth factor TGF- β , their ability to bind to this growth factor and to type X collagen may lead to the formation of a reservoir of this growth factor, specifically held within the hypertrophic zone of the epiphyseal growth plate. Breakdown of the hypertrophic matrix, containing type X collagen bound to decorin

or/and biglycan, may cause the release of TGF- β , thus allowing it to act on components present in the hypertrophic region of the growth plate and on invading cells such as osteoblasts at the vascular front. Previous studies have demonstrated that hypertrophy and apoptosis of chick chondrocytes in culture is associated with the release and activation of TGF- β 2, this has been suggested to provide a mechanism controlling the processes of vascular invasion of growth cartilage and the deposition of bone matrix on nearby cartilage remnants (Gibson et al., 2001).

a. Regulatory ?



b. Structural ?



c. Promoting endochondral ossification ?

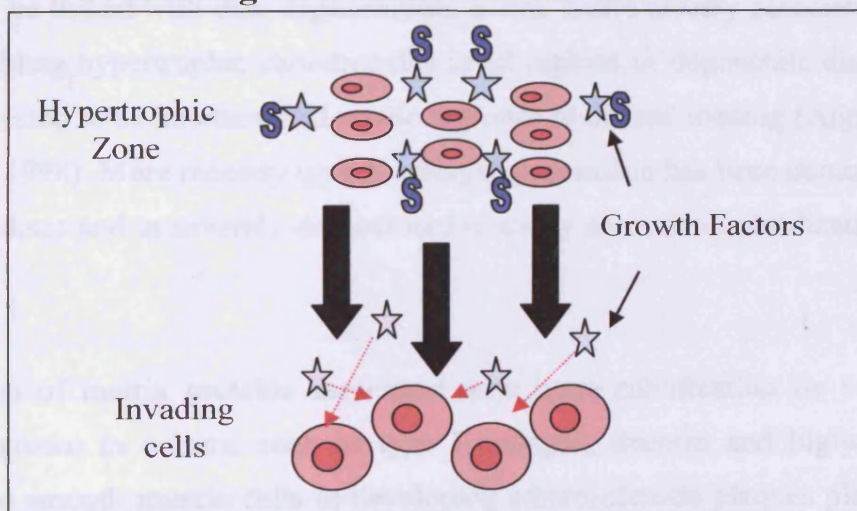


Figure 6.1: Potential roles of an interaction between type X collagen and the SLRPs decorin and biglycan.

6.3.2 Involvement in Pathology

The identified interactions of type X collagen with decorin and biglycan may have roles in pathology as well as normal physiological development. Pathological calcification can occur in multiple tissues throughout the body. Decorin and biglycan are widely expressed, whereas type X collagen has a much more restricted distribution. Type X collagen, decorin and biglycan have all been implicated in the pathology of osteoarthritis. In a study of human late stage osteoarthritic cartilage, decorin and biglycan transcription and translation was found to be up-regulated (Bock et al., 2001), and synthesised by fibroblast-like chondrocytes (Tesche and Miosge, 2005). Strong expression of type X collagen has been found to co-localise with the deposition of calcium within regions of osteoarthritic meniscal cartilage enriched with cell clusters (Hellio Le Graverand et al., 2001).

Another site where type X collagen, decorin and biglycan have been implicated in pathology is the intervertebral disc. A study of intervertebral disc degeneration found that different regions of the disc respond to degeneration differently. Cells of the nucleus pulposus decrease biosynthetic processes, whereas they are upregulated in the annulus fibrosus. In severely degenerated discs aggrecan synthesis was found to be decreased and the concentration of the small proteoglycan decorin and biglycan was increased. This finding was suggested to be influential on the biomechanical properties and hence the function of the disc, as well as being indicative of an inappropriate repair process (Cs-Szabo et al., 2002). Type X collagen has also been found to be linked with disc degeneration, it was found closely associated with clusters of cells resembling hypertrophic chondrocytes in all regions of degenerate discs and this also has been suggested to be an attempted repair response to altered loading (Aigner et al., 1998; Roberts et al., 1998). More recently type X collagen expression has been demonstrated in fetal intervertebral discs and in severely degenerated discs by an in situ hybridization study (Xi et al., 2004).

The production of matrix proteins associated with bone calcification by vascular smooth muscle cells grown in culture, such as type I collagen, decorin and biglycan, led to the suggestion that smooth muscle cells in developing atherosclerotic plaques play an important role in the deposition of ECM involved in calcification of developing lesions. Decorin has been found to induce calcification of arterial smooth muscle cell cultures and co-localises to mineral deposition in human atherosclerotic plaques, suggesting that decorin functions as a promoter of intimal calcification (Fischer et al., 2004). In a study of the atherosclerotic

process in rat hearts, calcified tissue in coronary arteries was found to contain type X collagen, among other markers of cartilage and bone tissue (Fitzpatrick et al., 2003).

Osteoarthritic cartilage, degenerating intervertebral discs and atherosclerotic plaques are examples of pathological situations where types X collagen, decorin and biglycan have all been implicated. Whether the identified interactions involving these molecules are involved in these processes remains to be studied.

6.4 Future Work

There are a number of other experiments that could be done to substantiate the characterised interactions of type X collagen with decorin and biglycan. High resolution co-localisation studies of type X collagen and the SLRPs decorin and biglycan could provide important information on the roles of these interactions *in vivo*. Sections of tibial growth plate could be probed with specific antibodies and different size gold particles could be used as markers for different proteins, TEM could then be used to study co-localisation. This technique would offer far better resolution than immunohistochemistry using the light microscope and would provide direct evidence of an interaction occurring *in vivo*. Artificial cross linking agents could be used on epiphyseal growth plate tissue, the tissue could be homogenized and the proteins extracted, analysis by SDS-PAGE and western blotting of the extracted proteins could also confirm interactions of type X collagen.

The clones produced during this study which contain fragments of the NC1 domain should be utilised after further optimisation of recombinant protein production to characterise the binding site for decorin and biglycan on the NC1 domain. The interaction of type X collagen with decorin and biglycan is in contrast to interactions with other collagen types which involve the triple helical domain. Decorin and biglycan bind to the N-terminal end of the triple helix of type VI collagen (Wiberg et al., 2001) and decorin binds to the triple helical region of type I collagen (Keene et al., 2000). The finding that decorin and biglycan interact with different domains in different collagen types reinforces their importance in collagen biology. Additionally, the site of interaction on the decorin and biglycan core protein should be mapped. Previous studies have demonstrate that leucine-rich repeats 4 and 5 are involved in the binding of decorin to type I collagen (Svensson et al., 1995) and this binding occurs on the concave face of the decorin 'horse-shoe' model (Weber et al., 1996). More recently the crystal structure of a decorin dimer has been resolved; which challenges this view. The dimer

involves a high affinity interaction of the concave surface of two ‘banana-shaped’ decorin molecules, which would suggest that the previously characterised interactions involving the concave surface could not occur (Scott et al., 2004).

Additional interacting partners for type X collagen could be identified by methods such as a yeast two hybrid screen. Other potential interacting partners for type X collagen include fibromodulin and epiphygan, two members of the SLRP family which are known to be present in the growth plate (Johnson et al., 1997; Saamanen et al., 2001). Perlecan is another potential interacting partner known to be present in the growth plate, it has been suggested that perlecan is involved in MMP regulation within the growth plate matrix (Gustafsson et al., 2003). A possible association between type X collagen and heparan sulphate containing proteoglycans was proposed when analysis of transgenic type X collagen mice growth plates showed a decompartmentalised chondro-osseous junction (Jacenko et al., 2001).

To establish whether the interaction of type X collagen with SLRPs have physiological roles, the use of transgenic mice would be ideal. Mice that are deficient in type X collagen could be used and compared with wild type animals. The expressed message, synthesis and localisation of SLRPs could be studied using a variety of methods, such as in situ hybridization and immunohistochemistry to determine if there are differences at the molecular and protein level within the growth plate. Differences in levels, distribution and activity of growth factors could be assessed. Changes to the histological arrangement; the onset of calcification, or changes at the vascular front could also be analysed. Mice deficient in decorin, biglycan or both could also be studied to look for growth plate abnormalities and changes to the distribution of type X collagen. Data generated from animal models may substantiate in vitro interaction data by proving a biological significance when the interactions are lost in a knock-out model.

6.5 Closing Comments

A high affinity interaction of type X collagen with decorin and biglycan has been described. The characterised interactions are likely to have functional roles in endochondral ossification during normal growth and development, but could also be involved in pathological calcification. Characterisation of these molecular interactions which are likely to be important for the structure and hence the function of the hypertrophic ECM, could help define the precise roles of these components during the process of endochondral ossification.

Chapter 7: References

- Abbaszade, I., Liu, R. Q., Yang, F., Rosenfeld, S. A., Ross, O. H., Link, J. R., Ellis, D. M., Tortorella, M. D., Pratta, M. A., Hollis, J. M., *et al.* (1999). Cloning and characterization of ADAMTS11, an aggrecanase from the ADAMTS family. *J Biol Chem* 274, 23443-23450.
- Aigner, T., Greskötter, K. R., Fairbank, J. C. T., von der Mark, K., and Urban, J. P. G. (1998). Variation with age in the pattern of type X collagen expression in normal and scoliotic human intervertebral discs. *Calcif Tissue Int* 63, 263-268.
- Alini, M., and Roughley, P. J. (2001). Changes in leucine-rich repeat proteoglycans during maturation of the bovine growth plate. *Matrix Biology* 19, 805-813.
- Alvarez, J., Sohn, P., Zeng, X., Doetschman, T., Robbins, D. J., and Serra, R. (2002). TGFbeta2 mediates the effects of hedgehog on hypertrophic differentiation and PTHrP expression. *Development* 129, 1913-1924.
- Ameye, L., and Young, M. F. (2002). Mice deficient in small leucine-rich proteoglycans: novel in vivo models for osteoporosis, osteoarthritis, Ehlers-Danlos syndrome, muscular dystrophy, and corneal diseases. *Glycobiology* 12, 107-116.
- Amizuka, N., Davidson, D., Liu, H., Valverde-Franco, G., Chai, S., Maeda, T., Ozawa, H., Hammond, V., Ornitz, D. M., Goltzman, D., and Henderson, J. E. (2004). Signalling by fibroblast growth factor receptor 3 and parathyroid hormone-related peptide coordinate cartilage and bone development. *Bone* 34, 13-25.
- Anderson, H. C. (1995). Molecular biology of matrix vesicles. *Clin Orthop*, 266-280.
- Anderson, H. C. (2003). Matrix vesicles and calcification. *Curr Rheumatol Rep* 5, 222-226.
- Antonsson, P., Heinegard, D., and Oldberg, A. (1991). Posttranslational modifications of fibromodulin. *J Biol Chem* 266, 16859-16861.
- Apte, S., Mattei, M. G., and Olsen, B. R. (1991). Cloning of human alpha 1(X) collagen DNA and localization of the COL10A1 gene to the q21-q22 region of human chromosome 6. *FEBS Lett* 282, 393-396.
- Apte, S. S., and Olsen, B. R. (1993). Characterisation of the mouse type X collagen gene. *Matrix* 13, 165-179.
- Apte, S. S., Seldin, M. F., Hayashi, M., and Olsen, B. R. (1992). Cloning of the human and mouse type X collagen genes and mapping of the mouse type X collagen gene to chromosome 10. *Eur J Biochem* 206, 217-224.
- Arikawa-Hirasawa, E., Watanabe, H., Takami, H., Hassell, J. R., and Yamada, Y. (1999). Perlecan is essential for cartilage and cephalic development. *Nat Genet* 23, 354-358.
- Aszodi, A., Pfeifer, A., Wendel, M., Hirpi, L., and Fassler, R. (1998). Mouse models for extracellular matrix diseases. *Journal of Molecular Medicine* 76, 238-252.
- Ballock, R. T., and O'Keefe, R. J. (2003). Physiology and Pathophysiology of the Growth Plate. *Birth Defects Research* 69, 123-143.
- Banyard, J., Bao, L., and Zetter, B. R. (2003). Type XXIII collagen, a new transmembrane collagen identified in metastatic tumor cells. *J Biol Chem* 278, 20989-20994.
- Barber, R. E., and Kwan, A. P. L. (1996). Partial characterization of the C-terminal non-collagenous domain (NC1) of collagen type X. *Biochemical Journal* 320, 479-485.
- Bateman, J. F., Freddi, S., Natrass, G., and Savarirayan, R. (2003). Tissue-specific RNA surveillance? Nonsense-mediated mRNA decay causes collagen X haploinsufficiency in Schmid metaphyseal chondrodysplasia cartilage. *Hum Mol Genet* 12, 217-225.

- Bengtsson, E., Neame, P. J., Heinegard, D., and Sommarin, Y. (1995). The primary structure of a basic leucine-rich repeat protein, PRELP, found in connective tissues. *J Biol Chem* 270, 25639-25644.
- Bentz, H., Nathan, R. M., Rosen, D. M., Armstrong, R. M., Thompson, A. Y., Segarini, P. R., Mathews, M. C., Dasch, J. R., Piez, K. A., and Seyedin, S. M. (1989). Purification and characterization of a unique osteoinductive factor from bovine bone. *J Biol Chem* 264, 20805-20810.
- Bianco, P., Fisher, L. W., Young, M. F., Termine, J. D., and Robey, P. G. (1990). Expression and localization of the two small proteoglycans biglycan and decorin in developing human skeletal and non-skeletal tissues. *J Histochem Cytochem* 38, 1549-1563.
- Blochberger, T. C., Vergnes, J. P., Hempel, J., and Hassell, J. R. (1992). cDNA to chick lumican (corneal keratan sulfate proteoglycan) reveals homology to the small interstitial proteoglycan gene family and expression in muscle and intestine. *J Biol Chem* 267, 347-352.
- Bluteau, G., Labourdette, L., Ronziere, M., Conrozier, T., Mathieu, P., Herbage, D., and Mallein-Gerin, F. (1999). Type X collagen in rabbit and human meniscus. *Osteoarthritis and Cartilage* 7, 498-501.
- Bock, H. C., Michaeli, P., Bode, C., Schultz, W., Kresse, H., Herken, R., and Miosge, N. (2001). The small proteoglycans decorin and biglycan in human articular cartilage of late-stage osteoarthritis. *Osteoarthritis and Cartilage* 9, 654-663.
- Bogin, O., Kvansakul, M., Rom, E., Singer, J., Yayon, A., and Hohenester, E. (2002). Insight into schmid metaphyseal chondrodysplasia from the crystal structure of the collagen X NC1 domain trimer. *Structure* 10, 165-173.
- Boot-Handford, R. P., Tuckwell, D. S., Plumb, D. A., Rock, C. F., and Poulosom, R. (2003). A Novel and Highly Conserved Collagen (pro α 1(XVII)) with a Unique Expression Pattern and Unusual Molecular Characteristics Establishes a New Clade within the Vertebrate Fibrillar Collagen Family. *J Biol Chem* 278, 31067-31077.
- Border, W. A., Noble, N. A., Yamamoto, T., Harper, J. R., Yamaguchi, Y., Pierschbacher, M. D., and Ruoslahti, E. (1992). Natural inhibitor of transforming growth factor-beta protects against scarring in experimental kidney disease. *Nature* 360, 361-364.
- Bourdon, M. A., Krusius, T., Campbell, S., Schwartz, N. B., and Ruoslahti, E. (1987). Identification and synthesis of a recognition signal for the attachment of glycosaminoglycans to proteins. *Proc Natl Acad Sci USA* 84, 3194-3198.
- Brass, A., Kadler, K. E., Thomas, J. T., Grant, M. E., and Boot-Handford, R. (1992). The fibrillar collagens, collagen VIII, collagen X and the C1q complement proteins share a similar domain in their C-terminal non-collagenous regions. *FEBS Letters* 303, 126-128.
- Briggs, M. D., and Chapman, K. L. (2002). Pseudoachondroplasia and multiple epiphyseal dysplasia: mutation review, molecular interactions, and genotype to phenotype correlations. *Human Mutation* 19, 465-478.
- Brown, J. C., and Timpl, R. (1995). The collagen superfamily. *Int Arch Allergy Immunol* 107, 484-490.
- Burgeson, R. E., Hebda, P. A., Morris, N. P., and Hollister, D. W. (1982). Human cartilage collagens - comparison of cartilage collagens with human type V collagen. *Journal of Biological Chemistry* 257, 7852-7856.
- Burke, D., Wilkes, D., Blundell, T. L., and Malcolm, S. (1998). Fibroblast growth factor receptors: lessons from the genes. *Trends Biochem Sci* 23, 59-62.
- Carlevaro, M. F., Cermelli, S., Cancedda, R., and Descalzi Cancedda, F. (2000). Vascular endothelial growth factor (VEGF) in cartilage neovascularization and chondrocyte differentiation: auto-paracrine role during endochondral bone formation. *J Cell Sci* 113, 59-69.
- Caterson, B., Flannery, C. R., Hughes, C. E., and Little, C. B. (2000). Mechanisms involved in cartilage proteoglycan catabolism. *Matrix Biol* 19, 333-344.

- Chakravarti, S., Magnuson, T., Lass, J. H., Jepsen, K. J., LaMantia, C., and Carroll, H. (1998). Lumican regulates collagen fibril assembly: skin fragility and corneal opacity in the absence of lumican. *J Cell Biol* 141, 1277-1286.
- Chan, D., and Jacenko, O. (1998). Phenotypic and biochemical consequences of collagen X mutations in mice and humans. *Matrix Biology* 17, 169-184.
- Chan, D., Weng, Y. M., Graham, H. K., Silience, D. O., and Bateman, J. F. (1998). A nonsense mutation in the carboxyl-terminal domain of type X collagen causes haploinsufficiency in Schmid Metaphyseal Chondrodysplasia. *Journal of Clinical Investigation* 101, 1490-1499.
- Chatterjee, A., Faust, C. J., and Herman, G. E. (1993). Genetic and physical mapping of the biglycan gene on the mouse X chromosome. *Mamm Genome* 4, 33-36.
- Cheah, K. S. E., Niewiadomska, A., Dung, W. F., Lau, Y. B., Hunziker, E. B., Aszodi, A., Gustafsson, E., Yamada, Y., Zhou, Z., Tryggvason, K., *et al.* (2004). Perlecan compartmentalizes collagen X in the mammalian growth plate. Paper presented at: XIXth Meeting of the Federation of the European Connective Tissue Societies (Taormina - Giardinia Naxos, Italy.).
- Cheng, F., Heinegard, D., Malmstrom, A., Schmidtchen, A., Yoshida, K., and Fransson, L. A. (1994). Patterns of uronosyl epimerization and 4-/6-O-sulphation in chondroitin/dermatan sulphate from decorin and biglycan of various bovine tissues. *Glycobiology* 4, 685-696.
- Chou, M. Y., and Li, H. C. (2002). Genomic organization and characterization of the human type XXI collagen (COL21A1) gene. *Genomics* 79, 395-401.
- Corsi, A., Xu, T., Chen, X. D., Boyde, A., Liang, J., Mankani, M., Sommer, B., Iozzo, R. V., Eichstetter, I., Robey, P. G., *et al.* (2002). Phenotypic effects of biglycan deficiency are linked to collagen fibril abnormalities, are synergized by decorin deficiency, and mimic Ehlers-Danlos-like changes in bone and other connective tissues. *J Bone Miner Res* 17, 1180-1189.
- Cs-Szabo, G., Ragasa-San Juan, D., Turumella, V., Masuda, K., Thonar, E. J., and An, H. S. (2002). Changes in mRNA and protein levels of proteoglycans of the annulus fibrosus and nucleus pulposus during intervertebral disc degeneration. *Spine* 27, 2212-2219.
- D'Angelo, M., Billings, P. C., Pacifici, M., Leboy, P. S., and Kirsch, T. (2001). Authentic matrix vesicles contain active metalloproteases (MMP). a role for matrix vesicle-associated MMP-13 in activation of transforming growth factor-beta. *J Biol Chem* 276, 11347-11353.
- D'Angelo, M., Yan, Z., Nooreyazdan, M., Pacifici, M., Sarment, D. S., Billings, P. C., and Leboy, P. S. (2000). MMP-13 is induced during chondrocyte hypertrophy. *Journal of Cellular Biochemistry* 77, 678-693.
- Danielson, K. G., Baribault, H., Holmes, D. F., Graham, H., Kadler, K. E., and Iozzo, R. V. (1997). Targeted disruption of decorin leads to abnormal collagen fibril morphology and skin fragility. *J Cell Biol* 136, 729-743.
- Danielson, K. G., Fazzio, A., Cohen, I., Cannizzaro, L. A., Eichstetter, I., and Iozzo, R. V. (1993). The human decorin gene: intron-exon organization, discovery of two alternatively spliced exons in the 5' untranslated region, and mapping of the gene to chromosome 12q23. *Genomics* 15, 146-160.
- Deere, M., Johnson, J., Garza, S., Harrison, W. R., Yoon, S. J., Elder, F. F., Kucherlapati, R., Hook, M., and Hecht, J. T. (1996). Characterization of human DSPG3, a small dermatan sulfate proteoglycan. *Genomics* 38, 399-404.
- Di Cesare, P. E., Chen, F. S., Moergelin, M., Carlson, C. S., Leslie, M. P., Perris, R., and Fang, C. (2002). Matrix-matrix interaction of cartilage oligomeric matrix protein and fibronectin. *Matrix Biol* 21, 461-470.
- Dugan, T. A., Yang, V. W., McQuillan, D. J., and Hook, M. (2003). Decorin binds fibrinogen in a Zn²⁺-dependent interaction. *J Biol Chem* 278, 13655-13662.

- Ehnis, T., Dieterich, W., Bauer, M., Kresse, H., and Schuppan, D. (1997). Localization of a binding site for the proteoglycan decorin on collagen XIV (undulin). *J Biol Chem* 272, 20414-20419.
- Ekins, R., and Chu, F. (1997). Immunoassay and other ligand assays: present status and future trends. *J Int Fed Clin Chem* 9, 100-109.
- Elima, K., Eerola, I., Rosati, R., Metsaranta, M., Garofalo, S., Perala, M., Crombrughe, B. D., and Vuorio, E. (1993). The mouse collagen X gene : complete nucleotide sequence, exon structure and expression pattern. *Biochemical Journal* 289, 247-253.
- Eyre, D., and Wu, J. J. (1995). Collagen structure and cartilage matrix integrity. *Journal of Rheumatology* 22, 82-85.
- Fichard, A., Kleman, J., and Ruggiero, F. (1994). Another look at collagen V and XI molecules. *Matrix Biol* 14, 515-531.
- Fischer, J. W., Steitz, S. A., Johnson, P. Y., Burke, A., Kolodgie, F., Virmani, R., Giachelli, C., and Wight, T. N. (2004). Decorin promotes aortic smooth muscle cell calcification and colocalises to calcified regions in human atherosclerotic lesions. *Arterioscler Thromb Vasc Biol* 24, 2391-2396.
- Fisher, L. W., Heegaard, A. M., Vetter, U., Vogel, W., Just, W., Termine, J. D., and Young, M. F. (1991). Human biglycan gene. Putative promoter, intron-exon junctions, and chromosomal localization. *J Biol Chem* 266, 14371-14377.
- Fisher, L. W., Termine, J. D., and Young, M. F. (1989). Deduced protein sequence of bone small proteoglycan I (biglycan) shows homology with proteoglycan II (decorin) and several nonconnective tissue proteins in a variety of species. *J Biol Chem* 264, 4571-4576.
- Fitzpatrick, L. A., Turner, R. T., and Ritman, E. R. (2003). Endochondral bone formation in the heart: a possible mechanism of coronary calcification. *Endocrinology* 144, 2214-2219.
- Fukuta, S., Oyama, M., Kavalkovich, K., Fu, F., and Niyibizi, C. (1998). Identification of Types II, IX and X Collagens at the Insertion Site of the Bovine Achilles Tendon. *Matrix Biology* 17, 65-73.
- Funderburgh, J. L., Corpuz, L. M., Roth, M. R., Funderburgh, M. L., Tasheva, E. S., and Conrad, G. W. (1997). Mimecan, the 25-kDa corneal keratan sulfate proteoglycan, is a product of the gene producing osteoglycin. *J Biol Chem* 272, 28089-28095.
- Gendelman, R., Burton-Wurster, N. I., MacLeod, J. N., and Lust, G. (2003). The cartilage-specific fibronectin isoform has a high affinity binding site for the small proteoglycan decorin. *J Biol Chem* 278, 11175-11181.
- Gerber, H. P., and Ferrara, N. (2000). Angiogenesis and bone growth. *Trends Cardiovasc Med* 10, 223-228.
- Gerber, H. P., Vu, T. H., Ryan, A. M., Kowalski, J., Werb, Z., and Ferrara, N. (1999). VEGF couples hypertrophic cartilage remodeling, ossification and angiogenesis during endochondral bone formation. *Nat Med* 5, 623-628.
- Gibson, G. (1998). Active role of chondrocyte apoptosis in endochondral ossification. *Microscopy Research and Technique* 42, 191-204.
- Gibson, G., Lin, D. L., Wang, X., and Zhang, L. (2001). The release and activation of transforming growth factor beta2 associated with apoptosis of chick hypertrophic chondrocytes. *J Bone Miner Res* 16, 2330-2338.
- Gibson, G., Schor, S. L., and Grant, M. E. (1982). Effects of matrix macromolecules on chondrocyte gene expression: synthesis of a low molecular weight collagen species by cells cultured within collagen gels. *Journal of Cell Biology* 93, 767-774.
- Gibson, G. J., Beaumont, B. W., and Flint, M. H. (1984). Synthesis of a low molecular weight collagen by chondrocytes from the presumptive calcification region of the embryonic chick sterna: the influence of culture with collagen gels. *J Cell Biol* 99, 208-216.

- Gibson, G. J., Schor, S. L., and Grant, M. E. (1981). Partial characterisation of a low molecular weight collagen synthesised by chondrocytes cultured in collagen gels. *Biochemical Society Transactions* 9, 550-551.
- Gill, M. R., Oldberg, A., and Reinholt, F. P. (2002). Fibromodulin-null murine knee joints display increased incidences of osteoarthritis and alterations in tissue biochemistry. *Osteoarthritis Cartilage* 10, 751-757.
- Goldberg, M., Septier, D., Rapoport, O., Young, M., and Ameye, L. (2002). Biglycan is a repressor of amelogenin expression and enamel formation: an emerging hypothesis. *J Dent Res* 81, 520-524.
- Gori, F., Schipani, E., and Demay, M. B. (2001). Fibromodulin is expressed by both chondrocytes and osteoblasts during fetal bone development. *J Cell Biochem* 82, 46-57.
- Grant, W. T., Wang, G.-J., and Balian, G. (1987). Type X collagen synthesis during endochondral ossification in fracture repair. *The Journal of Biological Chemistry* 262, 9844-9849.
- Gress, C. J., and Jacenko, O. (2000). Growth plate compressions and altered hematopoiesis in collagen X null mice. *The Journal of Cell Biology* 149, 983-993.
- Grover, J., Chen, X. N., Korenberg, J. R., Recklies, A. D., and Roughley, P. J. (1996). The gene organization, chromosome location, and expression of a 55-kDa matrix protein (PRELP) of human articular cartilage. *Genomics* 38, 109-117.
- Gustafsson, E., Aszodi, A., Ortega, N., Hunziker, E. B., Denker, H. W., Werb, Z., and Fassler, R. (2003). Role of collagen type II and perlecan in skeletal development. *Ann N Y Acad Sci* 995, 140-150.
- Handler, M., Yurchenco, P., and Iozzo, R. V. (1997). Developmental expression of perlecan during murine embryogenesis. *Developmental Dynamics* 210, 130-145.
- Hardingham, T., Burditt, L., and Ratcliffe, A. (1984). Studies on the synthesis, secretion and assembly of proteoglycan aggregates by chondrocytes. *Prog Clin Biol Res* 151, 17-29.
- Hashimoto, T., Wakabayashi, T., Watanabe, A., Kowa, H., Hosoda, R., Nakamura, A., Kanazawa, I., Arai, T., Takio, K., Mann, D. M., and Iwatsubo, T. (2002). CLAC: a novel Alzheimer amyloid plaque component derived from a transmembrane precursor, CLAC-P/collagen type XXV. *Embo J* 21, 1524-1534.
- Hassell, J., Yamada, Y., and Arikawa-Hirasawa, E. (2003). Role of perlecan in skeletal development and disease. *Glycoconj J* 19, 263-267.
- Hedbom, E., and Heinegard, D. (1989). Interaction of a 59-kDa connective tissue matrix protein with collagen I and collagen II. *J Biol Chem* 264, 6898-6905.
- Heinegard, D., Larsson, T., Sommarin, Y., Franzen, A., Paulsson, M., and Hedbom, E. (1986). Two novel matrix proteins isolated from articular cartilage show wide distributions among connective tissues. *J Biol Chem* 261, 13866-13872.
- Hellio Le Graverand, M. P., Sciore, P., Eggerer, J., Rattner, J. P., Vignon, E., Barclay, L., Hart, D. A., and Rattner, J. B. (2001). Formation and phenotype of cell clusters in osteoarthritic meniscus. *Arthritis & Rheumatism* 44, 1808-1818.
- Henry, S. P., Takanosu, M., Boyd, T. C., Mayne, P. M., Eberspaecher, H., Zhou, W., de Crombrughe, B., Hook, M., and Mayne, R. (2001). Expression pattern and gene characterization of asporin, a newly discovered member of the leucine-rich repeat protein family. *J Biol Chem* 276, 12212-12221.
- Hildebrand, A., Romaris, M., Rasmussen, L. M., Heinegard, D., Twardzik, D. R., Border, W. A., and Ruoslahti, E. (1994). Interaction of the small interstitial proteoglycans biglycan, decorin and fibromodulin with transforming growth factor beta. *Biochem J* 302, 527-534.

- Hirako, Y., Usukura, J., Uematsu, J., Hashimoto, T., Kitajima, Y., and Owaribe, K. (1998). Cleavage of BP180, a 180-kDa Bullous Pemphigoid Antigen, Yields a 120-kDa Collagenous Extracellular Polypeptide. *Journal of Biological Chemistry* 273, 9711-9717.
- Hobby, P., Wyatt, M. K., Gan, W., Bernstein, S., Tomarev, S., Slingsby, C., and Wistow, G. (2000). Cloning, modeling, and chromosomal localization for a small leucine-rich repeat proteoglycan (SLRP) family member expressed in human eye. *Mol Vis* 6, 72-78.
- Hocking, A. M., Shinomura, T., and McQuillan, D. J. (1998). Leucine-rich repeat glycoproteins of the extracellular matrix. *Matrix Biol* 17, 1-19.
- Hocking, A. M., Strugnell, R. A., Ramamurthy, P., and McQuillan, D. J. (1996). Eukaryotic expression of recombinant biglycan. Post-translational processing and the importance of secondary structure for biological activity. *J Biol Chem* 271, 19571-19577.
- Holden, P., Meadows, R. S., Chapman, K. L., Grant, M. E., Kadler, K. E., and Briggs, M. D. (2001). Cartilage oligomeric matrix protein interacts with type IX collagen, and disruptions to these interactions identify a pathogenetic mechanism in a bone dysplasia family. *Journal of Biological Chemistry* 276, 6046-6055.
- Holmbeck, K., Bianco, P., Caterina, J., Yamada, S., Kromer, M., Kuznetsov, S. A., Mankani, M., Robey, P. G., Poole, A. R., Pidoux, I., *et al.* (1999). MT1-MMP-deficient mice develop dwarfism, osteopenia, arthritis, and connective tissue disease due to inadequate collagen turnover. *Cell* 99, 81-92.
- Horner, A., Kemp, P., Summers, C., Bord, S., Bishop, N. J., Kelsall, A. W., Coleman, N., and Compston, J. E. (1998). Expression and distribution of transforming growth factor-beta isoforms and their signaling receptors in growing human bone. *Bone* 23, 95-102.
- Huang, X., Birk, D. E., and Goetinck, P. F. (1999). Mice lacking matrilin-1 (cartilage matrix protein) have alterations in type II collagen fibrillogenesis and fibril organisation. *Developmental Dynamics* 216, 434-441.
- Hunter, G. (1991). Role of proteoglycan in the provisional calcification of cartilage. *Clinical Orthopaedics and Related Research* 262, 256-280.
- Hunziker, E. B. (1994). Mechanism of longitudinal bone growth and its regulation by growth plate chondrocytes. *Microsc Res Tech* 28, 505-519.
- Hunziker, E. B., Schenk, R. K., and Cruz-Orive, L. M. (1987). Quantitation of chondrocyte performance in growth-plate cartilage during longitudinal bone growth. *J Bone Joint Surg Am* 69, 162-173.
- Ikegawa, S., Nakamura, K., Nagano, A., Haga, N., and Nakamura, Y. (1997). Mutations in the N-terminal globular domain of the type X collagen gene (COL10A1) in patients with Schmid metaphyseal chondrodysplasia. *Hum Mutat* 9, 131-135.
- Imai, K., Hiramatsu, A., Fukushima, D., Pierschbacher, M. D., and Okada, Y. (1997). Degradation of decorin by matrix metalloproteinases: identification of the cleavage sites, kinetic analyses and transforming growth factor-beta1 release. *Biochem J* 322 (Pt 3), 809-814.
- Inoki, I., Shiomi, T., Hashimoto, G., Enomoto, H., Nakamura, H., Makino, K., Ikeda, E., Takata, S., Kobayashi, K., and Okada, Y. (2002). Connective tissue growth factor binds vascular endothelial growth factor (VEGF) and inhibits VEGF-induced angiogenesis. *Faseb J* 16, 219-221.
- Iozzo, R. V. (1998). Matrix proteoglycans: from molecular design to cellular function. *Annu Rev Biochem* 67, 609-652.
- Iozzo, R. V. (1999). The biology of the small leucine-rich proteoglycans. Functional network of interactive proteins. *J Biol Chem* 274, 18843-18846.
- Isaka, Y., Brees, D. K., Ikegaya, K., Kaneda, Y., Imai, E., Noble, N. A., and Border, W. A. (1996). Gene therapy by skeletal muscle expression of decorin prevents fibrotic disease in rat kidney. *Nat Med* 2, 418-423.

- Jacenko, O., Chan, D., Franklin, A., Ito, S., Underhill, C. B., Bateman, J. F., and Campbell, M. R. (2001). A dominant interference collagen X mutation disrupts hypertrophic chondrocyte pericellular matrix and glycosaminoglycan and proteoglycan distribution in transgenic mice. *American Journal of Pathology* 159, 2257-2269.
- Jacenko, O., Ito, S., and Olsen, B. R. (1996). Skeletal and hematopoietic defects in mice transgenic for collagen X. *Annals of New York Academy of Sciences* 785, 278-280.
- Jacenko, O., Luvalle, P., and Olsen, B. R. (1993). Spondylometaphyseal dysplasia in mice carrying a dominant negative mutation in a matrix protein specific for cartilage to bone transition. *Nature* 365, 56-61.
- Jacenko, O., Roberts, D. W., Campbell, M. R., McManus, P. M., Gress, C. J., and Tao, Z. (2002). Linking Hematopoiesis to Endochondral Skeletogenesis through Analysis of Mice Transgenic for Collagen X. *Am J Pathol* 160, 2019-2034.
- Jepsen, K. J., Wu, F., Peragallo, J. H., Paul, J., Roberts, L., Ezura, Y., Oldberg, A., Birk, D. E., and Chakravarti, S. (2002). A syndrome of joint laxity and impaired tendon integrity in lumican- and fibromodulin-deficient mice. *J Biol Chem* 277, 35532-35540.
- Johnson, H. J., Rosenberg, L., Choi, H. U., Garza, S., Hook, M., and Neame, P. J. (1997). Characterisation of epiphycan, a small proteoglycan with a leucine-rich repeat core protein. *Journal of Biological Chemistry* 272, 18709-18717.
- Johnson, J., Shinomura, T., Eberspaecher, H., Pinero, G., Decrombrughe, B., and Hook, M. (1999). Expression and localization of PG-Lb/epiphycan during mouse development. *Dev Dyn* 216, 499-510.
- Johnstone, E. W., Leane, P. B., Kolesik, P., Byers, S., and Foster, B. K. (2000). Spatial arrangement of physeal cartilage chondrocytes and the structure of the primary spongiosa. *J Orthop Sci* 5, 294-301.
- Kamiya, N., Shigemasa, K., and Takagi, M. (2001). Gene expression and immunohistochemical localization of decorin and biglycan in association with early bone formation in the developing mandible. *J Oral Sci* 43, 179-188.
- Keene, D. R., San Antonio, J. D., Mayne, R., McQuillan, D. J., Sarris, G., Santoro, S. A., and Iozzo, R. V. (2000). Decorin binds near the C terminus of type I collagen. *J Biol Chem* 275, 21801-21804.
- Kember, N. F. (1978). Cell kinetics and the control of growth in long bones. *Cell Tissue Kinet* 11, 477-485.
- Kielty, C., and Grant, M. E. (2002). *Connective Tissue and Its Heritable Disorders. Molecular, Genetic and Medical Aspects.*, Second Edition edn (New York, Wiley-Liss).
- Kielty, C. M., Kwan, A. P., Holmes, D. F., Schor, S. L., and Grant, M. E. (1985). Type X collagen, a product of hypertrophic chondrocytes. *Biochem J* 227, 545-554.
- Kirsch, T., Harrison, G., Golub, E. E., and Nah, H.-D. (2000). The roles of annexins and types II and X collagen in matrix vesicle mediated mineralisation of growth plate cartilage. *The Journal of Biological Chemistry* 275, 35577-35583.
- Kirsch, T., and Pfaffle, M. (1992). Selective binding of anchorin CII (annexin V) to type II and X collagen and to chondrocalcin (C-propeptide of type II collagen). Implications for anchoring function between matrix vesicles and matrix proteins. *FEBS Lett* 310, 143-147.
- Knudson, C. B. (2003). Hyaluronan and CD44: Strategic Players for Cell-Matrix Interactions During Chondrogenesis and Matrix Assembly. *Birth Defects Research* 69, 174-196.
- Koch, M., Foley, J. E., Hahn, R., Zhou, P., Burgeson, R. E., Gerecke, D. R., and Gordon, M. K. (2001). alpha 1(Xx) collagen, a new member of the collagen subfamily, fibril-associated collagens with interrupted triple helices. *J Biol Chem* 276, 23120-23126.

- Kresse, H., and Schonherr, E. (2001). Proteoglycans of the extracellular matrix and growth control. *J Cell Physiol* 189, 266-274.
- Krumdieck, R., Hook, M., Rosenberg, L. C., and Volanakis, J. E. (1992). The proteoglycan decorin binds C1q and inhibits the activity of the C1 complex. *J Immunol* 149, 3695-3701.
- Krusius, T., and Ruoslahti, E. (1986). Primary structure of an extracellular matrix proteoglycan core protein deduced from cloned cDNA. *Proc Natl Acad Sci U S A* 83, 7683-7687.
- Kwan, A. P. L., Cummings, C. E., Chapman, J. A., and Grant, M. E. (1991). Macromolecular organisation of chicken type X collagen in vitro. *Journal of Cell Biology* 114, 597-604.
- Kwan, K. M., Pang, M. K. M., Zhou, S., Cowan, S. K., Kong, R. Y. C., Pfordte, T., Olsen, B. R., Sillence, D. O., Tam, P. P. L., and Cheah, K. S. E. (1997). Abnormal Compartmentalization of cartilage matrix components in mice lacking collagen X : implications for function. *The Journal of Cell Biology* 136, 459-471.
- Laemmli, U. K. (1970). Cleavage of Structural proteins during the assembly of the head of bacteriophage T4. *Nature* 227, 680-682.
- Lammi, P., Inkinen, R. I., von der Mark, K., Puustjarvi, K., Arokoski, J., Hyttinen, M. M., and Lammi, M. J. (1998). Localization of type X collagen in the intervertebral disc of mature beagle dogs. *Matrix Biol* 17, 449-453.
- Lee, E. R., Lamplugh, L., Davoli, M. A., Beauchemin, A., Chan, K., Mort, J. S., and Leblond, C. P. (2001). Enzymes active in the areas undergoing cartilage resorption during the development of the secondary ossification center in the tibiae of rats ages 0-21 days: I. Two groups of proteinases cleave the core protein of aggrecan. *Dev Dyn* 222, 52-70.
- Liu, C. Y., Birk, D. E., Hassell, J. R., Kane, B., and Kao, W. W. (2003). Keratocan-deficient Mice Display Alterations in Corneal Structure. *J Biol Chem* 278, 21672-21677.
- Liu, C. Y., Shiraishi, A., Kao, C. W., Converse, R. L., Funderburgh, J. L., Corpuz, L. M., Conrad, G. W., and Kao, W. W. (1998). The cloning of mouse keratocan cDNA and genomic DNA and the characterization of its expression during eye development. *J Biol Chem* 273, 22584-22588.
- Liu, J., Laue, T. M., Choi, H. U., Tang, L. H., and Rosenberg, L. (1994). The self-association of biglycan from bovine articular cartilage. *J Biol Chem* 269, 28366-28373.
- Long, F., Chung, U. I., Ohba, S., McMahon, J., Kronenberg, H. M., and McMahon, A. P. (2004). Ihh signaling is directly required for the osteoblast lineage in the endochondral skeleton. *Development* 131, 1309-1318.
- Lorenzo, P., Aspberg, A., Onnerfjord, P., Bayliss, M. T., Neame, P. J., and Heinegard, D. (2001). Identification and characterization of asporin, a novel member of the leucine-rich repeat protein family closely related to decorin and biglycan. *J Biol Chem* 276, 12201-12211.
- Luckman, S. P., Rees, E., and Kwan, A. P. (2003). Partial characterization of cell-type X collagen interactions. *Biochem J* 372, 485-493.
- LuValle, P., Daniels, K., Hay, E. D., and Olsen, B. R. (1992). Type X collagen is transcriptionally activated and specifically localized during sternal cartilage maturation. *Matrix* 12, 404-413.
- LuValle, P., Ninomiya, Y., Rosenblum, N. D., and Olsen, B. R. (1988). The type X collagen gene. Intron sequences split the 5'-untranslated region and separate the coding regions for the non-collagenous amino-terminal and triple-helical domains. *J Biol Chem* 263, 18378-18385.
- Madsen, L. B., Petersen, A. H., Nielsen, V. H., Nissen, P. H., Duno, M., Krejci, L., Bendixen, C., and Thomsen, B. (2003). Chromosome location, genomic organization of the porcine COL10A1 gene and model structure of the NC1 domain. *Cytogenet Genome Res* 102, 173-178.

- Maeda, S., Dean, D. D., Gomez, R., Schwartz, Z., and Boyan, B. D. (2002). The first stage of transforming growth factor beta1 activation is release of the large latent complex from the extracellular matrix of growth plate chondrocytes by matrix vesicle stromelysin-1 (MMP-3). *Calcif Tissue Int* 70, 54-65.
- Makihira, S., Yan, W., Murakami, H., Furukawa, M., Kawai, T., Nikawa, H., Yoshida, E., Hamada, T., Okada, Y., and Kato, Y. (2003). Thyroid hormone enhances aggrecanase-2/ADAM-TS5 expression and proteoglycan degradation in growth plate cartilage. *Endocrinology* 144, 2480-2488.
- Marcum, J. A., and Thompson, M. A. (1991). The amino-terminal region of a proteochondroitin core protein, secreted by aortic smooth muscle cells, shares sequence homology with the pre-propeptide region of the biglycan core protein from human bone. *Biochem Biophys Res Commun* 175, 706-712.
- Markey, F. (2000). *Real-Time Analysis of Biomolecular Interactions* (Tokyo, Springer).
- Marks, D. S., Gregory, C. A., Wallis, G. A., Brass, A., Kadler, K. E., and Boot-Handford, R. P. (1999). Metaphyseal chondrodysplasia type schmid mutations are predicted to occur in two distinct three dimensional clusters within type X collagen NC1 domains that retain the ability to trimerize. *The Journal of Biological Chemistry* 274, 3632-3641.
- Matsushima, N., Ohyanagi, T., Tanaka, T., and Kretsinger, R. H. (2000). Super-motifs and evolution of tandem leucine-rich repeats within the small proteoglycans--biglycan, decorin, lumican, fibromodulin, PRELP, keratocan, osteoadherin, epiphygan, and osteoglycin. *Proteins* 38, 210-225.
- McLaughlin, S. H., Conn, S. N., and Bulleid, N. J. (1999). Folding and assembly of type X collagen mutants that cause metaphyseal chondrodysplasia-type schmid - evidence for co-assembly of the mutant and wild-type chains and binding to molecular chaperones. *The Journal of Biological Chemistry* 274, 7570-7575.
- Mochida, Y., Duarte, W. R., Tanzawa, H., Paschalis, E. P., and Yamauchi, M. (2003). Decorin modulates matrix mineralization in vitro. *Biochem Biophys Res Commun* 305, 6-9.
- Mundlos, S. (1994). Expression patterns of matrix genes during human skeletal development. *Prog Histochem Cytochem* 28, 1-47.
- Mundlos, S., and Olsen, B. R. (1997). Heritable diseases of the skeleton II. Molecular insights into skeletal development-matrix components and their homeostasis. *The FASEB Journal* 11, 227-233.
- Murdoch, A. D., Dodge, G. R., Cohen, I., Tuan, R. S., and Iozzo, R. V. (1992). Primary structure of the human heparan sulphate proteoglycan from basement membrane (HSPG2/perlecan). A chimeric molecule with multiple domains homologous to the low density lipoprotein receptor, laminin, neural cell adhesion molecules, and epidermal growth factor. *Journal of Biological Chemistry* 267, 8544-8557.
- Mwale, F., Tchetina, E., Wu, C. W., and Poole, A. R. (2002). The assembly and remodeling of the extracellular matrix in the growth plate in relationship to mineral deposition and cellular hypertrophy : An in situ study of collagens II and IX and proteoglycan. *Journal of Bone and Mineral Research* 17, 275-283.
- Myllyharju, J., and Kivirikko, K. I. (2001). Collagens and collagen-related diseases. *Ann Med* 33, 7-21.
- Nagai, H., and Aoki, M. (2002). Inhibition of growth plate angiogenesis and endochondral ossification with diminished expression of MMP-13 in hypertrophic chondrocytes in FGF-2-treated rats. *J Bone Miner Metab* 20, 142-147.
- Nareyeck, G., Seidler, D. G., Troyer, D., Rauterberg, J., Kresse, H., and Schonherr, E. (2004). Differential interactions of decorin and decorin mutants with type I and VI collagens. *FEBS Lett* 271, 3389-3398.
- Nawachi, K., Inoue, M., Kubota, S., Nishida, T., Yosimichi, G., Nakanishi, T., Kanyama, M., Kuboki, T., Yatani, H., Yamaai, T., and Takigawa, M. (2002). Tyrosine kinase-type receptor ErbB4 in chondrocytes: interaction with connective tissue growth factor and distribution in cartilage. *FEBS Lett* 528, 109-113.
- Neame, P. J., Choi, H. U., and Rosenberg, L. C. (1989). The primary structure of the core protein of the small, leucine-rich proteoglycan (PG I) from bovine articular cartilage. *J Biol Chem* 264, 8653-8661.

- Niyibizi, C., Sagarrigo Visconti, C., Gibson, G., and Kavalkovich, K. (1996). Identification and immunolocalization of type X collagen at the ligament-bone interface. *Biochem Biophys Res Commun* 222, 584-589.
- Okamoto, O., Suzuki, Y., Kimura, S., and Shinkai, H. (1996). Extracellular matrix 22-kDa protein interacts with decorin core protein and is expressed in cutaneous fibrosis. *J Biochem (Tokyo)* 119, 106-114.
- Olsen, B. (1992). *Molecular biology of cartilage collagens*. (New York, Raven Press).
- Ornitz, D. M., and Marie, P. J. (2002). FGF signaling pathways in endochondral and intramembranous bone development and human genetic disease. *Genes Dev* 16, 1446-1465.
- Ortega, N., Behonick, D. J., and Werb, Z. (2004). Matrix remodeling during endochondral ossification. *Trends Cell Biol* 14, 86-93.
- Orth, M. W., Luchene, L. J., and Schmid, T. M. (1996). Type X collagen isolated from the hypertrophic cartilage of embryonic chick tibiae contains both hydroxylslyl- and lysyl pyridinoline cross-links. *Biochemical and Biophysical Research Communications* 219, 301-305.
- Pavasant, P., Shizari, T., and Underhill, C. B. (1996). Hyaluronan contributes to the enlargement of hypertrophic lacunae in the growth plate. *J Cell Sci* 109 (Pt 2), 327-334.
- Pavasant, P., Shizari, T. M., and Underhill, C. B. (1994). Distribution of hyaluronan in the epiphyseal growth plate: turnover by CD44-expressing osteoprogenitor cells. *J Cell Sci* 107 (Pt 10), 2669-2677.
- Peters, K. G., Werner, S., Chen, G., and Williams, L. T. (1992). Two FGF receptor genes are differentially expressed in epithelial and mesenchymal tissues during limb formation and organogenesis in the mouse. *Development* 114, 233-243.
- Polgar, A., Falus, A., Koo, E., Ujfalussy, I., Sesztak, M., Szuts, I., Konrad, K., Hodinka, L., Bene, E., Meszaros, G., *et al.* (2003). Elevated levels of synovial fluid antibodies reactive with the small proteoglycans biglycan and decorin in patients with rheumatoid arthritis or other joint diseases. *Rheumatology* 42, 522-527.
- Poole, A. R., Matsui, Y., Hinek, A., and Lee, E. R. (1989). Cartilage macromolecules and the calcification of cartilage matrix. *Anat Rec* 224, 167-179.
- Poole, C. A., Ayad, S., and Schofield, J. R. (1988). Chondrons from articular cartilage. Immunolocalisation of type VI collagen in the pericellular capsule of isolated canine tibial chondrons. *Journal of Cell Science* 90, 635-643.
- Price, J. S., Oyajobi, B. O., and Russell, R. G. G. (1994). The cell biology of bone growth. *European Journal of Clinical Nutrition* 48, 131-149.
- Prockop, D. J., and Kivirikko, K. I. (1995). Collagens: molecular biology, diseases, and potentials for therapy. *Annu Rev Biochem* 64, 403-434.
- Promega (2001). Technical Bulletin. Wizard Plus SV Minipreps DNA Purification System.
- Promega (2003). pGEM-T and pGEM-T Easy Vector Systems. Technical manual number 042.
- QIAGEN (2003). The QIAexpressionist. A handbook for high-level expression and purification of 6x His-tagged proteins.
- Reardon, A. J., Le Goff, M., Briggs, M. D., McLeod, D., Sheehan, J. K., Thornton, D. J., and Bishop, P. N. (2000). Identification in vitreous and molecular cloning of opticin, a novel member of the family of leucine-rich repeat proteins of the extracellular matrix. *J Biol Chem* 275, 2123-2129.
- Rees, S. G., Flannery, C. R., Little, C. B., Hughes, C. E., Caterson, B., and Dent, C. M. (2000). Catabolism of aggrecan, decorin and biglycan in tendon. *Biochem J* 350 Pt 1, 181-188.

- Reichenberger, E., Beier, F., LuValle, P., Olsen, B. R., von der Mark, K., and Bertling, W. (1992). Genomic organisation and full-length cDNA sequence of human collagen X. *FEBS Lett* 311, 305-310.
- Roach, H. I., Erenpreisa, J., and Aigner, T. (1995). Osteogenic differentiation of hypertrophic chondrocytes involves asymmetric cell divisions and apoptosis. *J Cell Biol* 131, 483-494.
- Roberts, S., Bains, M. A., Kwan, A., Menage, J., and Eisenstein, S. M. (1998). Type X collagen in the human intervertebral disc : an indication of repair or remodelling? *Histochemical Journal* 30, 89-95.
- Rosati, R., Horan, G. S. B., Pinero, G. J., Garofalo, S., Keene, D. R., Horton, W. A., Vuorio, E., Crombrughe, B. d., and Behringer, R. R. (1994). Normal long bone growth and development in type X collagen mice. *Nature genetics* 8, 129-135.
- Rosenberg, K., Olsson, H., Morgelin, M., and Heinegard, D. (1998). Cartilage oligomeric matrix protein shows high affinity zinc-dependent interaction with triple helical collagen. *J Biol Chem* 273, 20397-20403.
- Roughley, P. J. (2001). Articular cartilage and changes in arthritis: noncollagenous proteins and proteoglycans in the extracellular matrix of cartilage. *Arthritis Res* 3, 342-347.
- Roughley, P. J., White, R. J., and Mort, J. S. (1996). Presence of pro-forms of decorin and biglycan in human articular cartilage. *Biochem J* 318 (Pt 3), 779-784.
- Rucklidge, G. J., Milne, G., and Robins, S. P. (1996). Collagen type X: a component of the surface of normal human, pig, and rat articular cartilage. *Biochem Biophys Res Commun* 224, 297-302.
- Ruoslahti, E., and Yamaguchi, Y. (1991). Proteoglycans as modulators of growth factor activities. *Cell* 64, 867-869.
- Saamanen, A. M., Salminen, H. J., Rantakokko, A. J., Heinegard, D., and Vuorio, E. I. (2001). Murine fibromodulin: cDNA and genomic structure, and age-related expression and distribution in the knee joint. *Biochem J* 355, 577-585.
- Santra, M., Danielson, K. G., and Iozzo, R. V. (1994). Structural and functional characterization of the human decorin gene promoter. A homopurine-homopyrimidine S1 nuclease-sensitive region is involved in transcriptional control. *J Biol Chem* 269, 579-587.
- Sasaki, T., Fassler, R., and Hohenester, E. (2004). Laminin: the crux of basement membrane assembly. *Journal of Cell Biology* 164, 959-963.
- Sasaki, T., Larsson, H., Tisi, D., Claesson-Welsh, L., Hohenester, E., and Timpl, R. (2000). Endostatins derived from collagens XV and XVIII differ in structural and binding properties, tissue distribution and anti-angiogenic activity. *J Mol Biol* 301, 1179-1190.
- Sato, H., Kinoshita, T., Takino, T., Nakayama, K., and Seiki, M. (1996). Activation of a recombinant membrane type 1-matrix metalloproteinase (MT1-MMP) by furin and its interaction with tissue inhibitor of metalloproteinases (TIMP)-2. *FEBS Lett* 393, 101-104.
- Sawhney, R. S., Hering, T. M., and Sandell, L. J. (1991). Biosynthesis of small proteoglycan II (decorin) by chondrocytes and evidence for a procure protein. *J Biol Chem* 266, 9231-9240.
- Schmid, T. M., and Linsenmayer, T. F. (1983). A short chain (pro)collagen from aged endochondral chondrocytes. Biochemical characterization. *J Biol Chem* 258, 9504-9509.
- Schmid, T. M., and Linsenmayer, T. F. (1984). Denaturation-renaturation properties of two molecular forms of short- chain cartilage collagen. *Biochemistry* 23, 553-558.
- Schmid, T. M., and Linsenmayer, T. F. (1985). Immunohistochemical localization of short chain cartilage collagen (type X) in avian tissues. *J Cell Biol* 100, 598-605.

Schmid, T. M., and Linsenmayer, T. F. (1989). Chains of matrix-derived type X collagen: size and aggregation properties. *Connect Tissue Res* 20, 215-222.

Schmid, T. M., and Linsenmayer, T. F. (1990). Immunoelectron microscopy of type X collagen: Supramolecular forms within embryonic chick cartilage. *Developmental Biology* 138, 53-62.

Schmid, T. M., Mayne, R., Bruns, R. R., and Linsenmayer, T. F. (1984). Molecular structure of short-chain (SC) cartilage collagen by electron microscopy. *J Ultrastruct Res* 86, 186-191.

Schmid, T. M., Mayne, R., Jefferey, J. J., and Linsenmayer, T. F. (1986). Type X collagen contains two cleavage sites for a vertebrate collagenase. *Journal of Biological Chemistry* 261, 4184-4189.

Scholzen, T., Solursh, M., Suzuki, S., Reiter, R., Morgan, J. L., Buchberg, A. M., Siracusa, L. D., and Iozzo, R. V. (1994). The murine decorin. Complete cDNA cloning, genomic organization, chromosomal assignment, and expression during organogenesis and tissue differentiation. *J Biol Chem* 269, 28270-28281.

Schönherr, E., Broszat, M., Brandan, E., Bruckner, P., and Kresse, H. (1998). Decorin core protein fragment Leu155-Val260 interacts with TGF-beta but does not compete for decorin binding to type I collagen. *Arch Biochem Biophys* 355, 241-248.

Schönherr, E., Hausser, H., Beavan, L., and Kresse, H. (1995). Decorin-type I collagen interaction. Presence of separate core protein-binding domains. *J Biol Chem* 270, 8877-8883.

Schönherr, E., Levkau, B., Schaefer, L., Kresse, H., and Walsh, K. (2001). Decorin-mediated signal transduction in endothelial cells. Involvement of Akt/protein kinase B in up-regulation of p21 (WAF1/CIP1) but not p27 (KIP1). *J Biol Chem* 276, 40687-40692.

Schönherr, E., O'Connell, B. C., Schittny, J., Robenek, H., Fastermann, D., Fisher, L. W., Plenz, G., Vischer, P., Young, M. F., and Kresse, H. (1999). Paracrine or virus-mediated induction of decorin expression by endothelial cells contributes to tube formation and prevention of apoptosis in collagen lattices. *Eur J Cell Biol* 78, 44-55.

Scott, J. E., and Orford, C. R. (1981). Dermatan sulphate-rich proteoglycan associates with rat tail-tendon collagen at the d band in the gap region. *Biochem J* 197, 213-216.

Scott, P. G., Grossmann, J. G., Dodd, C. M., Sheehan, J. K., and Bishop, P. N. (2003). Light and X-ray scattering show decorin to be a dimer in solution. *J Biol Chem* 278, 18353-18359.

Scott, P. G., McEwan, P. A., Dodd, C. M., Bergmann, E. M., Bishop, P. N., and Bella, J. (2004). Crystal structure of the dimeric protein core of decorin, the archetypal small leucine-rich repeat proteoglycan. *PNAS* 101, 15633-15638.

Serra, R., Karaplis, A., and Sohn, P. (1999). Parathyroid hormone-related peptide (PTHrP)-dependent and -independent effects of transforming growth factor beta (TGF-beta) on endochondral bone formation. *J Cell Biol* 145, 783-794.

Shen, G. (2005). The role of type X collagen in facilitating and regulating endochondral ossification of articular cartilage. *Orthod Craniofacial Res* 8, 11-17.

Sherratt, M. J., Graham, H. K., Kielty, C. M., and Holmes, D. F. (2000). ECM macromolecules: rotary shadowing and scanning transmission electron microscopy. *Methods Mol Biol* 139, 119-132.

Sherwin, A. F., Carter, D. H., Poole, C. A., Hoyland, J. A., and Ayad, S. (1999). The distribution of type VI collagen in the developing tissues of the bovine femoral head. *The Histochemical Journal* 31, 623-632.

Shinomura, T., and Kimata, K. (1992). Proteoglycan-Lb, a small dermatan sulfate proteoglycan expressed in embryonic chick epiphyseal cartilage, is structurally related to osteoinductive factor. *J Biol Chem* 267, 1265-1270.

- Shinomura, T., Kimata, K., Oike, Y., Noro, A., Hirose, N., Tanabe, K., and Suzuki, S. (1983). The occurrence of three different proteoglycan species in chick embryo cartilage. Isolation and characterization of a second proteoglycan (PG-Lb) and its precursor form. *J Biol Chem* 258, 9314-9322.
- Siebler, T., Robson, H., Shalet, S. M., and Williams, G. R. (2001). Glucocorticoids, thyroid hormone and growth hormone interactions: implications for the growth plate. *Horm Res* 56, 7-12.
- Sires, U. I., Schmid, T. M., Fliszar, C. J., Wang, Z. Q., Gluck, S. L., and Welgus, H. G. (1995). Complete degradation of type X collagen requires the combined action of interstitial collagenase and osteoclast derived cathepsin -B. *Journal of Clinical Investigation* 95, 2089-2095.
- Slot, J. W., and Geuze, H. J. (1985). A new method of preparing gold probes for multiple-labeling cytochemistry. *Eur J Cell Biol* 38, 87-93.
- Somerville, R. P., Oblander, S. A., and Apte, S. S. (2003). Matrix metalloproteinases: old dogs with new tricks. *Genome Biol* 4, 216.
- Sommarin, Y., Wendel, M., Shen, Z., Hellman, U., and Heinegard, D. (1998). Osteoadherin, a cell-binding keratan sulfate proteoglycan in bone, belongs to the family of leucine-rich repeat proteins of the extracellular matrix. *J Biol Chem* 273, 16723-16729.
- Spicer, A. P., Tien, J. L., Joo, A., and Bowling Jr, R. A. (2002). Investigation of hyaluronan function in the mouse through targeted mutagenesis. *Glycoconj J* 19, 341-345.
- Stamenkovic, I. (2003). Extracellular matrix remodelling: the role of matrix metalloproteinases. *J Pathol* 200, 448-464.
- Steffensen, B., Xu, X., Martin, P. A., and Zardeneta, G. (2002). Human fibronectin and MMP-2 collagen binding domains compete for collagen binding sites and modify cellular activation of MMP-2. *Matrix Biol* 21, 399-414.
- Stephan, S., Sherratt, M. J., Hodson, N., Shuttleworth, C. A., and Kielty, C. M. (2004). Expression and Supramolecular Assembly of Recombinant {alpha}1(VIII) and {alpha}2(VIII) Collagen Homotrimers. *J Biol Chem* 279, 21469-21477.
- Stevens, D. A., and Williams, G. R. (1999). Hormone regulation of chondrocyte differentiation and endochondral bone formation. *Molecular and Cellular Endocrinology* 151, 195-204.
- Strazynski, M., Eble, J. A., Kresse, H., and Schonherr, E. (2004). IL-6 and IL-10 Induce Decorin mRNA in Endothelial Cells, but Interaction with Fibrillar Collagen is Essential for its Translation. *Journal of Biological Chemistry* 279, 21266-21270.
- Sugars, R. V., Milan, A. M., Brown, J. O., Waddington, R. J., Hall, R. C., and Embery, G. (2003). Molecular interaction of recombinant decorin and biglycan with type I collagen influences crystal growth. *Connect Tissue Res* 44 Suppl 1, 189-195.
- Svensson, L., Aszodi, A., Heinegard, D., Hunziker, E. B., Reinholt, F. P., Fassler, R., and Oldberg, A. (2002). Cartilage oligomeric matrix protein-deficient mice have normal skeletal development. *Mol Cell Biol* 22, 4366-4371.
- Svensson, L., Aszodi, A., Reinholt, F. P., Fassler, R., Heinegard, D., and Oldberg, A. (1999). Fibromodulin-null mice have abnormal collagen fibrils, tissue organization, and altered lumican deposition in tendon. *J Biol Chem* 274, 9636-9647.
- Svensson, L., Heinegard, D., and Oldberg, A. (1995). Decorin-binding sites for collagen type I are mainly located in leucine- rich repeats 4-5. *J Biol Chem* 270, 20712-20716.
- Takagi, M., Kamiya, N., Urushizaki, T., Tada, Y., and Tanaka, H. (2000). Gene expression and immunohistochemical localization of biglycan in association with mineralization in the matrix of epiphyseal cartilage. *Histochem J* 32, 175-186.

Takeuchi, Y., Kodama, Y., and Matsumoto, T. (1994). Bone matrix decorin binds transforming growth factor-beta and enhances its bioactivity. *J Biol Chem* 269, 32634-32638.

Takigawa, M. (2003). CTGF/Hcs24 as a Multifunctional Growth Factor for Fibroblasts, Chondrocytes and Vascular Endothelial Cells. *Drug News Perspect* 16, 11-21.

Tapanadechpone, P., Hassell, J. R., Rigatti, B., and Couchman, J. R. (1999). Localization of Glycosaminoglycan Substitution Sites on Domain V of Mouse Perlecan. *Biochem Biophys Res Commun* 265, 680-690.

Tasheva, E. S., Funderburgh, J. L., Corpuz, L. M., and Conrad, G. W. (1998). Cloning, characterization and tissue-specific expression of the gene encoding bovine keratocan, a corneal keratan sulfate proteoglycan. *Gene* 218, 63-68.

Tasheva, E. S., Koester, A., Paulsen, A. Q., Garrett, A. S., Boyle, D. L., Davidson, H. J., Song, M., Fox, N., and Conrad, G. W. (2002). Mimecan/osteoglycin-deficient mice have collagen fibril abnormalities. *Mol Vis* 8, 407-415.

Tesche, F., and Miosge, N. (2005). New aspects of the pathogenesis of osteoarthritis: the role of fibroblast-like chondrocytes in late stages of the disease. *Histol Histopathol* 20, 329-337.

Thomas, J. T., Cresswell, C. J., Rash, B., Nicolai, H., Jones, T., Solomon, E., Grant, M. E., and Boot-Handford, R. (1991a). The human collagen X gene. Complete primary translated sequence and chromosomal localisation. *Biochemical Journal* 280, 617-623.

Thomas, J. T., Kwan, A. P. L., Grant, M. E., and Boot-Handford, R. (1991b). Isolation of cDNAs encoding the complete sequence of bovine type X collagen. Evidence for the condensed nature of mammalian type X collagen genes. *Biochemical Journal* 273, 141-148.

Toole, B. P. (1969). Solubility of collagen fibrils formed in vitro in the presence of sulphated acid mucopolysaccharide-protein. *Nature* 222, 872-873.

Tortorella, M. D., Burn, T. C., Pratta, M. A., Abbaszade, I., Hollis, J. M., Liu, R., Rosenfeld, S. A., Copeland, R. A., Decicco, C. P., Wynn, R., *et al.* (1999). Purification and cloning of aggrecanase-1: a member of the ADAMTS family of proteins. *Science* 284, 1664-1666.

Towbin, H., Staehelin, T., and Gordon, J. (1979). Electrophoretic transfer of proteins from polyacrylamide gels to nitrocellulose sheets: procedure and some applications. *Proc Natl Acad Sci U S A* 76, 4350-4354.

Trask, B. C., Trask, T. M., Broekelmann, T., and Mecham, R. P. (2000). The microfibrillar proteins MAGP-1 and fibrillin-1 form a ternary complex with the chondroitin sulfate proteoglycan decorin. *Mol Biol Cell* 11, 1499-1507.

Tufvesson, E., and Westergren-Thorsson, G. (2002). Tumour necrosis factor-alpha interacts with biglycan and decorin. *FEBS Lett* 530, 124-128.

Ungefroren, H., and Krull, N. B. (1996). Transcriptional regulation of the human biglycan gene. *J Biol Chem* 271, 15787-15795.

Vetter, U., Vogel, W., Just, W., Young, M. F., and Fisher, L. W. (1993). Human decorin gene: intron-exon junctions and chromosomal localization. *Genomics* 15, 161-168.

Vogel, K. G., Koob, T. J., and Fisher, L. W. (1987). Characterization and interactions of a fragment of the core protein of the small proteoglycan (PGII) from bovine tendon. *Biochem Biophys Res Commun* 148, 658-663.

Vogel, K. G., Paulsson, M., and Heinegard, D. (1984). Specific inhibition of type I and type II collagen fibrillogenesis by the small proteoglycan of tendon. *Biochem J* 223, 587-597.

von der Mark, K., Kirsch, T., Nerlich, A., Kuss, A., Weseloh, G., Gluckert, K., and Stoss, H. (1992). Type X collagen synthesis in human osteoarthritic cartilage. Indication of chondrocyte hypertrophy. *Arthritis Rheum* 35, 806-811.

Vortkamp, A. (2001). Interaction of growth factors regulating chondrocyte differentiation in the developing embryo. *Osteoarthritis and Cartilage* 9, 109-117.

Vortkamp, A., Lee, K., Lanske, B., Segre, G. V., Kronenberg, H. M., and Tabin, C. J. (1996). Regulation of rate of cartilage differentiation by Indian hedgehog and PTH-related protein. *Science* 273, 613-622.

Vu, T. H., Shipley, J. M., Bergers, G., Berger, J. E., Helms, J. A., Hanahan, D., Shapiro, S. D., Senior, R. M., and Werb, Z. (1998). MMP-9/Gelatinase B is a key regulator of growth plate angiogenesis and apoptosis of hypertrophic chondrocytes. *Cell* 93, 411-422.

Vynios, D. H., Papageorgakopoulou, N., Sazakli, H., and Tsiganos, C. P. (2001). The interactions of cartilage proteoglycans with collagens are determined by their structures. *Biochimie* 83, 899-906.

Wai, A. W., Ng, L. J., Watanabe, H., Yamada, Y., Tam, P. P., and Cheah, K. S. (1998). Disrupted expression of matrix genes in the growth plate of the mouse cartilage matrix deficiency (cmd) mutant. *Dev Genet* 22, 349-358.
Wang, W., and Kirsch, T. (2002). Retinoic acid stimulates annexin-mediated growth plate chondrocyte mineralization. *J Cell Biol* 157, 1061-1070.

Warman, M. L., Abbott, M., Apte, S. S., Hefferon, T., McIntosh, I., Cohn, D. H., Hecht, J. T., Olsen, B. R., and Francomano, C. A. (1993). A type X collagen mutation causes schmid metaphyseal chondrodysplasia. *Nature genetics* 5, 79-82.

Weber, I. T., Harrison, R. W., and Iozzo, R. V. (1996). Model structure of decorin and implications for collagen fibrillogenesis. *Journal of Biological Chemistry* 271, 31767-31770.

Wegrowski, Y., Pillarisetti, J., Danielson, K. G., Suzuki, S., and Iozzo, R. V. (1995). The murine biglycan: complete cDNA cloning, genomic organization, promoter function, and expression. *Genomics* 30, 8-17.

Whinna, H. C., Choi, H. U., Rosenberg, L. C., and Church, F. C. (1993). Interaction of heparin cofactor II with biglycan and decorin. *J Biol Chem* 268, 3920-3924.

Wiberg, C., Hedbom, E., Khairullina, A., Lamande, S. R., Oldberg, A., Timpl, R., Morgelin, M., and Heinegard, D. (2001). Biglycan and decorin bind close to the n-terminal region of the collagen VI triple helix. *J Biol Chem* 276, 18947-18952.

Wiberg, C., Heinegard, D., Wenglen, C., Timpl, R., and Morgelin, M. (2002). Biglycan organizes collagen VI into hexagonal-like networks resembling tissue structures. *J Biol Chem* 277, 49120-49126.

Wiberg, C., Klatt, A. R., Wagener, R., Paulsson, M., Bateman, J. F., Heinegard, D., and Morgelin, M. (2003). Complexes of matrilin-1 and biglycan or decorin connect collagen VI microfibrils to both collagen II and aggrecan. *J Biol Chem* 278, 37698-37704.

Wilda, M., Bachner, D., Just, W., Geerkens, C., Kraus, P., Vogel, W., and Hameister, H. (2000). A comparison of the expression pattern of five genes of the family of small leucine-rich proteoglycans during mouse development. *J Bone Miner Res* 15, 2187-2196.

Wingfield, P. T. (1997). Purification of recombinant proteins. *Current Protocols in Protein Science* 6, 601-647.
Winnemoller, M., Schon, P., Vischer, P., and Kresse, H. (1992). Interactions between thrombospondin and the small proteoglycan decorin: interference with cell attachment. *Eur J Cell Biol* 59, 47-55.

Woessner, J. F. (1976). *The Methodology of Connective Tissue Research* (Oxford, Joynson-Bruvvers Ltd).

Wu, L. N. Y., Genge, B. R., Lloyd, G. C., and Wuthier, R. E. (1991). Collagen binding proteins in collagenase released matrix vesicles from cartilage. *The Journal of Biological Chemistry* 266, 1195-1203.

Wu, W., Mwale, F., Tchetina, E., Kojima, T., Yashuda, T., and Poole, R. (2001). Cartilage Matrix Resorption in Skeletogenesis. In *Molecular Basis of Skeletogenesis* (John Wiley & Sons Ltd.), pp. 158-170.

Xi, Y. M., Hu, Y. G., Lu, Z. H., Zheng, H. J., Chen, Y., and Qi, Z. (2004). Gene expression of collagen types IX and X in the lumbar disc. *Chin J Traumatol* 7, 76-80.

Xu, T., Bianco, P., Fisher, L. W., Longenecker, G., Smith, E., Goldstein, S., Bonadio, J., Boskey, A., Heegaard, A. M., Sommer, B., *et al.* (1998). Targeted disruption of the biglycan gene leads to an osteoporosis-like phenotype in mice. *Nat Genet* 20, 78-82.

Yamaguchi, N., Benya, P. D., vanderRest, M., and Ninomiya, Y. (1989). The cloning and sequencing of alpha 1 (VIII) collagen cDNAs demonstrate that type VIII collagen is a short chain collagen and contains triple-helical and carboxyl-terminal non-triple-helical domains similar to those of type X collagen. *J Biol Chem* 264, 16022-16029.

Yamaguchi, Y., Mann, D. M., and Ruoslahti, E. (1990). Negative regulation of transforming growth factor-beta by the proteoglycan decorin. *Nature* 346, 281-284.

Yamaguchi, Y., and Ruoslahti, E. (1988). Expression of human proteoglycan in Chinese hamster ovary cells inhibits cell proliferation. *Nature* 336, 244-246.

Yang, V. W., LaBrenz, S. R., Rosenberg, L. C., McQuillan, D., and Hook, M. (1999). Decorin is a Zn²⁺ metalloprotein. *J Biol Chem* 274, 12454-12460.

Young, M. F., Kerr, J. M., Ibaraki, K., Heegaard, A. M., and Robey, P. G. (1992). Structure, expression, and regulation of the major noncollagenous matrix proteins of bone. *Clin Orthop*, 275-294.

Young, R. D., Vaughan-Thomas, A., Wardale, R. J., and Duance, V. C. (2002). Type II collagen deposition in cruciate ligament precedes osteoarthritis in the guinea pig knee. *Osteoarthritis and Cartilage* 10, 420-428.

Zelzer, E., McLean, W., Ng, Y. S., Fukai, N., Reginato, A. M., Lovejoy, S., D'Amore, P. A., and Olsen, B. R. (2002). Skeletal defects in VEGF(120/120) mice reveal multiple roles for VEGF in skeletogenesis. *Development* 129, 1893-1904.

Zhang, Y., and Chen, Q. (1999). The noncollagenous domain 1 of type X collagen- a novel motif for trimer and higher order multimer formation without a triple helix. *The Journal of Biological Chemistry* 274, 22409-22413.

Zhang, Y., and Chen, Q. (2000). Changes of matrilin forms during endochondral ossification. Molecular basis of oligomeric assembly. *J Biol Chem* 275, 32628-32634.

Zou, H., Wieser, R., Massague, J., and Niswander, L. (1997). Distinct roles of type I bone morphogenetic protein receptors in the formation and differentiation of cartilage. *Genes Dev* 11, 2191-2203.

